Springer Series in Materials Science 134

Alexander Savvatimskiy

Carbon at High Temperatures

Springer

Springer Series in Materials Science

Volume 134

The Springer Series in Materials Science covers the complete spectrum of materials physics, including fundamental principles, physical properties, materials theory and design. Recognizing the increasing importance of materials science in future device technologies, the book titles in this series reflect the state-of-the-art in understanding and controlling the structure and properties of all important classes of materials.

More information about this series at http://www.springer.com/series/856

Alexander Savvatimskiy

Carbon at High Temperatures

Springer

Alexander Savvatimskiy
Department of Experimental
Thermo-Physics
Joint Institute for High Temperatures
Russian Academy of Sciences
Moscow
Russia

ISSN 0933-033X ISSN 2196-2812 (electronic)
Springer Series in Materials Science
ISBN 978-3-319-21349-1 ISBN 978-3-319-21350-7 (eBook)
DOI 10.1007/978-3-319-21350-7

Library of Congress Control Number: 2015947400

Springer Cham Heidelberg New York Dordrecht London

Printed on acid-free paper

Springer International Publishing AG Switzerland is part of Springer Science+Business Media (www.springer.com)

Foreword

The book *Carbon at High Temperatures* by Alexander I. Savvatimskiy presents a comprehensive review of properties of carbon materials at high temperatures. It combines an interesting narrative of the history of the subject development and rigorous treatment of the relevant physical properties of carbon materials near their melting point. The book gives a rare glimpse at science in making by providing a photo supplement about notable events in the world of carbon science and thermal physics. The advent of graphene with its unique electronic and thermal properties resulted in renewed interest to graphite and all other carbon allotropes and derivatives. It turned out that not only graphene, a single atomic plane of carbon atoms, has interesting properties for electronic and thermal management applications. Thin films of graphite can also be gated electrostatically and used as transparent current conductors or channels in sensors. They can also conduct heat better than metal or semiconductor films of the same thickness. The thermal management applications of graphite and, more recently, graphene require knowledge of their properties at high temperature. In this sense, *the book by Savvatimskiy provides a wealth of information.* The properties of carbon materials at high temperature will also be of major importance for numerous proposals of carbon electronics, which would combine various allotropes including carbon nanotubes, synthetic diamond, graphene, amorphous carbon and diamond-like carbon. *The present book fills a major gap in the scientific literature*. I am sure that it will serve as an important reference source for scientists and engineers working in the field of carbon materials. Graduate students pursuing higher education in materials science and engineering, physics and chemistry will also benefit from the information contained in this book.

Web-Site and GoogleScholar: http://www.ee.ucr.edu/∼balandin/

Alexander A. Balandin
Fellow of APS, MRS, IEEE, OSA, SPIE, IOP, AAAS;
University of California Presidential Chair;
Professor of Electrical Engineering; Founding Chair of Materials Science and Engineering; University of California—Riverside

Preface

This book consists of 11 chapters and presents a mostly not previously published review and critical analysis of past and present studies on carbon at very high temperatures. The author tried, to some extent, to preserve the temporal sequence of a very heterogeneous set of experiments and to group them around what he considers as key issues.

The book begins with general considerations on graphite and diamond. This introduction is followed by a description of the first attempts to melt graphite, since 1911, and to produce artificial diamonds.

In Chap. 2, experimental facts (obtained by A. Cezairliyan) about the electric resistance of graphite and its heat capacity in solid phase up to 3000 K are discussed. Knowledge of these properties has been the key to rational attempts to measure the triple point of carbon, at which the three phases coexist: solid, liquid and gaseous state. Then, the numerous attempts to reliably obtain the triple point of carbon are described in Chap. 3.

The experiments of F. Bundy (USA) and S. Lebedev (Russia) to record the melting area are discussed in Chap. 4. The results of pulse milliseconds heating of graphite and pulse microseconds heating are compared. It is claimed that the heating time, from seconds to microseconds, does not affect the obtained results for the melting temperature of carbon. Experimental studies of the scientists (M. Sheindlin and A. Kirillin; A. Cezairliyan; G. Pottlacher and R. Hixon) of the melting temperature and emissivity are compared to each other. The difficulties in measuring melting point under laser heating are mentioned.

Stationary studies (by L. Buchnev et al.) of the properties of graphite in the solid phase up to 3800 K, as well as calculations up to 4900 K are presented in the Chap. 5 to emphasize the importance of steady state research at a high professional level. The results of these experiments are in good agreement with pulse heating experiments.

In Chap. 6, milliseconds experiments (M. Togaya) at high pressures (up to 94 kbar), and microseconds pulse heating (G. Gathers et al. and J. Shaner; V. Korobenko and A. Savvatimskiy) without temperature measurements, are listed.

Their interpretation gives properties of liquid carbon as a function of input energy only. However, these results allowed to determine the appearing of the liquid phase and to obtain a non-trivial dependence of resistance at high pressure.

The experimental setup for pulse heating experiments is reviewed in Chap. 7. This material is extremely important to experimenters for further development of research methods for carbon at high temperatures. Pulse heating results on measuring carbon temperature (up to 12,000 K) are shown.

The ultimate goal of all of these experiments is to reliably develop a phase diagram of carbon. The history of the construction, over decades, of the phase (P-T) diagram of carbon (including modified diagram for nanocarbon) is discussed in Chap. 8. Modeling of carbon phase diagram and the agreement with the experiments are discussed, including the new publications of 2014–2015 years.

Chapter 9 displays the results of recent experiments (J. Eggert, G. Collins et al. USA) with carbon at extreme parameters: pressure level of millions bar and temperatures of about 10^4 K.

Chapter 10 is devoted to the study of graphene at high temperature (based on A. Balandin investigations). Graphene usually does not contain defects and impurities. This chapter does not only discuss graphene at temperatures of practical use (300–1000 K) but also gives the data on the melting of a Graphite HAPG (with the minimum defects) under pulse heating. In the last experiments in the year 2015, the melting temperature of the Graphite HAPG equals 4900 K, which coincides with the value for bulk carbon UPV-1T (HOPG graphite).

Moscow Alexander Savvatimsky

Acknowledgments

The first priority experiments with graphite under pulse heating were carried out by the author in conjunction with S.V. Lebedev in the years 1972–1986. Experimental studies on carbon were continued with the financial support of the atomic center of France (CEA Centre, grant number 3665, CEA/DAM). Experimental studies of carbon, in general, were fulfilled with the financial support of several initiative grants of the Russian Foundation for Basic Research (RFBR), headed by Savvatimskiy.

The participation (in some publications on this direction) of academician V.E. Fortov contributed to its effective development. The author is grateful to V.N. Korobenko and A.D. Rakhel—active participants of carbon study that took place in the laboratory of electro-explosion processes of Joint Institute for High Temperatures Russian Academy of Sciences, for providing experimental and computational efforts under pulse heating of carbon. The author is grateful to Prof. Gerard Vignoles (Université Bordeaux, France) for close examination of the manuscript and to Prof. Alexander Balandin (University of California—Riverside, USA) for useful additions to Chapter on Graphene.

Contents

Symbols

σ	Conductivity
γ	Density (g/cm^3) (p. 28)
ρ	Electrical resistivity (μΩ·cm; μΩ·m; mΩ·cm; μOhm·cm)
ε	Emissivity
δ	Penetration depth of the heat wave (Sect. 6.2.4 and 7.3.3)
λ	Thermal conductivity (J/cm·s·C) (in the formula 6.1 and in Sect. 7.3.3)
λ	Wave length of radiation (nm; microns)
Δt	Time interval
ε_λ	Spectral emissivity
ε_n	Normal emissivity
"*a*"	Radius of the wire (in the Fig. 6.31)
"a" and "c"	(a-face and c-face) lattice parameters (planes)
"reflectivity ρ"	(Sometimes, Sect. 4.2.1)
° C	Temperature in Celsius
μs	Microsecond
$3Nk_B$	Dulong-Petit limit in specific heat
Å	Angstrom
A	Cross-section (Chap. 2)
A	Thermal diffusivity (Sect. 7.3.2)
AIREBO	Interatomic potentials for carbon
AL-124A	Light Emitting Diode
*B*φ	Magnetic field induction (in the formula of Sect. 6.2.6)
C	Designation of carbon symbol
C	Light velocity $3 \cdot 10^{10}$ cm/s (in the formula of Sect. 6.2.6)
C1, C2, C3,…	Mixture of carbon molecules
C-196	High voltage voltmeter
C_P	Heat capacity under constant pressure (J/g·K)
C_V	Heat capacity under constant volume
DC	Direct current
E	Input electrical energy: (J/g)

E	Input energy (inserted energy) (J/g; kJ/g; MJ/kg)
EMF	Electromotive force
F	Capacitance (in farads)
G5-63	Russian pulse generator
GC-30	Glassy carbon (density 1.48 g/cm^3)
H	Enthalpy (J/g; kJ/g; J/mol; kJ/mol)
HAPG	Graphite (highly ordered and annealing pyrolytic graphite)
HOPG	Graphite (highly ordered pyrolytic graphite)
HPG-S3	Spectroscopic graphite (density 1.6 g/cm^3)
HVR APC	Low-inductance resistor disk
I, i	Current
I_1, I_2, I_3	Intensities of the spectral lines (P. 208)
IKM 50/3	Capacitor (50 kV, capacity 3 μF)
IVTAN	Institute for High Temperatures of Academy of Sciences (Subchapter 4.1.2)
J	Supplied energy (in Togaya publications) (kJ/mol) (P. 111)
Je	End of melting (in Togaya publications) (kJ/mol)
J_S	Start of melting (in Togaya publications) (kJ/mol)
K	Temperature in Kelvin
K	Thermal conductivity (W/m·K)
k_B	Boltzmann's constant
L, l	Length
LANG	Graphite grade (graphite for atomic industry)
LCBOP	Interatomic potentials for carbon
LCBOP-I	Model of atomistic calculations (Fig. 8.16)
LCBOP-II	Model of atomistic calculations (Fig. 8.16)
L_f	Inductance
M	Pearson Electronics current monitor (110A, 5046)
M	Mass (g, kg)
MF-307	Isotropic graphite of high initial density, 2.2 g/cm^3 (Japan production)
ms	(msec), millisecond
N	Avogadro number
N	Number
NIIGRAFIT	Moscow Institute for Graphite Investigation
NPO	Scientific and production Association
OIVT RAN	Joint Institute for High Temperatures Russian Academy of Sciences
P	Pressure (bar; kbar; pascal (Pa); GPa)
PDA-10A	Photodetector (Thorlabs production)
POCO AXF-5Q	Vitreous carbon, like glassy-carbon (density 1.83 g/cm^3) (Sect. 4.2.2 and Sect. 6.1.3)
POCO AXF-Q1	Graphite grade
POCO AXM-5Q	Graphite grade
Pyroid	Pyrolytic graphite (density 2.22 g/cm^3)

q	Specific absorbed heat (J/g; kJ/g; J/mol; kJ/mol)
Q (or ΔH)	Heat of fusion (J/g; kJ/g; J/mol; kJ/mol)
R	Electrical resistance (Ohm; Ω)
R	Radius (in the formula of Sect. 6.2.6)
RVU-2	Russian powerful spark gap
RW1	Graphite grade (density 1.55 g /cm^3)
S^0	Entropy (J/mol·K)
T	Temperature
T_m	Melting temperature
T	Time
T1, T2	Hydrogen thyratron #1 and #2
T_C	Critical point temperature
TCR	Temperature coefficient of resistance
TDS3034B	Digital oscilloscope Tektronix (300 MHz)
TDS-754C	Digital oscilloscope Tektronix (500 MHz)
T_{el}	Electron temperature
TGI1-1000/25	Hydrogen thyratron (1000A constantly, 25 kV)
T_i	Ion temperature
Tr	Radiation temperature
TVO-60	Russian ballast resistor (heat resistant, moisture resistant, three-dimensional), high-power
U	Voltage (Volts; kVolts)
U_0	Initial voltage
U_C	Voltage of the condense battery
(UPV-1T)	Russian grade graphite like HOPG
(UPV-1TMO); (UPV-1TKhMO)	Russian grade graphite like HAPG
V	Current volume
V/V_0	Relative volume
V_K	Capillary tube volume
V_O	Initial volume
VS-20-10	Russian rectifier unit
W/cm^2	Laser power (kwatt/cm^2 (Sect. 3.1.3)
wt.%	Weight quantity
ρ^0	Electrical resistivity referred to the initial dimensions
a_1, a_2, a_3	Constants
Φ^0	Thermodynamic function (J/mol·K)

Chapter 1
The First Attempts of Carbon Melting and Obtaining Diamond Phase of Carbon (1911–1939)

Abstract Astrophysical and terrestrial aspects of carbon investigations are discussed. Carbon and diamond structures are shown in comparison. A practical role of carbon in industry is underlined. The clue steady state experimental studies (starting with 1911 year), was discussed up to 1963 year. Particularly the estimation data of Leipunskiy (Russia) are shown to obtain diamond at high pressure (more than 40 kbar) for carbon with dissolved iron and at elevated temperature (higher 1500 K).

1.1 Astrophysical and Terrestrial Aspects of the Carbon Study

Carbon is a unique element of the periodic table, it is formed a huge amount of carbon compounds on the basis of carbon. Organic chemistry as a science emerged due to the existence of carbon. Not coincidentally, it belongs to the boundary matter between living and nonliving matter. One form of carbon—graphite is among the most refractory substances, which explains its widespread use in the industry. Construction of a complete phase diagram of carbon at high temperatures has always been the aim of the experimenters, because it allowed them to predict the properties required for practical applications. Modern energy industry, including pulse technique, required knowledge of the physical properties of carbon at high temperatures, normally comprised its liquid state. To solve this problem has not been enough steady state research methods, as for crucible there is no more refractory matter than the graphite itself. Transient research methods (rapid heating by laser or electric pulse current); have been intensively developed for several decades, first to study metals, and then graphite. The main problem under this study remains the measuring a true temperature of the specimen. There is evidence that for polycrystalline metals fast heating (up to fractions of a microsecond) may obtain, in general, the equilibrium thermal properties (enthalpy of the solid and liquid phase, heat capacity, heat of fusion) as well as temperature. Under graphite

A. Savvatimskiy, *Carbon at High Temperatures*, Springer Series in Materials Science 134, DOI 10.1007/978-3-319-21350-7_1

heating there are more significant features related to: its complex structure (anisotropy), sublimation of the solid phase, the density dependence of the manufacturing process, the initial heterogeneity of structure, etc. These features affect the measurement of temperature of graphite, especially near the melting point.

Motivation for scientists to study carbon has two major components: (1) astronomy and (2) the practical needs of space exploration and development of nuclear technology. We denote these two areas in more detail.

(1) The planets of our solar system (Mercury, Venus, Earth and Mars) are composed of silicates based on silicon. However, as was predicted by astronomers in 2005 [1] may exist planets consisting mainly of carbon. Theorists M. Kuchner, (Princeton University) and S. Seager (Carnegie Institution of Washington) presented a model in which some exoplanets (planets orbiting their stars) may consist mainly of carbon compounds. Carbon planets are more common in the center of the galaxy, because the carbon concentration is higher than near the solar system. Carbon planets contain carbon in various phase states. Kuchner and Seager believe that their idea is consistent with the discoveries of planets located close to their parent stars—much closer than Mercury is to the Sun. In such a planet, they argue, significantly more likely to survive at high temperatures near the star. Exoplanets revolve around stars (such as stars already discovered more than a hundred); most of them must contain a large amount of carbon, as resulted from the condensation of coal dust and gas rich in carbon. They may consist of solid carbon components, including silicon carbide SiC. On such planets cannot be excluded deposits of almost pure carbon. The upper layers of carbon deposits can be graphite, and the lower (due to pressure)—diamond.
Experimental confirmation of the existence of carbon planets appeared in 2010 [2]: an analysis of multi-wavelength photometry of the exoplanet WASP-12b showed a high concentration of carbon in the atmosphere. Recent images of Titan—Saturn obtained with the probe “Huygens” shows that the Methane Rivers and lakes are on its surface. Astrochemical Katharina Lodders from Washington University in St. Louis, Missouri, suggested that methane-rich atmosphere of Jupiter—proof that the planet was formed around of the carbon-based nucleus. The knowledge of the properties of carbon at high pressures and temperatures is one of the main problems in the physics of extreme conditions.

(2) Relevance of research on the properties of carbon depends on the fact that carbon and its compounds are increasingly used as structural materials for scientific and industrial high-temperature devices. For example, the development of space launch programs directly related to the search for new materials that can withstand significant thermal load (protective tiles on the “Buran-rocket”; nosecone missiles whose temperature reaches more than 3000 K at the entrance to the Earth’s atmosphere, and finally, the exhaust nozzle of the last missiles of the latest pattern. Nozzle of up-to date missiles performed on the basis of carbon compounds must to withstand a temperature

of about 4000–4500 K for 1–2 min. Such coatings are used to create micro-fuel spheres in nuclear technology. Matrixes for nuclear fuels consist mainly of compounds of refractory metals, carbides and carbon. Using carbon nuclear rocket engines and nuclear reactors requires accurate knowledge of the P-T phase diagram up to 1000 atmospheres. Investigation of high-temperature properties of these materials (high temperature carbides and graphite) and the task of research teams, as the calculation of practical problems of development (such as space, and new industrial technologies) requires knowledge of the properties of refractory materials, depending on the temperature. These properties should include substances primarily: density, resistivity, specific heat, heat capacity and thermal conductivity, for both solid and liquid states.

However, these studies have not only applied but also of great scientific importance. Development of science itself requires knowledge of the substance properties in a broad aspect, for example, the creation of phase diagrams of substances (depending on the pressure, density, composition, temperature)—allow to understand the behavior of materials in a wide temperature range and open the way for the creation of new and better materials. In particular, the study of the enthalpy and heat capacity is directly related to understand the cause of more intensive changes in heat capacity at high temperatures, the study of the role of structural processes as thermally activated formation of defects in the crystal lattice, un-harmonization of atomic vibrations, pre-melting. Finally, the establishment of a common theory of the liquid state is still awaiting its decision.

As an example, we recall that the phase diagram of carbon has not yet obtained the final form. To the melting point of graphite (4800 K), the experimental data are limited; moreover, still there is a debate in the scientific literature about the melting point of carbon. As for the properties of liquid carbon, the published data of direct experiment are rare. These properties can be obtained by applying to study the process of heating the carbon short pulse of electric current or laser pulse. Such heating during—nanoseconds or microseconds time interval very effectively as:

- loss of energy during the heating—low (fractions of a percent);
- specimen shape (cylindrical or rectangular) is preserved during heating;
- high-speed digital oscilloscope and pyrometer allow accurately record parameters (voltage, current, temperature) during heating.

Recall the difference in structures of diamond and graphite (Fig. 1.1), which are one and the same element—carbon. We use data from different reference books.

In diamond, each carbon atom has four tetrahedral located neighbors to form a cubic structure. Carbon atom has four valence electrons. Cubic structure corresponds to the maximum covalent bond, and all 4 electrons of each carbon atom forms a high-strong C–C bond, i.e. the conduction electrons are absent in the structure. Therefore, diamond has a high hardness and lack of conductivity, but (here's the paradox), good thermal conductivity. It is the hardest known substances. Breaking C–C bond (bond length 1.54 Å, hence the covalent radius of 1.54/2 = 0.77

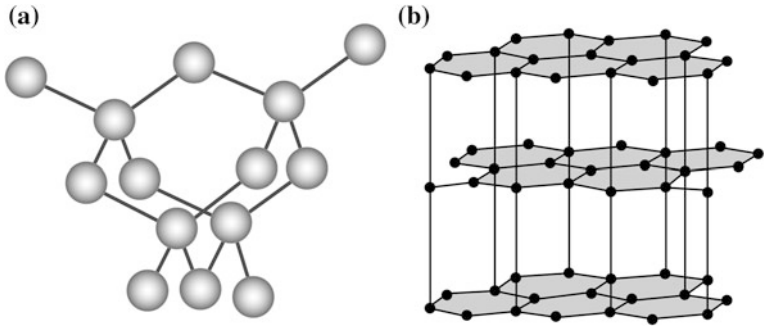

Fig. 1.1 (http://www.krugosvet.ru/enc/nauka_i_tehnika/himiya/UGLEROD.html) [3]. The structure of the diamond (**a**) and graphite (**b**). Parallel layers of graphite (**b**) are slightly displaced relative to each other. In rhombic lattice position of flat layers are not repeated over one layer in **a** hexagonal (as in this figure), but over two

Å) in tetrahedral coordination requires more energy, so the diamond, along with exceptional hardness, characterized by a high melting point.

Another allotropic form of carbon is graphite, very different from the properties of diamond. Graphite—a soft light layer of substance small crystals, characterized good electrical conductivity (if the initial density—high). Therefore, graphite is used where it is necessary to create high temperatures. High purity graphite is used in nuclear reactors as a neutron moderator. Graphite has a very high melting point (4800 K), but it is necessary to use high pressure for melting. Graphite is sublimated at ambient pressure and at a high temperature and cannot be transferred into the liquid state. Indeed, if the graphite specimen is heated for a long time at atmospheric pressure or in a vacuum, it sublimates only until the disappearance of the entire specimen.

The hexagonal structure of graphite is a condensed system of hexagonal rings with bond length of 1.42 Å (shorter than for diamond), but wherein each carbon atom has three (instead of four as in diamond) covalent bonds with three neighbors, and the fourth connection (3.4 Å) is too long for a covalent bond and weakly binds graphite layers stacked parallel to each other. It is the fourth electron of carbon determines thermal and electrical conductivity of graphite. This longer and less strong bond forms less compact graphite, which is reflected in its lower density compared to diamond (maximum density of 2.26 g/cm^3 for graphite, diamond—3.51 g/cm^3). For the same reason graphite slippery to the touch and flakes easily separates the substance that is used for the manufacture of lubricants and pencil rods. Many grades of graphite in the interests of industry are produced having a density is much lower (1.9–1.5) g/cm^3. This allows obtaining a solid structural material with good workability. Low-density graphite has a high porosity of such grades (it gives high electrical resistance). Therefore it is necessary to distinguish between bulk density of graphite (1.9–1.5) g/cm^3, which takes into account the presence of pores, and the X-ray density (2.26) g/cm^3, for which the presence of

pores is not considered. The quasi-monocrystalline graphite has a minimum number of pores, so it is approaching the bulk density of the X-ray.

Electrical conductivity of single crystals of graphite (density 2.26 g/cm^3) in a direction parallel to the basal plane is close to the metal, in the perpendicular—of hundreds or thousands of times smaller than that of metals.

Before proceeding to a brief review of earlier experimental studies and discussion of key studies on carbon, we should say that such a review was published in 1981 by Sheindlin [4] on the determination of the triple point parameters for graphite-liquid-gas sublimation curve and the boiling curve. Earlier (as the author [4] consider) these problems almost are not discussed in the domestic (Russian) literature.

Set out below is the point of view for the author of this book sometimes for publications already considered in [4] (1981), but this monograph focuses on pulse heating in recent years (the last 30 years since the publication of the survey [4], many new studies have appeared). Steady state research methods are thoroughly discussed in this monograph to show the problems of carbon investigation under slow heating of sublimated carbon. As for the beginning of experimental studies of graphite, let us mention the work [5] (1911 year) as one of the first and key. Ironically, still in 1911 it was clear for astute researchers that at atmospheric pressure there is no reason to expect melting graphite.

1.2 State of the Art with Graphite Melting in 1911 Year

The problem of graphite melting was considered in experimental study in 1911 [5]. In this work it has been criticized other work of the same year [6]. In the work [6] it was reported of sagging heated graphite rods, the presence of globular structures on the surface of the graphite pieces destroyed by electrical arc and gently rounded at the rods ends, as evidence of graphite melting at normal pressures. However, Watt and Mendenhall [5] prove in his experiments that the presence micro-globules and sagging graphite rods heated in the temperature range from 2150 °C up to temperatures of 3500–3800 °C cannot be related to the melting of graphite, but most likely indicates the condensation of steam and continuous growth plasticity graphite with increasing temperature.

Another observation in [5] is remarkable: there is an activity sublimation of the heated rods was watched at normal pressures. As with the surface and into the internal micro-cavities of the graphite rod, which leads to rod destruction to separate pieces to form an electrical arc between them. The melting rods are not observed in the report [5]. Curvature at the ends of the destroyed rod the authors explain the action of the electric arc that appears in the field gap of the rod. Temperature in [5] was measured with an optical pyrometer. The authors note that the measured surface temperature of 3250 °C, reassessed to the true 3500 °C (with extrapolation curve used suggested by the authors [5]). In a vacuum, only managed to fix the temperature up to 3100 °C in air at 1 atm—up to 3500 °C (reassessing

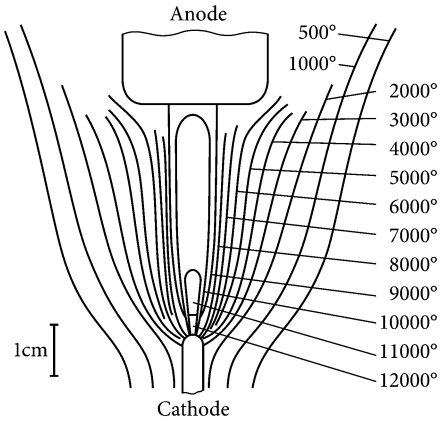

Fig. 1.2 The temperature distribution in different parts of the electric arc column (Illustration "The temperature in different parts of the cord of an electric arc"—from Great Soviet Encyclopedia)

gives a true temperature 3800 °C). The authors [5] considered that specimens are destroyed as soon as the inner temperature of the specimens (which is higher than the surface temperature) reaches the temperature of the arc. It is assumed that the measured pyrometer temperature of electric arc burning in the air, between the metal electrodes, is about 3800 °C. The reason for this conclusion is that the arc burning in air, was covered with a layer of metallic vapor (vapor of the electrodes) —it underestimates the measured temperature. In fact, the actual temperature of the electric arc is from 8000 to 12,000 K (Fig. 1.2).

It should be noted that Mendenhall is the author of the wedge blackbody model, which it was first proposed, designed and published in the same 1911 [7]. The question of measuring the melting temperature of carbon, including through the wedge blackbody model will be discussed in Sect. 7.2.

1.3 The First Substantial Experiments of Stationary Study of Graphite by Pirani 1925–1939

In 1923 Pirani and Alterthum [8] began to investigate the melting point of refractory metals under stationary heating by alternating electrical current, but the detailed investigation was set out in their study [9] in 1930. The control experiments were carried out on the metals.

Note experiment by Pirani in 1939 (under a small external pressure), which subsequent researchers has been interpreted differently, until the extreme view that Pirani melted carbon, which in fact was not. It often happens that the examination of original works of scientists allow us to formulate an adequate view of the results of their work, rather than their interpretation of other researchers. Consider the studies of Pirani [9] in more detail.

Metal rods of 7 mm in diameter were manufactured, and the small diameter holes were drilled perpendicular to the axis of the rods. Drilled holes played the role

of blackbody emitter at temperature measurements. The rods were heated by electrical alternating current in the atmosphere of neutral gas, and their temperature was measured by an optical pyrometer sighted inside the small hole. Moment of melting was detected in change luminosity holes and appearance of liquid metal from the hole. Further, in [9] states: if the rods are made of fused material with high reflectivity, such as nickel, the walls of drilled holes should be smoothed and the hole will therefore not look as blackbody radiation. Emissivity (the coefficient of radiation) should be only about 75 %. If the investigated material is made of pressed powder, then the surface of the drilled hole looks like a blackbody radiation because of a roughness [9].

For comparison, recall that for the wedge blackbody model mirror sidewalls gives a "black" radiation due to a larger number of reflections, see Chap. 4 of the temperature measurement, with the discussion on [5].

To test the efficiency of this method it was determined melting point of tungsten and molybdenum in [9]. Tungsten rods were pressed from pure metal powder (carbon content less than 0.01 %) and sintered at 1450 °C. Then, these rods were placed between two water-cooled clamps. Pyrometer was sited into the central drill. The rods were heated by AC (in a stream of hydrogen) to a temperature close to the melting point, and left them at that temperature for a while to complete sintering (a sign that—resistance becomes constant). Current fluctuations are aligned with regulation of the resistance by a transformer in the circuit. Then gradually increase a current, especially slowly near the melting temperature.

Since the location of the rod cross-section sighted its smallest, this is where there is a slight "overheating" of the material causes it to melt. The molten metal is sometimes stood out from the hole in the form of droplet. The external surface of the rod is lower because of radiation cooling and hydrogen jet, and it is approximately 80 °C lower than the temperature in the middle of the rod. Melting of the metal within the holes is always starting from the center to the exterior surface.

The temperature inside the hole was observed using a calibrated Kurlbaum-Holborn pyrometer. Under measurement the hole seemed bright circle on a dark surface of the wall, but at the time of melting at a very slow increase in temperature —a small dark spot suddenly appeared in the bright circle. With increasing in temperature all the hole suddenly becomes dark because the emissivity of the smooth molten surface significantly less than rough background. Thus the melting temperature was determined for molybdenum −2840 ± 40 K, and for tungsten 3660 ± 60 K.

The same method for determining the melting point was used by the author [9] to carbon. Figure 1.3 illustrates the experiences of coal melting under current 8000 A at 8 V, in a hydrogen atmosphere at a pressure of 800 mm Hg. Coal rod was made of pressed electro-graphite by Siemens Company (140 mm long and 37 mm in diameter). In the middle of the rod there was a transverse drilled hole diameter of 3 mm and a depth −18 mm (half of the diameter). This hole with allegedly spread and overflow carbon is shown in Fig. 1.3.

Figure 1.3 published in [9], it was shown exactly in this position (vertical specimen position). Consequently, bulging graphite did not constitute a fluid body;

Fig. 1.3 Graphite spread out of the drilled hole

it is probably hard and has a plastic state. Plasticity of carbon observed in the paper [5] (1911), which also discussed the problem of the graphite melting and its plasticity at high temperatures. During the publication of the works of M. Pirani 1923–1930 [8, 9] there was not perfect equipment for experimental studies of graphite at a high technical level and solid graphite sublimation were not considered. Pyrometer measuring of the graphite has not commented on by the author [9]. Result by the melting temperature of graphite (3500 °C)—is given in the hope that the methodology applied in [9] previously to metals at low ambient pressure will give a fair result for the carbon at low pressure (800 mm Hg). In fact, the author [9] observed graphite bulging out of the hole (3 mm in diameter). The graphite rod itself was heated slowly by alternating current. Pyrometer recorded the temperature of this bulged portion; the entire rod (diameter 37 mm) of course does not melt.

In [9] the author indicates the carbon melting point of the specimen as 3500 °C. Today, it is known that the melting point of carbon is 4800 K. Probably, the author

has watched the bulging of graphite from the hole and believed that graphite has melted. However, the appearance of the graphite from the hole may be explain due to the fact that at high temperatures, the graphite becomes highly plastic and with increasing in volume it is forced out of the hole. Thus, in [9], the carbon specimens were failed to melt and the graphite was observed only as bulging out of the hole.

1.4 Estimated Study for Obtaining Diamond by Leipunsky 1939

In 1939 Leipunsky [10] obtained an equilibrium phase diagram for carbon on the base of thermodynamic data for graphite and diamond (Fig. 1.4). Leipunsky have said: "*Only after the work of Nernst* [11], *who measured the heat capacity in 1911 for graphite and diamond, and the work of Rota* [12], *who obtained the heat of combustion for transition of graphite to diamond from the difference in the heat combustion of graphite and diamond* (*correct sign but wrong value*),—*it was possible to calculate the thermodynamic functions for graphite and diamond and determine the steady state conditions for both modifications*" [10, p. 1524].

Leipunsky performed thermodynamic calculations and extrapolated known data (at 1400 K) to a higher temperature and pressure. Volume change on graphite melting was not known. For most metals, it does not exceed 5 % of the volume. Taking this value into account Leipunsky expresses the dependence of the graphite melting temperature against pressure by the next equation:

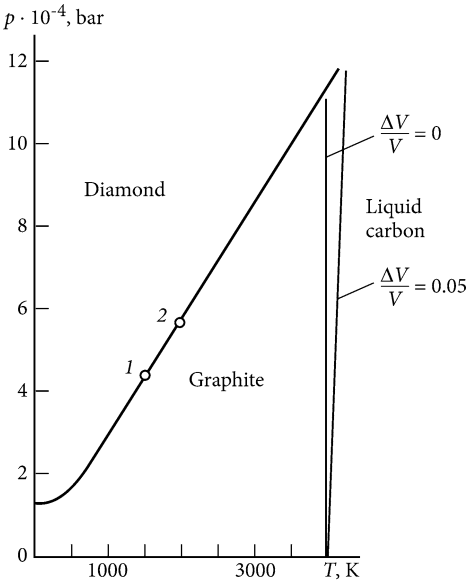

Fig. 1.4 Phase diagram of carbon proposed by Leipunsky in [10]: *1* minimum parameters (P = 42 kbar and T = 1500 K) for the crystallization of diamond from graphite and iron solution; *2* the same from the solid graphite (P = 60 kbar and T = 2000 K)

$$T = T_0 \times e^{\pm 0.05PV/Q,}$$

where T_0—initial known temperature; Q—heat of fusion for carbon.

In accordance with this formula: if for the pressure of 1 bar the melting temperature is 4000 K, then for 100 kbar pressure the melting temperature will rise by only 240 K and should be 4240 K (*Author of the monograph: It should be noted that the notion on the graphite as an ordinary metal unproductive because graphite increases its volume by 70 % at the melting point, see* Sect. 5.2).

Key recommendations of Leipunsky are as following. First, it is necessary to heat the graphite not less than 2000 K for carbon atoms can move from place to place. Secondly, it is necessary to compress graphite not less than 60,000 atmospheres. Leipunsky was the first who pointed out the possible way of diamond synthesis and predicted parameters at which a transition from graphite to diamond takes place in the presence of metal catalyst such as iron (on the grounds that the iron partially dissolves carbon).

Furthermore, Leipunsky considered the crystallization kinetics of the different forms of carbon, in particular transition graphite—diamond. Its main conclusions during the diamond crystallization contain: (1) the use of such pressures at which the diamond is more stable phase than graphite; (2) use of low transition rates, "*not to allow the advantages of graphite as a kinetically more likely environment*" [10, p. 1529]; (3) the use of such temperatures that reconstruction in the crystal lattice was possible, so that in case of graphite formation, the latter could go into a diamond. Leipunsky recommendations were extremely useful for further targeted experiments.

Using estimates of high-temperature kinetic reactions Leipunsky indicated lower limit of direct transition graphite-diamond (at least 40 kbar and 1250 K). Moreover, Leipunsky gives an example of diamond crystallization under cooling of the solution of carbon in iron. The latter technique is used by current technology of catalytic production of diamond in the presence of metals such as Fe, Ni, Co, etc. Leipunsky also supposed that the melting temperature of graphite is 4000 K, and it should slightly increase with increasing pressure.

Lower, we describe the work of Leipunsky according to the Journal [13]. Leipunsky tried to interest various departments to begin production of synthetic diamonds for industrial purposes, but never met understanding. For example, in the Ministry of Oil Industry at a special meeting at the department of drilling and hard materials, it was stated that they do not need diamonds. He also made a memorandum addressed to All-Union Economic Council on the organization of a special laboratory for the production of diamonds, but received no response. But later, when the United States sued the USSR for use diamonds in their patents with global circulation, Soviet officials have realized the problem, and created the following document.

Scientific discovery "Regularity of diamond formation (creation of artificial diamonds from graphite)".

Formula of the discovery "Theoretically established previously unknown conformity of crystallization (synthesis) of diamond from carbon—formation of diamond in the region of its stability in a liquid medium, dissolving carbon or come in unstable chemical compounds at a pressure and a temperature greater than 1400 K, *corresponding to the condition:*

$P > 5, 5 + 26, 42022\ 10^{-3}\ T$ K *(in thousand atmospheres)"*

Author: O.I. Leipunsky.

Number and date of priority: № 101, August ***1939***

Filing Date: January 5, ***1971***

Ovsey Ilyich Leipunsky—Doctor of Physical and Mathematical Sciences, disciple of the academicians Ya. Zel'dovich and N. Semenov, worked in the Atomic Project (for which he was awarded the Order of Lenin), participated in the first and all subsequent tests of atomic bombs near Semipalatinsk; in 1960s he became involved in the Institute of Chemical Physics (ICP) and deal with solid propellant.

Experimental study of P-T carbon phase diagram causes problems when performing normally incompatible requirements while maintaining a high temperature and high pressure for the specimen. With the development of technology of ultrahigh-pressure industry a possibility appeared first of synthesis of diamond, and then carefully examines the coexistence curve of the graphite- diamond, finding the minimum pressure and temperature at which the catalytic synthesis is still possible. Later, the American scientist Francis Bundy [14] succeeded in exploring the melting curve of graphite at very high pressures (up to 100 kbar), define the conditions of non-catalytic synthesis of diamond from graphite and obtain triple point parameters diamond-graphite-liquid ($P \sim 100$ kbar).

References

1. M.J. Kuchner, S. Seager, Astrophys. J. Lett. **0504214**, 2 (2005)
2. N. Madhusudhan, J. Harrington, K.B. Stevenson, et al., Nature **09602**, (2010)
3. (http://www.krugosvet.ru/enc/nauka_i_tehnika/himiya/UGLEROD.html)
4. M.A. Sheindlin, The phase diagram of carbon at high temperatures. High Temp. **19**(3), 467–488 (1981)
5. O.P. Watts, C.E. Mendenhall, On the fusion of carbon. Phys. Rev. (Series 1), **33**, 65–69 (1911)
6. M. LaRosa, Uber das Schmelzen des Kohlenstoffs mittels des Jouleschen Effektes. Ann. Der Physik **339**(1), 95–105 (1911)
7. C.E. Mendenhall, On the emissive power of wedge-shaped cavities and their use in temperature measurements (An International Review of Spectroscopy and Astronomical Physics). Astrophys. J. **33**(2), 91–97 (1911)
8. Pirani u. Alterthum, Z. fur Elektrochemie **29**, 5/8 (1923)
9. M.S. Pirani, in *Elektrothermie; die elektrische Erzeugung und technische Verwerdung hoher Temperaturen,* ed. by M.S. Pirani (Springer, Berlin, 1930)
10. O.I. Leipunsky, About artificial diamonds. Chem. Uspekhi **8**(10), 1519 (1939)
11. Nernst, Ann d. Phys. **36**, 395 (1911)
12. Roth u. Wallach, Z. Electrochem. **21**, 1 (1915)
13. State Resource Management. № 9/51/2009 (in Russian)
14. F.P. Bundy, Melting of graphite at very high pressure. J. Chem. Phys **38**, 618–630 (1963)

Chapter 2
Resistivity and Heat Capacity for Solid Graphite up to 3000 K

Abstract The carefully executed experiments by Ared Cezairliyan (USA) are reviewed. Cezairliyan obtained resistivity and specific heat of graphite grade POCO up to 3000 K. The specimens were made of commercial graphite POCO; electrical resistivity and heat capacity were obtained against temperature. Temperature was measured with the help of a blackbody model under millisecond current heating (heating rate—from 600 up to 6500 K/s).

In 1985 Ared Cezairliyan and Miiller [1] reported, as always carefully performed work on the study of graphite heated by pulse current during the fraction of a second. It was selected well-known commercial graphite POCO AXM-5Q. In the introduction, the authors note that graphite has every reason to become a standard material (reference material) for the study of materials at high temperatures, in connection with its use in thermal protection systems and refractory composites. This work was put under program CODATA to create high-standard materials, in particular with respect to thermal conductivity.

All experiments were performed in a vacuum of 10^{-5} mm Hg. The specimens were in the form of tube with the length of 76 mm, an outer diameter of 6.4 mm and wall thickness of 0.5 mm.

A rectangular hole 0.5 × 1 mm for pyrometer measurements was in the center of the tube gives blackbody model for temperature investigation.

To compensate the heterogeneity of the cross section, the part of the specimen ground off along the length of the specimen, except for the place opposite to the hole. The pyrometer temperature measurements were divided into six overlapping regions for convenience, so pyrometer used only for its range of temperatures at every heating. In this connection, the heating speed of the specimens was ranged from 3000 to 5000 K/s in different series of measurements. To determine the possible effects that may be associated with different heating rate it was performed 16 additional experiments in the temperature range 1900–2100 K, using a heating rate from 600 to 6500 K/s. The results of these additional experiments were not included in the final calculations of the specific heat and electrical resistivity. Pyrometer was again calibrated with a standard tungsten lamp after completion of all experiments.

A. Savvatimskiy, *Carbon at High Temperatures*, Springer Series in Materials Science 134, DOI 10.1007/978-3-319-21350-7_2

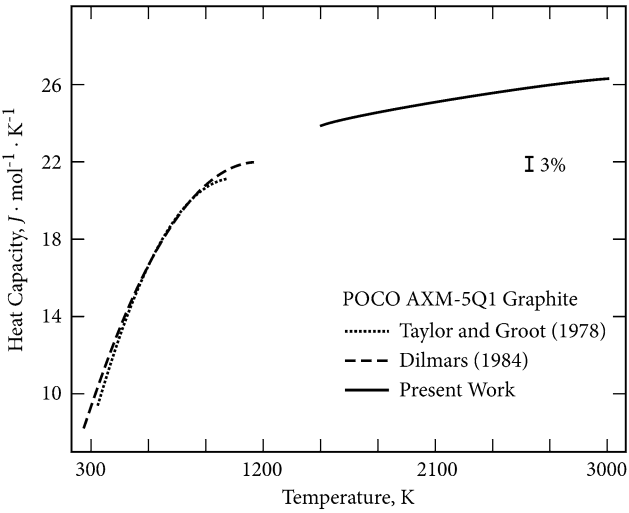

Fig. 2.1 [1] Heat capacity of graphite POCO AXM-5Q; experimental results (*solid line*) and published data

Experimental data on the current and voltage were approximated by a polynomial least squares, which are then used to obtain the resistivity and heat capacity for each temperature range. Heat capacity was calculated according to the formula

$$C_P = (UI - H_{rad})/n \times dT/t,$$

where U—voltage; I—current; H_{rad}—losses by thermal radiation; n—number of moles.

Heat losses were calculated from experiments on the cooling of the same specimens after the appropriate heating. For example, for a temperature of 1500 K, the heat loss was 4 % of the input power; for 2000 K—10 %; for 2500 K—19 %; and for 3000 K—34 %. As a result, an expression was obtained for the specific heat $C_P = 19{,}438 + 3{,}6215 \times 10^{-3}T—4{,}4426 \times 10^{-7}T^2$, where C_P in J/mol K, the atomic weight of 12,011 was used. Data are shown in Fig. 2.1.

Figure 2.2 shows the results obtained for the specific heat of graphite POCO AXM-5Q in comparison with other graphite grades (published data).

Resistivity (referred to the initial size) was calculated as $\rho = RA/L$, where R—electrical resistance; A—cross-section; L—length of the specimen between the electrodes. The cross section of graphite was calculated from the density (1.709 and 1.744 g/cm^3) for the two different deliveries and the weight measurement of the specimen. A considerable difference ($\sim$10 %) was observed in the magnitude of the resistivity for the specimens of different density, so the final results approximated by polynomials are shown separately for specimen 1 and specimen 3 in Fig. 2.3.

Prior to the experiments the initial electrical resistance was measured for the three specimens, the results were obtained: 1735, 1533, 1545 μΩ cm. The final

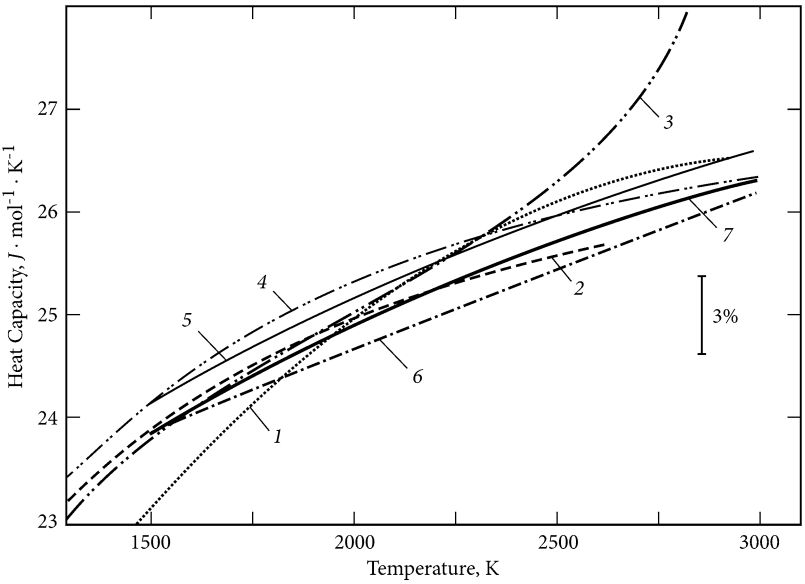

Fig. 2.2 The heat capacity of different grades and forms of graphite: the results (*solid thick line*) and the data published in the literature. *1* Rasor and McClelland 1960 [2]. *2* West and Ishikava 1965. *3* A.E. Sheindlin et al. 1972 [3], Soviet grades. *4* Buchnev et al. 1973 [4], Crystal, Pyrolytic. *5* Cezairliyan and Righini 1975 [5] AXM-5Q. *6* Cezairliyan and Righini 1975 [5] Pyrolytic. *7* Present Work, AXM-5Q1 References are referred to this monograph

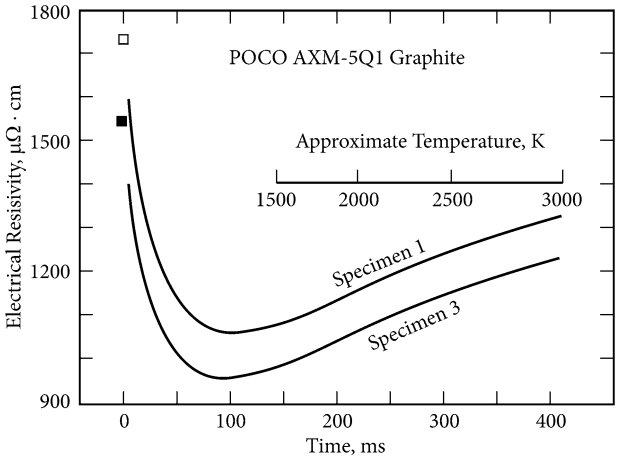

Fig. 2.3 Electrical resistivity (referred to initial dimensions) for graphite POCO AXM-5Q1 against time for the specimens heated in the range from room temperature to 3000 K. The corresponding temperature scale (non-linear) is shown for the last phase of heating

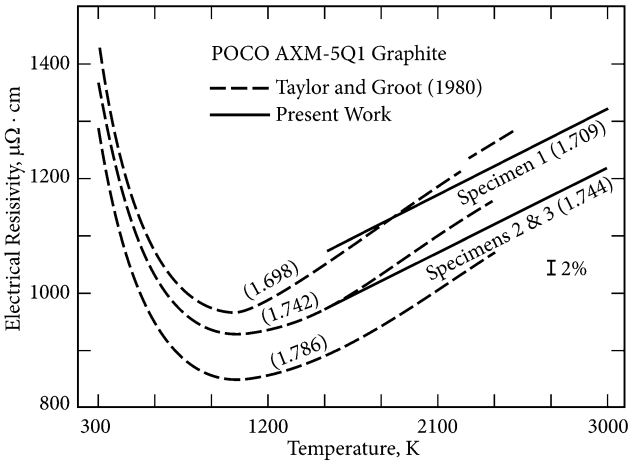

Fig. 2.4 Electrical resistivity (referred to initial dimensions) for graphite POCO AXM-5Q1 (specimen number 1 and number 2, *thick lines*) compared with literature data (*dotted line*) for graphite of the same grade, but with slightly differing density (in the parentheses)

results for the two previously mentioned specimens (No. 1 and No. 2) were presented in Fig. 2.4 with a density of 1,709 and 1.744 g/cm^3 accordingly, and a comparison with results of other authors for the same grade of graphite, but with a different density is shown.

References

1. A. Cezairliyan, A.P. Miiller, Heat capacity and electrical resistivity of POCO AXM-5Q1 graphite in the range 1500-3000 K by a pulse-heating technique. Int. J. Thermophys. **6**(3), 285–300 (1985)
2. N.S. Rasor, McClelland JD. Thermal properties of graphite, molybdenum and tantalum to their destruction temperature, the physics and chemistry of solids, pergamon press **15**, 17–26 (1960)
3. A.E. Sheindlin, I.S. Belevich, I.G. Kozhevnikov, Teplofizika Vysokikh Temperatur **10**(5), 997–1001 (1972) (in Russian)
4. L.M. Buchnev, V.I. Volga, B.K. Dimov, N.V. Markelov, Investigation of the enthalpy of the carbons in the range 500–3250 K. High Temp. **11**(6), 1198–1202 (1973). (in Russian)
5. A. Cezairliyan, F. Righini, Measurements of heat capacity, electrical resistivity and hemispherical total emittance of two grades of graphite in the range 1,500 to 3,000 K by a pulse heating technique. Rev. Int. Hautes Temp. et Refract, **12**, 124 (1975)

Chapter 3
Carbon Triple Point (Graphite/Liquid/Vapor)

Abstract Determination of parameters (P, T) for the triple point of carbon (solid–liquid–gaseous) began in 1939 (Basset), and continued in 1959 (Noda). But the impressive result was obtained only in 1976 (Gokcen) for the pressure at the triple point of carbon (~120 bar). Study of Shoessov at pressures up to 1000 bar, however, had no progress in temperature measurement. The study only by Haaland (1976) [18] gave a truthful value for the melting temperature (close to 5000 K). In addition, Haaland gave a brief analysis of the main results on different high-temperature carbon investigations, noting that the vapor (more precisely, carbon sublimate) affect the quality of the temperature measurements. Later researchers have taken a number of measures to avoid that of the steam jet (sublimate) has appeared in the optical path under temperature measurements. The determination of specific input energy under beginning of melting, enabled investigators to interpret the accuracy of the temperature measurements near the melting point of graphite. Millisecond heating current (M. Sheindlin) allowed us to obtain reliable dependence of enthalpy (input energy) against temperature of the graphite in the solid state up to 4500 K. This experiment is discussed in this chapter. Experiments of different duration (from seconds to nanoseconds) showed no dependence of the melting temperature on the heating rate (Table 3.3). The results of the various experiments performed as under heating by current or by laser heating give the matching results on the melting temperature of graphite (4800–4900 K), provided that the pressure is maintained above 110 bar.

3.1 First Attempts to Obtain Triple Point Parameters (1939–1976)

3.1.1 The First Experimental Evidence of the Pressure at the Triple Point Slightly Higher 100 Bar

In 1939 year Basset [1] determined the parameters of the triple point of carbon (P = 105–110 bar; T = 4000 K) and the melting curve of carbon to 11,500 bar. He used electrical current as a heating method. Basset heated graphite specimen

A. Savvatimskiy, *Carbon at High Temperatures*, Springer Series in Materials Science 134, DOI 10.1007/978-3-319-21350-7_3

diameter 2 and 6 mm length, with the current up to 300 A at a voltage of 12–30 V, measuring the temperature by an optical pyrometer until the specimen destruction. The author [1] used carbon arc crater as a high-temperature calibration point, whose temperature equals 3800 K, it was believed that this temperature was determined with high accuracy. In the survey [2] the Basset study was presented in detail, so we show a brief result given in [2]. Based on their measurements Basset proposed phase diagram of carbon, in which the temperature of the crater of the carbon arc (T = 3800 K at P = 1 bar) corresponds to equilibrium solid–gas at P = 1 bar. According to Basset heat of carbon fusion is 203 kcal/g atom that differs sharply with the result of Bundy pilot study [3] (25 kcal/g atom at a pressure of 48 kbar). Thus, the phase diagram proposed by Basset, is in contradiction with thermodynamics of phase transitions, which is a result of incorrect determination of the triple point parameters.

Noda [4] in 1959 repeated the experiments of Basset on the characterization of the triple point for carbon. The pressure vessel was reconstructed in the autoclave and is provided with electrodes and a viewing window. The specimen was a graphite rod with a diameter from 3 to 4 mm and a length of about 30 mm, the middle part of the rod is reduced in diameter and should be fully melted. The vessel was evacuated and filled with argon to a pressure of about 90 atm. Argon pressure increased as far as the specimen is heated by current. The conditions for melting specimen, which had an average diameter of 4 mm and a length of 25 mm: voltage from 21 to 23 V and a current—350 to 400 A at an argon pressure of 150–160 atm. Fused carbon usually was obtained as a bead with a diameter of 1–3 mm, but if the argon pressure was less than 100 atm, the bead did not appear and soft graphite condensed around the rod. At pressures greater than 110 atm molten beads were obtained, and the amount of condensed carbon decrease with increasing argon pressure and at pressures above 130 bar it was barely noticeable.

The temperature was measured through the window by an optical pyrometer, graded on a standard lamp. Absorption in the glass was also calibrated. To verify accuracy of calibration, the temperature was measured in the anode crater in the vessel at a pressure of 1 atm. Previously it was known that the temperature should be 3810 ± 7 °C; it was obtained value of 3810 ± 10 °C.

The maximum temperature carbon before the very melting point considered to be the melting point for carbon in this experiment. The experiment was repeated twelve times, but sometimes melting could not be seen by the pyrometer, since the specimen was broken before melting occurs. The average result of five specimens equals to 4020 ± 50 K (six experiments were used); it has been adopted as the melting point of carbon. Sixth specimen was not taken into account when calculating the average data, since condensed carbon was seen at the specimen. Melting temperature turned out to be low, if the specimen is contaminated with fine carbon condensed particles, which being in the vapor phase absorb radiation. As the pressure at the triple point it was taken P = 105 ± 5 bar.

A beadle obtained in this experiment was a plastic small ball and easily deformed. Lattice parameters were measured on the X ray diffractometer and found to be $C_0 = 6.7078 \pm 0.0007$ and $a_0 = 2.4614 \pm 0.0002$, which indicates the degree of

crystallization of fused carbon, close to natural graphite. Electron microscopic study showed that re-melted graphite—it is a well-developed single crystal.

In 1960, a paper [5] has appeared, which, along with metals (Mo, Ta) there was studied graphite "*to the temperatures of their destruction*" (as the authors [5] has told). Coal tube furnace was used; the temperature was measured by pyrometer. Particular achievement of this work was to obtain the specific heat C_P for graphite up to 4000 K. After reaching a constant level of heat capacity (0.5 cal/mol K) at a temperature of 3000 K, a sharp rise of heat capacity was obtained near 3500 K (up to 1.0 cal/mol K at 4000 K). Authors [5] indicate the error of the measurements $C_P = \pm 5$ %. This accuracy is questionable, because the cause of the steep growth of the heat capacity by the authors is not commented.

Careful measurements by Gokcen in 1976 [6] gave a convincing proof of the existence of the triple point of carbon at elevated pressure (120 bar), Fig. 3.1.

Bundy leads (as he says) convincing and reproducible results of Gokcen (Fig. 3.1), which he cannot say about the results of Whittaker (assumption of the triple point pressure equal to atmospheric pressure). Weaknesses in Gokcen are temperature measurements; it was introduced various assumptions and corrections due to clouds of carbon surrounding the specimen. However, Bundy sees no reason to doubt in his pressure measurements.

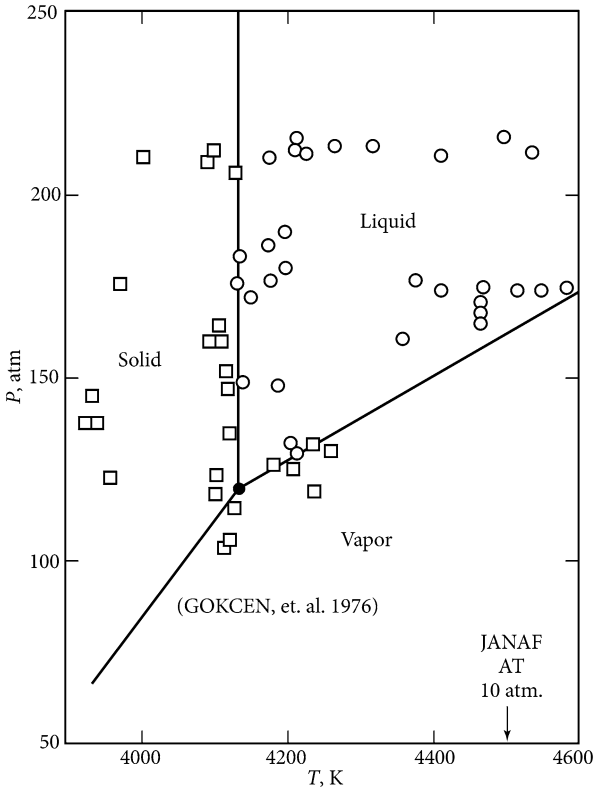

Fig. 3.1 Experimental data by Gokcen et al. [6] of 1976 year, under heating the graphite in argon high pressure (50–250 atm). *Circles* indicate observation of liquid phase, thus defined triple point of carbon (*Figure is a copy from the paper of F.P. Bundy* [48] *of 1980 year*)

In 1979, Ferraz and March [7] (Okcford University) published theoretical work with the assumption that liquid carbon has both insulating phase and conductive. Bundy later rejected this assumption [8]. The adoption Bundy that liquid carbon at high pressure to be denser than graphite is essential, and his opinion that resistivity of the liquid carbon must be noticeably lower than resistivity of graphite before melting is fundamental.

In the survey [2] the study of Gokcen et al. [6] is considered as a very interesting, as it was conducted at a pressure much larger (up to 220 bar) than in the work of Whittaker [9–12]. A study of the triple point of graphite-liquid-vapor also used laser heating. HF-laser with the power of 1.4 kW heated the pyrolytic graphite specimen in a chamber with high pressure inert gas. The brief comments are shown lower from the survey [2] concerning the work of Gokcen.

HF laser beam (λ = 25,000–30,000 Å) focused on an area of $\sim$3 mm^2. The temperature was measured using a monochromatic pyrometer with the disappearing thread at a wavelength of 0.65 μ. The optical pyrometer is directed onto the object in such a way that the optical axis of the pyrometer as close as possible to the axis of the laser beam. According to the authors [6] it helped to preserve the optical path to the specimen "clean" (without soot), which in the case of formation is evaporated by a laser beam.

Duration of the experiment was about 5 s. It was assumed that the pressure in the chamber corresponds to equilibrium vapor pressure of carbon. After the experiment it was conducted examining a specimen under a microscope to detect the presence of melt, as well as to study the structure of the melt by X-ray diffraction, and ion microprobe to determine the possible impurities. The signs of a brilliant melt were marked on the specimens that were heated at a pressure of ≥120 bar and T > 4130 K. Gokcen et al. conducted a large number of experiments and obtained a number of points corresponding to the presence of fluid (Author of this book: *a very important data* (Fig. 3.1) *of the study by Gokcen will be presented in the analysis of study by Francis Bundy*). Analyzing the data, the authors [6] have led to the following values of the triple point of carbon: P = 120 ± 10 bar and T = 4130 K. These values are in satisfactory agreement with measurements made by Basset, Noda and Schoessov.

"*Studies of graphite at high pressures show that graphite can be melted, and the triple point pressure of about 100 bar. Scatter in the temperature of the triple point of graphite is quite large, and not less than 400 K. There is evidence of new polymorphic forms of carbon, different from graphite and diamond. However, in many cases, the amount of the received new crystalline modification is extremely small, which does not allow investigating their thermal and other properties. Currently there is no reliable evidence of their thermodynamic stability and therefore there is no reason to consider them when constructing phase diagram of carbon.*"

By these words M.A. Sheindlin generally ends in his review in 1981 [2] discussion of Gokcen.

3.1.2 *Effort to Search Phase Boundary Solid–Liquid at a Pressure up to 1000 Bar*

In the experimental study by Schoessov [13], the triple point of graphite (electrical current heating), and an attempt was made to determine the phase boundary solid–liquid at pressures up to 1000 bar.

The pressure of the triple point of graphite was determined as 103 atm. The last operation in the manufacture of the specimens for graphitization was 2620 K for 4 h. Triple point temperature was varied for three grades of graphite and was from 4183 ± 10 to 4299 ± 25 K. The temperature at the solidus–liquidus measured for one of the grades increased from 4247 to 4306 K with increasing pressure from 103 to 1000 atm.

To create high-pressure helium gas cell was used. It was found that helium is better than argon, because a signal detected by pyrometer, was more stable in helium, especially at high temperatures.

A specimen with outer diameter 11.5 mm, was melted by an electric current at the central axial line of the specimen but it remains solid at the outer surface near the melting point. Radial hole in the melting region results as a cavity of a blackbody model for optical measurements. Monochromatic pyrometer was calibrated (at the U. S. National Bureau of Standards) by blackbody radiation for all temperature measurements. As the author of [13] noted, an additional calibration check was performed on the operating facility in measuring the melting point for gold, molybdenum and tungsten. The results of these tests to verify the accuracy of the pyrometer with instrumentation, and showed that the measured temperatures are very close to known values. It should be noted (by the author of this monograph) that the calibration on metals does not allow to consider the optical measurements with carbon certainly valid, because of fundamental differences of experimental conditions (graphite begins actively sublimate from the surface at high temperatures, that affects the measurement of temperature by means of an optical pyrometer). Perhaps trying to take this into account the author of [13] used the vent hole (in the outer surface of the specimen, see Fig. 3.2, hoping to reduce the impact of carbon vapor cloud). Nevertheless, the author notes the appearance of black clouds at the highest temperatures near the hole for pyrometer measurements up to the blockage of the hole (the author admits these separate experiments he tried not to include in the final results).

Signs of melting the author considered, in particular the observation of graphite spheres, considering them as formed from a molten phase, and "*the rapid growth of the voltage across the specimen, which is the result of increasing the resistivity of the specimen at the initiation of the phase transition (i.e., melting or sublimation)*" [14]. It should be noted that the graphite spheres may occur as a result of condensation of the vapor phase, as was indicated by Watts and Mendenhall in 1911 [14]. As was shown by the study of Francis Bundy and our work of later years—for melting the resistivity corresponds to drop, but not growth.

Temperature was calibrated in the central cavity [13] with respect to the input power at temperatures below the threshold of visible amount of carbon vapor. This calibration is then used to extrapolate to the past, as the author [13] writes, "*several*

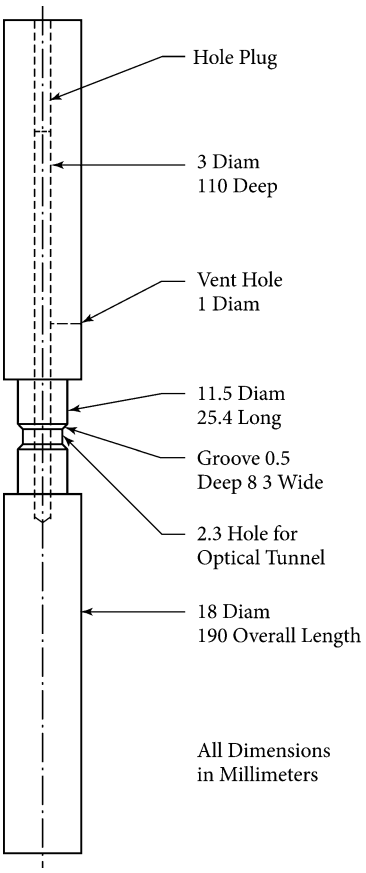

Fig. 3.2 Details of the specimen in the Schoessov's study

hundred degrees" to the melting point, using "*appropriate equation*". Thus, we can assume that direct measurements of the melting temperature of graphite were absent in [13]. However, the authors [13] give temperature dependence of the pressure P (in Fig. 3.3) supposedly with high accuracy (although temperature measurements in [13] are unsatisfactory).

In the study [13] it was obtained that the triple point pressure equals 103 bar and temperature—from 4180 to 4300 K; T = 4300 K corresponds to spectral pure graphite. As noted in his review by M.A. Sheindlin [2]: "*the temperature of the triple point in* [13] *exceeds the 200–300 K temperatures that were obtained earlier. Results* [13] *are of fundamental importance, as they measured the temperature of the melt surface and the obtained values significantly exceed the data of other measurements. Due to the fact that when using a monochromatic pyrometer it may take place only underestimated temperature, the value T = 4300 K sets the lower limit for the temperature of the triple point*" [2].

The survey [2] contains a detailed summary of the work of Whittaker and his colleagues [9–12], who proposed a phase diagram showing the position of carbon

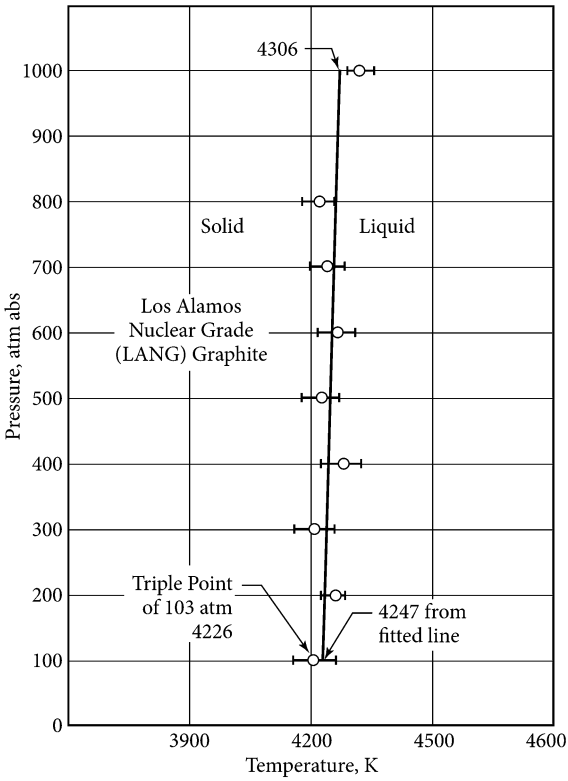

Fig. 3.3 P-T phase diagram for the graphite (grade LANG) up to 1000 bar

carbine (C=C=C) in this phase diagram, from 2600 to 3800 K. The temperature of the triple point of carbon proposed by Whittaker: T = 3800 K, and the pressure P = 0.2 bar. Since the carbine was not the subject of our research, we refer the reader to the survey [2], in which the phase diagram is investigated in detail with Carbine used. To add this issue (relatively fresh) information published in 1999–2004, about getting new forms of carbon (see publications [15–17]).

3.1.3 Detailed Investigations of Carbon Under Laser Heating by Haaland and His Critical Review of Previous Determination of Triple Point Parameters (All the Conclusion Made by Haaland, but not the Author of the Monograph)

Experimental study of the triple point of carbon was made by David Haaland in Sandia National Laboratory, USA, in 1976 [18].

For the annotation of this work Haaland gives following text. "*Continuous 440-watt Nd: YAG laser thermal heater served. The pressure of the triple point was defined as 107 ± 2 atm (10.8 ± 0.2 MPa). To confirm that melting was used, and X-ray diffraction analysis of the recrystallized microstructure of graphite. Experiments were performed by melting carbon in a helium atmosphere, and argon, the specimen size was varied and the density of the laser power to ensure melting under pressure at the triple point of carbon and also prove that only pairs of carbon present on the specimen surface during melting. We measured the maximum rate of mass loss, which proves the insignificance of non-equilibrium pressure deviations. Generated by laser luminous vapor or glowing particles trickle prevented temperature measurement, thus was not allowed to determine the temperature of the triple point of carbon. The density of liquid carbon near the triple point was calculated from the quantitative measurements of the density of voids and solidified melt. This density was determined as 1.37 ± 0.06 g/cm*^{3}."

Details of these experiments were published by Haaland in [19]. Below is the most important material of this publication. No less interesting are reviewed Haaland on research on carbon made earlier than his own experiments.

As pointed out by Haaland, in 1939 Basset [1, 20] performed the first quantitative measurements of pressure at the triple point of carbon and received 102 atm pressure at which the graphite begins to melt.

Next Haaland leads list of publications since 1939, which gave the facts of determination the triple point of carbon. Let us, for clarity, the list in Table 3.1 (without details).

As noted by Haaland, in comments to this table, some researchers have argued (until 1939), they observed that the boiling melt of carbon on the surface of arc electrode during combustion of electric arc at atmospheric air pressure, for example, Otto Lummer in 1914 (*Lummer and Vien suggested in 1995 year a method of creating a completely black-body cavity with a small hole*).

However, more recent experiments by Stanley showed that observation of Otto Lummer—the result of oxidative processes, and they cannot characterize the electric arc burning in an inert environment. The appearance of the droplets after the experiment cannot be characterized as a melt, as they are the result of condensation of steam, said Stanley.

(Note of the author of the monograph: *The more correctly to say "condensation of sublimate" rather than condensation of the vapor, as the reader hearing the word "vapor" imagines that it was obtained from the liquid*).

In this regard, the observation of spherical formations does not always mean that you see a drop of carbon after melting. It's time to mention the work [21], in which spherical carbon formation obtained (Fig. 3.4), as a result of the carbon deposition of the sublimate on the surface of the "whisker" at a temperature of 1,000°. Part of the readers can take them as solidified liquid droplets, although it is a misconception, as the temperature does not rise above 1000°.

In this study pyrocarbon "whiskers" were obtained at a temperature of 900–1000° under vacuum at a residual pressure of 10–40 mm Hg out of benzene vapor without using any diluent gas flow in the reactor with the graphite substrate and a

Table 3.1 The triple point of carbon (data of Haaland)

Authors	Year	Method	Pressurized gas	Pressure (bar)	Temperature (K)
Basset	1939	Heating by current	Ar	102	4000
Steinle	1940	The same	Ar, N_2	100	3670
Jones	1958	The same	Ar	100	3840
Noda	1959	The same	Ar	110–120	4020
Fateeva et al.	1963	The same	Ar	100 ± 10	4650
Fateeva et al.	1969	The same	Ar	100	4040
Schoessow	1967	The same	He	103	4180–4300
Diaconis et al.	1971	Heating by current and the analysis of electrical current image	Ar, N_2	102	4100–4300
Gokcen	1976	HF laser	Ar, Ne, Kr	120 ± 10	4130
Whittaker and Kintner	1975	CO_2 laser	Ar	0.19	3870
Haaland	1975	Nd:YAG laser, 1.06 μm	Ar, He	107 ± 2	–
	Evaluation of the theory				Temperature calculation
JANAF	1961	Extrapolation of vapor pressure		100	5200
Palmer and Shelef	1968	Analysis of the vapor pressure		100	4570
Leider et al.	1973	New heat functions, the heat of formation, the analysis of the vapor pressure		103	4765

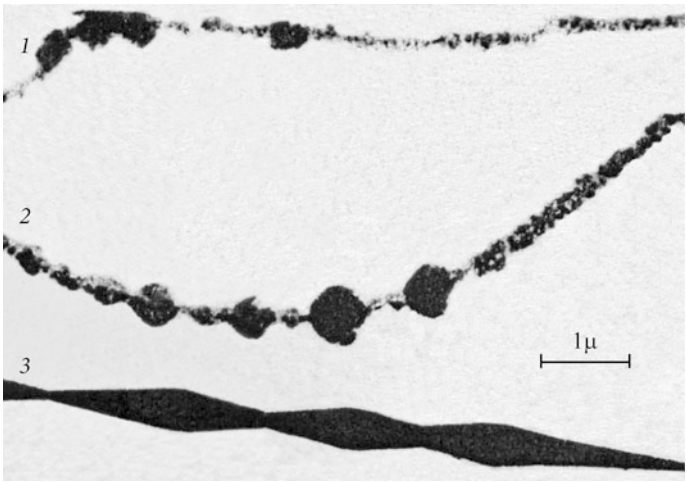

Fig. 3.4 [21]. Different formations of deposits on the central rod of carbon whiskers: *1* deposition of dispersed particles, *2* formation of a shell of dispersed particles, *3* deposition of pyrolytic carbon

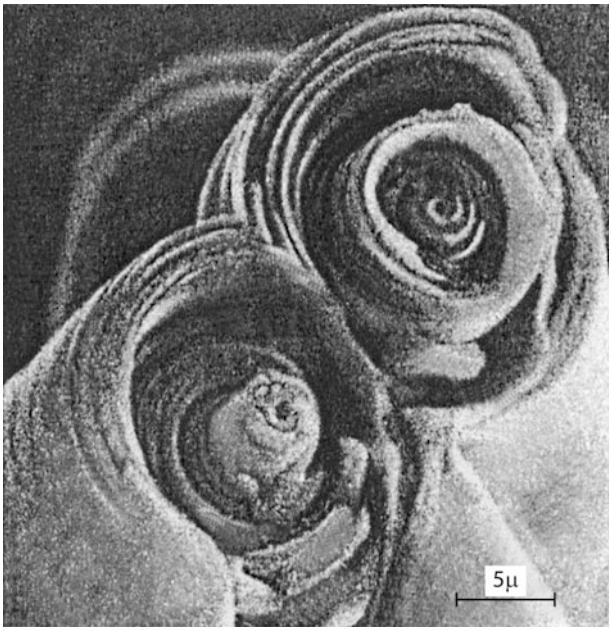

Fig. 3.5 [21]. Carbon whisker breaks with layered deposits of pyrolytic carbon

metal catalyst. Whiskers at the initial time of detection (by using the appropriate optics) have a thickness of 0.1–0.4 μ and consist of a central rod with a diameter of 100–200 Å and the shell. The central rod is a formation with a very high degree of orientation. Directly on the surface of the central rod are shaped aggregates which consist of particles having a size equal to (or slightly larger) diameter of the rod, with the diameter 100–300 Å. Dispersed particles formed a solid shell on the rod in the form of chain made of docked spindle formations. Thickness of whiskers increases with time and reaches 40–100 μ after 30 min. Later, we investigated specimens of such kind (Fig. 3.5), with the average bulk density of 1.8–1.9 g/cm^3, under pulsed heating (see Chap. 4, Figs. 4.13 and 4.14).

We return to the research of Haaland and his remarks.

In 1958, Jones repeated the experiments of Basset and Stanley and got similar results. Optical pyrometer at a wavelength of 0.65 μ showed that the brightness temperature on the surface of not shielded (*apparently meaning the temperature measured through a layer of sublimate, note the author of the monograph*) carbon rod was 3620 K and does not vary with pressure from 1 to 100 atm. An attempt to measure the temperature of the screened (shielded) graphite (in the drilling, that is in the model simulates a blackbody) led to an increase in temperature by 220 K with the changing of a pressure from 1 to 100 atm. In the conclusion, Jones leads the temperature of the triple point of carbon as 3840 K.

In 1976 year Haaland gives the next comments, concerning experiment by Schoessov.

In 1968 Schoessov fulfilled the experiments [13] using perpendicular drilling of the rod (blackbody model). It was shown inextricable difficulties in recording temperature due to convection flows of gas and soot formation near the melting point. Under these conditions, the hole for measuring the temperature, sometimes slaughter soot, preventing accurate temperature measurements near the melting point. Schoessov was forced to begin to extrapolate the input power before reaching the melting temperature, recording power as $P = a_1T^4 + a_2T + a_3$, where a_1, a_2, a_3—constants. This method allowed Schoessov to estimate the melting temperature, by measuring the input power to each specimen. It gave the deletion of some difficulties, but not all. Although the bore have increased emissivity, but the effectiveness of the blackbody model still low due to axial temperature gradients. Besides the very form of the equation for input power does not fully take into account the loss of heat by evaporation (sublimation) under high temperatures near the melting point. Schoessov gives carbon melting temperature from 4180 to 4300 K, depending on the type of graphite used.

In the works of Whittaker [11, 12] the conclusion on melting of carbon have been done on the basis of observation of spherical formations after the experiment (at a pressure of 0.25 atm) and observation of the high-speed color film. In addition, he noticed a small break in the dependence of the vapor pressure of carbon at 0.19 atm, attributing it also to the characteristics of the triple point of carbon. As gently noticed Haaland: "*obvious the interpretation of Whittaker—not the only one that can follow from consideration of his experiences*." After careful analysis of previous works Haaland concludes that the results of the triple point pressure equal to atmospheric pressure in Whittaker's experiments, were misinterpreted by Whittaker.

Add to that problem some of the data of Whittaker published in his work.

Interpretation of the parameters for the triple point of carbon has been declared (but not measured) by Whittaker [11, 12]: for the triple point P = 1 bar, T = 3800 K. The author studied the vapor pressure of the temperature using a pyrometer for temperature measurement, but he gave no details of temperature measurement and calibration. The quality of temperature measurements in [11, 12] may be characterized by the following quotations: "*At 100 bar the optical density of carbon gas would be quite high. Hence, a pyrometer may not be able to "see" the surface of the condensed phase at this pressure. In this case the reported temperatures would have little meaning*") [12, p. 696]. In another publication [22, p. 255], the same author adds: "*The solidification droplets were observed, when temperature reached 3800 K, and more*". Obviously, this approach is not direct measurements of the melting point of graphite.

Unlike Whittaker the work by Haaland features a thorough study of the results of previous experiments, it is significantly different from most other studies in which the authors do not want to take into account and thoroughly analyze the way science has already passed. Haaland used graphite specimens (pyrolytic graphite HOPG by production of Union Carbide) to form a rod of length 12 mm and a diameter from 0.75 to 2.5 mm. The rod was placed vertically in a chamber with high pressure; the

rod axis was the axis "c". The laser heats the narrow drive on the basal plane (*apparently rod rotated about its axis, note the author of the monograph*), that is, from the side of the rod. Heat losses were considered small, since the axis of the "c"—has a low thermal conductivity. Heating spot size ranged from 1/3 to 1/2 the diameter of the rod. It has been found that heating of the rod diameter of 1.5 mm in a helium atmosphere, the heat loss was too large to melt graphite at a pressure of 107 atm. 111 atm pressure required to melt this specimen. Laser heating of other brands of graphite (POCO AXF-Q1 and spectroscopic graphite SPK) is unlikely to give (as noted by Haaland) a positive result on the melting of the specimens in this geometry, as these grades of polycrystalline graphite have much higher thermal conductivity along the axis of the specimen and a high emissivity than graphite grades used by Haaland. For maximum power that could provide the laser in Haaland experiment (80 kW/cm^2), heating the specimen with 1 mm in diameter (POCO AXF-Q1) would require a pressure of 130 atm in argon, and absolutely would not melt when heated in helium at a pressure of 165 atm. Thus, under the available power of the laser, there is a delicate balance between the energy input and heat losses. Only specific properties of used pyrolytic graphite yielded data on the triple point in the experiments of Haaland. The diagram of the experiment by Haaland [19] is shown in Fig. 3.6.

Much attention was paid by Haaland to temperature measurements. He became convinced that the sublimation of the specimen at the approach to the melting temperature plays a crucial (negative) role in the temperature measurements, to which subsequent experimenters often ignored. One of the most successful and specific temperature measurements in [19] is shown in the Fig. 3.7.

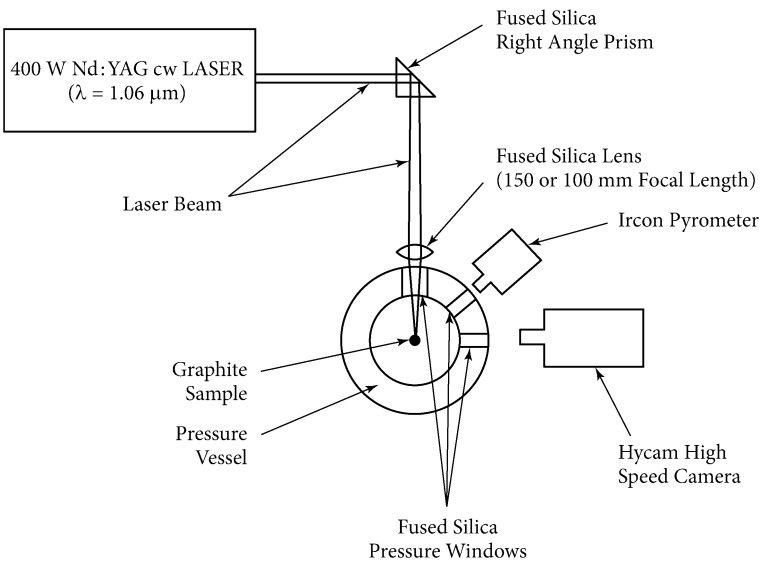

Fig. 3.6 The experimental scheme for laser heating by Haaland [19]

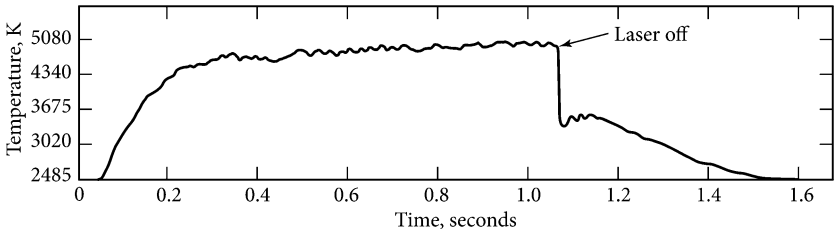

Fig. 3.7 Pyrometer temperature signal as a function of time in the work of Haaland. Moment of switching off the laser marked with an *arrow*

The author notes that the pyrometer output is nonlinear with respect to temperature, and that the pyrometer is insensitive to temperatures below 2500 K. The brightness temperature was recorded, which takes into account the passage of radiation through the window of fused silica. The diameter of pyrolytic graphite specimen was 1.5 mm; heated under argon at 147 atm; laser power 35 kW/sm^2.

Haaland notes that the measured temperature was considerable variation (from 4000 to 5500 K). Temperature does not reflect the state of the surface, but the dense (steam) jets in front of graphite rod under conditions of high pressure. This conclusion is based on several observations.

(1) High-speed photography showed that jets shaded surface of the specimen, and it was proven that it is not the result of exposure (saturation) of the film.
(2) Temperatures measured in argon, were consistently higher than in helium. That is, vapor (or jets consisting of particles) was intensively cooled in helium due to the higher thermal conductivity of helium.
(3) Under turn off the laser heating, the temperature dropped sharply and then weakly growing up to the final diminishes to room temperature (Fig. 3.7). The author explains this picture as follows: steam jets quickly cooled and condensed into soot, which blocks the radiation of the specimen.

Pyrolytic graphite rod was subjected to laser exposure (at a pressure of 147 atm in argon). After the experiment the specimens were polished and examined under polarized light for a detailed study of the structure. At the bottom of the crater there were observed drops of recrystallized melt. The author of [19] indicates signs that the melt was subjected to a substantial contraction during cooling. Heating the graphite at the same laser power, but under a pressure of 105 atm (i.e., at a pressure below triple point) showed no signs of melt recrystallization and the presence of microscopic droplets.

Thus the work of Haaland is an example for all researchers of any scientific problems, not only in the study of graphite. It is necessary careful examine previous studies to avoid repeating mistakes. In particular, in this monograph a lot of attention paid to the previous studies so that the reader had the opportunity to get acquainted with the comparative characteristics of previous studies and was able himself to evaluate the most promising works that have been done recently.

3.2 The Role of the Condensed Graphite Vapor at the Laser Heating

Despite the fact that Vereschagin [23–25] had the conflicting results (pressure is about 100 bar) to the melting temperature of graphite (4650 and 4035 K), he warned about the need to use a solid-state optical fiber for pyrometer measurements at high pressure and at high temperatures. This avoids convection of vapor flow leading to heterogeneous vapor density that prevents reliable temperature measurements [23–25].

In 1981, it was published a detailed review by Sheindlin [2] on the different experimental studies on the heating of the graphite specimens. This review provides evidence about the difficulties of various authors "*... under the measurement of temperatures close to the melting point, due to the emergence of carbon vapor, substantially understates the temperature*" [2, c. 637].

The authors of [26] believe that "*the amount of vapor rises sharply when approaching the sublimation temperature ≥3000 K. The weakening in the layer of condensed vapor of graphite leads to underestimation of brightness temperature, which... increases with increasing temperature*" [26, p. 368].

A stationary laser heating was used in [27, 28] to determine the melting temperature of graphite MPG-6 at a pressure of 223–277 bar. "*The melting point was found at a temperature corresponding to the horizontal section under heating or cooling the specimen ... ... horizontal section can be identified as the level of the liquid phase crystallization*" [27]. This temperature (4000 ± 100 K), the authors [27, 28] consider to be a melting temperature. But there is another point of view on laser heating, supported by the experimental studies. Under slow heating of the graphite in [27, 28] a pyrometer could register glow of condensed vapor but not a glow of solid surface. We will show this point by analyzing the results of the studies [29, 30].

Laser heating has certain peculiarities. The first necessary condition for obtaining reliable experimental data by laser pulse heating—it is uniformity of power dissipation at the spot heating. For example, in [31], a laser was used within 5 % uniformity of its power, that ensure a constancy in heat released in the focal spot with the diameter of 3 mm. Such a laser was also used in [29, 30] when heated surface on the plane "a" for the specimens of graphite HOPG. Both scientific groups give 4750–4800 K as the melting point of graphite.

The second necessary condition for obtaining reliable data for laser heating is to limit the volume above the surface of the graphite specimen with the following purpose:

- To reduce the vapor stream as the vapor (condensing into soot) prevents correct measurements by pyrometer [32];
- To prevent the release of energy in condensing vapor above the surface of the specimen [29, 30];

- To provide a thin transparent layer of vapor [29, 30]; (Vereshchagin [32] advised to use a solid-state fiber for the same purpose).

Restriction of the distance between the specimen and the cover glass has been used, for example, in [52], this distance was 50 mm. Then, [53], it was reduced to 2.3 mm (in order to eliminate the influence of convection flows of hot gas in the chamber).

More stronger limit above the graphite surface (0.15–0.05 mm) was used in [29, 30]. This made it possible to control the laser power allocated in graphite specimens of grade HOPG (initial density 2.26 g/cm^3). The study [29, 30]—this is a unique case of fix the melting temperature plateau under pulsed laser heating of the surface "a" of anisotropic graphite. A surface "a" of highly oriented graphite grade UPV-1TMO was heated by laser pulse of 700 ms in a helium atmosphere (P = 150 bar). The quartz plate was placed above the specimen [30].

In option 1, the distance between the specimen and the quartz plate was 12 mm. In this case, the plateau was fixed at thermogram signal only under the cooling stage at corresponding temperatures 3400–4200 K. To calculate the true temperature an emissivity was assumed to be 0.65, and it did not depend on temperature. It was shown that in the area over the specimen after switching off the laser pulse it was observed a flash glow of condensing vapor cloud. This flash recorded in the form of a temperature plateau, was born not on the specimen surface but at the distance $\sim$1 mm above surface. This fact has been verified by the orientation of the optical axis of the pyrometer along the specimen surface. The temperature of this condensed vapor above the graphite surface was 3400–4200 K, i.e., it is the level of temperature which is called in [33] as a melting point of graphite (3700 K, 4000 K). This experimental fact has forced the authors [29, 30] apply the restriction on the free volume above the surface of the graphite.

In option 2, the distance between the specimen and the quartz plate was 0.05–0.15 mm (the larger gap reduced the results to the first option). This ensured transparency of the thin vapor layer over the surface and the lack of released energy of the laser pulse in the condensing vapor above the surface. In this case, the temperature plateau was reproducibly recorded at the heating stage (T = 4750 ± 150 K), which refers to the melting point of graphite. The traces of melting were not observed at a pressure of P < 100 bar.

A high thermal conductivity along the plane of heating for anisotropic graphite ($\sim$3000–4000 W/m K [34]) helps to equalize the temperature through the spot of heating. To calculate the true temperature the emissivity was assumed to be 0.65, and it was supposed that it is not depend on temperature. In [27, 28, 33] no measures have been taken (or are not reported) to ensure the quality of temperature measurements, such as those that have been taken in [29–31].

In contrast to [29, 30] M.A. Sheindlin and M.V. Brykin with the colleagues [31] show that the laser heating of specimens of the two types of graphite (HOPG and artificial graphite RW1) have different results: liquid carbon has a very high surface tension under poor wettability of basal plane "a" for the pyrolytic graphite HOPG.

According to the authors [31] it is for this reason that a film of liquid carbon removed (disappeared) from the surface "a" during the experiment, which made it impossible to observe the liquid carbon on the surface "a" for the HOPG specimens after the experiment. That's why instead of HOPG graphite in [31] it was used graphite RW1 (initial density 1.55 g/cm^3). For this graphite grade the molten part of a specimen retained on the surface after the experiment [31].

3.3 The Start of Graphite Melting Recorded by the Enthalpy

In the history of graphite melting it was repeatedly recorded the specific energy input corresponding to the beginning of melting. Table 3.2 presents data on the enthalpy and the specific heat capacity of the solid phase graphite before melting and at the melting point obtained by various authors (in chronological order).

Analyzing the studies listed in the Table 3.2, we can conclude that the specific energy input (10.4–10.5 kJ/g) corresponding to the start of melting for graphite—is a firmly established value in experimental studies [34–37, 39]. Taking the average heat capacity for the solid graphite at high temperatures $C_P \sim 3.0$–3.2 J/g K (Table 3.2), and knowing that the enthalpy of 6.3 kJ/g corresponds to 3500 K (or 7.1 kJ/g corresponds to 3800 K, steady state data [38] 1987), it is possible to calculate the melting temperature of graphite for the reliable fixed enthalpy at the beginning of the melting point (10.5 kJ/g).

One can obtain a result in carbon melting temperature 4600–4900 K, but not 3700–4000 K, as was stated in the papers [27, 28, 33], in which there are no own measurements of specific energy input.

3.4 Start of Melting Obtained at Milliseconds Heating

In [39] an experimental dependence of the enthalpy H of pyrolytic graphite (initial density $\sim$2 g/cm^3) against temperature T was obtained up to 4500 K. It was also obtained the dependence of the specific heat C_P up to 4500 K (with the uncertainty better than 5 %). Pyrolytical graphite of the initial density near 2 g/cm^3 was heated by electrical pulse current during 0.5–2 ms. According to Fig. 3.8 the enthalpy at 4500 K is 9.1 kJ/g (with the uncertainty 2.5 %). Temperature was measured with the uncertainty 2 % at T = 4500 K. According to [39]: "*The maximum temperature to which it was able to heat the graphite at a rate of up to 2 × 10^7 K/s, was 4700 K. This value is obtained by measuring temperature in five experiments and sets the lower limit for the melting temperature of graphite*."

Table 3.2 The start of graphite melting recorded by the energy input (H) with corresponding pressure, temperature, and heat capacity (C_P) measurements

No.	Author, year, ref.; method, type of graphite, density	Enthalpy (specific energy input) at the beginning of melting H_{solid}, kJ/g	Corresponding pressure, bar	Melting point, K; Heat capacity Cp
1	Bundy 1963 [34] current pulse (several ms); spectroscopic graphite, 1.6 g/cm^3	**10.45** for pressures 9–31 kbar and 67–97 kbar 12.2 for pressures of 50–60 kbar (H_{solid} determined by the drop of electrical resistance at the beginning of melting)		Not determined
2	Buchnev et al. 1984 [41] steady-state investigation of UPV-1T (2.26 g/cm^3) graphite and glassy carbon	T = 3800 K corresponds to the enthalpy of 7.1 kJ/g	Tmelt = 4890 K (estimated) at 100 bar. The temperature was measured by standard optical pyrometer EOP-66 up to 3818 K in argon at atmospheric pressure. Cp (3800 K) = 2.5 J/g K (measured); Cp (4500 K) = 3.3 J/g K (extrapolation)	
3	Lebedev and Savvatimskiy 1986 [49] current pulse (tens of microseconds); UPV-1T (2.26 g/cm^3) and pyrolytic (density of about 1.9 g/cm^3) graphite	H_{solid} = **10** kJ/g (estimated) Experiments in water, colophony, and in quartz capillary tubes	~1 kbar Uniform heating of graphite of different densities was analysed. For the energy input of 18 kJ/g, the specimen expansion amounted to 68 %	
4	Sheindlin et al. 1988 [39] current pulse (1–2 ms); pyrolytic graphite with a density of about 2 g/cm^3; presumably, UPV-1T graphite, 2.14–2.17 g/cm^3	The temperature of 4500 K corresponds to the enthalpy of 9.1 kJ/g. The pyrometer was focused onto the c-plane of a square anisotropic specimen	Pressure of 1 kbar. At 4700 K, graphite still does not melt (five experiments). The temperature dependence of enthalpy (error of 2.5 %) was obtained. Cp = 3.1 J/g K (for 4500 K) 52, 38 [50, 51]	
5	Baitin et al. 1990 [35] current pulse (2 ms); UPV-1TMO graphite (density of 2.26 g/cm^3)	H_{solid} = **10.4** kJ/g The beginning of the temperature plateau of melting was recorded (on the a-plane)	1–2 kbar →	5080 ± 70 K (measured for the supposed emissivity of liquid graphite 0.6)
6	Korobenko et al. 1998 [42] and Korobenko et al. 1999 [36] current pulse (1.5 μs); UPV-1T graphite	H_{solid} = 12 kJ/g (inaccurate value), recorded by pyrometer on the a-plane at a pressure of about 1 kbar		5000 ± 500 K; Cp (solid) = 3.2 J/g K; Cp (liquid) ~4 J/g K (measured) at 5000–10,000 K
		H_{solid} = **10.5** kJ/g. The melting plateau recorded by pyrometer on the c-plane at a high pressure (tens of kbar)		

(continued)

Table 3.2 (continued)

No.	Author, year, ref.; method, type of graphite, density	Enthalpy (specific energy input) at the beginning of melting H_{solid}, kJ/g	Corresponding pressure, bar	Melting point, K; Heat capacity Cp
7	Kerley and Chhabildas 2001 [50] the equation of state for graphite is constructed from 0–10^8 K	9 kJ/g (the estimation obtained in simulating of different experiments)	Pressure at the triple point, 170 bar (estimation)	Temperature at the triple point, 4660 K (estimation)
8	Korobenko [37] current pulse (1.5 μs); UPV-1T graphite	(a) **10.5** kJ/g The melting plateau recorded by pyrometer on the a-plane at a pressure of about 1 kbar (a correction was introduced because of the cooling of the surface layer under conditions of close contact with glass)		Heat capacity (liquid) = 4.2 J/g K (measured)
		(b) A melting design of graphite blackbody → with calibration against the melting of a model of tungsten blackbody at 3690 K (embedded in resin)		T_{melt} = 4800 ± 200 K (measured)

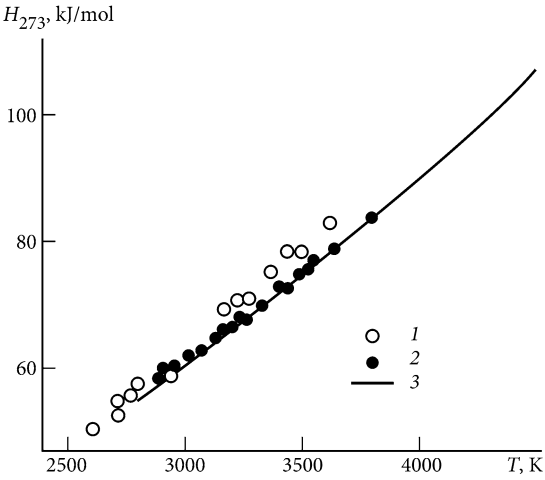

Fig. 3.8 [39] (1988). Enthalpy of pyrolytic graphite with high initial density depending on the temperature. *1*—[40]; *2*—[41]—both stationary measurements; *3*—[39]—pulse milliseconds measurements

One can see in Fig. 3.8 that heat capacity as derivate dH/dT is positive and grows near the temperature 4500 K.

Note that the calculations in [35] gives the enthalpy 9.2 kJ/g at 4500 K. We emphasize that in both studies [35, 39] it was obtained the increasing of the heat capacity with increasing temperature for solid graphite.

The time of pulsed current heating in [39] equals 0.5–2 ms at a pressure of 100 MPa in a gas atmosphere (Ar, He). Enthalpy measurement error—less than 2.5 % at a temperature of 4500 K. The error for the temperature measurement equals 2 %. Temperature 4500 K at the corresponding enthalpy of 4.1 kJ/g was used by some researchers as a calibration point of energy input to determine the temperature scale. In these calculations it was obtained: Cp = 2.8 J/g K for 4200 K; Cp = 3.08 J/g K for T = 4500 K. The error of the calculation for the heat capacity Cp equals 5 %, at a temperature of about 4500 K. Under the heating rate 2×10^7 K/s [39] it was obtained a maximum temperature of 4700 K. This value was obtained for the five experiments and sets (according to the authors [39]) lower limit melting point of graphite.

In the experimental work [35] it was received the maximum melting temperature of graphite for all considered pulsed experiments under milliseconds pulse heating. But the heating rate was slow enough to see the complete melting (Fig. 3.9).

The authors [35] suggested that the maximum temperature in the thermogram (near the point A in Fig. 3.9) is not a melting point and they extrapolated the curve 1 to the line 3 (perhaps, relying on the known value of enthalpy at melting). In our opinion, this procedure led to an overestimation of the melting temperature in [35]: 5080 K. It is possible to get a reliable and lower temperature in Fig. 3.9, if one considers a steady temperature plateau at higher enthalpy value to be a melting point (curve 2). This will give the temperature of 4860 K, which seems more likely.

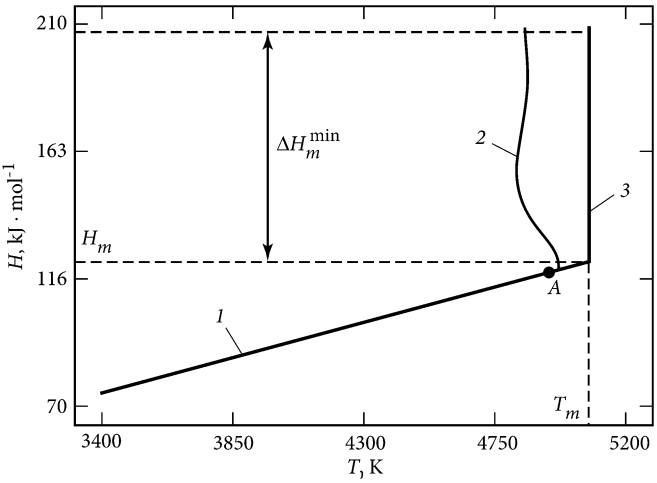

Fig. 3.9 [35] (1990). The dependence of the enthalpy H (kJ/mol) versus temperature near the melting point of graphite. *1*—heating of solid graphite; *2*—heating of the two-phase region; *3*—melting temperature under the assumption of the authors [35], which equals 5080 ± 80 K; *Hm*—the enthalpy for the onset of melting; *ΔHm*—the minimum enthalpy is going to melt graphite

For this case maximum pyrometer signal at the beginning part of the plateau can be attributed to a change in emissivity of the surface of graphite at the start of melting. A similar effect (pyrometer signal drop after the onset of melting) is known for refractory metals under pulsed heating (Nb, Re, W). It has been observed by us as well as by Ared Cezairliyan (USA). Explanation for the metals is that the alignment of roughness on the surface under melting of metals requires a certain (albeit short) time. Vanishing roughness is the cause of falling signal pyrometer (emissivity) at the beginning of melting. These reasons cannot be excluded for graphite at the start of melting at the certain velocity of heating.

Note that the dependence of the enthalpy H (T) graphite temperature for the solid state is linear, as shown in Fig. 3.9 (curve 1), whereas the same dependence [39] (Fig. 3.8) (published by the same leading researchers M. Sheindlin and V. Senchenko) —nonlinear. According to Fig. 3.8 the nonlinearity H (T) gives the heat capacity Cp increasing with increasing temperature T, which was observed in our experimental studies on graphite under fast pulsed heating [36, 42], as well as for stationary measurements [38]. Perhaps the fact that the graphite of different brands (and even different specimens) with different number of internal defects will respond differently to the pulse heating: specimens with a large number of defects will show a larger heat capacity.

In the laboratory of electro-explosion processes (JIHT RAS, Moscow) V.N. Korobenko managed to hold direct temperature measurement of melting point of graphite for pressures above 1 kbar. It was obtained melting temperature (Tm = 4800 ± 200 K for graphite UPV1-T). The radiation was recorded from the flat surface of graphite as well as from the blackbody model design. At the same time this temperature value corresponds to the measured enthalpy at the start of the melting (10.5 kJ/g). This enthalpy value coincides with the data of other authors for a slower pulse electrical heating.

3.5 Temperature at the Melting Point Obtained in the Experiments with the Different Velocity of Heating

Since 1963, among 10 research centers from different countries, only in two (Whittaker [11, 12, 22, 33]) it was obtained the lowest melting temperature of graphite 3700–4000 K. Excluding work of Vereschagin [32] as uncertain for its dual result (4040 and 4650 K). In most other reasonably it were represented 4530–5080 K.

The authors of the study [33] considered only some of the works on the melting temperature measurement of the graphite (5 references show numerical values, including estimates, only 3 values are direct measurements). For the minimum melting temperature (4035 K) specified in [33, Table 1], literary references refer to 1939–1971 years. And for some references the primary experimental data belong to

an even earlier time. In most of these studies [33] carbon sublimation before melting usually not taken into account. In [33] it is claimed that the melting temperature of graphite depends on the heating time: the shorter heating time—the higher the temperature is fixed. Such a conclusion cannot be considered reasonable by analyzing a wider range of experimental data of the recent years. For example, in Table 3.3 below there are presented data for several experimental studies of 1981–2003 years (about 8 numeric values are considered). The melting point of graphite

Table 3.3 Melting point of graphite (depending on the time of heating and heating rate

	Heating time	Heating rate (K/s)	Melting temperature T, K, method	Pressure P (bar)	References
1	10 s	$5 \cdot 10^2$	**5000 ± 200** laser	100	[52, 53]
2	Several seconds	$1 \cdot 10^3$	**4650** (1963 year)	100 (in gas, using a solid-state light guide);	[32]
			4040 (1968 year) current	100 (with the specimen embedded in NaCl);	
3	20–30 ms	$1.6 \cdot 10^5$	**4800 ± 150** laser	110–2500 bar[a]	[31]
4	15 ms	$3 \cdot 10^5$	**4530 ± 150** current; emissivity of 0.8	140–200[b]	[54]
5	1–3 ms	10^6–$2 \cdot 10^7$	**4700 ± 80** current	500–2200[c] (gas pressure)	[26]
6	2 ms	$2.3 \cdot 10^6$	**>4700** current	1000	[39]
7	1.7 ms	$3 \cdot 10^6$	**5080 ± 70** current; emissivity equals 0.6	1000–2000	[35]
8	0.7 ms	$6.8 \cdot 10^6$	**4750 ± 150** laser; emissivity equals 0.64	150	[29]
9	0.2 ms	$3 \cdot 10^7$	**4800 ± 100** laser; emissivity equals 0.65 from 2750 up to 4800 K	150	[30]
10	~20 μs	$2.4 \cdot 10^8$	**4900 ± 200** current	3000	[55]
11	1 μs	$4.8 \cdot 10^9$	**4800 ± 200** current	Melting of a blackbody design, P ≥ 1000	[37]
12	8 ns × 1000 (averaged over 1000 pulses)	$\geq 4.8 \cdot 10^9$	**(4765–5000) ± 200** laser	The sum of measured values of partial pressure (C_1–C_7) gives ~100 bar at 4979 K	[43]

[a]According to [31], the change in pressure from 110 to 2500 bar did not affect the measured value of the melting temperature

[b]The oxygen in the pressure chamber (for the transfer graphite vapor to optically transparent gas CO and CO_2) led to an increase in the measured temperature (oxygen partial pressure of 40 bar gives rise to 80 K)

[c]According to [26], the change in pressure from 500 to 2200 bar did not affect the measured melting point

(depending on the time of heating and heating rate) showing the heating method (by current or by laser) are presented in Table 3.3.

L.F. Vereschagin experimental data [32] (number 2 in Table 3.3) is contradictory, since in fact one and the same measurement method by optical pyrometer gives different results. We draw attention to the fact that the use of solid fiber in [32], is resulted in a higher temperature of recording, as it allows to avoid temperature understating at the expense of streams of coagulating vapor occurring during sublimation of solid graphite.

Data marked with numbers 1 and 12 in Table 3.3, were obtained through changing the slope of the dependence of saturation pressure against temperature. These two results have the same method of assessment and have almost the same result (4765–5000 K), but the heating rate varies $\sim 10^7$ times. Vapor pressure of high density polycrystalline graphite at temperatures of 4100–7100 K was measured in [43] (item 12 in Table 3.3), using the mass-spectrometric method with a time resolution. The quadruple mass spectrometer was set to 56 cm from the specimen. Nd: YAG high-power laser was used (8 ns, 532 nm).

The result on the composition of the vapor molecules (from C1 to C7) is averaged for 1000 laser pulses. Measurements (the total pressure for vapor temperature) showed a change in the slope, indicating the presence of a phase transition solid–liquid near the temperatures 4765–5000 K. Temperature measurement has an error ±200 K [43]. For temperature 4979 K it was obtained: C1 (the partial pressure of P = 41.29 bar); C2 (P = 9.36 bar); C3 (P = 49.4 bar); C5 (P = 0.23 bar); C7 (P = 0.146 bar). Thus, in [43], by the independent measurements it was obtained graphite melting point and the corresponding vapor pressure of graphite (about 100 bar).

Others are listed in Table 4.2 data can be regarded as direct temperature measurements. The depending of the melting temperature against heating time is not observed. I.I. Klimovsky (Institute for High Temperatures RAS, Moscow) drew attention to the possible dependence of the melting temperature of graphite is not on the time interval, but on the heating rate. Such dependence may be obtained on the data of Table 3.3, but it also does not show the dependence of the melting temperature on the heating rate (in the considered range of heating speeds), despite the fact that the latter varies by at least 4 orders of magnitude.

As a result, there are two sets of measurements: fast heating to give a melting temperature of 4530–5080 K, and a low heating rate (the excluding the effect of sublimation; time of heating equals a minute or more), which gives 3,700 or 4,000 K. The difference between these two groups is related to various capabilities of the temperature measurements on the graphite surface, which begin to sublime even in the solid phase at a low ambient pressure.

In the case of graphite investigation the fast heating is preferable as the specimen is at high temperature only a short period of time, which minimizes the amount of sublimated graphite. One can imagine that the slower heating, the greater the amount of carbon vapor (and, consequently, the condensate) is formed before the optical path of the pyrometer. This may underestimate the measured temperature, which could happen in [27, 28, 33]. Under heating in a graphite container of large

volume, we may measure the surface temperature by the pyrometer (calibrated in a steady state conditions) and obtain underestimated temperature.

Practically graphite melting temperature measurement depends exclusively on the experimental conditions, in particular on the presence of condensed vapor, which affects recording pyrometer temperature not equipped with a solid state optical light guide.

It should be noted that for solid carbon at high temperatures it is better to use the word "sublimate" instead of the word "vapor" because in the last case a reader think that vapor comes from a liquid (as it will be for usual liquids). And further, we usually used the word "condensation" for appearing a liquid from the vapor, but for "condensation" of a sublime the result should be a solid state (not a liquid). Therefore for sublime the "condensation" should be as coagulation, which leads to appearing a soot.

In other words the graphite specimens (which sublime at a temperature below the triple point) graphite vapor (that was obtained by sublimation of the solid body), is "condensed" according to the type of vapor-solid transition, instead of the vapor-liquid-solid.

3.6 Temperature of the Triple Point Under Steady State Laser Heating

In 1982 it was published the work by Evseev et al. [44] "Study of the phase diagram of carbon in a wide range of pressures using laser heating". The aim was to investigate the equilibrium curve of the liquid and vapor phase of carbon. Stationary laser heating was used (Nd-YAG laser at a wavelength of 1.06 μ) in a chamber with high gas pressure (up to 400 bar). Heating of the samples was carried out from below; during the heating a crater was appeared with the diameter 1.5–2.5 mm. The heat flux density was 10 kW/cm^2 at the specimen surface. The specimens were made of spectrographic and pyrographite. Brightness pyrometer was used (wavelengths of 530 and 650 nm) for temperature measurement. It was calibrated through tungsten lamp (to 2400 K) and by graphite blackbody model up to 3500 K. Experimental results showed that within the error of the temperature measurements (200 K at 5000 K), the temperature of the crater does not depend on the type of buffer gas (He, Ne, Ar), nor from the heating mode (constant power or linear rise of the power during 8 s), or the value formed by the crater. Conclusion the authors of [44] is that the surface temperature of the crater equals to the temperature of the phase transition at a pressure equals to the pressure of a buffer gas. The temperature of the crater at a pressure of 100 bar, (equaled to the pressure at the triple point), is mentioned in the work as 4900 ± 200 K. Judging by the literary reference in [44] to Bassett, Schoessow, Gokcen, the authors of [44] took the pressure at the triple point equaled to 100 bar—according to the literature data. By the way on the thermogram, published in [44], there was not fixed region of melting (temperature plateau).

In 1985 there was published an article by A.V. Kirillin with the colleagues [45], an experimental study fulfilled also at the Institute for High Temperatures (JIHT RAS). It was published the results of stationary laser heating to investigate carbon vapor pressure in the temperature range 5000–7000 K. It was clarified the parameters of the triple point of graphite-liquid-vapor: the pressure P = 102 bar and the temperature T = 5000 ± 200 K were obtained. It was measured the heat of vaporization for liquid carbon (30 ± 2 kJ/g). Two types of graphite were used: pyro-graphite in the form of rod as obtained by carbon sedimentation on graphite fiber from the gas phase (the highest thermal conductivity along the axis) and fine-grained graphite B-1. Heating of the graphite carried out under an inert gas (He, Ne, Ar). The authors of [45] note that the density of the gas amounts to 1 g/cm^3 at high pressure used, so the scattering of the laser beam on the optical heterogeneities associated with density gradients, was essential. Laser beam was focused (from the bottom) on the surface of the specimen, spot diameter of 1–1.5 mm. Such a position of the specimen reduced the negative influence of convective flows. The brightness pyrometer was calibrated on a temperature lamp to 2400 K and on graphite blackbody model to 3500 K. Extrapolation to higher temperatures was made using Wien's law. The correction for the transition from Wien to Planck was made by calculation. After measuring the vapor pressure of carbon the authors [45] obtained an equation of the relationship of vapor pressure with temperature. When substituting into this equation the average value of the triple point pressure (102 bar), it was obtained the temperature of the triple point T = 5000 ± 200 K. The authors of [45] also note that the reliably fusion traces (by brilliant sites in electronic micro-photos of a crater) managed to be found with pressure over 150 bars. A reference is shown in [45] to the previous work of 1982 year [44] giving a result of the temperature at the triple point for carbon as 4900 ± 200 K (P = 100 bar).

It should be mentioned that temperature at the triple point in [44] and in [45] is not a result of direct measurements.

3.7 The Result of the Discussion on the Triple Point Parameters

During several 10 years non-stationary methods of research intensively have been developed (rapid heating by laser or electric pulse), first for the study of metals and then graphite. The main problem remains the measuring a true temperature of the specimen. There is evidence that for pure metals the fast heating (up to fractions of a microsecond) allows to obtain the equilibrium thermophysical properties (enthalpy at the beginning of the melting and heat of fusion), and melting temperature also [46]. Under heating graphite there are more additional significant features related to: its complex structure (anisotropy), sublimation in the solid phase, the density dependence of the manufacturing process, the initial

heterogeneity of a structure, etc. These features affect the measurement of the graphite temperature, especially near the melting point.

After 1963, the numerous studies have been performed with graphite recording high melting temperature of graphite (4530–5080 K). The stable set value of the pressure at the triple point it is called more than 100 bar. A new interpretation of the parameters of the triple point of carbon has been declared (but not measured) by A. G. Whittaker in 1978 [11, 12]: at the triple point P = 1 bar, T = 3800 K. Whittaker investigated the vapor pressure on the temperature using a pyrometer for temperature measurements, but he did not give no details of the temperature measurement and calibration. The following quotes can characterize the quality of temperature measurements in [11, 12] by the author himself: "*At 100 bar the optical density of carbon gas would be quite high. Hence, a pyrometer may not be able to "see" the surface of the condensed phase at this pressure. In this case the reported temperatures would have little meaning*" [12, p. 696]. In another article, the same author adds: "*The solidificated droplets were observed, when temperature reached 3800 K, and more*". Obviously, this approach is not direct measurements of the graphite melting temperature. Unfortunately, many authors of the estimated work (without its own thorough analysis of the results of different experiments) took the publication of Whittaker and Asinovskii as reliable sources of information about the parameters of the triple point (the temperature below 4000 K and the pressure is near 1 atm).

After 1963, the numerous studies have been performed with graphite recording high melting temperature of graphite (4530–5080 K).

As a result the review of the main experimental data on the parameters of the carbon triple point, that was shown in this chapter, with a high degree of confidence can say that the pressure P equals 107–110 bar, temperature T = 4800–4900 K. All the experiments, which published a melting point lower than (or equal to) 4200 K, are not reliable, as it does not take into account the influence of active sublimation of carbon on temperature measurements. All the publications, which postulated the pressure at the triple point closed to atmospheric, do not have reliable evidence of the appearance of the liquid phase.

In 1996, Bundy et al. [8] presented a new phase diagram for carbon with its melting temperature of 5000 K, the most likely temperature of the triple point of measurement in recent years. Review [8], mainly devoted to the phase transitions of graphite at high pressures, and particularly in the diamond phases at pressure P = 100 kbar to pressures in excess of 1 Mbar. It was shown a new phase diagram for carbon, where the authors [8] gives "*5000 K as being the most probable value for the temperature at the triple point*" [8, p. 144]. The melting point of 5000 K was taken from [35], besides in [8] it was noted that for temperature values in other studies, (where only the enthalpy was measured, for example, in [47]), the data [39] of 1988 year was used on the dependence of the enthalpy on temperature (up to 4500 K). With regard to the maximum temperature attainable on the boundary melting curve graphite-liquid (on the level 50 kbar), the authors [8] preferred study [47] (5200 K), as this study was performed using more perfect equipment. The parameters of the critical point of carbon [8] estimated as 6800 K at 2 kbar.

In [8] it was noted that the condensation of carbon vapor to graphite or to diamond—has equivalent probability. By controlling the condensation conditions, a metastable diamond can be obtained at low pressures. The presence of organic molecules is of importance for the condensation of carbon vapor to the diamond, and it has found practical application in the preparation of the diamond coatings from the plasma phase.

3.8 Give the Experimental Facts on Carbon (Just Near the Melting Point)

1. At the pressures below 107–110 bar (triple point pressure of carbon) graphite begins active sublimation from the surface at a temperature of 3000 K and higher, which leads to appearing soot around the specimen. For slow heating process even calibrated pyrometer will underestimate the temperature.
2. It should be recognized that finally established: to melt graphite requires pressure of at least 107–110 bar. If graphite is heated at a lower pressure, at the energy input near ~10 kJ/g, there is a "volume sublimation"—graphite expands throughout the volume and resistivity sharply increases.
3. The melting temperature of graphite in the form of a dense form (~2.2 g/cm^3): 4800 ± 100 K; calculated melting temperature for graphene (alone layer)—4900 K. Under melting graphite its initial volume increases in ≈2 times (~70 % only during melting).
4. At not very high pressures (up to several kbar) the melting input energy at the beginning of melting E ~ 10.5 kJ/g; the heat of fusion ~10 kJ/g; the energy input for the liquid phase (at melting) ~20.5 kJ/g.
5. If a current pulse to heat loose graphite of low initial density ~1.8 g/cm^3 (even at pressures above 107–110 bar), at a high temperature of about 3400 K (even in the solid phase!) graphite is compressed to a higher density.

References

1. M.J. Basset, Fusion of graphite under pressure of argon of 1 to 11500 bar: determination of the triple point and the establishment of a provisional diagram for the solid, liquid and gaseous states of carbon. J. Phys. Radium **10**, 217 (1939)
2. M.A. Sheindlin, The phase diagram of carbon at high temperatures. High Temp. **19**(3), 467–488 (1981)
3. F.P. Bundy, Melting of graphite at very high pressure. J. Chem. Phys **38**, 618–630 (1963)
4. T. Noda, in *Proceedings of an International Symposium on High Temperature Technology*, Asilomar, California, 6–9 October 1959 (McGrow-Hill Book Company, Inc., New York, 1960)
5. N.S. Rasor, J.D. McClelland, Thermal properties of Graphite, Molybdenum and Tantalum to their destruction temperature. Phys. Chem. Solids **15**, 17–26 (1960). Pergamon Press

6. N.A. Gokcen, E.T. Chang, T.M. Poston, D.I. Spencer, Determination of graphite-liquid-vapor triple point by laser heating. High temperature Sci. **8**, 81 (1976)
7. A. Ferraz, N.H. March, Phys. Chem. Liq. **8**, 289 (1979)
8. F.P. Bundy, W.A. Basset, M.S. Weathers, R.J. Hemley, H.K. Mao, A.F. Goncharov, Review article the pressure-temperature phase and transformation diagram for carbon; updated through 1994. Carbon **34**(2), 141–153 (1996)
9. K. Whittaker, R. Nelson, With laser heating system for the study of the properties of materials at high temperatures in a wide range of pressures. Res. Instrum. **6**, 52 (1977)
10. A.G. Whittaker, P.L. Kintner, Comments on the solid-liquid-vapor triple point of carbon. High. Temp. Sci. **9**(1), 71 (1977)
11. A.G. Whittaker, Carbon: a new view of its high-temperature behavior. Science **200**, 763–764 (1978)
12. A.G. Whittaker, The controversial carbon solid-liquid-vapour triple point. Nature **276**, 695–696 (1978)
13. G.J. Schoessov, Graphite triple point and solidus-liquidus interface experimentally determined up to 1000 atm. Phys. Rev. Lett. **21**(11), 738–741 (1968)
14. O.P. Watts, C.E. Mendenhall, On the fusion of carbon. Phys. Rev. (Series 1) **33**, 65–69 (1981)
15. V.D. Blank, B.A. Kulnitskiy, Ye.V. Tatyanin, O.M. Zhigalina, A new phase of carbon. Carbon **37**, 549–554 (1999)
16. G.K. Moiseev, N.A. Vatolin, Assessment of thermodynamic properties of a number of condensed carbon compounds. J. Phys. Chem. **76**(3), 424–428 (2002). (in Russian)
17. Yu.M. Korolev, New forms of crystalline carbon. Doklady **394**(1), 36–39 (2004). (in Russian)
18. D.M. Haaland, Graphite-liquid-vapor triple point pressure and the density of liquid carbon. Carbon **14**(6), 357–361 (1976)
19. D.M. Haaland, Determination of the solid-liquid-vapor triple point pressure of carbon. Report SAND 76-0074, pp. 1–48 (1976)
20. J. Basset, The fusion of graphite under a very high pressure of argon up to 4000 kg/cm^2. Comptes Rendus **208**, 267 (1939)
21. A.S. Fialkov, N.M. Sidorov, B.N. Smirnov, B.I. Dyuzhikov, Features of the structure and growth of filamentous structure of pyrocarbon. Doklady **211**(1), 158–161 (1973). (in Russian)
22. A.G. Whittaker, P.L. Kintner, Carbon solid-liquid-vapor triple point and the behavior of superheated liquid carbon. Contract # F04701-4-0075 US Air Force Space and Missile System Organization (SAMSO), pp. 45–47 (1975)
23. N.S. Fateeva, L.F. Vereshchagin, V.S. Kolotygin, Optical method for measuring the melting temperature of graphite up to 3 kbar. Doklady USSR **152**(1), 88 (1963). (in Russian)
24. L.F. Vereshchagin, N.S. Fateeva, Melting curves of graphite, tungsten and platinum up to 60 kbar. JETP **28**(4), 597–600 (1969)
25. N.S. Fateeva, L.F. Vereshchagin, On the graphite melting curve to 90 kbar. JETP Lett. **13**(3), 110–111 (1971)
26. V.N. Senchenko, M.A. Sheindlin, Experimental investigation of caloric properties for tungsten and graphite in the vicinity of their melting point. High Temp. **25**(3), 364–368 (1987)
27. E.I. Asinovsky, A.V. Kirillin, A.V. Kostanovskii, The phase diagram of carbon in the neighboroughood of the solid- liquid-vapor triple point. High Temp. **35**(5), 704–709 (1997)
28. E.I. Asinovsky, A.V. Kirillin, A.V. Kostanovskii, V.E. Fortov, On the parameters of carbon melting. High Temp. **36**(5), 716–721 (1998)
29. A.Yu. Basharin, V.E. Fortov, Parameters of the triple point of graphite, in *Abstracts of the 14th Symposium on Thermophysical Properties*, (June 25-30 2000, Boulder, USA). Compiled and edited by Haynes W.M. and Stevenson B.A., National Institute of Standards and Technology (NIST), p. 159 (2000)
30. A.Yu. Basharin, M.V. Brykin, M. Marin, I.S. Pakhomov, S.F. Sitnikov, Ways to improve the measurement accuracy in the experimental determination of the melting temperature of graphite. High Temp. **42**(1), 60–67 (2004)

31. M. Musella, C. Ronchi, M. Brykin, M. Sheindlin, The molten state of graphite: an experimental study. J. of Applied Physics **84**(5), 2530–2537 (1998)
32. L.F. Vereshchagin, Solid state at a high pressure. Nauka, 286 (1981). (in Russian)
33. E.I. Asinovsky, A.V. Kirillin, A.V. Kostanovskii, Experimental investigation of the thermal properties of carbon at high temperatures and moderate pressures. Phys. Uspekhi **45**, 869–882 (2002)
34. F.P. Bundy, R.H. Wentorf, Direct transformation of hexagonal Boron Nitride to denser forms. J. Chem. Phys. **38**(1733815), 6 (1963)
35. A.V. Baitin, A.A. Lebedev, S.V. Romanenko, V.N. Senchenko, M.A. Sheindlin, The melting point and optical properties of solid and liquid carbon at pressures up to 2 kbar. High Temp. - High Press. **21**, 157–170 (1990)
36. V.N. Korobenko, A.I. Savvatimski, R. Cheret, Graphite melting and properties of liquid carbon. Int. J. Thermophys. **20**(4), 1247–1256 (1999)
37. V.N. Korobenko, PhD dissertation for the degree of candidate of physical and mathematical sciences, in *Experimental Study of the Properties of Liquid Metals and Carbon at High Temperatures* (Moscow: Institute for High Temperatures RAS, 2001). (in Russian)
38. L.M. Buchnev, A.I. Smyslov, I.A. Dmitriev, A.F. Kuteinikov, V.I. Kostikov, Experimental study of the enthalpy of kuazi-moncrystal graphite and glassy carbon in the temperature range 300-3800 K. High Temp. **25**(6), 816–821 (1987)
39. M.A. Sheindlin, V.N. Senchenko, Experimental study of the thermodynamic properties of graphite near the melting point, Sov. Phys. Dokl. **33**, 142–145 (1988)
40. A.E. Sheindlin, I.S. Belevich, I.G. Kozhevnikov, Teplofizika Vysokikh Temp. **10**(5), 997–1001 (1972). (in Russian)
41. L.M. Buchnev, A.I. Smyslov, I.A. Dmitriev, et al., Doklady **278**(5), 1109 (1984)
42. V.N. Korobenko, A.I. Savvatimskiy, Electrical resistivity of liquid carbon. High Temp. **36**(5), 700–707 (1998)
43. M. Joseph, N. Sivakumar, P. Manoravi, High temperature vapour pressure studies on graphite using laser pulse heating. Carbon (Letters to the Editor) **40**(11), 2021–2040 (2002)
44. V.N. Evseev, A.V. Kirillin, M.A. Sheindlin, Investigation of carbon phase diagram in the wide range of pressure with laser heating used. Ind. Heat Eng. **4**(3), 87–91 (1982). (in Russian)
45. A.V. Kirillin, M.D. Kovalenko, M.A. Sheindlin, V.S. Zhivopiscev, Experimental study of carbon vapor pressure in the temperature range 5000-7000 K using a stationary laser heating. High Temp. **23**(4), 557–563 (1985)
46. S.V. Onufriev, A.I. Savvatimskiy, A.M. Kondratyev, Tantalum melting temperature under fast (microseconds) heating: overheating is not found. High Temp.-High Press. **43**(2–3), 217 (2014)
47. M. Togaya, Pressure dependences of the melting temperature of graphite and the electrical resistivity of liquid carbon. Phys. Rev. Lett. **79**(13), 2474–2477 (1997)
48. F.P. Bundy, The P, T phase and reaction diagram for elemental carbon, 1979. J. Geophys. Res. **85**(B12), 6930–6936 (1980)
49. S.V. Lebedev, A.I. Savvatimskiy, The electrical resistivity of graphite in a wide range of condensed state. High Temp. **24**(5), 671–678 (1986)
50. G.I. Kerley, L. Chhabildas, Multicomponent-Multiphase Equation of State for Carbon, in *Sandia Report: SAND2001-619*, USA, Sandia National Laboratories, pp. 1–50 (2001)
51. L.M. Buchnev, Volga VI Dimov BK, Markelov NV Investigation of the enthalpy of the carbons in the range 500–3250 K. High Temp. **11**(6), 1198–1202 (1973). (in Russian)
52. A.V. Kirillin, S.P. Malyshenko, M.A. Sheindlin, V.N. Evseev, Study of phase transformations of condensed phase—carbon gas in the vicinity of the triple point of graphite-liquid-vapor under pressure up to 400 bar. Doklady **257**(6), 1356–1359 (1981). (in Russian)
53. A.V. Kirillin, M.D. Kovalenko, S.V. Romanenko, L.M. Heifetz, M.A. Sheindlin, Apparatus and methods for examining the properties of refractory substances at high temperatures and pressures by stationary laser heating. High Temp. **24**(2), 286–290 (1986)

54. A. Cezairliyan, P. Miiller, Measurement of the radiance temperature (at 655 nm) of melting graphite near its triple point by a pulse-heating technique. Int. J. Thermophys. **11**(4), 643–651 (1990)
55. G. Pottlacher, R.S. Hixon, S. Melnitzky, E. Kaschnitz, M.A. Winkler, H. Jager, Thermophysical properties of POCO AXF-5Q graphite up to melting. Thermochimica Acta **218**, 183–193 (1993)

Chapter 4
Resistivity up to Melting and the Recording of Melting Area

Abstract Clue experimental data (starting with 1963 year, and up to 1996) by Francis Bundy (USA) are discussed in detail (under heating graphite by milliseconds electrical current pulse). Francis Bundy was the first who obtain imparted energy and resistivity of carbon near melting point. Bundy—may be the first who has been constructed phase diagram for carbon simultaneously with his experimental activity during many years. In spite of the fact that Bundy did not measure temperature, a thorough analysis of the experimental data (resistivity and enthalpy at different pressures, up to 100 kbar) gives him an advantage before other investigators. Experimental investigation of graphite at high temperatures under heating by pulse of electrical current within microseconds time interval actively started at the Institute for High Temperatures (IVTAN) in 1972, in Moscow, in the group headed by S.V. Lebedev (the pioneer of electrical explosion method). Specimens were made of isotropic graphite of low initial density, and of anisotropic pyrolytical graphite UPV-1T (like HOPG) of the high density. At the initial stage only resistivity and input energy were measured, but restricted volume around the specimen was used that gives a possibility to investigate heated graphite at high pressure. This method gives the estimation of the start of melting (in kJ/g units) and the heat of graphite melting (10 kJ/g) was obtained long before obtaining nearly the same value (10.5 kJ/g) under the temperature measurements. Next experiments of milliseconds heating by electrical current by M. Sheindlin with co-workers (Joint Institute for High Temperatures) are discussed. A special high-pressure chamber and fast pyrometer were used that give a start of graphite melting at $\sim$ 5000 K at elevated pressure. It was obtained the dependence of emissivity for anisotropic graphite UPV1-TMO against temperature. The total error for temperature measurement ±4 %, error for emissivity measurements ±6 %. The original data of Ared Cezairliyan (USA) was obtained that the addition of oxygen into the chamber leads to an increase of the detected temperature of melting (oxygen reacts with the steam, forming a transparent carbon monoxide). It confirms that carbon vapor (sublimate) plays a leading role in underestimation of melting temperature measuring for graphite. The whole temperature plateau under graphite melting was obtained (for the first time) under microseconds heating of low density graphite as in Austria by Gernot Pottlacher as in Los Alsmos, USA by Robert Hixon. But the difficulties has

A. Savvatimskiy, *Carbon at High Temperatures*, Springer Series in Materials Science 134, DOI 10.1007/978-3-319-21350-7_4

appeared with the specimen density measurements because of low initial graphite density. The last point of this chapter devoted to the difficulties in recording melting temperature under laser heating.

4.1 Graphite Resistivity (Versus Inserted Energy Only) Under Pulse Current Heating

4.1.1 Graphite Resistivity (Versus Inserted Energy) at High Pressure

This chapter begins a series of experimental studies in which Francis Bundy (one of the first) used a pulse (milliseconds) electrical heating to investigate graphite properties at high pressures.

Francis Bundy (with colleagues Hall, Wentorf, and Strong) synthesized diamond in the frame of project, announced by General Electric in 1955. This group used a high pressure, graphite and catalyst to obtain diamond for industrial applications.

The four researchers found that graphite has strong interatomic bonds that prevent conversion of graphite into diamond. Using iron sulfide as a catalyst, they managed to weaken interatomic bonds in carbon. While applying high pressure, they managed to get the first artificial diamonds in December 1954.

Diamonds have a wide range of application due to its outstanding characteristics: increased hardness and thermal conductivity. It is an ideal material for cutting, grinding and polishing. Annually manufactured over 100 tons (450 million carats) of artificial diamonds for industrial use (Fig. 4.1).

Elaboration of artificial diamonds—it was a top of achievement by Francis Bundy. In 1963, Francis Bundy of "General Electric" (after the publication of De Carli and Jamieson in 1961 the results of explosion experiments at 300 kbar and T = 1200 °C, and obtaining diamond nanoparticles) was able to establish a direct conversion of graphite into diamond under static pressure exceeding 130 kbar (under pulse electrical current heating up to 2000 °C). The size of the diamond particles appeared to 5 times more than was obtained in 1961. However, his studies of carbon, graphite melting and obtaining of liquid carbon—are no less fascinating story, which ran in parallel with the diamond theme.

In [1] Bundy makes a general conclusion about the beginning of melting for spectroscopic graphite (initial density is not specified, but, apparently, is 1.6 g cm^{-3}) and gives specific enthalpy for start of melting, depending on the applied pressure (at 9, 21, 31, 48, 67, 96 and 97 kbar). The onset of melting of the graphite it was considered the beginning of the fall of the resistivity. This fact was previously defined by Bundy with metallographic analysis of thin section of the specimens, after the heating. In this case, the specific enthalpy at the start of melting Hm had the following values. For pressures 9, 21, 31 kbar, as well as for 67, 96 and

Fig. 4.1 Francis P. Bundy Born Sept.1, 1910—Died Febr. 23, 2008 (picture from the Internet). In 1987, by the International Association, he was awarded a gold medal Bridgman for outstanding achievements in science and technology of high pressure

97 kbar Hm = 10.45 kJ/g, and at the pressures 48 and 67 kbar Hm = 12.2 kJ/g. Based on these 7 experiments the author [1] concludes that for 50–60 kbar has a flat maximum and Hm $\sim$ 12.2 kJ/g. For the most other pressure solid phase enthalpy upon melting Hm $\sim$ 10.45 kJ/g.

Note that to a large extent the value of melting heat obtained in [1] is calculated. Thus, from the total energy input to a single specimen the only 30–50 % goes to the melting of the specimen. The rest—is the thermal losses of various kinds. More rapid heating (microseconds) has allowed reducing these losses practically to zero. The author's conclusion [1] is very important that after solidification of molten graphite (various grades) resistivity of the cooled graphite specimens has the same value, smaller than the electrical resistance heated along the plane "a" at the beginning of the graphite melting. This indicates that graphite specimens of different grades heated along the plane "a", after the melting are one and the same liquid.

Melting heat ΔH defined in [1] in two ways ("on heating" and "on cooling").

The calculated value of the heat of fusion ("on heating") averaged 8.7 kJ/g (4 specimens are exhibited such a spread: 8.71; 8.36; 9.06; 8.36). For six specimens in the process ("on cooling") it was received an average specific heat of fusion, which is close to the previous value of ΔH = 8.7 kJ/g, but with a large spread (6.6; 11.1; 10.1; 7, 3; 7.7; 8.4). In any case, as mentioned in [1], specific melting heat is in the range of 7–10.45 kJ/g.

For higher pressures of 70–80 kbar and the negative slope of the melting curve of graphite indicates that the liquid state denser than the solid phase. The question

of the density of liquid carbon for lower pressures is not discussed in [1]. However, the positive slope of the melting curve for the lower pressures, given in [1], suggesting that at lower pressures graphite melting accompanied by an increase in volume with a corresponding decrease in density. This was confirmed in further experiments. Before publication [1] a theory gave a heat of fusion of graphite equals to 3.5 kJ/g, suggesting that liquid graphite—are the long molecular chains. Author [1], having the estimated value ΔH = 8.7 kJ/g, comes to the conclusion that liquid carbon has smaller molecules and a greater degree of freedom than the theory suggested. However, 8.7 kJ/g, still much less than 61 kJ/g (heat of vaporization), then there is a very small part of the bonds in the graphite lattice should be broken during melting. Therefore, the author in [1] concludes that the molecules of the liquid phase—are the probably similar-graphite fragments.

Uncertainty of heat losses of different forms under millisecond heating confirmed Bundy remark: "*heating loss through the walls and the faces of the pistons during the input of energy cannot be calculated exactly.*"

Graphite specimen in Bundy's work was surrounded by a sleeve of refractory material and is electrically connected to the pistons via the graphite discs at the end of the specimen.

The following are experimental results of the first significant work Bundy on graphite [1]. Graphite rods have diameter of 0.04 in. (0.04 × 25.4) = 1.016 mm, a length of 0.28 in. (0.28 × 25.4 = 7.11 mm). With this specimens sizes the resistivity can be easily calculated (related to the initial size). For example, if the resistivity at the start of melting Rb = 0.043 Ω (Fig. 4.2), the electrical resistivity equals ρ = R × S/l, where: S—cross section, l—length. We find that at the beginning of melting (Fig. 4.2) ρ = 490 μΩ cm under 48 kbar pressure.

Bundy recognized that the physical meaning of these various points it was not clear at the beginning of his experimental research. As described in [1] 70 % of the

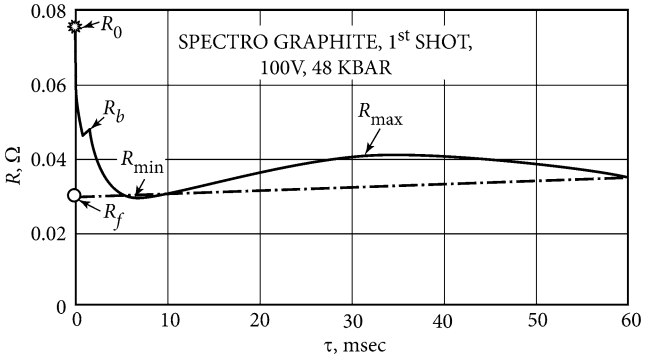

Fig. 4.2 The dependence of the resistivity against time at the first pulse heating spectroscopic graphite (48 kbar pressure). Pulse current was provided by the initial voltage of 100 V. R_0 initial resistance; R_b resistance at the beginning of melting; R_{min} resistance at the maximum of melting; R_{max} resistance at the completion of the solidification; R_f finite resistivity at room temperature, but is still under pressure

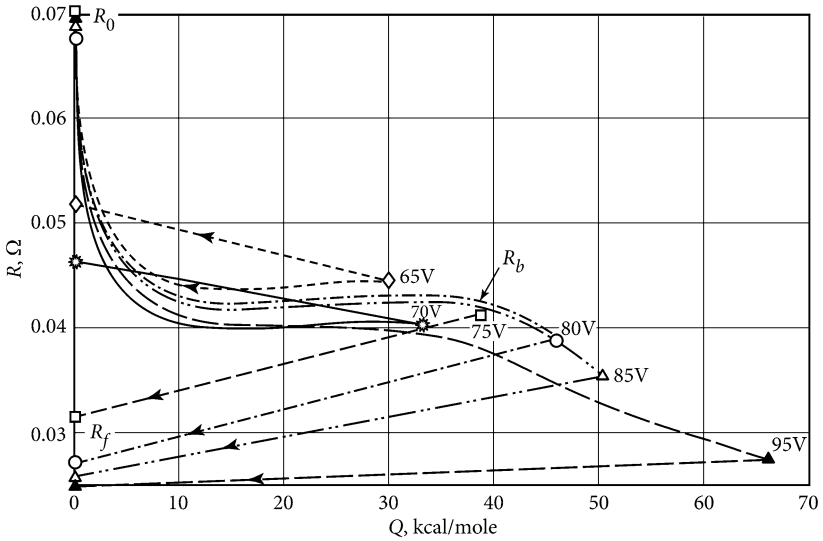

Fig. 4.3 The family of resistivity curves R (Ohms) versus energy input Q (kcal/mol) for the rods of spectroscopic graphite coated with boron nitride under a pressure of 48 kbar. The battery voltage (in volts) is indicated near the *curves*

energy was imparted for the first 3 ms, and 98 %—during 7 ms. After 7 ms the curve corresponds to cooling of the specimen. The mark (Rb) appears on the resistance curve at the imparted energy of about 38 kcal/mol.

The initial part of the heating curve is shown in more detail in the following figure (Fig. 4.3).

In this figure, R_b—resistance at the beginning of melting is indicated by an arrow. Each curve is the result of heating during the first 5 ms, so at the voltage 65 V a specimen absorbs 30 kcal/mol during the first 5 ms, whereas in the case of 95 V a specimen absorbs 66.5 kcal/mol for the same time interval. Straight lines connect the end of each curve with a finite resistance (R_f) at room temperature and do not show which way the final state is reached. The Fig. 4.3 observed general characteristics of the heating process: (1) a rapid fall in the beginning of the electrical energy input at 5–10 kcal/mol; (2) the resistance begins to diminish when the input energy is greater than 38 kcal/mol, reflecting the beginning of melting; (3) the final resistance during cooling is less than R_b when the input energy reaches point R_b, whereas at energy input lower than R_b the finite resistance R_f is greater than R_b. The latter effect is shown graphically in Fig. 4.4.

Figure 4.4 shows that the energy input from 35 to 42 kcal/mol radically changes the state of graphite. The further energy input does not affect the ratio R_f/R_0. It is assumed that input energy 42 kcal/mol is sufficient to melt all the intercrystalline zones of graphite, which are poorly conduct current up to this point.

Bundy polished section specimens subjected to heat and received a series of photos of these thin sections. When input energy reaches 32 kcal/mol (65 V) a

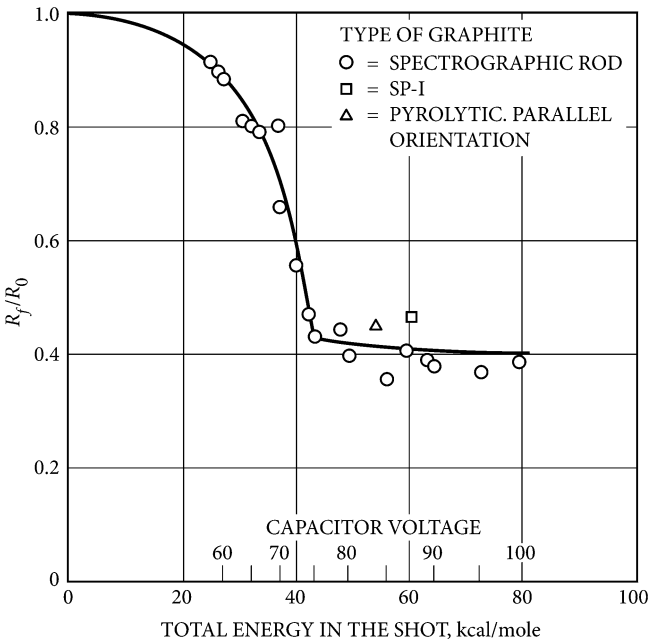

Fig. 4.4 The resistance ratio (final to initial R_f/R_0) for graphite specimens which are heated at a pressure of 50 kbar under imparted the different energies (kcal/mol). Scale energy input compared with the scale of the battery voltage (60–100 V)

structure was close to the initial one. At 37 kcal/mol (70 V) it may be seen an increase of small grains, some crystals showed a sharp boundary. At 43 kcal/mol (75 V), the author observed a dramatic change in the center (at the half of the diameter), in the central zone of the crystals were larger and had a sharply defined edges. At 49 kcal/mol (80 V) the region of strongly modified material was larger and the radial traces of the crystal structure appeared in the center, which grew rapidly with the rising of input energy. This radial crystal structure, pronounced for large energy input—the result of the rapid cooling of the completely liquefied rod. Dendrite crystals have grown from the periphery (colder region) to the center. In this case, the preferred direction of growth (crystals of graphite) was "a" direction, since the thermal conductivity for the graphite crystals is more in "a" direction and not in "c" direction.

General conclusion is that: input energy up to 35 kcal/mol does not give melting. Between 38 and 48 kcal/mol melting occurs around the crystals and grains, pseudo —liquid (mushy phase) state appears, which solidified in the form of radial oriented crystals almost an ideal electrical conductivity at final pressure. The melting is achieved in the center of the specimen at about 48 kcal/mol. With further energy input it is formed a larger diameter of the molten graphite. "*The resistivity of the liquid carbon less than a solid at the same temperature*" ([1], p. 620).

Bundy indicates the value of electrical resistivity of liquid carbon at a pressure of about 100 kbar—150 μΩ · cm. In the future, after the experiments by Motohiro Togaya (see Chap. 6) and by our experiments it was clear that this result is too low: the value of about 400–600 μΩ · cm (for pressures of 50–90 kbar) is more reliable. In a further publication in 1996 (it will be discussed later) Bundy admits that by measuring the electrical resistance of carbon data by Togaya is more reasonable. This is the more likely since the new modern recording techniques have appeared.

In this regard, it is interesting to see the dependence of the resistivity (one and the same grade of graphite) against input energy for different pressures. You may notice that the value of the resistivity depends essentially on pressure (Fig. 4.5).

One can see in Fig. 4.5 a flat maximum energy under 35 kcal/mol for 50–60 kbar, as well as changing the course of the resistance at 30 kcal/mol for the higher and lower pressures. According to Bundy, "*the most striking effect is the significant influence of pressure on the resistance of solid graphite at the melting temperature*" ([1], p. 622). At 97 kbar, the resistance is about half of what it was under 9 kbar. The same effect is observed for a liquid state, but to a lesser extent. Thus, the effect of high pressure is lowered resistance to graphite at high temperature and to the liquid carbon.

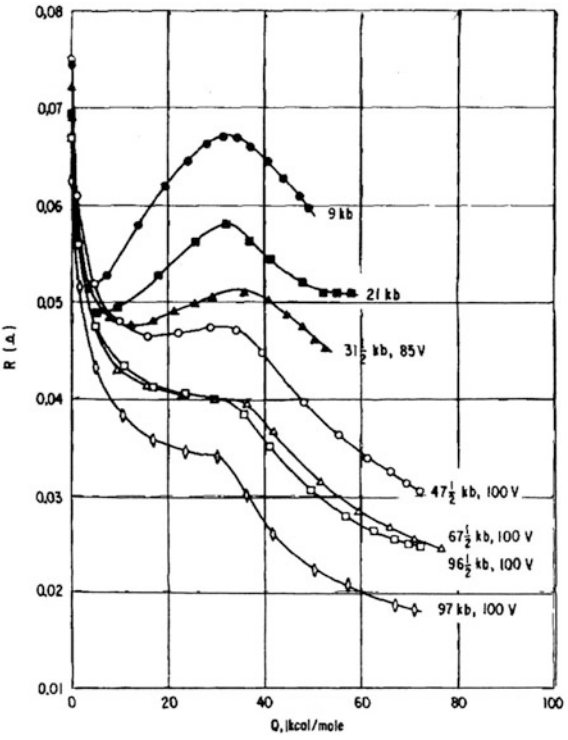

Fig. 4.5 Resistivity R (Ohm) of spectroscopic graphite (coated with boron nitride) against the energy input Q (kcal/mol) for various pressures (from 9 to 97 kbar). The battery voltage (in volts) is shown near the *curves*

Graphite is a lot of different types arranged in a variety of structural forms.

However Bundy assumes that any solid form must be melted in the same liquid ([1], p. 623). Bundy analyze the known heat capacity data for graphite at high temperatures C_P, and comes to the conclusion to make a linear extrapolation of the heat capacity (known at T = 3200 K) up to 5000 K. Under these assumptions Bundy constructed carbon phase diagram (Fig. 4.6) which has a maximum melting point of 4600 K for a pressure of 60–70 kbar (accordingly about 4200 K at pressures of about 100 bar).

Analyzing the possibility of assessing the heat of fusion for graphite Bundy concludes on approximately of the assessment and indicates 25 kcal/mol, as the most probable value for the heat of fusion for graphite at the pressure 48 kbar (noting that apparently it is between 20 and 30 kcal/mol). For other pressures Bundy does not give any estimates. The essential remark of Bundy it is a structure of liquid carbon. Since the heat of fusion of carbon is sufficiently small (25 kcal/mol) in comparison with the heat of vaporization (175 kcal/mol), it is only a small part of bonds will be broken during melting. Consequently, the liquid carbon molecules look like graphite-like fragments.

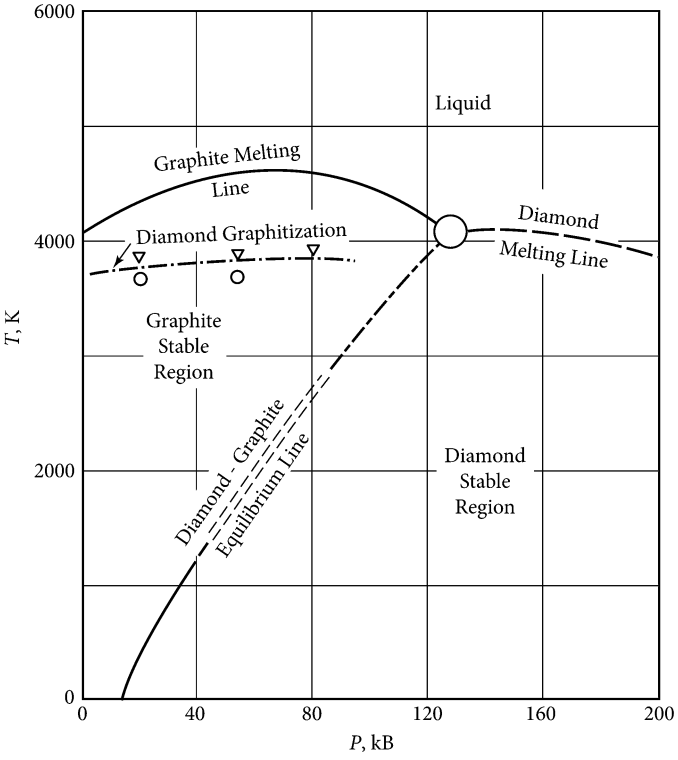

Fig. 4.6 Graphite melting temperature T (K) against pressure P (kbar) [1]

Bundy compares his millisecond heating of graphite with the rapid heating by capacitor banks (exploding wire) and notes their significant differences: (1) Bundy experiments have thousands of times slower, (2) In the experiments of Bundy a pressure so great that the conductor limited in expansion and in the vapor or the arc phase appearing, (3) The current density was too low to create a large magnetic pressure or plasma state. From this comparison it follows that Bundy was not sufficiently informed about the possibilities of rapid (microseconds) pulse electrical heating. Bundy cites Bridgman's data on the compressibility of graphite up to 100 kbar (by 1948 year) and Berman and Simon data on the thermal expansion of the graphite (by 1955 year), and notes that if mentally to imagine that graphite is heated at constant volume to 4000 K, the pressure that generate the graphite itself will consist of 95 kbar. In this regard, we note that in the Bundy's experiments there is no possibility to fix a constant volume, because the graphite specimen is surrounded by a material with a similar module and density. So Bundy's experiments are close to static experiments. In concluding the article Bundy takes attention to the proximity of the melting entropy for graphite, silicon and germanium—they are neighbors in the periodic Mendeleev's table (accordingly 5.4, 6.5, 6.7 kcal/mol K). We can add: if one can see the latest research data for carbon, the agreement will be even closer.

In the same 1963 year Francis Bundy published the second significant study on carbon at high pressure [2]. Consider this publication, including its translation into Russian [3]. The following Figs. 2.6–2.9 were taken from Bundy's paper [2]. In this paper, Bundy used two types of specimens. Specimen type "b" was (Fig. 4.7) a cylinder with the diameter of approximately 0.76 mm and a length of 1.02 mm, surrounded by a sleeve of a refractory material such as pyrophyllite or ThO_2 and electrically connected to the graphite pistons via the end discs. When the resistance of the specimen is 0.03–0.07 Ω the circuit characteristics allow to get a discharge of the unitary pulse with the 90 % imparted energy of the whole pulse during 3–6 ms

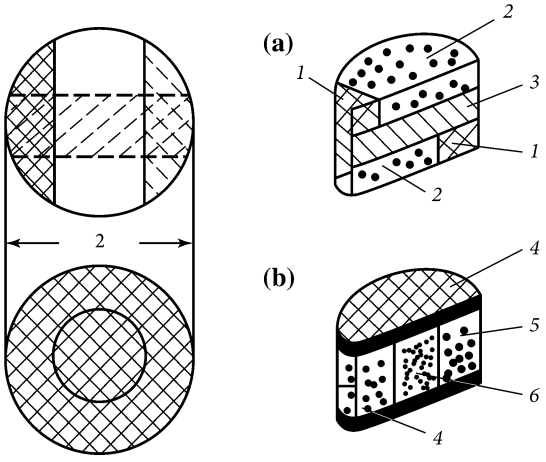

Fig. 4.7 Specimens in the form of the bar (**a**) and cylinder (**b**) applied to the device "Belt" in the high-pressure experiments by Bundy: *1* graphite electrode; *2* pyrophyllite; *3* graphite block; *4* end graphite disk; *5* pyrophyllite, MgO, ThO_2, or Al_2O_3; *6* graphite cylinder

time interval. The cooling of the specimen after the current pulse lasts about 30 ms. Bundy consider that just that is why the input of energy can be regarded as adiabatic, but says: "*heat losses through the walls and the faces of the pistons during imparting the energy cannot be calculated accurately*" [2, p. 633].

Bundy calculated the temperature from the input energy and the available data on the specific heat capacity (C_p), published in references 1955 and 1958. The plotted curve temperature—input energy was used in the cited paper. The same year 1963 Bundy together with Wentorf published the study of direct conversion of hexagonal boron nitride to more dense forms [4].

Pulse energy input adequate voltage 30 V battery. At a pressure of 140 kbar, the resistance increased dramatically (typical for the beginning of the diamond formation) at about 8 J of input energy.

(Author's monograph note. If we calculate the specific energy imparted to the specimen used Bundy's dimensions: diameter of 0.76 mm, length 1.02 mm and a density of 1.6 g/cm^3 for spectroscopic graphite, the input of 8 J correspond to the specific energy of 10.8 kJ/g. According to our measurements, the amount of energy at the start of melting under pulsed electrical heating at the triple point is 10.5 kJ/g).

In experiments at high pressures Bundy stated: "*there is almost no doubt that the melting of carbon derived from the diamond phase.*" The fundamental difference between these two experiments (in our experiment in the water and in Bundy's experiment at a high pressure) is the difference in pressure value: below the triple point (pressure lower 107 bar) by heating in water, and significantly higher than the triple point pressure (tens kbar) in Bundy's experiment. Anyway, there is intrigue of this effect: proof of the correctness of his interpretations can only be the result of an experiment to determine the expansion of the specimen (bulk sublimation) at the input energy 10.5–10.8 kJ/g at low external pressure. If this expansion would be small it should indicate that there is a transition of the graphite to diamond at low external pressure. If there would be a significant volume growth (which may explain the increase in electrical resistance)—then it is the bulk sublimation takes place. To substantiate our point of view we note an important experimental fact: if you limit the expansion of graphite before rising of the resistivity, the high rise of resistivity is not happening.

Now back to work of Bundy. Thus, the dense black polycrystalline diamond cylinder with a diameter and a length of about 0.76 mm was obtained by Bundy. This result cannot be explained as a simple process of melting and solidification. The transition of graphite to the diamond is essentially a conversion of the solid to solid. Earlier, just before the investigation of diamond problem, Bundy performed extensive research of graphite melting [4], which showed that the melting of graphite required significantly more energy and, consequently, achieve higher temperatures.

Bundy concludes his analysis: "*Thus, it is clear that the transformation of graphite into diamond occurs at a temperature corresponding to about two-thirds of the energy required to bring the graphite specimen to its melting point. Tests with other cell geometry and other grades of graphite give the same results.*"

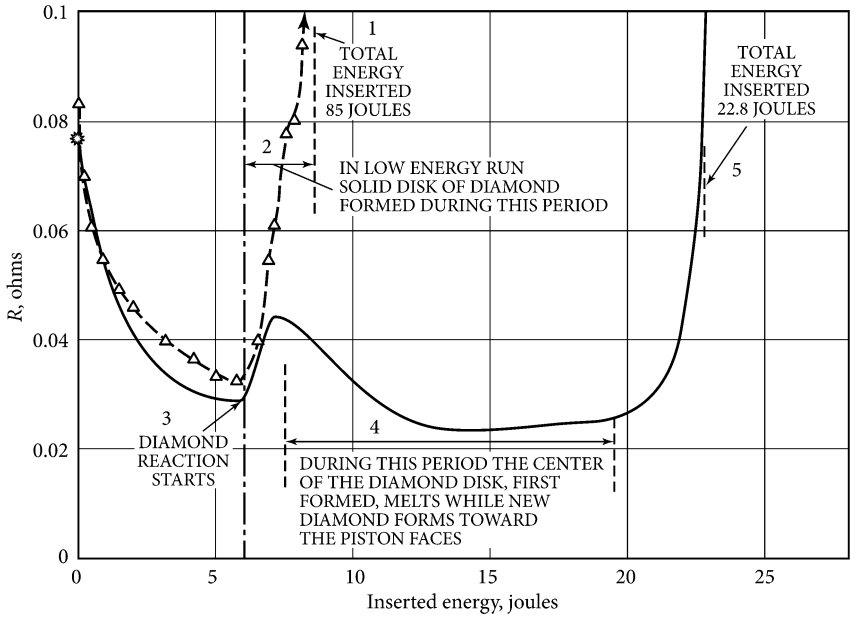

Fig. 4.8 [2]. The change of resistance R as a function of inserted energy in the experiments for graphite with the addition of boron. Numerals: *1* the total input energy of 8.5 J (up to *dashed vertical line*); *2* in the experiment with the low inserted energy, diamond compact disc formed during this period; *3* beginning of the diamond reaction appearing; *4* during this time the central portion of the diamond disk melts, while the new diamond is formed in the direction of the ends of the pistons; *5* the total input energy equals 22.8 J

The start of diamond reaction (Fig. 4.8) occurs under energy input of about 6 J. If we calculate the input energy for a specimen having dimensions: diameter 0.76 mm, length 1.02 mm, density 1.6 g/cm^3, just as for spectroscopic graphite, the input of 6 J corresponds to specific energy of 8.1 kJ/g. The maximum of curve 1 at 7.5 J (apparently—the start of melting for diamond or graphite), corresponds to a specific energy of 10.14 kJ/g (the start of melting graphite in our experiments—at 10.5 kJ/g). The finish of melting may occur at ~20 J, i.e. prior to the start rise of the resistance. Then melting ends at 27 kJ/g (in our experiments—at 21 kJ/g).

Calculation of the electrical resistivity in Fig. 4.8 based on the original specimen size (diameter of 0.76 mm and a length of 1.02 mm, the electrical resistance R = 0.0233 Ohm) gives the electrical resistivity of the liquid phase of carbon 1035 μΩ cm (to the right side of the field 4, at E = 20 J). (Remind that this result was obtained with graphite with the addition of boron).

Figure 4.8 shows that the diamond reaction starts at one and the same input energy (i.e., temperature). It is worth mentioning Bundy remark: "*there is little doubt that the liquid carbon obtained by melting the diamond rather than graphite.*" Indeed, if we look at Fig. 2.12, the formation of the diamond occurs before the

formation of a liquid phase (in the same energy input axis). Later it allowed Bundy to say: to produce liquid carbon requires much more energy than for producing diamond.

Regarding the resistivity of the liquid carbon Bundy [1] has obtained 350 μΩ cm at a pressure of 48 kbar. Togaya has obtained 460 μΩ cm at 56 kbar pressure [5]. Bundy noted [6] that the electrical resistance measured by Togaya is more reliable as more perfect registration was used. As noted Bundy in [6] "*Baitin* et al. [7] *found the emissivity of liquid carbon at λ = 0.65 μm to be about 0.6; this is close to values for liquid metals and is therefore consistent with liquid carbon being metallic*".

Close value was obtained by Shaner J.W. (USA) [8] with microsecond pulse heating of graphite (about 1000 μΩ cm). As it will be shown below in this chapter (study of Lebedev and Savvatimskiy [9]) for pure graphite was obtained about 700 μΩ cm, using analog oscilloscopes, and later study [10–13]) 600–640 μΩ cm with a digital oscilloscope used for the case of elevated pulse pressure. The latter result coincides with measurements by Motohiro Togaya (630 μΩ cm) [14]. If previously Togaya argued that liquid carbon—it is rather a non-conductor, a such lowest recorded value of the electrical resistance, that they declared in 2010, allowed M. Togaya (in his last study) assert that liquid carbon—is a "*weakly conductive metal.*"

In [4] the electrical and laser heating of graphite were considered. It was concluded by Bundy *(on the resistivity values) that: "All the results listed above, except for those of* Malvezzi et al. [15], *are consistent with liquid carbon having semimetallic properties*" [6], p. 144. According to [6], there is no reason to believe that liquid carbon exists in insulating form. Bundy expressed in that case: "*There appears to be no firm evidence from the most recent experiments that supports the existence of an electrically insulating form of liquid carbon*" [6]. In spite of these words and the results of the most experiment results, the researchers (who deal with the computing modeling) happily continue calculations conductive and non-conductive liquid phases of carbon. It is obvious that computer account allows one to feel the joy of fellowship with science regardless of the validity of the obtained result.

4.1.2 Correspondence of the Author with Francis Bundy, 1999

In 1999, when we published a rather capacious work on the metals and graphite together with Fortov and Cheret [16], I dared sending the article to Bundy (found his home address). Surprisingly, I received a response from Bundy (Fig. 4.9).

At the same letter it was flaunted (color) personal stamp with Bundy home address. The letter was written by accurate, school handwriting (I admit that it was written by his grandson or granddaughter, by dictation). Just here this letter:

"*Dear Doctor Savvatimski, thank you very much for sending me reprints of your recent publications about the thermophysical properties of metals, and carbon, up through the liquid state at high temperatures, studied by fast electrical pulse-heating.*

Fig. 4.9 Envelope letter from Francis Bundy, which I received in Moscow in 1999

I appreciate receiving them especially because of being retired (age 88). I no longer live near access to university libraries where I can read the latest scientific literature. I do subscribe to several "general science" journals such as SCIENCE, SCIENTIFIC AMERICAN, etc.*, and attend every 2 years the Gordon Conference on High Pressure Science. Also, my younger colleagues keep me informed of their work.*

I have studied your article carefully and I am impressed by the skill and the honesty with which you have performed and interpreted your experiments. I feel pleased that the graphite melting, and direct transition of graphite into diamond experiments that I did rather hurriedly in 1962 have "stood the test of time" and still are quite valid. As you show,—the experimental difficulties at very high temperatures are strong and one has to be very cautious about them.

Your method of making diamond powder by the very rapid pulse-heating method is very interesting,—and valid. Whether it can become of commercial significance will depend upon the cost of production (energy, equipment, maintenance, materials, etc.*) and the commercial need and price of the diamond powder product that is produced. The present shock-compression commercial process is relatively efficient and inexpensive, and will be hard to beat.*

Keep up your good scientific work and continue to expand our knowledge and understanding of materials at high temperatures and pressures!

Sincerely, Francis P. Bundy."

Being at a world conference on carbon in Byarritz (France, 2009), I met a researcher Judd Diefendorf who knew Bundy and admiringly spoke of him, calling him the enthusiast in researching carbon. I learned from him the sad news that Francis Bundy died in 2008. Really, Bundy was the enthusiast and outstanding leader in carbon investigation.

4.1.3 *Resistance Against Inserted Energy up to Melting (Fast Electrical Heating)*

In 1939 year Pirani fulfilled one of the first significant experimental studies of graphite [17] by stationary heating with an alternating electric current at atmospheric pressure. He was failed to melt the graphite rod with a diameter of 37 mm, while only buckling of the graphite was observed at T ~ 3500 °C from the side hole of 3 mm in diameter (Fig. 1.3). Further experiments showed that only the pulse heating allows to increase the specific power dissipation and to obtain data for the melting point of graphite.

Experimental investigation of graphite at high temperatures under heating by pulse of electrical current within microseconds time interval actively started at the Institute for High Temperatures (IVTAN) in 1972, in Moscow, in the group headed by S.V. Lebedev (Figs. 4.10, 4.11 and 4.12).

Sergey Vladimirovich Lebedev (1913–1990) is a world leader in the application of pulse electrical heating of conductors. He pioneered in the use of short pulse heating (microseconds and nanoseconds) for the study of metals at high temperatures. More milestones of the biography of S.V. Lebedev were presented in [18, 19].

Remind the method and the data obtained by S.V. Lebedev (1913–1990) who (maybe the first) investigated special metal properties at high temperatures under

Fig. 4.10 S.V. Lebedev in 1968 year (Photo by Vladimir Lebedev)

Fig. 4.11 S.V. Lebedev during his work at the Institute for High Temperatures (IVTAN), 1986 year. Photo by Valery Platonov (1939–2008), our qualified technician at the IVTAN

Fig. 4.12 Vladimir Lebedev (the son of S.V. Lebedev)—professor of faculty "Quantum Radiophysics" at MIPT, working in 2014 as a head of the theoretical sector "Optics of non-equilibrium environments" in Physical Institute (FIAN, Moscow). Nowadays Vladimir Lebedev—professor of the Moscow physics and technical Institute, MIPT, the same Institute where S.V. Lebedev taught students in 1948–1965 years

fast (microseconds) electrical heating. W.G. Chace and Moore H.K., the editors of the well-known proceedings on the exploding wires [20] devoted to pulse heating, called him "*a pioneer of exploding wire phenomenon*".

Remind one of the article [21] published by S.V. Lebedev in 1954 year (in Russian).

It should be emphasized that he used fast (several microseconds up to tens of microseconds) electrical heating for studying properties of the refractory metal wires. Later it would be clear that the fast heating is more preferable for measuring properties because the inertia gives specimen of a high density a time to stay at the initial position. It gives a possibility to measure properties for unchanged geometry of the specimens that is very important for expansion and resistivity recording.

Figure 4.13 shows one of the first result of the pulse heating of pyrolytic carbon rods (bulk density of 1.9 g/cm^3) provided in the Institute "Elektrougli" (located near Moscow). These rods (diameter from 0.3 to 0.05 mm) were prepared by freely borne under depositing carbon on graphite filaments in the volume of high-temperature cameras during pyrolysis of carbonic gas.

According to suppliers data: the structure of pyrolytic carbon is close to a single crystal, but it is not a single crystal. It has been argued that these specimens do not melt, they will only sublimate. This opinion corresponded to the point of view of many experts at that time who are not familiar with the problem of the carbon melting.

We have found that the pulse heating the graphite in air leads to a shunting discharge along graphite specimen (as was the case earlier when pulsed heating of the refractory metal wires in air was used). Therefore, the carbon specimens at this

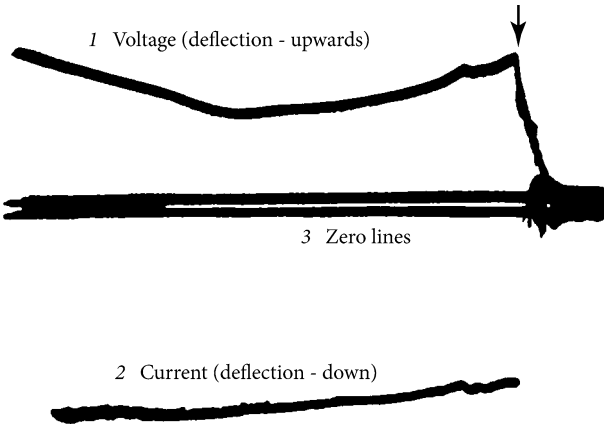

Fig. 4.13 The first (in our study) experiment (March 15, 1972) with pulse heating of a thin graphite rod. Voltage 1 (upward deflection from zero line) on graphite un-annealed specimen (rod with the diameter of 0.26 mm, submerged in water) by passing a current (curve 2) with a nearly flat top, i.e. the voltage waveform reflects the dependence of the resistivity versus time (in arbitrary units). Abscissa—the total time of about 30 μs. The current was forced shut down at the last stage of the experiment (*arrow*). The waveforms were recorded by the analog oscilloscope OK-17M

stage of study were heated in water. In particular, the electrical resistivity of the specimen at the beginning of heating equals ~880 μΩ cm, then diminishing to a minimum of ~400 μΩ cm, and then continued to rise (Fig. 4.13). Before forcing of interrupting a current at the input energy ~14 kJ/g, a rough estimate shows that according to the magnitude of input energy, graphite could be partially melted. As it was our first experiment with graphite, we have not considered at the time an important requirement for high pressure for successful melting graphite. However, this was our first experiment (Fig. 4.13) demonstrated that the electric current to heat the graphite in microseconds time scale can be also successfully used, just as for the metals.

In 1970 [22] it was found by our investigations that it is possible to study the heating of refractory metals in the air without the formation of shunt discharge on the surface, placing them in a limited isolated volume. Metal wire placed in the internal volume of the capillaries (even up to 25 times larger than the volume of the original wire). The same technique was applied to graphite. The heating of graphite specimens in tubes of different internal cross-sections allowed:

(a) prevent the appearing discharge along the surface at atmospheric pressure (as for metals);
(b) to create a high pressure (thermo-compression) in the graphite in the case of closer placement of graphite specimens in the tube.

In 1986, Lebedev and Savvatimskiy [9] carried out investigation of the properties of graphite of the two grades: cylindrical obtained in the Institute of Elektrougli (density of about 1.8–1.9 g/cm^3) and planar graphite specimens (grade UPV-1T) with a density of ~2.15 g/cm^3. Base to the start of this research were the following considerations. The physical mechanism of the loss of conductivity (with considerable energy input by electrical pulse) and the associated destruction of the graphite could be different than in the case of metal heating. Graphite is significantly different from metal by high initial resistance and significantly higher pressure at the triple point (equals or over 100 atm). Also should be remained the possibility of a kind of "overheating" of solid graphite and (hypothetically) obtaining the electrical explosion of solid state by its rapid heating at a pressure less than the pressure at the triple point.

Specimens in the form of cylindrical graphite (diameter of 0.3 mm, length 20 mm) were fixed in copper lead electrodes by pouring tin. The electrical resistivity at room temperature was 1500 μΩ cm. Results for cylindrical un-annealed specimens are presented in Fig. 4.14. The diminishing of the electrical resistivity up to the energy ~10 kJ/g, i.e. almost to melting, leading to non-uniform heat dissipation during heating of such specimens by electrical current (in those portions of the specimen where the resistance is lower,—it was released the higher power).

It was found that pulse heating of graphite by electrical current in the open air (at atmospheric pressure) leads to bypass current discharge along graphite specimen. So graphite specimen at the initial stage of the research was heated in water, and then in the isolating capillaries (Fig. 4.14, [9]).

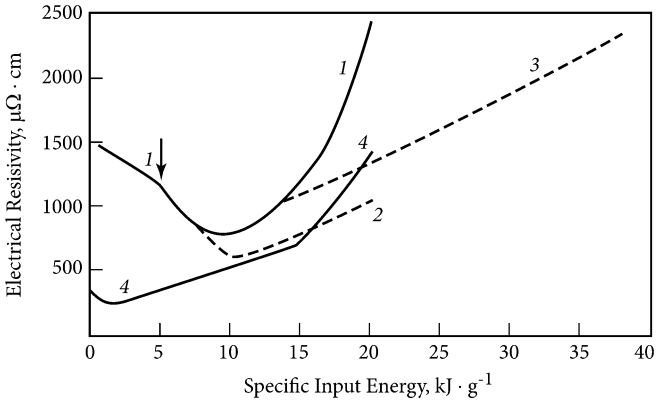

Fig. 4.14 [9], 1986. Electrical resistivity (referred to initial dimensions) of the pyrolytic graphite specimens of different initial densities under pulse electrical heating

(1) Pyrolytic un-annealed graphite is in the form of a rod (density 1.9 g cm^{-3}) under pulse heating in a water. Arrow indicates the point of compression of the graphite in solid phase.
(2) The like specimen in a glass capillary tube (V/V_0 = 1.19, where V—internal volume of the tube, V_0—graphite specimen volume). Start heating is along the curve 1, and then, after filling of the graphite tube,—by the dashed curve 2.
(3) The like specimen in a glass capillary tube (V/V_0 = 1.45). Start heating is along the curve 1, and then, after filling the glass tube—by the dotted curve 3.
(4) Pulse heating of dense graphite UPV-1T in solid colophony. Flat pyrolytic graphite with the density 2.15 g/cm^{-3}. Slight decrease at the beginning of the electrical heating—the result of an insufficient annealing. Steeper increase in resistivity at 15 kJ/g—the result of a free expansion of the specimen in the melted colophony.

Arrow indicates the moment (at the input energy E $\sim$ 5 kJ/g), of increasing the density of solid graphite with low initial density; this effect was also recorded in [23].

As it is seen in Fig. 4.14 the restriction of the volume around graphite specimen (it is analog to high pressure) reduces heterogeneity of heating for low density graphite.

Experiments by Bundy and our measurements show that the onset of graphite melting corresponds to the input specific energy E = 10.5 kJ/g, and the end of E = 20.5 kJ/g. We will consider the results of experiments for these specific energy input is related to the beginning and end of melting, respectively, for all types of graphite with different initial densities studied in similar conditions (for example, close the same external pressure). This approach is justified, because the specific energy refers to a unit mass of a substance. It should be remembered that the value of input specific energy (for example, at the phase transition) may depend on the pressure value.

First experiments with the heated graphite specimens in the glass and quartz tubes are shown in Fig. 4.14 [9] for pyrolytic graphite with different initial bulk density. Diminishing for the electrical resistivity of graphite specimens of low initial density until the input energy 10 kJ/g (Fig. 4.14, curve 1), i.e. almost to the onset of melting, may causes a non-uniform heat dissipation during electrical heating.

An electrical resistivity kink is regularly observed on the decreasing curve at the input energy of ~5 kJ/g. As it turned out, this corresponds to the compression of graphite to the higher density. By the way, in 1986, we determined the density of cylindrical specimens by dividing the weighted cut of graphite on the volume (density 1.94 g/cm^3 was obtained and used in a publication [9]). However it was later revealed, that in the center of the circle specimen there was a thin filament with the lower density. Thus, the average density should be considered as 1.8 g/cm^3. The start of increasing resistivity begins at the input energy 9–10 kJ/g under heating in the water (curve 1 in Fig. 4.14). This increasing rise further up to the highest value of resistivity and destruction of the specimen.

Plane specimens of pyrolytic graphite (grade UPV-1T) were obtained by deposition at T = 2450 K. The total amount of impurities is less than $5 \cdot 10^{-3}$ wt%. Initial crystallographic characteristics in the deposition plane "a" consists 2,450 Å (crystallite size of 260 ± 30 Å); in the plane of "c"—6,856 Å (crystallite size of 100 ± 10 Å). Bulk density was measured for the various pieces of graphite in rectangular form with the volume of 0.2–1.0 cm^3. It were obtained values of 2.10–2.15 g/cm^3; in the calculation of the value of 2.10 g/cm^3 was used.

The electrical resistivity for flat highly oriented graphite (un-annealed specimens) is presented in the Fig. 4.15, depending on the enthalpy and temperature. Later the specimens made of grade UPV1-T were annealed in vacuum to obtain a low initial resistivity (~50 μΩ cm). It has led to continued growth of graphite electrical resistance from the start of heating (i.e., to the lack of falling resistance at the beginning of heating, which is visible in Fig. 4.15).

Stationary experiments up to 2300 K are shown by crosses [24]. Circles [25] from 1500 to 3000 K—the results of slow process by pulse electric heating of pyrolytic graphite. By the way gives the details of this excellent study (abstract [25]):

"*Measurements of heat capacity, electrical resistivity and hemispherical total emittance of Poco and pyrolytic graphite in the temperature range 1,500–3,000 K by a subsecond duration pulse heating technique are described. For a given graphite grade, heat capacities of different specimens were in agreement within 0.5 %. The difference between the results of the two different grades was about 1.8 %: the results of Poco being higher than those of pyrolytic. Electrical resistivity of the Poco graphite was about four times greater than that of pyrolytic graphite (parallel to basal planes). Hemispherical total emittance of Poco graphite was almost twice that of pyrolytic graphite*".

The temperature scale in Fig. 4.15 is graded according to the data of Institute NIIGRAFIT [26].

The data (Fig. 4.16) were obtained by heating of un-annealed graphite in the colophony, in order to create an excessive pressure during the experiment (5 μs).

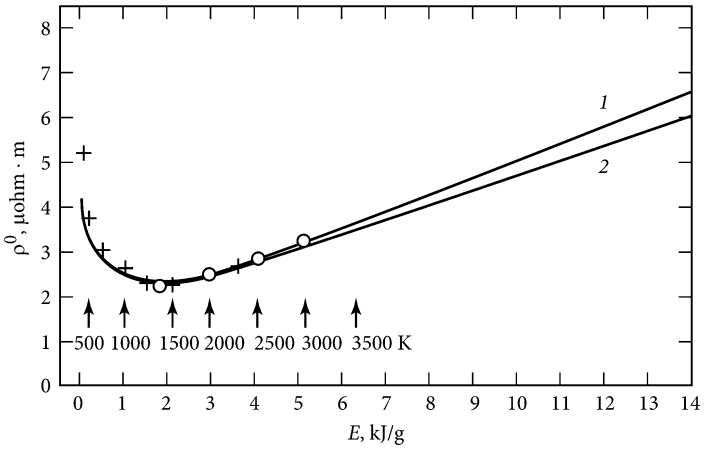

Fig. 4.15 [9] The resistivity of pyrolytic graphite ρ^0 (referred to initial dimensions) along the planes of deposition, heated in colophony. *1*, *2* Data of the two experiments [9] for heating time of 5 μs. When the input energy E (equals enthalpy H) is less than 5 kJ/g, the curves 1 and 2 coincide. I (crosses)—we used some fixed point of steady state data [24] up to 2300 K. II (*circles*)—pulse data (parts of a second) [25] up to 3000 K

Comparison in Fig. 4.16 shows that at the energy input lower 2 kJ/g at a rapid diminishing of electrical resistance occurs during fast heating, such as in the case of slow heating. For the large energy input (difficult to achieve in stationary experiments) the resistivity of graphite increases monotonically without noticeable features that could be associated with the area of fusion.

Ordinate axis: resistivity ρ^0 (μΩ m) referred to the initial dimensions. Curve 3: planar graphite specimen with the cross-section 0.22 mm × 0.26 mm in a glass capillary tube with internal diameter 0.349 mm, external diameter 5.2 mm. The

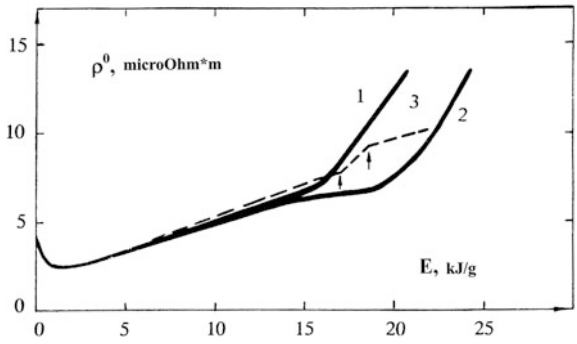

Fig. 4.16 [9] Resistivity versus input energy E: fast heating of planar pyrolytic graphite (initial density 2.2 g/cm^3) in boiled water (*1*), colophony (*2*), and in a glass capillary tube (*3*). Under H < 15 kJ/g curves 1 and 2 coincides. The limit for the curves (*right-hand side*) is connected with occurrence of bypass discharge (*1*, *2*), the beginning of the destruction of the capillary (*3*)

right-hand arrow shows the moment at which the rate of change of the resistivity with input energy changes abruptly. This moment is attributed to the filling of the inner tube volume with the thermally expanded graphite. The relative volume at that moment $V/V_0 = 1.68$ for the input energy (enthalpy) ~18.5 kJ/g, which is just before the completion of melting (20.5 kJ/g).

Note the remarkable result of obtaining the electrical resistivity (referred to the initial dimensions) $\rho^0 = 900$ μΩ cm for the graphite specimen filling the internal volume of a thick-walled glass tube [9] (Fig. 4.16, right-hand arrow in the curve 3). This time corresponds to the specific energy input E = 18.5 kJ/g, which is close to completion of fusion (20.5 kJ/g). As in Fig. 4.16 it was fixed the moment of filling the tube by the graphite specimen, the graphite was expanded freely up to this point. Expansion of graphite is sharply limited just after the filling the entire cavity of the capillary. We note that for the duration of the order of several microseconds of the experiment, and a ratio of length of the capillary to the diameter of its cavity (equals to 40) an outflow of graphite from the cavity can be neglected. Especially that the ends are closed by massive electrodes.

Knowing the initial volume of the cavity V_K and the volume of graphite V_0 ($V_K/V_0 = 1.68$), one can determine the density of graphite in a state where the whole cavity is filled with the graphite (right-hand arrow on the curve 3 in Fig. 4.16). Thus, we obtain the density ~ 1.25 g/cm^3 at the largest energy input of 18.5 kJ/g (for graphite of initial density 2.1 g/cm^3). It is also possible to calculate the electrical resistivity (in view of thermal expansion) for the case of low external pressure. This value will be $\rho = \rho^0 \times V/V_0$, where $V/V_0 = 1.67$ (V—volume of the cavity in the tube, V_0—graphite specimen volume). As a result, $\rho = 890 \times 1.67 \sim$ **1500** μΩ cm for graphite at E = 18.5 kJ/g (Fig. 4.16). Under pulse heating of less dense graphite (Fig. 4.14, curve 3) that the electrical resistivity $\rho \sim$ **1650** μΩ cm at the input energy 14 kJ/g ($V/V_0 = 1.45$).

Thus, freely expanding graphite at low pressures (up to ~ 1 kbar) has sufficiently high resistivity ρ (thermal expansion is taken into account) near the melting point. The reason is in a significant expansion of the volume for small external pressures, such as for Fig. 4.16 (curve 3)—67 % of the initial volume of graphite. This growth is fixed before the complete melting of the specimen, i.e. the rise of the volume (relative to the original) for the liquid state at the melting line will be slightly higher.

The appearance of a pressure exceeding the equilibrium vapor pressure of the graphite at very rapid heating (when the inertia effect of the environment takes place) can naturally be explained by evaporation of the substances with low melting temperature contacted with high temperature carbon,—water, colophony, or the wall material of the capillary. Note that at the same temperature, the equilibrium vapor pressure of silica is considerably higher than the vapor pressure of carbon [27].

Using data of handbook [26] it is able to estimate the energy at which should begin the melting of graphite. According to [26], the enthalpy of 6.3 kJ/g corresponds to the temperature of 3500 K. At this temperature, the carbon heat capacity equals 2.6 J/ g K. Considering the melting temperature $T \sim 5000$ K, we have obtain the energy equal to the start of melting ~ 10 kJ/g.

Note the interesting (and important) feature, that is known from the literature. According to [28] for different substances "*as the pressure corresponding to the triple point increases, the region of existence of the liquid is reduced.*" In particular, graphite has a narrow in comparison with metals, the existence region of the liquid state. Width of this area can be judged from the ratio of the critical point temperature T_C to the temperature at the triple point T_{TP} [28]. According to the calculations [29] for graphite $T_C/T_{TP} = 6810/4765 = 1.43$, whereas for tungsten the same ratio is equal 6.3 [28]. By the way it should be noted that the temperature at the critical point of carbon is an estimated value, and therefore is insufficiently reliable.

As with metals explosion after an explosion of graphite in a liquid medium the destructed products remaining in the liquid are indistinguishable with the optical microscope used. Under an explosion of graphite in a liquid the latter is darkened, and at break of current before a sharp rise in resistance—a liquid is transparent. For the same explosion of tungsten the products, making a dark liquid, have a particle sizes equal 100–200 Å [9, 18, 30–32]. A similar analysis was not obtained for graphite, except for the watched of the darkening of a liquid.

With the example of graphite one can give another argument against the idea of the electric explosion as a boiling of a conductive liquid. Since under the rapid heating of the graphite specimen the pressure on the specimen surface by its own vapor plus the pressure of water (and colophony or silicon) vapor are larger than carbon vapor pressure in the supposed carbon bubbles of a liquid carbon,—the growth of carbon bubbles are impossible. Consequently, a strong increase in resistance and volume (Fig. 4.16, curves 1, 2) cannot be explained by the volume boiling of carbon.

Continuing research of cylindrical graphite specimens, we later used thick sapphire tube. Results for the specific electrical resistivity of cylindrical graphite (it was an annealed specimen heated in the sapphire capillary tube), limiting expansion, shown in Fig. 4.17 [16]. Preliminary annealing of the specimens allowed reducing the initial electrical resistance and eliminating the fall of the resistance at the beginning of the electrical heating.

The results of these experiments confirmed that the graphite of low density has no any peculiarities on the electrical resistivity which may be considered as the signs of the graphite melting (from 10.5 to 20.5 kJ/g) under the conditions of both low and high pressures. Furthermore, in Fig. 4.17 there is a direct dependence of the resistivity of the liquid carbon (above 20.5 kJ/g) on the pressure: the higher the pressure, the lower the resistivity of the liquid phase. By the time we knew that the end of melting occurs at 20.5 kJ/g.

Specimens that have been made of various types of low density graphite (1.5–1.9 g/cm^3) typically have initial heterogeneity in structure (experimental fact), which may cause no uniform heat dissipation throughout the specimen volume. In the further experiments, we used highly oriented pyrolytic graphite UPV-1T—analog of HOPG (Highly Ordered Pyrolytic Graphite) that has a rectangular section. These specimens have the opportunity to expand independently in two axes. Electric current is passed through the plane "a" of high conductivity. In 1986 [9] Lebedev and Savvatimskiy showed the comparative characteristics of the pulse

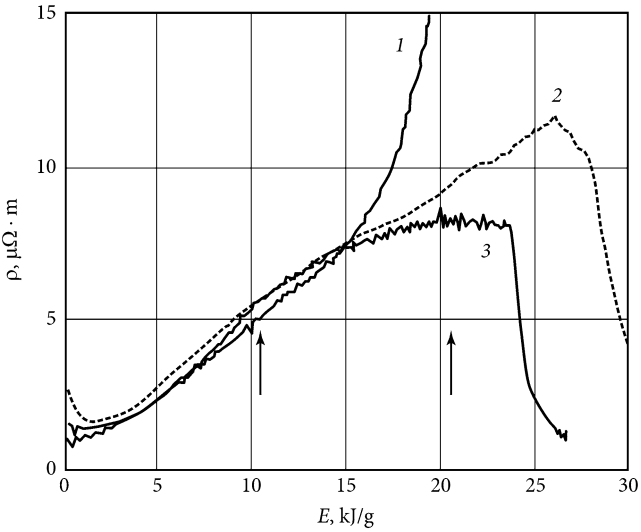

Fig. 4.17 [16] Resistivity of pyrolytic graphite specimens annealed (in needle form) versus specific imparted energy E. The start of the melting is at E = 10.5 kJ/g, the finish at E = 20.5 kJ/g. *1* heating in the water; *2* in the sapphire tube, $V/V_0 = 1.7$ (V—the volume of the tube, V_0—the initial graphite volume); *3* in the sapphire tube, $V/V_0 = 1.4$. Sharp diminishing in the curves 2 and 3—the destruction of the tubes due to high pulse pressure. The *arrows* indicate the start and the end of melting

heating of metals and graphite in a liquid medium (water, oil) and a solid medium (colophony). In this study, the most important results were obtained as the following conclusions:

- The growth rate of the resistivity (both annealed and un-annealed) graphite specimens of low density (1.5–1.9 g/cm^3) during melting usually has no any peculiarities, so there is no any possibility to determine the moment of melting by the electrical resistance;
- Assessment of the specific energy input at the beginning of melting (including heat capacity data) gives $\sim$10 kJ/g, which was later confirmed by direct experiment;
- Electrical explosion of graphite, i.e. the rapid expansion of the specimen with a steep increase in the electrical resistance, leads to appearance of a sol–colloidal solution (indistinguishable by eye fine particles) in a liquid environment (water, oil). Thus, the electrical explosion of graphite [9] is similar to the electric explosion of metal [18, 31, 32], and it starts at the same relative density ($\sim$0.6 from the initial).

Summary results of our measurements up to 1993 on the pulse of electrical heating of graphite [9] and metals [32] were published in [31].

The heating by current pulse has a major advantage (before pulse laser heating) in volumetric heat generation, which allows more accurate measurements of the specific material properties (density, electrical resistivity, energy input). Experiments have shown that heating by a current pulse allows to increase specific power dissipation (with respect to the stationary experiments) and provide graphite melting in a short time (a few microseconds). The absence of significant heat losses (at this rate of heating $\sim 5 \times 10^9$ K/s), it was set in the study of metals yet,—led to the use of short -time heating for graphite specimens, up to $\sim$1–3 μs. The advantages of these experiments consist, first, in the rapid heating (which prevents the molten liquid specimen to change the shape during heating). Secondly—isochoric heating conditions were obtained under placing the specimens into the dielectric thick-walled tubes (for a short time of the experiment) accompanied by the emergence of pulse pressure. Assessment of specific energy input E(t) absorbed by a unit mass of graphite (Joule heat), was made on the measured current I and voltage U, taking into account the inductance of the specimen. The 4-channel digital oscilloscope Tektronix TDS-754C (bandwidth of 500 MHz) was used.

$$E(t) = \int_0^t \left[I^2(t) \cdot R(t)/m\right] dt$$

where m—mass of the specimen; I—current; R (t)—the electrical resistance, which is calculated by the formula R (t) = [U (t) − L (dI/dt)]/I (t), where U—voltage the specimen; L—inductance of the specimen. The total measurement error of the specific energy input E does not exceed 5 %.

4.2 Melting Area Recorded Under Pulse Heating and Emissivity Estimation

4.2.1 The Start of Melting and Graphite Emissivity at Milliseconds Current Heating

Recall that the emissivity of the high-density graphite UPV-1TMO (kuazi-monocrystall) studied in detail in [7] (1990).

Experimental study of the graphite melting was fulfilled in [7] under pulse electrical heating during 2–3 ms. Pyrolytic graphite of high quality was used (brand-UPV-1TMO), heat-treated, with the density of 2.25 g/cm^3. The crystallite size has 10 μ, the orientation angles of the crystallites relative to the axis “c”—30 min. Due to the high plasticity of this graphite the difficulties arise in the preparation of desired geometry. Final specimens were rods with square section 1 × 1 mm and with the length 20 mm (Fig. 4.18).

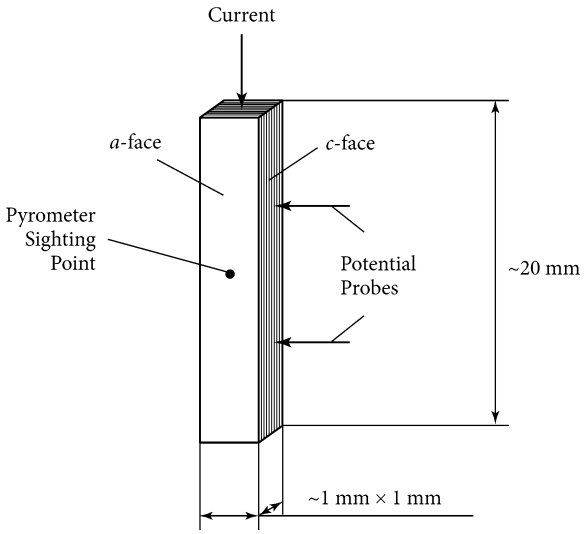

Fig. 4.18 Specimen for graphite UPV-1TMO designed for pulsed current heating

As the Fig. 4.18 shows, pyrometer was sighted on the plane of deposition (a-plane). Voltage signal was removed by the potential electrodes (tungsten), which were attached to the plane "c". The scheme of high-pressure chamber is shown in Fig. 4.19.

A chamber was filled with argon at high pressure (up to 2 kbar). The temperature plateau under graphite melting is shown in Fig. 4.20 (the shape of pulse current—in Fig. 4.21).

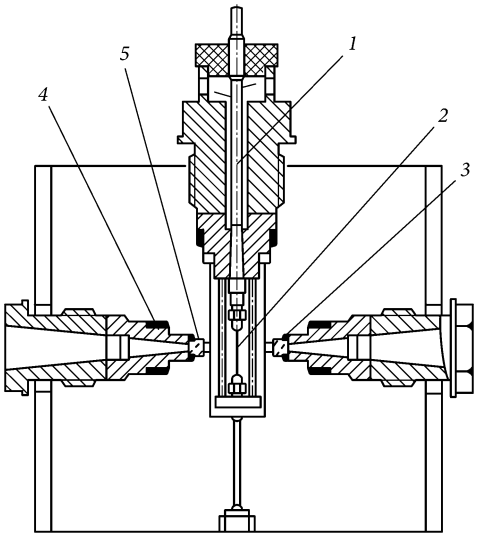

Fig. 4.19 High-pressure chamber (*1* input; *2* specimen; *3* seal; *4* gasket; *5* sapphire window)

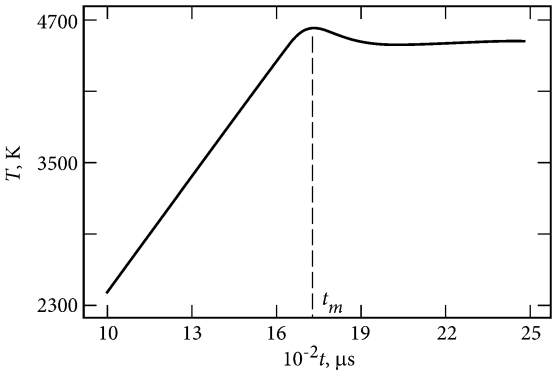

Fig. 4.20 ([7], 1990). The start of melting temperature plateau at the surface "a" for flat specimen of highly oriented graphite grade UPV1-TMO. Y-axis—the brightness temperature, K; abscissa—time from 1 ms (symbol 10) to 2.5 ms (symbol 25). T (at the melting point) = 5080 ± 70 K [7]. Measured emissivity ε at a temperature 4000 K equals 0.71; (ε at the melting point is taken equals 0.6)

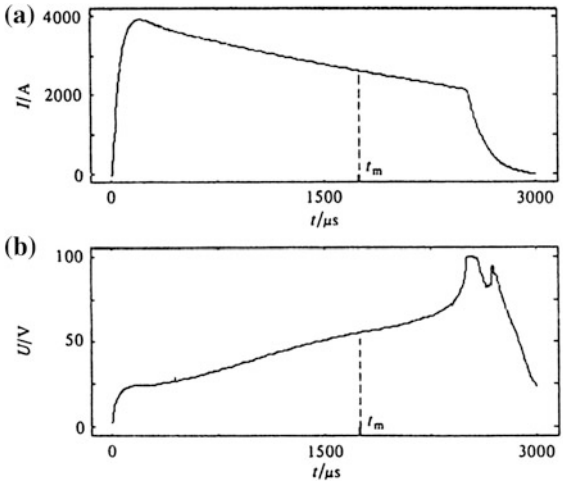

Fig. 4.21 The shape of the current pulse (**a**) and the voltage at the potential electrodes (**b**) versus time **t** (in microseconds); **t**m—the start of melting, fixed in the previous Fig. 4.20

Previously, the study of graphite grade UPV-1T [33] in 1988 year, it was carried out temperature measurement, when fixing the pyrometer on the plane "c". The emissivity of that plane was 0.95 for the wavelength of 0.65 μ, and weakly dependent on temperature. In this study [7], the plane "a" was used giving a better reproducibility of the temperature signal for specimen UPV-1TMO. However, the authors [33] did not know the exact value of the monochromatic emissivity of the plane "a", so additional measurements were performed in [7].

Pyrometer was calibrated by a standard tungsten lamp up to 2500 K and by a blackbody model in the range 2000–3300 K. The reflection of helium-neon laser

pulse on the "a" plane allowed to estimate emissivity ε of the plane "a" by a formula ε = 1—ρ, where ρ—reflectivity. The average value of the emissivity of liquid carbon (for 5 specimens used) was found to be 0.6; it is close to the emissivity of liquid metals.

The enthalpy at the beginning of melting is 10.4 kJ/g, the melting temperature equals 5080 K [7]. The result of reflectivity measurements is shown in Fig. 4.22.

In the same 1990 year Ared Cezairliyan investigated melting of graphite of low initial density, brand POCO graphite (Fig. 4.23).

Y-axis—the brightness temperature, K (at a wavelength of 655 nm), the x-axis—time in milliseconds. Argon pressure in the chamber equals 140–200 bar.

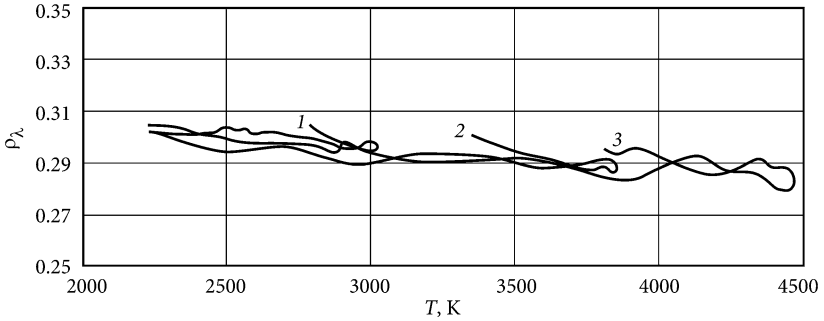

Fig. 4.22 Dependence of reflectivity ρ for UPV1-TMO (at the λ = 0.63 μ) against temperature for three series of the experiments. The total error for temperature measurement ±4 %, error for reflectivity measurements ±6 %. The emissivity value may be obtained as (1 − ρ)

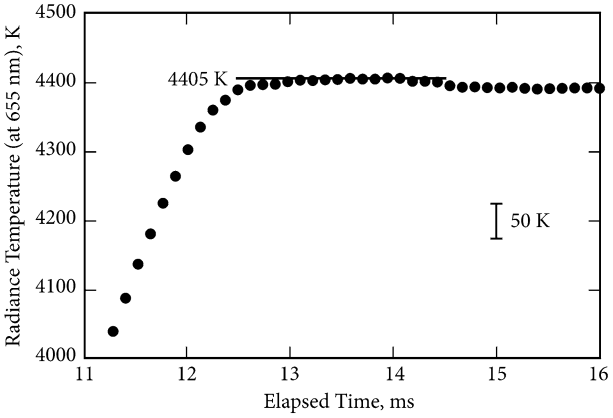

Fig. 4.23 ([34], 1990). The start of the radiance temperature plateau at the melting of the polycrystalline graphite, grade POCO

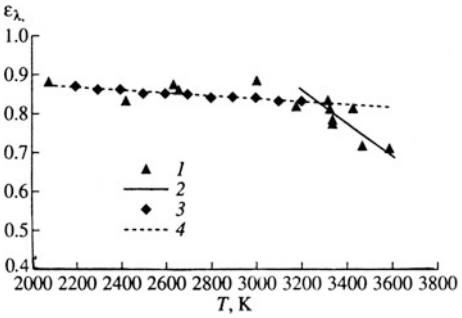

Fig. 4.24 Normal spectral emissivity ε for isotropic graphite MPG-7 (λ = 650 nm) against temperature [36]. The maximum measuring temperature of spectral emissivity ε was 3600 K. *1* Results of the study [36]; *2* smoothing; *3* Results of the handbook [35]; *4* smoothing of the handbook results

Introduction of oxygen into the high pressure chamber (for transferring graphite vapor to transparent gas CO_2) led to an increase in the measured temperature (the oxygen partial pressure of 40 bar will give a temperature rise of 80 K).

In [37] it was obtained the melting temperature 4530 ± 150 taking into account emissivity 0.8.

According to the reference data, the emissivity of graphite at high temperature (near 3000 K) is indeed equal to 0.8 [35]. At the same time for carbon, starting around 3200 K the normal spectral emissivity which has a falling character [36] but at temperatures around 3600 K it is reduced to 0.67 (Fig. 4.24).

4.2.2 The Whole Temperature Plateau Recording (First Published) for Graphite of Low Initial Density

In [9, 16] it was shown that at the heating by electric current of not very dense (less than 2 g/cm^3) graphite specimens (and also annealed below 3000 °C),—at the initial stage of heating the electrical resistance diminishes. This leads to the strengthening of not uniform heating of graphite by electric current, as the more power begins isolate in the micro-regions with the falling electric resistance. Thus, the high initial density of the graphite specimens and their deep annealing are the conditions for the homogeneous graphite heating. Initial resistivity of dense graphite after this preparation is 50 μΩ cm. Measuring the electrical resistance of graphite specimens can be an additional control of homogeneity of heating and achievement of fusion area.

For the first time a full temperature plateau under graphite melting was obtained in the work [37] in 1993 year. This is the main achievement of this work. Unfortunately the choice of the graphite brand was unsuccessful. As it was shown in the study, graphite of low initial density is heated unevenly, as a result the

resistivity of graphite in the field of melting poorly reproducible. The authors rightly noted that this graphite is not suitable for studies at the liquid state.

Reference [37] shows the experimental data on the thermal and electrical properties of graphite mechanically strong brand POCO (AXF-5Q), heated by electrical pulses. The heating time was ranged from the microseconds up to nanoseconds. This study was performed independently in two laboratories: in Graz (Austria) and in Los Alamos (USA) on specimens from the same batch. Initial density of graphite $\gamma = 1.83$ g/cm^3. Graphite specimens of diameter 1 mm, length 20 mm were investigated.

Based on the analysis of microphotographs of the surface and the fracture of the specimen the authors [37] have noted that despite the external macroscopic uniformity, there is microscopic inhomogeneity—irregularities in the structure. The external environment—water under pressure 3 kbar (Graz), and argon pressure of 3 kbar (Los Alamos).

In [37] it was obtained the temperature plateau in the time-temperature dependencies (Fig. 4.25).

As one can see, the plateau obtained in Graz, at a half of the range of melting has a growing nature. The plateau obtained in Los Alamos has significant curvatures at the start of melting and upon its completion. Melting point (under P = 3 kbar) obtained in measurements of the authors [37] is 4900 ± 200 K. In [37] it was shown a photo of the cylindrical graphite specimen with a separate bright shining spots on the surface, as the evidence of an inhomogeneous of electric heating graphite of a small initial density. Not accidentally, the authors of [37] claimed: "*this graphite is not suitable for studies of liquid state.*"

A comparison for specific enthalpies obtained under the maximum for Los Alamos T = 4775 K, gives 8.69 kJ/g (Graz) and 8.00 kJ/g (Los Alamos). The authors [37] give specific enthalpy at the start of melting: Hsolid = 9.02 kJ/g (Graz)

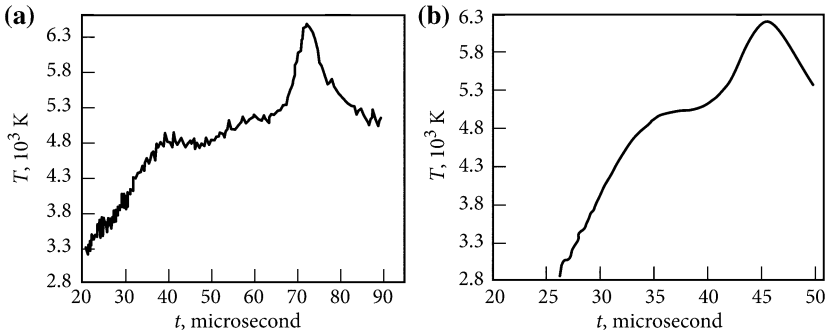

Fig. 4.25 ([37], 1993). Temperature plateau with a single pulse heated by electrical current of graphite POCO with low initial density (1.83 g/cm^3). **a** Experiment in Graz (Austria). **b** Experiment in Los Alamos (USA) with the same specimens of the same graphite grade. Emissivity is in the whole range of temperature measurements was taken equal to 0.8, according to Cezairliyan and Miiller [34]

for T = 4900 K. As we see, the experiments with non-uniform graphite give Hsolid smaller than were received by Bundy [1] (10.45–13.9 kJ/g).

The authors of [37] give a "*rough*" estimate of the heat of fusion: 8 kJ/g (Graz) and 9 kJ/g (Los Alamos). It was determined the heat capacity of the solid phase, which has a constant value over a wide temperature range: Cp = 2.64 J/g K for T = 3000–4950 K (Graz), Cp = 2.06 J/g K for T = 2840–4775 K (Los Alamos). Even more significant difference is observed in [37] for measuring the volume of the heated graphite. For the same of specific enthalpy 8.5 kJ/g (even for the solid phase) it was fixed volume as a relation to the initial volume: V/Vo = 1.69 (Graz) and 2.47 (Los Alamos).

That is, the volume of graphite even in a solid phase would increase significantly (diameter obtained by the illumination of the diameter of the cylindrical sample in a certain section). A significant expansion near melting the authors (Los Alamos) explained by the instabilities associated with the expansion of the less dense environment (expanded graphite) in a more dense medium (argon at high pressure). Apparently, there is a brittle fracture of the graphite before melting. Thus, the low density graphite may be destroyed before reaching the melting point. The micro-cracks may be appeared in the solid state of low initial density before melting, which can be allocated additional energy by burning electric arc.

This will lead to the strengthening of non-uniform heating and can also lead to high pressure (>100 bar) in some places collapsing sample [38, 39]. In this case the specimen will not melt, as a whole, but in some areas the melting can take place. Therefore, the visual observation of "traces of melting" for graphite (for example, in [40])—is not sufficient to argue that the pyrometer temperature recorded the entirely melted of graphite specimen.

According Fig. 4.25a, [37] the initial electrical resistivity equal to 1000 μΩ cm is growing up to a maximum of the 3700 μΩ cm (referred to the initial sizes of the specimen) at the input specific enthalpy H = 11.5–12 kJ/g (Graz). The calculation of the authors [37] for specific resistivity for solid graphite (including expansion) for the same input energy H = 8.05 kJ/g gives 4573 μΩ cm (Graz) and 3665 μΩ cm (Los Alamos). Error for resistivity measurement according to ([37]: 10–20) %. Apparently, the heating rate in these experiments was not high enough; along with the heterogeneity of the specimens;—all of this could lead to fracture of the specimens in the later stages of heating.

Back in 1998, after numerous experiments with low density graphite it was indicated [16], that the current heating of the graphite specimens only with high initial density UPV-1T (porosity is close to zero [41]) can lead to success in the study of liquid carbon, in particular under measuring the graphite thermal expansion.

This program was implemented in [10, 42] and the result was obtained for the melting point with application of solid-state optical fibers (4800 ± 200 K), enthalpy at the start of melting (10.5 kJ/g), the heat of fusion (10 kJ/g), the heat capacity (4.2 J/g K) for liquid carbon. Also it was measured electric resistivity of liquid carbon: 730 μΩ cm (±7 %) for the density 1.8 g/cm^3 (pressure–dozens kbar).

Estimation of thermal expansion under graphite melting gives 70 % [10, 11] (pressure P ~ 1 kbar); 45 % [43]; 50 % [44].

Recall that graphite is a complex structure with different expansion coefficients in the directions of "a" and "c" planes. The most modern experimenters have worked with specimens of high-oriented graphite with square section (density 2.26 g/cm^3), it is provided by independent expansion on two axes under electrical heating [7, 10, 11, 33, 42, 45].

4.2.3 *Particular Feature of Recording of Graphite Melting Under Laser Heating*

Consider the article [46], published with the description of the installation for slow laser heating, intended for research and evaporation of refractory materials at a gas pressure of up to 300 MPa and temperatures up to 8000 K. It was studied the evaporation of carbon at temperatures up to 7000 K. The pyrometer was used at a wavelength of 0.656 microns.

The maximum temperature curve (~7000 K), the authors [46] consider to be boiling point for carbon corresponding 1 kbar pressure. A break at a temperature of about 5500 K takes place in the curve of Fig. 4.26. The authors of [46] did not attach any importance to this break. In our opinion, a break— it's a melting point of the specimen. In this case, the derivative dT/dt diminishes at this point. The reason in the high thermal conductivity of this grade graphite (in the direction of the laser heating of the plane "c"). At this moment the input energy ensure melting and at the same moment the part of the input energy may be "sucked off" into the specimen melting.

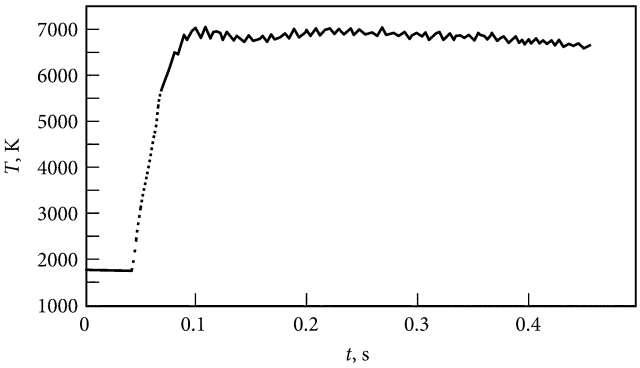

Fig. 4.26 Thermogram of laser heating of the pyrographite specimen in helium at a pressure of 1 kbar (heating of the laser spot on the plane "c"). The authors of [46] considered the temperature plateau at the level 7000 K to be a boiling temperature for carbon at 100 MPa

Give the second example for recording a start of graphite melting by laser pulse.

M.A. Sheindlin and M.V. Brykin with the colleagues [43] show that the laser heating of specimens of the two types of graphite (HOPG and artificial graphite RW1) have different results: liquid carbon has a very high surface tension under poor wettability of basal plane "a" for the pyrolytic graphite HOPG. According to the authors [43] it is for this reason that a film of liquid carbon removed (disappeared) from the surface "a" during the experiment, which made it impossible to observe the liquid carbon on the surface "a" for the HOPG graphite specimens after the experiment. That's why instead of HOPG graphite in [43] it was used graphite RW1 (initial density 1.55 g/cm^3).

For this graphite grade the molten part of a specimen retained on the surface after the experiment [43]. In [40, 47] no measures have been taken (or are not reported) to ensure the quality of temperature measurements, such as those that have been taken in [43, 48, 49]. Figure 4.27 shows the experimental data of temperature measurements obtained in [43]. Pay attention to the fact that the beginning of melting (at 5000 K) is recorded only on the change in the slope of the temperature signal that is growing with time. During the cooling phase, the temperature of solidification (4850 K) is recorded on the temperature delay of the temperature diminishing. The difference between these two temperatures is in the range of measurement error (±150 K) [43].

Such a break again was appeared in Fig. 4.27, but in contrast to the above mentioned Fig. 4.26, with increasing the derivative dT/dt. In a latter case, the density of the isotropic graphite RW1 is 1.55 g/cm^3 and it has a low thermal conductivity (the heat released on the surface has no possibility to be "sucked off"

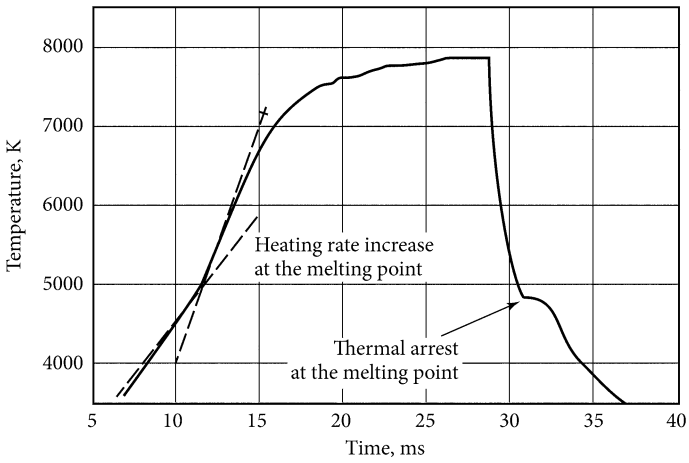

Fig. 4.27 The graphite melting RW1 (density 1.55 g/cm^3) at a laser heating [43]. The change in the slope at the front of growing temperature is interpreted by the authors of [43] as the start of melting

by inner layers of the specimen), which resulted in the acceleration of the heating of the surface layer of the graphite specimen.

Pay attention to the fact that the increase of the rate of heat at this point can be explained by the fact that after the melting of the surface layer it continues heating further, since the low heat conductivity of liquid carbon (5 W/m K 43 [41]) does not allow to remove heat quickly from the molten surface deep into the sample. That is why the derivative dT/dt is growing steeper after the start of the melting of the surface layer.

Figure 4.27 shows the experimental data of temperature measurements obtained in [43]. Pay attention to the fact that the beginning of melting (at 5000 K) is recorded only on the change in the slope of the temperature signal that is growing with time. During the cooling phase, the temperature of solidification (4850 K) is recorded on the temperature delay of the temperature diminishing. The difference between these two temperatures is in the range of measurement error (±150 K) [43]. Authors of [43] have carefully analyzed their measurement and the results provide evidence for the triple point of carbon: P = 110 ± 20 bar; T melt = 4800 ± 150 K (for the pressure 1–2 kbar).

The only case when temperature plateau was recorded under laser heating was published in [49]. The study [49]—this is a unique case of fix the melting temperature plateau under pulsed laser heating of the surface "a" of anisotropic graphite UPV1-TMO of highly oriented grade (like HOPG). Figure 4.28 shows a thermogram of the heating surface "a" (surface of deposition) for graphite HOPG by laser radiation while limiting the volume above the surface [49]. The diameter of the radiation spot equals 3 mm and the diameter of the pyrometer sight spot −0.5 mm.

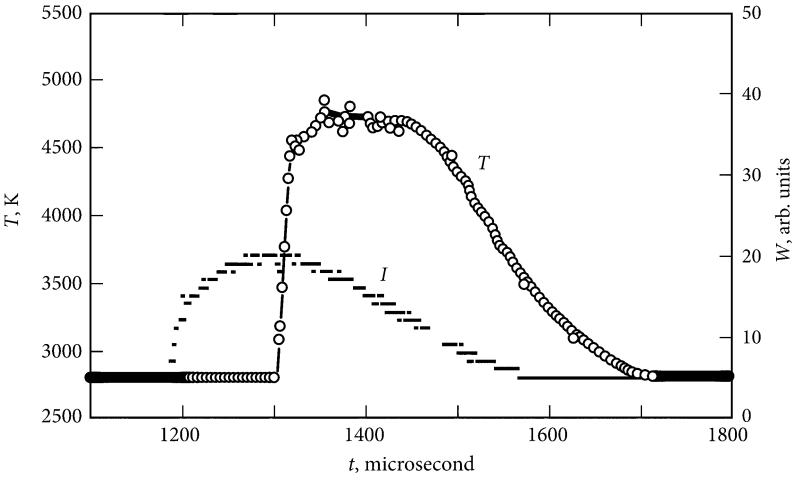

Fig. 4.28 [49] Thermogram for graphite heating by laser pulse while limiting the volume above the surface (the initial graphite density 2.26 g/cm^3). *I* The shape of the laser pulse. Y-axis on the right-hand side—the laser power in arbitrary units. T—temperature of the surface "a" of graphite. T melting = 4800 ± 100 K, (emissivity ε = 0.65)

A visible heterogeneity is seen at the start of the temperature plateau (by the opinion of the authors [49], melting begins in some separate hot spots and then spreads to the whole spot).

The true monochromatic normal emissivity ε_n was taken equal to 0.65 [50] in the range from 2750 K to the melting point during the conversion of the brightness temperature into the true temperature.

References

1. F.P. Bundy, Melting of graphite at very high pressure. J. Chem. Phys **38**, 618–630 (1963)
2. F.P. Bundy, Direct conversion of graphite to diamond in static pressure apparatus. J. Chem. Phys. **38**(3), 631–643 (1963)
3. I.I. Kornilov, *New Materials and Investigation Methods of Metals and Alloys* (Metallurgy, Moscow, 1966) (in Russian)
4. F.P. Bundy, R.H. Wentorf, Direct transformation of hexagonal Boron Nitride to denser forms. J. Chem. Phys **38**, 1733815 (1963). (6 pages)
5. M. Togaya, S. Sugiyama, E. Mizuhara, Melting line of graphite, in *AIP, Conference Proceedings 1994*, vol. 309, pt.1, pp. 255–258
6. F.P. Bundy, W.A. Basset, M.S. Weathers, R.J. Hemley, H.K. Mao, A.F. Goncharov, Review article: The pressure-temperature phase and transformation diagram for carbon; updated through 1994. Carbon **34**(2), 141–153 (1996)
7. A.V. Baitin, A.A. Lebedev, S.V. Romanenko, V.N. Senchenko, M.A. Sheindlin, The melting point and optical properties of solid and liquid carbon at pressures up to 2 kbar. High Temp. - High Press **21**, 157–170 (1990)
8. J.W. Shaner, Bull. Am. Phys. Soc. **32**, 608 (1987)
9. S.V. Lebedev, A.I. Savvatimskiy, The electrical resistivity of graphite in a wide range of condensed state. High Temp. **24**(5), 671–678 (1986)
10. V.N. Korobenko, A.I. Savvatimski, R. Cheret, Graphite melting and properties of liquid carbon. Int. J. Thermophys. **20**(4), 1247–1256 (1999)
11. V.N. Korobenko, A.I. Savvatimskiy, Blackbody design for high temperature (1800 to 5500 K) of metals and carbon in liquid states under fast heating. Temperature: its measurement and control in science and industry, in *AIP Conference Proceedings*, ed. by D.C. Ripple, 2003, vol. 7, Part 2, pp. 783–788
12. A.M. Knyazkov, A.I. Savvatimskiy, Electrical resistivity of liquid carbon during rapid heating of dense isotropic graphite in different environments. High Temp. **48**(2), 192–197 (2010)
13. A.I. Savvatimskiy, A.M. Kondratyev, S.V. Onufriev, Experiments on the graphite melting under heating by electrical current pulse, Izvestia Vuzov. Chem. Chem. Technol. **56**(7), 53–56 (2013). (in Russian)
14. M. Togaya, Electrical property changes of liquid carbon under high pressures. J. Phys.: Conf. Ser. **215**, 012–081 (2010)
15. A.M. Malvezzi, N. Bloembergen, C.Y. Huang, Phys. Rev. Letters **57**, 146 (1986)
16. A.I. Savvatimskiy, V.E. Fortov, R. Cheret, Thermophysical properties of liquid metals and graphite, and diamond production under fast heating. High Temp.-High Press **30**, 1–18 (1998)
17. M.S. Pirani, in *Elektrothermie; die elektrische Erzeugung und technische Verwerdung hoher Temperaturen*, ed. by M. S Pirani (J. Springer, Berlin, 1930)
18. A.I. Savvatimskiy, V.N. Korobenko, High-temperature properties of metals for nuclear industry (zirconium, hafnium and iron during melting and in the liquid state). MEI Publishing House, 2012, 216 pp. ISBN 978-5-383-00800-3 (in Russian)

19. V.M. Batenin, F.V. Bunkin, N.V. Karlov, V.A. Kirillin, L.P. Pitaevskii, A.M. Prokhorov, A.A. Rukhadze, A.I. Savvatimsky, E. FortovV, A.E. Sheindlin, In memory of Sergei Vladimirovich Lebedev. Phys. Usp. **161**(3), 181–183 (1991)
20. W.G. Chace, H.K. Moore H.K. (eds.) *Exploding wires*, vol. 1. (Plenum, New York, 1959)
21. S.V. Lebedev, Phenomena in tungsten wires before their explosion under high current action. JEPT **27**(5), 605–614 (1954)
22. S.V. Lebedev, A.I. Savvatimskiy, The density of liquid tungsten, at which the sharp drop in conductivity takes place in the process of electrical explosion. High Temp. **8**(3), 494–500 (1970)
23. G.R. Gathers, J.W. Shaner, D.A. Young, High temperature carbon equation of state, UCRL-51644. Livermor **1974**, 1–13 (1974)
24. V.A. Petrov, I.I. Petrova, VYa. Chekhovskoi et al., High Temp.-High Press **2**(2), 155 (1970)
25. A. Cezairliyan, F. Righini, Measurements of heat capacity, electrical resistivity and hemispherical total emittance of two grades of graphite in the range 1,500 to 3,000 K by a pulse heating technique. Rev. Int. Hautes Temp. et Refract **12**, 124 (1975)
26. S.E. Vyatkin, A.N. Deev, V.G. Nagorny et al., *Nuclear Graphite* (Atomizdat, Moscow, 1967), p. 279. (in Russian)
27. S. Dushman, *Scientific foundations of vacuum technology*, 2nd edn. (Wiley, New York, 1962)
28. A.R. Ubbelohde, *Melting and Crystal Structure* (Publishing Company MIR, Moscow, 1969), p. 420
29. H.R. Leider, O.H. Krikorian, D.A. Young, Thermodynamic properties of carbon up to the critical point. Carbon **11**, 555–563 (1973)
30. S.V. Lebedev, Phenomena in tungsten wires prior to their explosion by a high current. JEPT **27**(511), 605–614 (1954)
31. S.V. Lebedev, A.I. Savvatimskiy, in *Investigation of Metals and Graphite Under Conditions of Rapid Electric Heating*, ed. by A.E. Sheindlin, V.E. Fortov. Thermal Physics Reviews, Section B, vol 5, part 3 (Harwood Academic Publishers GmbH, Yverdon, 1993), pp. 1–79
32. S.V. Lebedev, A.I. Savvatimskiy, Metals during rapid heating by dense currents. Sov. Phys. Usp. **27**, 749–771 (1984)
33. M.A. Sheindlin, V.N. Senchenko, Experimental study of the thermodynamic properties of graphite near the melting point. Sov. Phys. Dokl. **33**, 142–145 (1988)
34. A. Cezairliyan, P. Miiller, Measurement of the radiance temperature (at 655 nm) of melting graphite near its triple point by a pulse-heating technique. Int. J. Thermophys. **11**(4), 643–651 (1990)
35. L.N. Latyev, V.A. Petrov, V.Y. Chekhovskoi, E.N. Shestakov, *Radiative Properties of Solid Materials*, ed. by A.E. Sheindlin. Handbook, 471 pp (Energiya, Moscow, 1974) (in Russian)
36. A.V. Kostanovskii, M.G. Zeodinov, M.E. Kostanovskaya, Experimental determination of the emissivity of isotropic graphite at temperatures above 2300 K. High Temp. **39**(1),159–161 (2001)
37. G. Pottlacher, R.S. Hixon, S. Melnitzky, E. Kaschnitz, M.A. Winkler, H. Jager, Thermophysical properties of POCO AXF-5Q graphite up to melting. Thermochim. Acta **218**, 183–193 (1993)
38. G.A. Mesyatz, D.I. Proskurovsky, *Pulsed Electrical Discharge in Vacuum*, 256 pp. (Nauka, Novosibirsk, 1984) (in Russian)
39. B.A. Koval, D.I. Proskurovsky, V.F. Tregubov, E.B. Yankelevich, JTP. Lett. **5**(10), 603 (1979). (in Russian)
40. E.I. Asinovsky, A.V. Kirillin, A.V. Kostanovskii, Experimental investigation of the thermal properties of carbon at high temperatures and moderate pressures. Phys. Uspekhi. **45**, 869–882 (2002)
41. YuS Virgilev, Thermal conductivity of structural carbon materials. Inorg. Mater. **30**(3), 353–362 (1994). (in Russian)
42. V.N. Korobenko, PhD dissertation for the degree of candidate of physical and mathematical sciences. Experimental study of the properties of liquid metals and carbon at high temperatures (Institute for High Temperatures RAS, Moscow, 2001) (in Russian)

43. M. Musella, C. Ronchi, M. Brykin, M. Sheindlin, The molten state of graphite: an experimental study. J. Appl. Phys. **84**(5), 2530–2537 (1998)
44. G.I. Kerley, L. Chhabildas, *Multicomponent-Multiphase Equation of State for Carbon, Sandia Report: SAND2001–2619* (Sandia National Laboratories, USA, 2001), pp. 1–50
45. V.N. Korobenko, A.I. Savvatimskiy, Electrical resistivity of liquid carbon. High Temp. **36**(5), 701–707 (1998)
46. A.V. Kirillin, M.D. Kovalenko, S.V. Romanenko, L.M. Heifetz, M.A. Sheindlin, Apparatus and methods for examining the properties of refractory substances at high temperatures and pressures by stationary laser heating. High Temp. **24**(2), 286–290 (1986)
47. E.I. Asinovsky, A.V. Kirillin, A.V. Kostanovskii, V.E. Fortov, Melting parameters of carbon. High Temp. **36**(5), 716–721 (1998)
48. A.Y. Basharin, V.E. Fortov, Parameters of the triple point of graphite, in *Abstracts of the 14th Symposium on Thermophysical Properties*, ed. by W.M. Haynes, B.A. Stevenson, National Institute of Standards and Technology (NIST), Boulder, USA, 2000, p. 159, 25–30 June 2000
49. A.Y. Basharin, M.V. Brykin, M. Marin, I.S. Pakhomov, S.F. Sitnikov, Ways to improve the measurement accuracy in the experimental determination of the melting temperature of graphite. High Temp. **42**(1), 60–67 (2004)
50. A.Y. Basharin, I.S. Pakhomov, M.A. Scheindlin, The optical properties of polished pyrographite. High Temp.-High Press. **23**, 543 (1991)

Chapter 5
Stationary Experiments on Physical Carbon Properties (Enthalpy and Thermodynamic Functions) Against Temperature

Abstract Experimental steady state data (by Buchnev et al.) on the enthalpy against temperature (steady state experiments up to 3800 K, and further calculation up to 4900 K) are discussed. These measurements is stated as the more reliable data among stationary investigations. The resulting data are close to the measurements under fast heating by pulse of electric current. The possible high expansion (50–70 %) of carbon under melting was obtained in some experiments.

5.1 Enthalpy Against Temperature (Steady State Experiments up to 3800 K, and Further Calculation up to 4900 K)

The classical studies of graphite were fulfilled in NIIGRAFIT, Moscow (Institute for graphite investigation) in 1973. The authors of [1] studied the temperature dependence of the enthalpy of various carbon materials. We may give the details of this study to show the difficulties faced by the experimenter during stationary study of high-temperature properties of carbon. Investigation of the enthalpy of carbon in this work was carried out by mixing method with the use of massive copper calorimeter.

Specimen temperature above 1200 K was measured by laboratory precision optical pyrometer EOP-66, sighting to the hole diameter 1 mm with the depth of 8–10 mm in the lateral surface of the specimen. Estimated degree of blackness hole equals 0.998. Corrects were included for the absorption of radiation by glass.

Glass of the viewing window was protected from dust of sublimating carbon by the water-cooled copper valve, which was opened by an electromagnet at the time of measuring the temperature of the specimen. At temperatures below 1200 K the measurements were made by platinum-rhodium thermocouple (GOST 6016-61), the juncture of which was protected from carbonization by a tip of the copper foil.

The juncture with the protective tip was placed in the hole drilled in the top of the specimen. To prevent the influence of the furnace to the calorimeter system a

A. Savvatimskiy, *Carbon at High Temperatures*, Springer Series in Materials Science 134, DOI 10.1007/978-3-319-21350-7_5

water-cooled pan was located at the bottom of the heater. Calorimeter was made of electrolytic copper and had a cylindrical shape with a diameter of 120 mm and a height of 150 mm. In axial recess inserted a copper sleeve with her wound bifilar heater wire for the calibration of the calorimeter.

Calorimeter was embedded in thermostat shell. System of copper screens was installed between calorimetric block and thermostat shell. Calorimeter temperature was measured by platinum resistance thermometer TSPN-2B, cladding temperature was recorded by copper resistance thermometer graded on a platinum thermometer.

Temperature control of the shell within ±0.002° was produced by water from the thermostat TC-15 through the heat buffer. Resistance of the thermometer, EMF of the thermocouples, current of the pyrometer lamp and heater power during calibration of the calorimeter were measured by DC potentiometer R-348 (accuracy Class 0.002). Battery to supply a potentiometer and thermometer, model coil resistance and regulatory resistance were housed in a temperature-controlled device table, in which during the experiment maintained temperature at 20 ± 0.01°. Calorimeter was graduated by heating of electric current. The temperature dependence of the intrinsic thermal value of calorimeter in the range 288–308 °C was obtained. The maximum deviation of the experimental points of graduation from the smoothing curve did not exceed 0.2 %. Error of calibration was checked by measuring the enthalpy of α-modified alumina. The test specimen containing 99.8 % of $A1_20_3$.

Standard deviation σ of the experimental points from the averaged data, recommended by the Institute of High Temperatures RAS, is 0.38 %. Specimens of quazi-monocrystal, pyrolytic carbon and glassy carbon were investigated. Some characteristics of the materials studied in [1] are listed in Table 5.1

The impurity content in the test specimens did not exceed 0.01 %. Before heating of the specimen the installation unit was evacuated to 0.001 mmHg and filled with high purity helium pressurized to 10 mm Hg. Exposure of the specimen at a setting temperature was not less than 1 h. The correction to the loss of heat by radiation during the falling the specimen into the calorimeter was calculated according to the integral degree of emissivity obtained for these materials by AA Dmitriev [2]. This correction was not more than 2 % at 3000 K. Correction to bring the experimental data to 0 K was calculated from the low temperature heat capacity, measured on the same specimens.

Table 5.1 Characteristics of the hydrocarbons under study [1]

Carbon	Volume mass (g/cm^3)	Dimension of the crystallite (Å)	Inter-plane distance (Å)	Heat conductivity at		Resistivity at	
				300 K	W/m K[a]	300 K	Ohm mm^2/m*
Quazimonocrystal	2.26	30000	3.354	1100	6.0	0.5	2000
Glassy carbon	1.45	60	3.60	6	5	45	45
Pyrolytic carbon	2.24	1000	3.36	600	4.5	2	–

[a] In the directions of maximum and minimum of the electro-conductivity

Table 5.2 Experimental data for investigated hydrocarbons, kJ/kg

T, K	H_T	$\frac{H_{exp}-H_{cal}}{H_{cal}}$ %	T, K	H_T	$\frac{H_{exp}-H_{cal}}{H_{cal}}$ %
Quazimonocrystal			Pyrolytic carbon		
298.16	84.10	+0.1	1187	1415	+0.1
500.0	282.8	−0.4	1224	1484	0.0
830.0	785.3	+1.8	1279	1596	+0.4
1140	1331	+0.5	1379	1808	+1.2
1523	2062	−0.5	1550	2101	−1.2
2005	3063	−0.2	1973	2999	−0.1
2010	3085	+0.1	2002	3043	−0.7
2504	4137	+0.02	2528	4176	−0.3
2353	4172	−0.8	2781	4757	+0.4
2773	4732	+0.2	2852	4886	−0.1
2789	4745	−0.2	2893	4982	−0.1
2958	5122	−0.06	2927	5067	+0.2
2956	5153	+0.6	2934	5050	−0.4
3257	5820	+0.7	3005	5228	0.0
σ = 0.5			3105	5478	+0.6
Glassy carbon			3222	5717	+0.2
1548	2177	−0.3	881	859.0	+0.2
1966	2996	+0.2	934	956.9	+0.8
2525	4165	−0.4	σ = 0.5		
2535	4192	−0.3			
2832	4853	+0.1			
2866	4924	+0.06			
2980	5167	−0.1			
534	326.3	−0.1			
757	659.8	+1.3			
858	812.9	−0.6			
1095	1247	+0.4			
σ = 0.5					

Experimental values of the enthalpy for investigated materials are shown in Table 5.2.

It is seen from Table 5.2 that the maximum temperature reached by the authors of the specimens not exceeds 3300 K, and this temperature is insufficient to melt the carbon specimen.

Next work of L.M. Buchnev was performed with colleagues in 1987 [3]. The new work contains very important stationary data results at extremely high temperatures. Experiments were conducted on quazi-monocrystal graphite and glassy carbon to the maximum possible temperature. To assess the validity of their calculations of the triple carbon point the authors [3] provide a reference to the experimental work [4], carried out under the guidance of A.V. Kirillin and M.A.

Table 5.3 Chemical content of investigated specimens

Impurity	Content of the impurity, 10^{-7} %		Impurity	Content of the impurity, 10^{-7} %	
	UPV-1T graphite	Glassy carbon		UPV-1T graphite	Glassy carbon
Fe	20–50	$4 \cdot 10^3$	Sn	0.3	10^3
Mg	10–30	10^3	Si	70–100	$2 \cdot 10^4$
Mn	1	10^2	Zn	30	–
Al	20–40	$2 \cdot 10^4$	Bi	3	10^2
Ti	5	10^3	Ag	0.3	–
Cu	3	$5 \cdot 10^2$	Cd	3	10^2
Ni	3	10^2	Au	3	–
Ca	50–160	10^4	Pb	3	10^2
Na	–	40	Co	–	10^2

Sheindlin in 1985, which shows the parameters of the triple point: P = 102 bar, T = 5000 ± 200 K.

Chemical composition of the investigated specimens in [3] are presented in Table 5.3.

Table 5.4 presents the results of experimental studies (up to T = 3818 K).

Results of Table 5.4 were used for calculations of the carbon properties at higher temperatures. Choosing of quazy-monocrystal graphite (UPV-1T) is due to the proximity of its structure to the single-crystal data and the presence of low-temperature data [5, 6]. In the frame of the joint work of NIIGRAFIT, NPO Metrologia and Institute for High Temperatures of RAS, the data were obtained in the form of Table of standard reference data [7]. To expand the temperature level reached earlier by the authors [7], they have developed a new high-temperature heater. A heater was elaborated in the form of two coaxial cylinders of graphite included in the electrical circuit in series and placed in protective covers of pyro-graphite. This design ensures reliable operation of the furnace up to 3800 K. The amendment on heat loss by radiation during the fall of the specimen in the calorimeter gives the main contribution to the error in determining the enthalpy under the temperatures above 2900 K. The value of this correction was 2.4 % for the temperature 2890 K and 8.8 % for the temperature 3818 K. The correction was calculated by Stefan-Boltzmann law (emissivity assumed to be equal 0.9).

X-ray diffraction analysis was carried out of the investigated specimens during experiments in process of temperature increase. The authors have made an important conclusion: "*The heating of quazy-monocrystal graphite and glassy carbon up to 3800 K did not lead to a change in the basic parameters of the crystal lattice of these materials.*" That is the melting of the specimens was not achieved. The temperature 3800 K is apparently maximum possible for the methods based on stationary calorimetric method. This important experimental results have not been considered further by researchers, for which the most appropriate melting temperature of graphite is considered to be 3800 K [8].

Table 5.4 Results of measurements and calculations

T, K	H(T) − H (0) (kJ/mol)	δH (%)	T, K	H(T)–H (0) kJ/mol	δH (%)	T, K	H(T)–H (0) (kJ/mol)	δH (%)
Quazy-monocrystal graphite								
(a) Primary Data								
298.16	1.010	0	2005	36.79	+0.1	2789	56.99	+0.2
500	3.398	0	2010	37.05	+0.5	2958	61.52	+0.2
830	9.432	+1.7	2504	49.69	+0.5	2956	61.89	+0.9
1140	15.99	+0.2	2535	50.11	−0.3	3257	69.90	+0.5
1523	24.77	−0.5	2773	56.84	+0.7			
(b) Installation with an improved calorimeter								
775.7	8.251	+0.6	2584	51.70	+0.3	2787	57.11	+0.4
847.3	9.637	0	2588	51.82	+0.4	2831	58.32	+0.6
995.2	12.75	+0.1	2595	51.75	−0.1	2843	58.46	+0.2
1096.2	14.96	−0.1	2621	52.63	+0.3	2872	5869	−0.7
1176	16.71	−0.3	2656	53.60	+0.4	2899	59.59	−0.4
1302	19.75	+0.4	2704	54.56	−0.2	2921	60.98	+0.9
2169	40.71	−0.4	2704	54.82	+0.3	3009	63.39	+1.0
2581	51.52	+0.1	2734	55.76	+0.5	3072	65.10	+1.0
(c) Improved Data								
2890	59.66	+0.1	3074	64.36	−0.3	3410	73.75	−0.1
2914	60.67	+0.7	3132	66.24	+0.2	3431	73.94	−0.6
2915	60.28	+0.1	3166	67.00	−0.3	3485	76.07	+0.1
2947	61.30	+0.4	3201	67.81	−0.2	3524	77.05	+0.8
3008	63.25	+0.8	3229	69.12	+0.5	3545	78.39	+0.9
3041	63.89	−0.1	3253	69.09	−0.5	3626	80.09	0
3056	63.96	−0.1	3313	71.14	+0.1	3790	85.03	+0.3
(d) Installation of NPO “Metrologia”								
1200	17.13	−1.1	1635	27.93	+1.1	2149	40.47	+0.2
1241	18.23	−0.1	1709	29.31	−0.4	2237	42.62	0
1373	20.98	−1.6	1770	30.84	−0.2	2286	44.01	+0.3
1401	21.82	−0.8	1864	33.36	+0.4	2359	46.08	+0.8
1453	23.11	−0.5	1930	34.99	+0.3	2423	48.05	+1.4
1583	26.31	−0.1	2072	38.41	−0.1	2500	49.34	−0.1
Glassy carbon								
(a) Primary Data								
534	3.919	+0.1	1548	25.43	−0.5	2535	50.35	+0.3
757	7.925	+1.1	1600	26.59	−0.6	2832	58.29	+0.5
858	9.764	−0.9	1966	35.98	+0.6	2866	59.14	+0.5
1095	14.98	+0.1	2525	50.03	+0.2	2980	62.06	0

(continued)

Table 5.4 (continued)

T, K	H(T) − H (0) (kJ/mol)	δH (%)	T, K	H(T)–H (0) kJ/mol	δH (%)	T, K	H(T)–H (0) (kJ/mol)	δH (%)
(b) Improved Data								
3130	65.51	−0.8	3545	77.44	−0.4	3723	83.48	+0.5
3402	72.86	−0.9	3587	78.94	0	3777	85.04	+0.4
3503	75.89	−0.8	3596	79.31	+0.1	3782	84.13	−0.9
						3818	86.10	+0.1

Buchnev et al. [3] note that remained unexplored temperature range is 3800–5000 K. The authors of [3] have an attempt to describe the obtained results on the basis of known physical representations, considering oscillatory components of internal energy in Debye approach; setting the temperature coefficient of thermal expansion ($20 \cdot 10^{-6}$ 1/K); volume of graphite; compressibility; anharmonicity constant; constant of electronic and vacancy components; energy of vacancies formation ($294 \cdot 10^{3}$ J/mol). The results of calculations of thermodynamic functions listed in Table 5.5.

Authors [3] also calculated the equilibrium line gas–solid and temperature of the triple point (Table 5.6). Data for the gas phase and the heat of sublimation is taken from [9]. Pressure at the triple point is assumed to be 102 atmospheres. Temperature of the triple point according to the authors [3] was 4900 K, which is very close to the result of [4] (5000 K).

Subsequently, in experimental studies with pulsed electric heating it was obtained melting temperature of carbon study will be discussed below. Therefore, we should recognize that calculations of Buchnev for temperature at the melting point of carbon are very close to the experimental results obtained in pulsed heating studies. For the example: (Sheindlin and Senchenko [10]—more 4700 K; Cezairliyan [11]—4530 K; Korobenko et al. [12]—4800 K; Pottlacher and Hixson [13]—4900 K; as well as Basharin et al. [14]—4800 K).

5.2 Expansion Graphite upon Melting (Calculation)

We write the Clausius-Clapeyron equation in the following form for the melting point of carbon, provided that this equation is also valid for an anisotropic material (graphite):

$$\mathrm{Vliquid/Vsolid} = 1 + \Delta\mathrm{Hmelting/Vsolid}\ (\mathrm{Tmelting} \times \mathrm{dP/dT}),$$

where Vliquid—volume of liquid phase at the melting point; Vsolid—volume of the solid phase at the melting point (Vsolid $\sim 1.2V_0$—literature data); Δ Hmelting—melting heat (10 kJ/g—our measurements); Tmelting—melting temperature

Table 5.5 Thermodynamic functions for graphite UPV-1T

T, K	H(T)–H(0) kJ/mol	C^0p J/molK	S^0 J/molK	$-\Phi^0$ J/molK
298.15	1.0098	8.606	5.432	2.045
300	1.026	8.67	5.48	2.07
400	2.062	11.95	8.44	3.29
500	3.398	14.70	11.41	4.62
600	4.982	16.87	14.29	5.99
700	6.758	18.56	17.03	7.38
800	8.680	19.86	19.60	8.75
900	10.72	20.88	21.99	10.08
1000	12.85	21.68	24.23	11.38
1200	17.32	22.85	28.30	13.87
1400	21.97	23.65	31.89	16.20
1600	26.76	24.25	35.09	18.36
1800	31.65	24.70	37.95	20.36
2000	36.63	25.07	40.58	22.27
2200	41.68	25.38	43.00	24.06
2400	46.78	25.68	45.24	25.74
2600	51.95	25.99	47.30	27.31
2800	57.19	26.37	49.20	28.78
3000	62.51	26.86	50.96	30.12
3200	67.94	27.54	52.68	31.45
3400	73.54	28.47	54.37	32.74
3600	79.35	29.73	56.06	34.02
3800	85.46	31.38	57.75	35.26
4000	91.93	33.48	59.46	36.48
4200	98.88	36.07	61.20	37.65
4400	106.41	39.18	62.98	38.80
4600	114.60	42.84	64.82	39.90
4800	123.58	47.04	66.74	41.00
4900	128.40	49.35	67.75	41.54

(4800 K—our measurements); dP /dT = 54 bar/K [15] or dP/dT = 300 bar/K [16]. The latter seems to be overestimated as compared with our and Bundy's data. Then we obtain: Vliquid/Vsolid $\sim$ 1.7

As it turned out, the graphite expands considerably during melting. Expansion during melting is $\sim$70 % for low pressures ($\sim$0.1–1 kbar). According to the phase diagram above 50 kbar pressure graphite during melting should be compressed. Our independent measurement technique using capillary sapphire tubes, obtained the relative rise of V/V_0 = 1.68 [17] when the specific energy input equals 18 kJ/g, which is close to the end of melting (20.5 kJ/g). Pressure level in [17] can be attributed to low pressures (up to 1 kb). This confirms the strong expansion under the graphite melting at pressures up to 1 kbar.

Table 5.6 Equilibrium vapor pressure of carbon

T, K	$P(C_1)$ atm.	$P(C_2)$ atm.	$P(C_3)$ atm.	$P(C_4)$ atm.	$P(C_5)$ atm.	∑P atm.
3000	0.000052	0.000034	0.000343	0.000001	0.000007	0.000437
3200	0.00031	0.00026	0.00254	0.00001	0.00009	0.00321
3400	0.0015	0.0016	0.0146	0.0001	0.0008	0.0186
3600	0.006	0.0076	0.0678	0.001	0.006	0.0884
3800	0.021	0.031	0.264	0.006	0.034	0.356
4000	0.062	0.108	0.880	0.026	0.159	1.235
4200	0.17	0.33	2.61	0.11	0.64	3.86
4400	0.42	0.92	6.89	0.37	2.19	10.79
4600	0.97	2.32	16.70	1.15	6.75	27.89
4800	2.0	5.35	37.0	3.20	18.34	65.9
4900	2.9	7.9	53.5	5.1	29.2	98.6
4908	–	–	–	–	–	102.0

For expanding substances during melting and the electrical resistivity in the liquid state ($\sim$700 μΩ cm), the molten graphite, apparently retains covalent bonds, which are usually characterize of solid graphite. Obviously, the liquid carbon has a complex molecular structure. Here it is pertinent to note that the pressure significantly affects the expansion of graphite during melting, expansion is directly related to the magnitude of the electrical resistivity. Initial observations can be stated as follows. The greater the pressure, the graphite expands less during melting, and the minimal resistivity liquid phase has upon melting. Conversely, the less pressure to be applied, the more the graphite expands by melting, and the greater has the resistivity of the liquid carbon.

One can imagine that the liquid carbon—it's as if tightly compressed carbon gas which expands freely as soon as the pressure is reduced. The reason for such behavior of the liquid carbon apparently lies in its ability to sublime even in the solid phase at low pressures, temperatures ranging from 2800 K (in vacuum) or 3600 K (with a pressure of 1 bar in a protective medium). Recall that in 1911 Watt and Mendenhall [18] noted that graphite sublimates at high temperatures not only from the surface but also in the internal pores, which leads to break of graphite (heated at low pressure).

Obviously, the pressure needed to convert solid carbon into the liquid, and then begins technology. For technological process it would be very tempting to manage the transformation of liquid carbon by acting upon it by external pressure, even in pulsed process. The place will add that the dissolution of the solid graphite in some liquid metals (V, Mo, and W), a diffusion of carbon is so high that corresponds to the diffusion of gases [19]. As noted by the authors of this paper: "*apparently occurs spontaneously dispersing of the graphite in contact with liquid metals and the formation of colloid graphite with a particle size of* 0.01 μ." [19], p. 163. The situation with the dispersion of solid graphite reminiscent of the collapse of liquid

metal on particles of the same size under the electric explosion (see references [17, 20–22]).

In conclusion, we note that since 1963, among 10 research centers of different countries, only in two [23–25, 26] it was obtained the lowest melting temperature of graphite 3700–4000 K (exclude the results published LF Vereshchagin [15] as uncertain in its double result, 4000, and 4600 K for different measurement conditions).

In most other reasonably it was represented 4530–5080 K. This difference is greater than the experimental error and indicates an attempt of the authors [26] to create a view of the melting graphite on the basis of incomplete information.

We assume that the reason for the differences between low melting temperature of graphite 3800–4000 K in [26–28] with the most other measurements is to neglect the role of condensed vapor above the surface of graphite at low external pressure, which led to errors in the temperature measurements.

This monograph presents the most reliable experimental data on the properties of graphite at its melting: enthalpy for the start of melting (10.5 kJ/g), enthalpy under completion of melting (20.5 kJ/g), melting heat (10 kJ/g), melting temperature for the melting of the blackbody model (4800 ± 200 K); specific heat capacity of liquid carbon C_P (4.2 J/g K for temperatures from 6000 to 12,000 K).

Experiments of different authors performed under pulse current heating confirm a significant expansion of graphite under melting (at pressure of 1 kbar). Under pulsed laser heating of graphite the expansion during melting is estimated as 45 ± (10 %) at a pressure of 0.3–2.5 kbar) [29]. In [29], it was obtained a melting temperature of graphite 4800 ± 150 K (emissivity is assumed equal to $\varepsilon = 0.65$ at a wavelength $\lambda = 650$ nm). Significant expansion of graphite at the melting point (at low external pressure) allows drawing conclusions about the complex molecular structure of liquid carbon. Recall that under atmospheric pressure expansion of alumina at the melting point is 29.5 % [30], so that a significant change in volume upon melting of molecular crystals—is rare event, but it happens.

With the significant expansion upon melting, and the high value of resistivity in the liquid state $\sim$2000 μΩ cm (for low pressures) the molten carbon apparently retains a covalent bonds, which typically characterize solid state of graphite. It is possible that liquid carbon—it is a mixture of the original graphite fragments with partially broken bonds. At the same time we must not forget that to get liquid carbon we need to spend a lot more energy than for the solid-state phase transition from graphite to diamond [31].

We have measured the electrical resistivity of liquid carbon under the melting $\sim$730 μΩ cm (1.8 g/cm^3 density and pressure estimated at $\sim$54 kbar) is in good agreement with the results of Togaya [16, 32] ($\sim$700 μΩ cm at a pressure of 56 kbar) for the melting curve. Under conditions of low pressures at the completion of melting (20.5 kJ/g) the density of liquid carbon equals 1.2 g/cm^3.

For obtaining the high-temperature data of graphite (near the melting region) under electrical heating it is necessary to use anisotropic graphite specimens of perfect structure (UPV-1T or HOPG),—it allows specimens to expand freely along two axes. This requires a high temperature preliminary annealing before the start of

heating by electrical current. It gives monotonically increasing resistivity which provides uniform heat dissipation. Only under this initial heat treatment one can clearly observe the moments of the beginning and the end of melting on the resistivity curve during the melting of graphite.

We were able to make the direct measurements of the melting temperature of graphite for pressures 1–10 kbar (Tm = 4800 ± 200 K). The surface radiation was used and the radiation of the blackbody design of the graphite was used also. To this value of measured temperature (4800 K) at the same time corresponds to the beginning of the melting the enthalpy equals 10.5 kJ/g). This value of enthalpy of fusion at the start of melting coincides with the data of other authors for a slower heating by pulse of electric current.

In the final experiments with the graphite obtained for a blackbody design made of two strips of graphite was obtained the melting temperature of graphite is also equal to 4800 ± 200 K. The following results for carbon are obtained: the beginning of fusion 10.5 kJ/g, the end of melting 20.5 kJ/g, the heat of fusion of 10 kJ/g, the electrical resistivity of liquid carbon 730 μΩ cm, the heat capacity C_P of liquid carbon 4.2 J/K.

The matching data were obtained by pulse laser heating [14] for the melting temperature of graphite and the crystallization temperature of liquid carbon. A quartz plate was fixed above graphite specimen with a very small gap between them. It prevents the interaction of hot carbon condensate with the cold buffer gas. The heating rate was 10^8 K/s, and the cooling rate of the melt 1.6×10^6 K/s. The coincidence was obtained for the melting and solidification temperature (4800 ± 100 K), indicating that the graphite melting is a quasi-equilibrium process at high rates of heating. These data also confirm the results of our measurements of the melting temperature of graphite (4800 ± 200 K) at a heating rate $\sim 10^9$ K/s under electric current heating.

Reasoned criticism of the few works (for example, [26], which is obtained melting temperature 3700 K by slow electrical heating), is presented in [33]. In the several papers by Korobenko and Savvatimskiy it were obtained experimental data on the properties of graphite under heating by pulse of electric current:

- Enthalpy for the start and the completion of melting: 10.5 and 20.5 kJ/g;
- Heat of fusion: (10 ± 1) kJ/g (estimated in 1986 [17] gives the same value);
- Electrical resistivity of liquid carbon ∼730 μΩ cm (for the density 1.8 g/cm^3, for a few tens of kbar pressure and temperature 5000–7000 K [12, 34];
- Experiment and estimation of thermal expansion of the graphite in the phase transition solid—liquid (using the Clausius-Clapeyron equation) gives about 70 % for pressures P ∼ 1 kbar.

It is known that with increasing temperature a graphite phase equilibrium curve of solid-liquid has a positive derivative (dP/dT > 0) at pressures up to ∼50 kbar (M. Togaya). Moreover, at low pressures (several units of kbar) dP/dT ∼ 50 bar/K, while at higher pressures dP/dT ∼ 300 Bar/K, i.e., the derivative following the curvature of the boundary curve. These derivative values (50 and 300) are found in the scientific literature. Above 50 kbar—the derivative dP/dT is negative

(dP/dT < 0). Thus, at the pressures above 50 kbar a graphite specimen during melting should be compressed (in the phase diagram Bundy this transition is observed at ~80 kbar).

A deep preliminary annealing of the specimens (at T ≥ 3000 °C) is needed. The need for this procedure is determined by the fact that under current heating a graphite specimen should have only increasing of the electrical resistance. This ensures a uniform heating, just as it is ensured by heating the metal in the solid state (with a monotonically increasing of resistivity with increasing temperature).

References

1. L.M. Buchnev, V.I. Volga, B.K. Dimov, N.V. Markelov, Investigation of the enthalpy of the carbons in the range 500–3250 K. High Temp. **11**(6), 1198–1202 (1973). in Russian
2. A.A. Dmitriev, V.I. Volga, A.I. Lutkov, A.V. Vtulkin, in *Proceedings of Report of 4th—All-Union Conference on Thermophysical Properties of Materials at High Temperatures*, Odessa, 1971
3. L.M. Buchnev, A.I. Smyslov, I.A. Dmitriev, A.F. Kuteinikov, V.I. Kostikov, Experimental study of the enthalpy of kuazi-moncrystal graphite and glassy carbon in the temperature range 300–3800 K. High Temp. **25**(6), 816–821 (1987)
4. A.V. Kirillin, M.D. Kovalenko, M.A. Sheindlin, V.S. Zhivopiscev, Experimental study of carbon vapor pressure in the temperature range 5000–7000 K using a stationary laser heating. High Temp. **23**(4), 557–563 (1985)
5. L.M. Buchnev, A.I. Smyslov, I.A. Dmitriev et al., Doklady **278**(5), 1109 (1984)
6. V.I. Volga, B.K. Dimov, V.P. Pukhlyakov et al., *Collection: Structural Materials Based on Graphite*, vol. 5 (Metallurgy, Moscow, 1970), p. 98. in Russian
7. Bergman G.A., Buchnev L.M., Petrova I.I., Senchenko V.N., Fokin L.R., Chekhovskoi V.Ya., Sheindlin M.A., Graphite kuazi-monokristall UPV-1T, M. GSSSD, P. 25–90 . Table of reference data, 1991
8. E.I. Asinovsky, The possibility of melting of graphite in an arc at atmospheric pressure. High Temp. **37**(3), 481–483 (1999)
9. Thermodynamic properties of individual substances, ed. by V.P. Glushko, vol. 2, Moscow: Nauka (1979). in Russian
10. M.A. Sheindlin, V.N. Senchenko, Experimental study of the thermodynamic properties of graphite near the melting point. Sov. Phys. Dokl. **33**, 142–145 (1988)
11. A. Cezairliyan, P. Miiller, Measurement of the radiance temperature (at 655 nm) of melting graphite near its triple point by a pulse-heating technique. Int. J. of Thermophys. **11**(4), 643–651 (1990)
12. V.N. Korobenko, A.I. Savvatimski, R. Cheret, Graphite melting and properties of liquid carbon. Int. J. Thermophys. **20**(4), 1247–1256 (1999)
13. G. Pottlacher, R.S. Hixon, S. Melnitzky, E. Kaschnitz, M.A. Winkler, H. Jager, Thermophysical properties of POCO AXF-5Q graphite up to melting. Thermochim. Acta **218**, 183–193 (1993)
14. AYu. Basharin, M.V. Brykin, M. Marin, I.S. Pakhomov, S.F. Sitnikov, Ways to improve the measurement accuracy in the experimental determination of the melting temperature of graphite. High Temp. **42**(1), 60–67 (2004)
15. L.F. Vereshchagin, Solid state at a high pressure, Nauka. 286 pp. (1981) in Russian
16. M. Togaya, S. Sugiyama, E. Mizuhara, Melting line of graphite, in *AIP Conference Proceedings*, no. 309, pt. 1, pp. 255–258 (1994)

17. S.V. Lebedev, A.I. Savvatimskiy, The electrical resistivity of graphite in a wide range of condensed state. High Temp. **24**(5), 671–678 (1986)
18. O.P. Watts, C.E. Mendenhall, On the fusion of carbon. Phys. Rev. (Series 1) **33**, 65–69 (1911)
19. N.N. Shipkov, V.I. Kostikov, E.I. Neproshin, A.V. Demin, *Recrystallized graphite* (Moscow, Metallurgy, 1979). in Russian
20. A.I. Savvatimskiy, V.N. Korobenko, *High-Temperature Properties of Metals For Nuclear Industry* (zirconium, hafnium and iron during melting and in the liquid state), MEI Publishing House, 216 pp. (2012). ISBN: 978-5-383-00800-3, in Russian
21. S.V. Lebedev, A.I. Savvatimskiy, Density of liquid tungsten, at sharp fall in electrical conductivity during an "electrical explosion". High Temp. **8**(3), 494–500 (1970)
22. S.V. Lebedev, A.I. Savvatimskiy, Metals during rapid heating by electric current of high density Phys. Uspekhi **27**, 749–771 (1984)
23. A.G. Whittaker, Carbon: a new view of its high-temperature behavior. Science **200**, 763–764 (1978)
24. A.G. Whittaker, The controversial carbon solid-liquid-vapour triple point. Nature **276**, 695–696 (1978)
25. A.G. Whittaker, P.L. Kintner, Carbon solid-liquid-vapor triple point and the behavior of superheated liquid carbon. Contract # F04701-74-0075 US Air Force Space and Missile System Organization (SAMSO), pp. 45–47 (1975)
26. E.I. Asinovsky, A.V. Kirillin, A.V. Kostanovskii, Experimental investigation of the thermal properties of carbon at high temperatures and moderate pressures. Phys. Uspekhi **45**, 869–882 (2002)
27. E.I. Asinovsky, A.V. Kirillin, A.V. Kostanovskii, On the carbon phase diagram in the vicinity of the triple point of the solid- liquid-vapor. High Temp. **35**(5), 704–709 (1997)
28. E.I. Asinovsky, A.V. Kirillin, A.V. Kostanovskii, V.E. Fortov, On the parameters of carbon melting. High Temperatures **36**(5), 716–721 (1998)
29. M. Musella, C. Ronchi, M. Brykin, M. Sheindlin, The molten state of graphite: an experimental study. J. of Applied Physics **84**(5), 2530–2537 (1998)
30. S.V. Stankus, P.V. Tyagelsky, Thermal properties of Al_2O_3 in the melting region. Int. J. Thermophys. **15**(2), 309 (1994)
31. F.P. Bundy, Melting of graphite at very high pressure. J. Chem. Phys **38**, 618–630 (1963)
32. M. Togaya, Pressure dependences of the melting temperature of graphite and the electrical resistivity of liquid carbon. Phys. Rev. Lett. **79**(13), 2474–2477 (1997)
33. A.I. Savvatimskiy, Melting point of graphite and liquid carbon. Phys. Usp. **46**, 1295–1303 (2003)
34. Korobenko V.N., and Savvatimskiy A.I., Blackbody design for high temperature (1800 to 5500 K) of metals and carbon in liquid states under fast heating, temperature: its measurement and control in science and industry, in *AIP Conference Proceedings*, ed. by Dean C. Ripple, vol. 7, Part 2, pp. 783–788 (2003)

Chapter 6
Liquid Carbon Properties Against Input Energy Only

Abstract The main discussed results were obtained at the high pressure (14–94 kbar) under slow (millisecond) heating by electrical current (Togaya et al.) during 1997–2010 years. In spite of the fact that only resistivity and enthalpy were measured the authors gave an important conclusion on the appearing liquid state of carbon and on the dependence of resistance versus pressure. Liquid carbon (at the melting point) diminishes its resistance at a pressure lower 50 kbar, and resistance rises at a pressure higher 50 kbar. American scientists (Gathers et al.) obtained experimental data under microseconds heating, that graphite is compacted even in a solid phase, reaching its maximum density near the input energy ~7.5 kJ/g (that is before melting). Thus, graphite of low initial density compacts to the maximum density (2.2 g/cm^3) in the time interval shorter than 1–2 microseconds, and then reaches melting point just as usual graphite of high initial density. The third part of this chapter (also microseconds heating) shows the behavior of resistance for different graphite grades under thermo-compression in sapphire capillary tubes. Korobenko and Savvatimskiy (JIHT, Russia) obtained the data on expansion of carbon at fast microseconds heating and estimated the resistivity of carbon near melting with an expansion included. A detailed data on resistivity versus input energy under fast heating of isotropic graphite MF-307 (Japan production) are discussed. It was mentioned a critical sensitivity of graphite to the start of melting under rising pressure. It was discussed the role of pinch pressure for graphite melting (except its surface). Discovered a critical sensitivity of graphite melting to the magnitude of applied pressure (experiments for graphite sticks heated inside sapphire capillary tubes).

A. Savvatimskiy, *Carbon at High Temperatures*, Springer Series in Materials Science 134, DOI 10.1007/978-3-319-21350-7_6

6.1 Resistivity Against Input Energy Near the Melting Point

6.1.1 Liquid Carbon Resistivity just at the Melting Point (Experiments by Togaya 1997 and 2000)

In 1997 the paper of Togaya [1] was published: the graphite melting line and the electrical resistivity of liquid carbon at high pressure (14–94 kbar) were obtained. The pulse heating of the spectroscopic graphite specimens was used in milliseconds time interval. The electrical resistivity of liquid carbon decreased from 900 to 600 μΩ cm with increasing pressure from 14 to 94 kbar.

The voltage on the capacitor bank was 120 V (the maximum possible for the conditions to maintain a high pressure with the system of 6–8 plungers). Isolation of specimens that are compressed by plungers cannot be made significantly higher than this voltage. Consequently, the heating time, which is related to the magnitude of the voltage, cannot be reduced, and Togaya was forced to use millisecond heating, which is characterized by much higher heat losses that are needed to consider.

In the abstract to the next work of the same author [2] it was mentioned that for measurement of the electrical resistivity of the liquid carbon and resistance changes during melting—three types of carbon were used in pulsed heating at 40 kbar (spectroscopic graphite, pyrolytic graphite and glassy carbon). In each case significant changes were observed during the melting of the resistivity for the same energy input. Spectroscopic graphite resistance decreases under melting, and for pyrolytic graphite, further, increases. Assuming a constant form factor (ratio of cross-section to length), the electrical resistivity of liquid carbon at 40 kbar is about 480 and 670 μΩ cm for pyrolytic graphite and spectroscopic respectively. Resistance decreases with increasing T (or energy) in the liquid phase to all three types of investigated carbon, demonstrating the fact that, at given P, T conditions, liquid carbon is not metallic (author of this book remind that for metals the growth of T is accompanied by increased of resistance). Later Togaya changed the opinion a little and consider liquid carbon—"a poor conducting metal".

At the very beginning of article Togaya reminds the historical background. Bundy gives the electrical resistivity of liquid carbon as metal type (150 μΩ cm at 100 kbar). Shaner [3] gives an almost constant electrical resistance $\sim$1000 μΩ cm up to $\sim$6000 K for liquid carbon at 4 kbar in pulsed experiments with carbon grade POCO graphite AXF-5Q with the density 1.83 g/cm^3. Heremans [4] heated pyrolytic graphite filament in air at a pressure of 1 bar, claimed to have received a metallic liquid carbon with electrical resistivity of 30 μΩ cm. Togaya [2, 5] reported the pulse experiment with spectroscopic graphite (density of 1.6 g/cm^3), in which it was found that the electrical resistivity of liquid carbon is reduced from 900 to 600 μΩ cm with increasing pressure from 14 to 94 kbar. Lebedev and Savvatimskiy [6], and Savvatimskiy et al. [7] in the pulse experiments with the pyrolytic graphite (density 2.1 g/cm^3) under limiting the volume around the specimen, showed that

this graphite has a resistivity of 700–800 μΩ cm in the melting region. Pressure as it was supposed in last study to be not more than several kbar.

Cell of octahedral type for research at 6–8 plunger high pressure system is presented in Fig. 3.5. Graphite is heated by discharge of electrolytic capacitors with total capacity of 96 mF. Carbon specimen was surrounded by a wall of refractory MgO. Heating current passed through one plunger, passed through a molybdenum electrode and graphite electrode and out to the electrodes on the other side to the opposite plunger. The voltage measured on the specimen from the two electrical probes made of Kish graphite (flake graphite, recrystallized from molten metal solder with carbon) of thickness 20 μ as shown in Fig. 6.1. This graphite probe is connected to the copper rod electrodes by a copper foil.

Three types of carbon were investigated in [2] (Table 6.1).

According Togaya: pyrolytic graphite is grown by chemical deposition, electrical resistance in the direction perpendicular to the c-plane is 1000 times greater than for a direction parallel to the c-plane. It should be noted that under a c-plane Togaya understands the deposition plane. I had a conversation with him on the

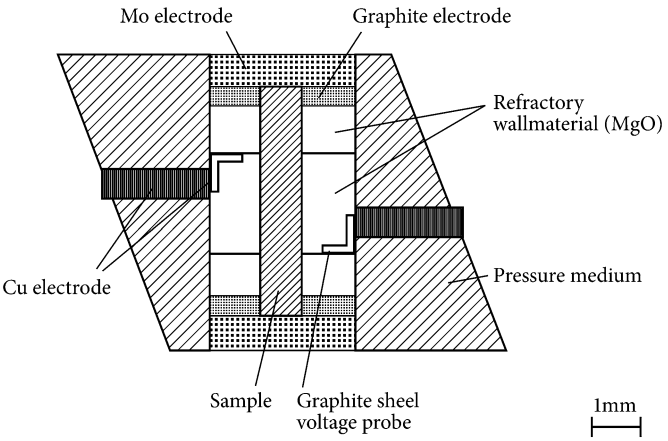

Fig. 6.1 [2] The unit cell used in the experiment

Table 6.1 Specimens used in these experiments

Specimen material	Dimensions (mm)	Weight (mg)	Density (g/cm^3)	Length[a] (mm)
HPG-S3 (spectroscopic) Impurities were not determined	∅0.7 × 5[b]	2.949	1.6	1.981
Pyroid (pyrolytic)	0.545 × 0.545 × 4.863[c]	3.200	2.22	1.991
GC-30 (glassy carbon)	0.545 × 0.545 × 4.825[c]	2.232	1.48	1.988

[a]length between both graphite sheet voltage probes as shown in Fig. 6.1
[b]specimen in a form of a cylinder
[c]specimen with square section

subject in 2007, when I made a special trip from Fukuoka (where I have participated in the International Asian Conference on Thermophysical Properties) to Osaka where Togaya lived and worked. Togaya's arguments are as follows: each plane is characterized by the perpendicular, restored to her, so formally the plane layer deposition (with high conductivity) is characterized by the perpendicular to it (perpendicular directs along the c axis), and then this plane should be called c-plane. This approach differs from that in Russia; the plane of deposition (with high conductivity) is called a-plane. Thus, under the c-plane according to Togaya, it should be understood as a-plane. It is better to say "a plane of the deposition"; it means as a-plane.

The weight of each specimen was measured independently and Table 6.1 shows the average size. Graphite specimen container made of refractory MgO, it had a square shape for the specimens of pyrolytic graphite and glassy carbon. Pressure in the cell for the unit of 8 plungers was calibrated using markers pressure at room temperature. Thermal pressure arising due to heating of the specimen was considered to be neglected, as it was not possible to calibrate the pulse pressure that occurs during the time of experiment 0.5–2 ms.

In Fig. 6.2 it was presented experimental results for the three grades of carbon: the dependence of resistance against energy input for a pressure of 40 kbar.

For the spectroscopic graphite (curve 2) the start of the melting occurs with falling resistance (J_S). These results were published for spectroscopic graphite by Togaya earlier. The original words by Togaya: "*At the energy J_e the irregular decrease on the resistance curve shows that the graphite placed between the voltage proves completely transformed to a molten state. The slight decrease of resistance after that seems to show the temperature dependence of resistance in*

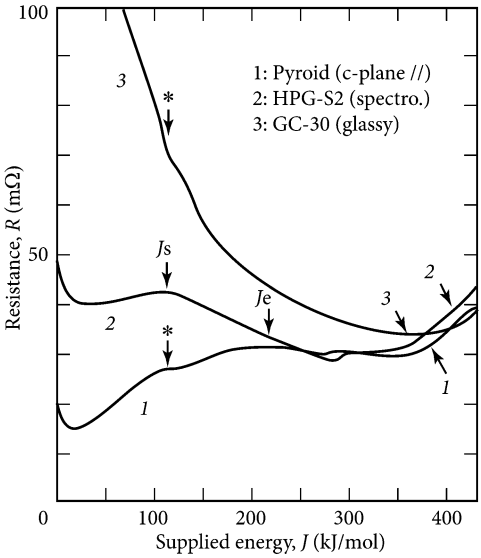

Fig. 6.2 Dependence of the resistance against energy input for the three types of carbon at 40 kbar. Curve number 2 (spectroscopic graphite): J_S the start of melting; *Je* the end of melting

liquid carbon." It would seem: there is no temperature dependence in the figure, but Togaya writes quite so: ".. *that seems to show the temperature dependence of resistance in liquid carbon*.", i.e. it is assumed that the input energy goes into increasing the temperature.

Glassy carbon (curve 3) has the semiconductor type with higher electrical resistance, it decreases more steeply with increasing input energy (temperature). After the characteristic moment indicated with an asterisk (*) in Fig. 6.2, the resistance still decreases with energy input. This moment marks the beginning of melting, because the energy introduced at this point, is the start of melting energy for spectroscopic graphite. However glassy carbon resistivity is higher than for the two other grades of carbon. Apparently this indicates heterogeneity heating as recorded significant difference in electrical resistance for the solid and for the liquid state. Therefore there is no reason to rely on the glassy carbon behavior under analysis of the resistance of liquid carbon.

Pyrolytic graphite (Pyroid) has metallic conductivity in the direction parallel to the c-plane (according to our view "a-plane", as mentioned earlier) and a semiconductor conductivity on the other axis. Under heating, the resistance of this grade of graphite increases (as for metals). The start of melting was determined in the same manner: the moment when the input energy is equal to that of the onset of melting for spectroscopic graphite. However, after the maximum resistivity which is connected with the end of melting, the resistance decreases with liquid carbon energy input (with increasing temperature) as for spectroscopic like. As noted Togaya [5], the diminishing of the resistance for liquid carbon with increasing temperature indicates the conductive mechanism in the semiconductor; and a such behavior is also observed under the measuring of the reflectance of molten graphite heated by a femtosecond laser pulse [8, 9].

Although femtosecond laser heating of carbon (in the first experiments with such short time interval) allowed only measuring of reflectivity, scientific journals have presented it as a sensation. Journal Nature in 1992 [10], citing the work [9], called its brief article as: "*First light on fluid carbon*". To be fair it should be noted that up to the year 1992 it has already been obtained thermal properties of liquid carbon obtained by pulsed electrical heating (Lebedev, Korobenko, Savvatimskiy, Sheindlin, Senchenko, Gathers, Shaner).

Togaya has fulfilled the quenching experiments for pyrolytic graphite, it was confirmed that it is the end of melting occurs at the maximum of the resistance (curve 2 in Fig. 6.2). Figure 6.3 shows the voltage, current and their derivatives; power W; resistance R; input energy J depending on the time. The cut off the current occurred at J = 237 kJ/mol (19.7 kJ/g).

Figure 6.4 shows a photograph (obtained in the microscope) of the cross-section in the center of the refractory wall of MgO, placed between two sheets of Kish graphite (voltage measuring instruments). As one can see in the figure: the size of solidified graphite is close to the original size, except for the more rounded corners. White spots on the photos—the result of reflection of light from the surface of the graphite crystals. No carbon contamination from the MgO was found in this solidified specimen.

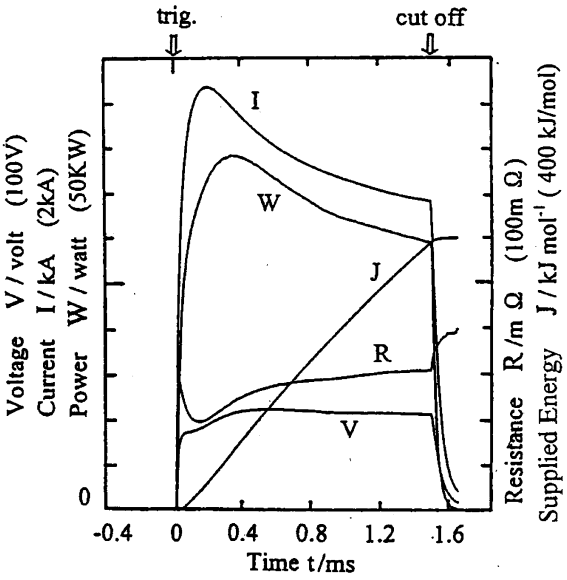

Fig. 6.3 The dependence of voltage *V*, current *I*, the power *W*, the resistance *R*, *J* input energy against the time of quenching experiments with cut off current at the input energy 237 kJ/mol. The values given in parentheses are the maximum for the axes

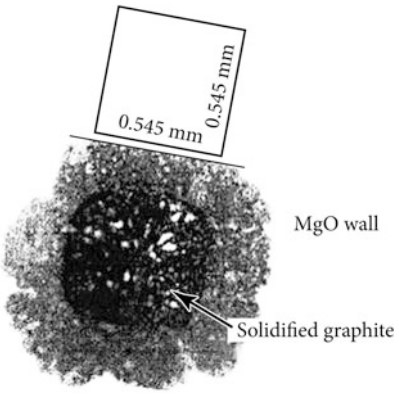

Fig. 6.4 The microscope photo of the specimen after the quenching experiment; it shows the average cross section of the specimen after the experiment. Square near the photos shows the initial section of the specimen size

As can be seen from Fig. 6.2 there is observed a small jump for pyrolytic graphite and spectrographic at input energy of 300 kJ/mol, after that the resistance begins to decrease with energy input. Togaya considers that the reason—the melting of the wall material and contamination of the heating zone, i.e. partial

melting MgO close to the contact with carbon. In the case of glassy carbon this jump occurs at a much greater input energy 430 kJ/mol. Author [2] explains this by overheating of the molten carbon (because of the heterogeneity of heating), which is surrounded by a cylindrical solid crust of unfused carbon, which prevents the contamination by magnesium oxide. After all this resistance is significantly increased for all three types of carbon. This may indicate, as noted in [2] for further contamination of molten carbon by molten and non-conductive MgO.

In conclusion, the author [2] notes the difficulty of estimating the exact value of the electrical resistivity of liquid carbon at high pressure: the change in volume of carbon under its thermal expansion—is unknown, also unknown is the change of the specimen shape during its compression by punches. If the resistance is recorded under the assumption of the constancy of the shape factor A/B, where A—cross-sectional area, B—distance between two electrical contacts, then multiplying factor A/B by the value of the resistivity, we obtain at the end of melting the electrical resistivity of liquid carbon equals 480 μΩ cm for pyrolytic graphite and 670 μΩ cm for spectroscopic graphite. As a result of his research, Togaya concludes liquid carbon—is not metallic. In the next study [11], 2010 year, Togaya will say that liquid carbon—"*is poorly conductive metal*."

6.1.2 Resistivity Against Pressure Just After the Melting

Note that the resistivity of liquid carbon is increasing in our experiment for isotropic dense graphite MF-307 (see lower Fig. 6.18) with the rising of input energy (or with the rising temperature) under conditions of fast quazy-isochoric heating. In the experiment of Togaya [12] it was observed the growth of the resistivity immediately after melting of the pyrolytic graphite of high density (2.2 g/cm^3) at relatively low pressures 14 kbar, wherever happens the completion of the melting (Fig. 6.5). It should be noted that in [12] the electrical resistivity of liquid carbon is shunted by molten layer of magnesium oxide: the similar calculation using the formula (6.1 in Sect. 6.2.4.4) given thickness of penetration layer for magnesium oxide equals 100 μ. Therefore, the electrical resistance above the melting point in [12] may be distorted by the influence of the molten layer of magnesium oxide. However, for a qualitative assessment at the melting point of carbon these data can be considered, especially for increasing of the electrical resistivity of carbon as a liquid magnesium oxide layer can only reduce the total electrical resistance.

Stationary pressure data (from 14 to 94 kbar) are shown in Fig. 6.5 near the curves; and *Je*—the end of melting. We present in Table 9.1, compiled from the data shown in Fig. 6.5 [12], related to the liquid phase of the carbon at the melting point at different pressures.

Most likely, the pulse pressure in our experiments did not reach the level of stationary pressure (25–94 kbar) used by Togaya. Under the conditions of isochoric heating shown in Chap. 4 the density of liquid carbon equals 1.18 g/cm^3. Electrical resistivity (including expansion) of the liquid phase at the melting point $\sim$1020 μΩ

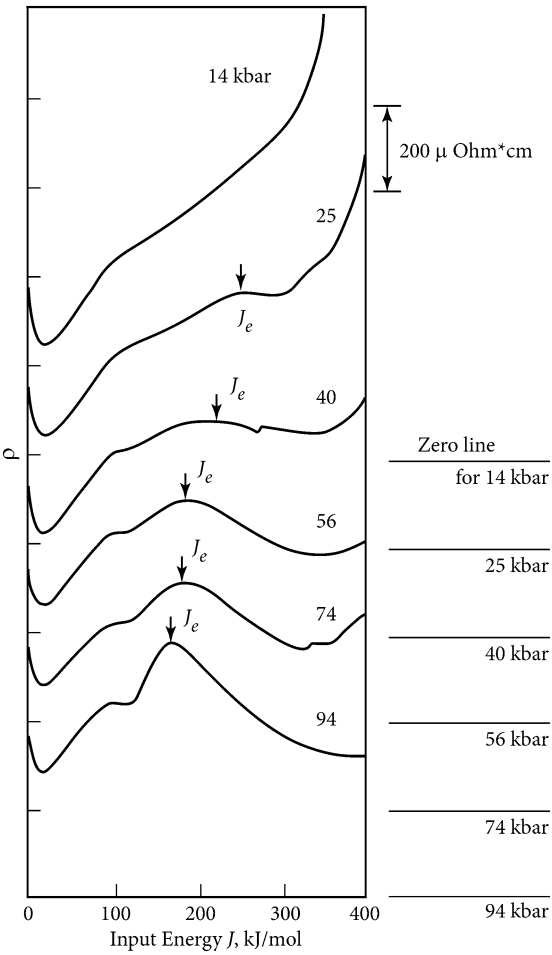

Fig. 6.5 This figure was published in 2002 by Togaya [12], that is, earlier than it was published analytical consideration of the same experiment in [11] in 2010. The experimental results in Fig. 6.5 obtained for the resistivity of pyrolytic graphite of high initial density (2.2 g/cm^3) at millisecond heating by pulse current and at the steady state pressure. Arrows (*Je*) indicate completion of melting for different pressures, from 25 to 94 kbar. The origin of the resistance for each curve is shifted

cm; and resistivity, excluding expansion, related to the initial size, equals 600 μΩ cm. It must be recalled that the electrical resistivity of liquid carbon depends on the pressure. The greater the pressure, the lower the resistivity (at the pressures less than about 50 kbar).

For example, a pressure of ~50 kbar specific (i.e. including expansion) the electrical resistivity of liquid carbon at the melting point equals ~600–800 μΩ cm [13], and for low pressures (but more than 110 bar) ~2200 μΩ cm [14]. We obtained the value of ~1000 μΩ cm indicated a not very high pressures (up to ~20 kbar). Therefore the growth of the electrical resistivity of liquid carbon in our experiments, for this level of pressure, this corresponds to the experimental data of Togaya [2].

A comparison on the value of resistivity ρ^0 (excluding the expansion) shows (Table 6.2), that in our case (600 μΩ cm) for the liquid phase at the melting point is

Table 6.2 (The part of the Table 6.3 shown lower) of experimental data [12] for stationary pressure

Input energy at the finish of melting J_e (kJ/g)	Pressure at the finish of the melting (kbar)	Resistivity ρ^0 (referred to initial dimensions) (μΩ cm)
20.8	25	**572**
18.3	40	**483**
15.8	56	**503**
14.6	74	**509**
14.2	94	**572**

not reached a pressure of 25 kbar, which is fixed in [12] (the appropriate resistance is 572 μΩ cm). This indicates of the pressures in our experiment as a rough estimate of about 20 kbar, not more.

6.1.3 Experiment by Togaya 2010 [11]

Pyrolytic graphite was melted by direct Joule heating, current flows parallel to c-plane. I'm reminded that Togaya understands under a c-plane—the plane of deposition, i.e. the plane of high conductivity. The argument by Togaya: the plane is characterized by the perpendicular restored to it. The resistance of the liquid at the melting point of carbon decreases from 630 to 470 μΩ cm with increasing pressure from 14 to 40 kbar and then increased from 490 μΩ cm to 565 with increasing pressure from 56 to 94 kbar. Judging by the resistance at the melting point the liquid carbon, according Togaya, "*is poorly conductive metal*".

On the other hand the resistance of liquid carbon has a tendency to change the metal-like behavior (resistance temperature coefficient $d\rho/dT > 0$) to a non-metallic or semiconductor as $d\rho/dT < 0$ for pressures 40–56 kbar. These results support our previous conclusion about the existence of a structural transition of carbon in the liquid state [15].

Figure 6.5 shows the dependence of the resistance against the input energy at pressures from 14 to 94 kbar. Resistance was calculated under the assumption that the ratio of length to section remained unchanged from zero to extremely high pressure. As shown in Fig. 6.5 the graphite resistance increases with increasing input energy, and graphite reaches a point J_S. Melting begins at irregular behavior of the electrical curve, and resistance increases further with increasing the melted region. When the input energy is compared with the melting enthalpy, melting comes to the end in *Je* point (Figs. 6.5 and 6.6). Under pressure conditions studied the liquid resistance of carbon is always greater than graphite resistance (along the planes of the deposition) at the start of heating.

Resistivity curves for liquid carbon show different behavior depending on the pressure. Above 56 kbar, the resistance decreases with energy input and the resistance growth rate becomes larger with increasing pressure. This implies that the

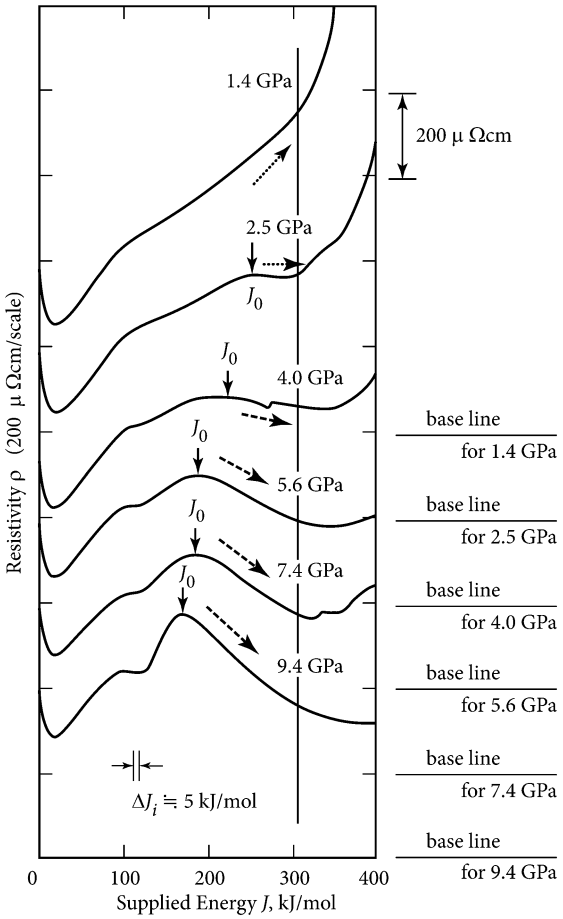

Fig. 6.6 [11] Resistance curves of energy input for the pressure of 14–94 kbar for specimens of pyrolytic graphite (parallel to the deposition plane)

temperature coefficient of resistance (TCR) for liquid carbon is negative ($d\rho/dT < 0$) and the liquid carbon has non-metallic character. On the other hand, the decrease in resistance of liquid carbon is very small at a pressure of 40 kbar, and at 25 kbar the resistance increases after a certain constant value. There is a significant increase in the resistance of liquid carbon at a pressure of 14 kbar, demonstrating the process of transforming into a liquid. Therefore the point of the end of melting is still insufficiently clear. In contrast to the behavior of the resistance above 56 kbar, we can say that lower than 25 kbar there is a tendency to increase with energy input, and the curve for 40 kbar, showing a slight decrease is an intermediate state.

6.1.4 Discussion on the Resistivity at the Carbon Melting Point

Anisotropic graphite with a high initial density (γ_0 = 2.25 g/cm^3).

The energy input up to the start of melting for pyrolytic graphite of high initial density at a pressure of 40 kbar (after correction for the heat losses) was 9.25 kJ/g according to Togaya [12]. At the end of melting [12] at a pressure of 40 kbar there was obtained 19.4 kJ/g. There is insignificant difference between the values obtained for the melting point in [12] and in our measurements (respectively 10.5 and 20.5 kJ/g) at low pressures. Moreover, our measurements during rapid heating do not require amendments to the heat loss. Togaya [12] argues that for the graphite of high initial density the input energy introduced to the start of the melting Js—is very weakly dependent on the pressure. The same result was presented in [1] for spectroscopic graphite of low initial density. Obviously, the data obtained by the author [12] for Js under quenching (at the compulsory termination of current and research of thin sections for the times specified in Fig. 6.2 by stars). However, the input energy at the finish of melting J_e—according to [11, 12] strongly depends on the pressure (Fig. 6.6).

The data published in [12] (2010) and in [11] (2002)—confirms the low level of pressure in our experiments in confined volume (judging by the resistivity).

A physical effect discovered by Togaya [11, 12] at the melting line, is the change of sign for the dependence of the resistivity of liquid carbon against pressure (Fig. 6.7). Resistivity of liquid carbon equals $\sim$600 μΩ cm, on the left line of the Fig. 6.7, corresponds to a pressure of about 20 kbar, not more. Thus, the behavior of the electrical resistivity of liquid carbon in our experiments, for this level of pressure, consistent with experimental data of Togaya [11, 12] obtained for the two grades of graphite of different initial densities.

For the same dense graphite at a pressure of 25 kbar the input energy at the completion of melting is 20.8 kJ/g, and at 94 kbar it is only 14 kJ/g (Fig. 6.6 and Table 6.3). The moment of melting completion in the Fig. 6.6 was determined by the maximum value of the dependence of the electrical resistivity against energy input (note that for the 14 kbar pressure this maximum is not observed). Thus, the energy required to melt the graphite drops drastically (from 20.8 to 14.2 kJ/g) with increasing pressure (from 25 to 94 kbar) for graphite of high initial density (Table 6.3).

It is difficult to draw a reliable comparison in Table 6.3, as the amendment to the volume expansion is unknown for the most experiments. Togaya says [2, p. 874] : “*... the volume change in the thermal expansion and the phase transformation to liquid is unknown in addition to the change of shape by compression*.” Nevertheless we see that our measurements of ρ with amendments on thermal expansion, give higher resistance: 640 and 790 μΩ cm (Table 6.3).

Togaya [12] explores how changes has the electrical resistivity ρ^0 (referred to initial dimensions) for liquid carbon after melting at different pressures (Fig. 6.6) and makes two observations: (1) the resistivity drop after melting suggests that

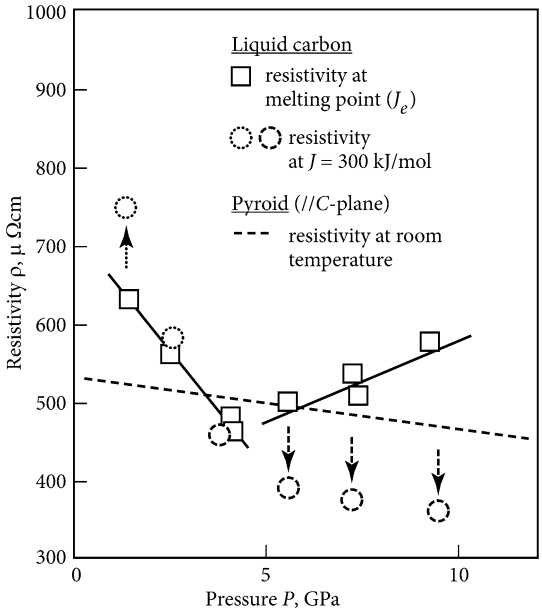

Fig. 6.7 [11]. Dependence of the of liquid carbon resistance versus pressure under input energy J = Je for the end of melting and resistance at the input energy J = 300 kJ/mol (25 kJ/g); (Je < 300 kJ/mol). At a pressure of more than 56 kbar, the resistance of liquid carbon after the onset of melting decreases with energy input until up to 300 kJ/mol (*down arrow*). Before 56 kbar the resistance within the specified range of input energy is increased (*up arrow*). The *dotted line* shows the pressure experiment, but without heating by pulse current (at room temperature)

Table 6.3 Input energy Je and the resistance ρ^0 and ρ at the end of melting depending on the pressure

Input energy at the end of melting Je (kJ/g)	Evaluation of pressure at the end of melting (kbar)	Resistance ρ^0 (excluding the expansion) or resistance ρ (including expansion (μΩ cm)	References
20.8	25	**572**	[12]
18.3	40	**483**	[12]
15.8	56	**503**	[12]
14.6	74	**509**	[12]
14.2	94	**572**	[12]
Data published in [43]			
18.7	≈38	$\rho^0 \approx$ **550**	
	Estimation of pressure through [43] for E = 18.7 kJ/g	ρ ≈ 640	
21	≈23	ρ^0 = **590**	
	Estimation of pressure through [43] for E ≈ 21 kJ/g	ρ = 730	

Comparing measurements made by Togaya [12] and our results

liquid carbon has a non-metallic character, and (2) the resistivity drop after a maximum value indicate the completion of melting. As to (1) we can again notice: falling of the given resistance ρ^0 not always means falling of specific resistance ρ (taking into account expansion). In the Fig. 6.6 it is shown that the falling of ρ^0 (upper curve for 14 kbar pressure) is not observed, on the contrary, there is a continuous increase in resistance. Unlike Togaya opinions, we believe that the liquid carbon has a metallic character. But the dependence on a high pressure is imposed on it. Under item (2) there is also a remark may be considered: according to Fig. 6.6 the rise of resistance takes place under 14 kbar pressure after the graphite melting. The resistance has practically a constant value at a pressure of 25 kbar after melting, and then rising under input energy more than 300 kJ/mol (more than $\sim$25 kJ/g). Therefore the conclusion of the author [12] of item (2) is not universal.

At the same time the heat of melting ΔE is almost independent of pressure in the works by M. Togaya for spectroscopic graphite of low initial density in [1]—9.2 kJ/g under 14 kbar, then the maximum value of 9.6 kJ/g at 56 kbar and further slight decrease to 9.2 kJ/g at 94 kbar pressure. This contradictory factual material related, in all probability, to the lack in studies of Togaya the temperature measurements for recording melting and ignorance of volume change on melting. The temperature in [1, 12] was not measured. The authors of these studies calibrated their final data for all grades of graphite according to result of Russian scientists [16] for graphite UPV-1T with high initial density. The temperature dependence of the enthalpy E (T) was obtained in [16] only for one (small!) pressure—1 kbar, and only up to a temperature of 4500 K. Nevertheless, in [1, 12] the authors assumed, that this dependence remains fair for the wide range of pressure (from 1 to 94 kbar). This assumption is not perfect, due to the strong dependence of the energy (required for the melting of dense graphite) on the pressure (Table 6.3) obtained in [1, 2, 12]. In the absence of temperature measurements in these studies, a check of the start and the end of graphite melting on resistivity curve—is difficult, and for the end of melting of spectroscopic graphite [1, 2, 12], is quite impossible.

Look at the results of experiments at high pressures by Togaya [12] with pyrolytic graphite of initial density of 2.2 g/cm^3. It is obtained [12] resistance of liquid carbon (referred to initial dimensions) at the melting line of graphite equals to ρ^0 = 580 μΩ cm, and this value doesn't change at pressure rise from 25 up to 94 kbar. For comparison we received $\rho^0 \sim$ 590 μΩ cm at pressure assessment in $\sim$50 kbar. A good agreement is observed between the results obtained in Joint Institute for High Temperatures RAS [15, 17], and results by Togaya [12] that given for the resistance (referred to initial dimension) ρ^0 at the melting line.

Figure 6.7 shows the dependence of the resistivity of liquid carbon against pressure at the melting point (open squares). Resistance decreases with increasing pressure up to about 40 kbar, but above 56 kbar the resistance begins to rise. At first glance, this dependence of the resistance versus pressure reflects the temperature dependence of the melting curve [5], in which the melting temperature is increased to 56 kbar and then decreases with increasing pressure (assuming that the liquid carbon has semiconductor properties and electrical properties do not change with pressure).

However, this view must be rejected, since the temperature coefficient of resistance (TCR) of liquid carbon behaves itself differently for pressures up to 56 kbar and above this pressure, as shown in Fig. 6.7. In order to describe features of the electrical properties of the liquid carbon in Fig. 6.7 the resistance at the energy input of 300 kJ/mol, (which is more than energy Je at the finish of melting) is shown by circles with an arrow up and by circles with an arrow down. In the cases above 56 kbar, the resistance of liquid carbon (after melting Je) decreases with an additional energy input of up to 300 kJ/mol and shows the properties of the negative temperature coefficient of resistance (TCR). On the other hand, at a pressure of 40 and 25 kbar liquid carbon resistance at 300 kJ/mol is almost the same as at the melting point, though TCR—very small both negative and positive, respectively. At a pressure of 14 kbar, the resistance of liquid carbon increases significantly with increasing energy input and shows a large value of TCR.

These serious changes in the dependence of the resistivity of liquid carbon versus temperature and pressure suggest the possibility of a structural transition at 56 kbar, to the same extent as the major changes of the melting curve, which suggests the existence of phase transition liquid-liquid, as was reported by Togaya in [12], published in 2002 (with an indication to Fig. 6.7).

In these experiments, the resistance of the liquid carbon was about 470–630 μΩ cm at pressures from 14 to 94 kbar, as shown in Fig. 6.7. These values of resistance are consistent with the resistance obtained in many recent experiments, for example, 625 μΩ cm at 300 kbar [9], 700–730 μΩ cm at 10–20 kbar [15]. On the other hand, the value of 150 μΩ cm at 100 kbar obtained by Bundy [18], is too small compared with the above mentioned (and Bundy himself gave priority resistivity measurements, that was made by Togaya).

Resistance of liquid carbon 30 μΩ cm, obtained in [4], is the result obviously erroneous measurements, and it is associated with the occurrence of shunting discharge at low external pressure. Resistance of liquid carbon is significantly higher than the resistivity of many metals (metals has from 80 to 320 μΩ cm). We can say (after M. Togaya) that liquid carbon—is poorly conductive metal.

Metal-like liquids have a positive temperature coefficient of linear expansion (TCLE), and a negative TCLE,—for non-metal like liquids. The temperature coefficient of resistance (TCR) of liquid carbon varies with pressure from negative to a positive value. This suggests a possible connection of the structural transition of liquid carbon at a pressure near 40–56 kbar.

The experimental results by Togaya can be summarized as follows.

(1) The resistance of the liquid at the melting point of carbon decreases from 630 to 470 μΩ cm with increasing pressure from 14 to 40 kbar, and then decreases from 490 to 560 μΩ cm with increasing pressure from 56 to 94 kbar.
(2) Resistance of liquid carbon at the melting point ranges from 470 μΩ cm to 630 μΩ cm within the pressure changes in the experiment. The resistance

value is greater than for metals with a large electrical resistance (such as Ba, Eu, etc.); consequently carbon is poorly conductive metal.

(3) Resistance of liquid carbon tends to change from metal-like behavior (temperature coefficient of resistance $d\rho/dT > 0$) to the nonmetal (or semiconductor) ($d\rho/dT < 0$) at pressures in the range of 40–56 kbar. This is an important result since the temperature dependence of the resistivity is associated with the structure factor $a(K)$ of the liquid.

(4) The results in the electrical resistance of liquid carbon and their dependence on the pressure and temperature confirms the existence of the structural transition in liquid carbon, liquid-liquid, which can be confirmed by analyzing the melting curve of graphite.

6.2 The Fast Electrical Heating of Different Grades of Carbon

6.2.1 Resistivity and Expansion at the Melting Point (Gathers et al.)

In this paper [19] it were obtained (with support of the U.S. Atomic Energy) the important experimental data under pulsed heating graphite (grade POCO AXF-5Q vitreous carbon) of initial density of 1.83 g/cm^3. The authors of [19] say: "*The choice of vitreous carbon avoided the severely anisotropic mechanical properties of graphite. It is believed that the microscopic structure consists of randomly-oriented graphite grains of 1 to 10 nm*". It was a polycrystalline nature of the specimen. In another part of the publication the author called graphite "*glassy carbon*". Heating time did not exceed 20 μs, i.e. it has been used quite rapid heating that allows to compare results obtained in [19] (Fig. 6.8) with the data of our experiments (Chap. 4) with the same heating rates.

The reason of compressing this graphite in solid state (E ~ 6–8 MJ/kg) may be as follows: it is well known that glassy carbon has closed pores inside; specimen reaches plastic stage under heating even in solid state, and the pores collapse under pressure 2–4 kbar (see result in Fig. 6.9).

If the assumption about fixing the melting region is valid in Fig. 6.11, the heat of fusion will be 5.5 kJ/g (for a pressure of 4 kbar) and the relative volume change under melting consists 50 %. Moreover, from the slope of the curve shown in Fig. 6.11, one can obtain the slope of the melting curve Clausius-Clapeyron equation (44 bar/K), if we assume that the melting point of carbon is 5000 K.

Reference [19] for the first time presents the quasi-equilibrium equation of state and specific resistance of carbon at the input energy than 2 times more that the energy needed to achieve carbon normal point of sublimation. The authors of [19]

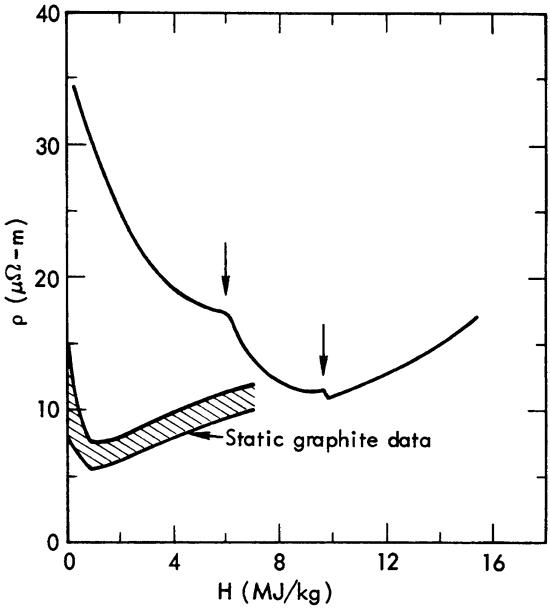

Fig. 6.8 Resistance versus input energy (*upper curve*). *Lower curve* a comparison with the results of steady-state measurements of various grades of graphite. *Left-hand arrow* the start of the compression, *right-hand arrow* the fixing of a pre-melting

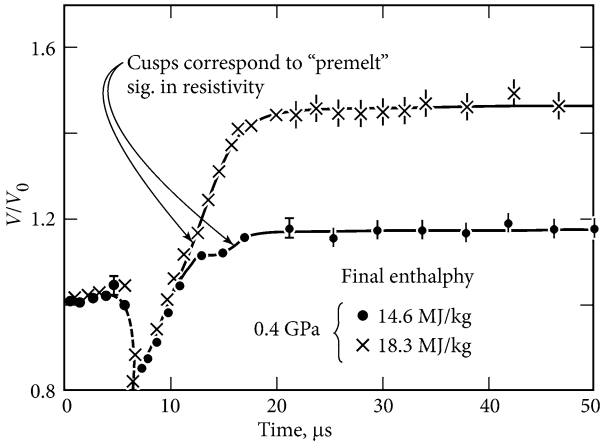

Fig. 6.9 Figure shows a weak thermal expansion of graphite for 6 μs after start-up, and then a compression of graphite takes place. After compression it is the period of continuous expansion with a break ("cusp" as a pre-melting)

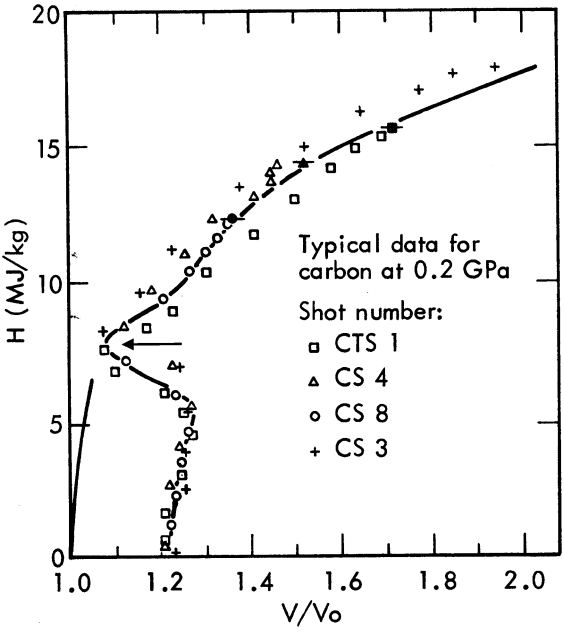

Fig. 6.10 It shows scattering of experimental points around the generalized curve for the dependence of energy input against the relative change in volume. Graphically it is represented as graphite is compacted in the solid phase, reaching its maximum density near the input energy ~7.5 MJ/kg (*arrow in Fig. 6.10*)

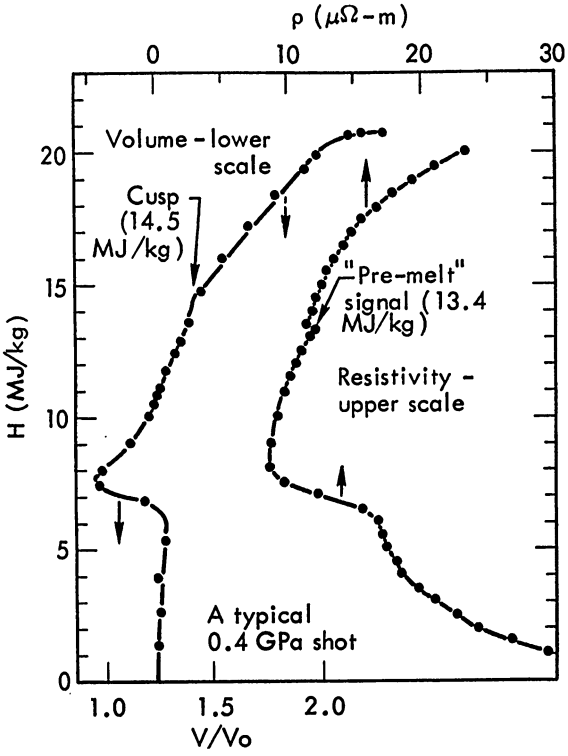

Fig. 6.11 Typical results of the experiment at a pressure of 4 kbar. From the input energy H = 14.4 kJ/g to about 20 kJ/g a noticeable linear part is shown for the curve enthalpy—volume. It is assumed by the authors [19] that this is a melting region

give (implicitly) the results for the critical point and parameters for the curve liquid-vapor region. They note that earlier [20] in 1973, it was calculated the critical temperature to be 6810 K, critical volume—1.56 cm^3/g, the critical pressure—2.2 kbar. Indicating poor agreement of the obtained data with the results of [20] the authors [19] explain this lack of harmonization of the equation of van Der Waals with the scaling obtained in [19] equation of state.

In Sandia laboratory [21] there it was built a new equation of state for carbon to very high temperature (10^8 K) and density (0−100 g cm^{-3}). In this model, the following parameters were used for the melting point of graphite [21]:

- The start of melting at the enthalpy of 9.1 kJ g^{-1} (our measurements give 10.5 kJ g^{-1});
- The enthalpy of melting of 12 kJ g^{-1} (our measurements give 10 kJ g^{-1});
- The finish of melting at the enthalpy of 21 kJ g^{-1} (our measurements give 20.5 kJ g^{-1});
- The change of density upon melting 50 % (our estimation gives 70 %);
- At the triple carbon point T = 4.660 K, P = 170 bar (our measurements give the melting temperature 4800 K);
- The temperature of intensive sublimation 3800 K.

Thus, the latter (relative to the newer) publication [21] is also confirmed that the melting point of graphite is higher 4600 K.

Remind that in the study of American scientists [19] a current pulse was used for heating the glassy carbon of initial density of 1.83 g/cm^3. It was shown that first, specimens were expanded a little bit, but later (at the input energy ~7 kJ/g) they compressed to nearly theoretical density at temperatures of about 4000 K, i.e. below the melting point (Fig. 6.12). A model of carbon heating was constructed in [21], it is shown in Fig. 6.12 (curves). Since the calculations were made for pore-free graphite (i.e. at the maximum density), only the results at the more than 7 kJ/g can be compared with experiment. According to the model [21] the start of melting occurs at H = 9 kJ/g. The slope of the curves changes dramatically upon the occurrence of melting. Melting is completed at H = 21 kJ/g, which corresponds to the final points of measurements (Fig. 6.12). Calculated enthalpy of melting—12 kJ/g; calculated change in density (at melting point)—50 %.

Pulsed heating of even very fast (picoseconds) at high pressure can successfully melt graphite. As an example, Fig. 6.13 shows the supposed route of a femtosecond laser heating of the surface of highly oriented graphite [22].

Melting point of graphite (the intersection of the melting line GRAPHITE-LIQUID) occurs, according to [22], at a pressure of about 10 kbar and temperatures slightly above 5000 K.

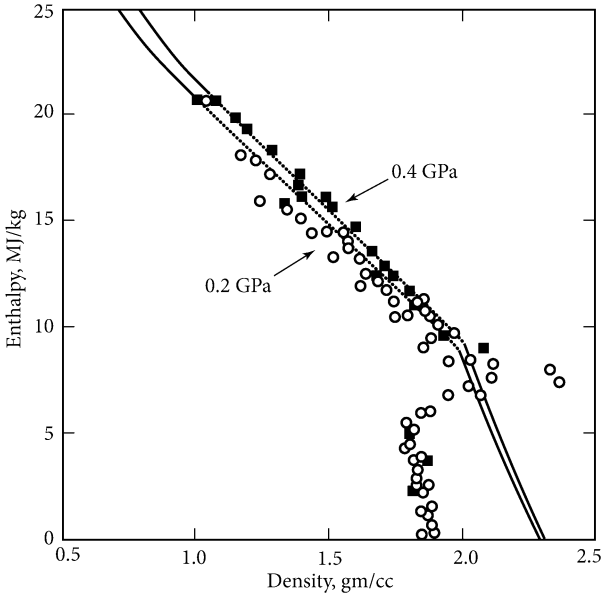

Fig. 6.12 [19, 21] Data on carbon isobaric expansion. Experimental data: *circles* at 2 kbar, *squares* at 4 kbar. *Curves* calculation model (*dashed part* shows two-phase system)

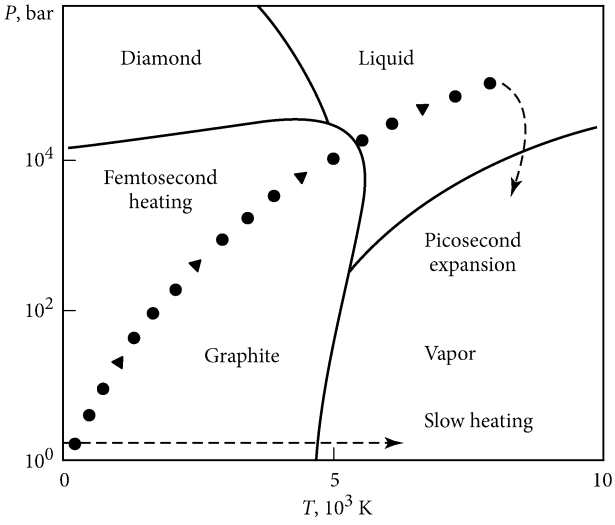

Fig. 6.13 P-T equilibrium phase diagram of carbon and path femtosecond laser heating of highly oriented graphite HOPG [22]

6.2.2 *Advantages of Fast Heating (Microseconds) by Electrical Pulse Current Before Slow (Milliseconds) Heating*

Parallel to experimental steady state investigations for several decades have been intensively developed transient research methods (rapid heating laser or electric-pulse current), first to study metals, and then graphite. The main problem remains measuring the true temperature of the specimen. It is possible to take for granted that for pure metals fast heating (up to fractions of a microsecond) allows obtaining the equilibrium thermo-physical properties (enthalpy at the beginning of the melting, heat of fusion) as well as temperature [23]. Under heating graphite, the more significant features are available related to: its complex structure (anisotropy), sublimation of the solid phase, the density dependence of the manufacturing process, the initial heterogeneity of structure, etc. These features affect the measurement of graphite temperature, especially near the melting point.

Obtaining properties of carbon in a liquid state required pulse heating (already there were not enough stationary methods of research), since for a crucible there is no more refractory material, than graphite. Currently pulsed heating remains perhaps the only way to get liquid carbon and study its properties.

Heating by current pulse has a major advantage (before the laser pulse) in volume heat release that allows you to measure the specific material properties (density, electrical resistivity, energy input). The novelty of our approach is to heat the graphite by fast heating. With a short heating time (1–5 μs) is eliminated most of the difficulties associated with the steady state heating (or slow pulse): accounting of thermal losses of all types; the loss of the shape by a specimen during experiment; need of crucible use; essential interaction with a material of a crucible and surrounding gas.

Application of refractory isolating capillaries by us is not only for fixing the volume of liquid carbon for a short time, but also allows to execute resistance measurements in an isochoric heating process, and also to execute measurements with high pulse (thermal-compression) pressures.

Graphite as the most refractory substances of other conductors, it is difficult to melt under conventional conditions. However, pulse heating for short time (several microseconds) enables successfully to melt graphite at a suitable pressure (more than 100–200 bar). For the purpose of constructing the phase diagram of carbon reliable at high temperatures it is necessary to investigate the graphite at the melting temperature (Tm = 4800 K), and to study the properties of the carbon in the liquid state.

6.2.2.1 Specimens

A diamond tools were used to obtain thin (0.2 mm) graphite strips. The block of quasi-monocrystal graphite UPV-1T were cut to the narrow (width 1 mm, 40 mm long) bars, that was then split into thin (0.2 mm) strips. Finally, the specimens had a size of 1 × 0.2 × 40 mm.

Specimen size and weight were determined with the use of optical methods and balance VLR-200 (measurement error is 0.15 mg). The copper layers were deposited to the ends of the graphite specimens by electrolytic method. The electrodes were soldered to the copper layers. Two such strips folded one by one, with a small (0.1 mm) gap from one side of this sandwich. A flat tip of an optic cable was inserted in this gap. A flat tip of an optic cable has 20–50 optical fibers (diameter of 50 μ each) that was arranged in one row. Then, the whole unit was fixed laterally by quartz plates, and the spacing between the plates was filled with epoxy glue. Thus the light transmitting medium is an epoxy glue and glass fiber. Under a short-time heating (1–5 μs) the heat losses are negligible, so the calculation of input energy absorbed by a unit mass of graphite was

$$E(t) = \int_0^t [I^2(t) \cdot R(t)/m]dt$$

where m—mass of the specimen; I—current; R (t)—the electrical resistance, which is calculated by the formula R (t) = [U (t)—L (dI/dt)]/I (t), where U—voltage along the specimen; L—inductance of the specimen.

Diagnostic equipment includes a digital 4-channel oscilloscope Tektronix TDS-754C for recording voltage and current signal, as well as high-speed pyrometer response.

Under the heating of the anisotropic pyrolytic graphite (that was grown in a cylinder form) the expanding in radial direction (plane "C ») becomes impossible because the cylindrical surface (plane "a ») restricts expansion—specimen may breaks before melting. We used a special method for the manufacture of cylindrical graphite specimens having the opportunity to expand in two axes (graphite grade UPV-1T). We applied serial pushing the specimens of square cross section UPV-1T through the diamond filers of all decreasing (step by step) diameter. Specimens were obtained with a diameter 0.87 mm. They were placed into a thick (outer diameter 11 mm) sapphire tubes which had an internal diameter slightly larger than the diameter of the specimens. Heating of such specimens in the tubes gave the results on the specific electrical resistivity of liquid carbon, assuming that the tube has not changed the inner diameter of sapphire tube during short heating of graphite. Recording the radiation from the graphite plane "c" through the wall of the sapphire tube, it was managed in the same experiments to fix the inclined temperature plateau of graphite at melting point [17].

Our experiments in a limited volume showed that the electrical resistivity of liquid carbon equals 730 μΩ cm at a density 1.8 g/cm^3 (specific volume of 0.55 cm^3/g) for pressures of a few tens of kbar and temperatures of 5000–7000 K (Fig. 6.14). In our opinion (based on the results of the experiments) the electrical resistivity of liquid carbon at high pressure has a metallic character. Numerically, it corresponds to the resistivity of extended (by four times) liquid refractory metals (W, Ta, Mo) [7].

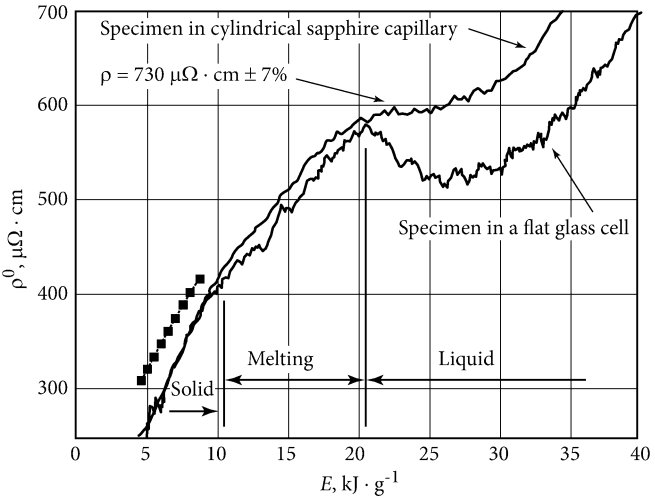

Fig. 6.14 [15, 17, 41] Specific (related to the initial size) electrical resistivity ρ^0 graphite, depending on the specific energy input E; (ρ—resistivity with the expansion included)

The figure contains the value of the specific ρ (including extension) resistivity (730 μΩ cm) at a pressure of tens of kbar. Glass cell—the plate graphite sandwiched in the thick plates of glass.

The specimen in a sapphire capillary—a cylindrical graphite specimen (diameter 0.87 mm) UPV-1T in a thick-walled (outer diameter 11 mm, internal 0.97 mm) sapphire tube.

Solid squares—reference [24]—by Senchenko (graphite in a solid state before melting).

Remind that for high input energy E = 38 kJ/g [6] (Fig. 4.14, curve 3) resistivity (with the expansion included) $\rho = \rho^0 \times V/V_0 = 2200 \times 1.84 \cong 4000$ μΩ cm (ρ^0 = 2200 μΩ cm—electrical resistance for input energy E = 38 kJ/g). Moreover, liquid carbon heated from E = 20.5 to 38 kJ/g in a quartz tube (with a true density $\gamma = 1.2$ g/cm^3) shows a linear increase of the electrical resistivity versus E, from E = 20.5 to 38 kJ/g. If we assume that for isochoric heating a heat capacity of liquid carbon C_V = 3 J/g K, according to the experiment [7], and it retains its value across the entire range of input energy after melting (from E = 20.5 to E = 38 kJ/g), the liquid carbon with a density $\gamma = 1.2$ g/cm^3 has a temperature T ∼ 10600 K for the specific energy input E = 38 kJ/g.

The special attention of researchers attracts graphite melting region, as in scientific terms, melting—a key knot for the theoretical calculations, and for practical applications, melting—this is the limit of stability of structural materials based on graphite. Previously, in [20] it was represented by the calculated phase diagram of carbon: carbon density dependence of the temperature for the solid phase, liquid phase and vapor. The density of the liquid phase at the triple point is taken to be 1.611 g per cubic

centimeter (obtained by averaging the data in the literature of previous years (until 1973) on the increase of graphite volume by 15–30 % during melting.

The density of liquid carbon was estimated in our experimental work [6] only on the basis of experiments of fast heating graphite in capillary tubes, depending on the changes of the electrical energy input. Result for the density of liquid graphite is close to 1 g per cubic centimeter. In milliseconds studies by Togaya [1] the electrical resistivity of liquid graphite was obtained excluding expansion. A slow technique (millisecond heating) is not possible to measure the expansion of graphite. Moreover, in the last work the melting temperature was not measured. Thus, the published works don't give a definite answer to a question of liquid carbon density, and its dependence on pressure. In our study [7], based on experimental practice we argued that only the densest graphite UPV-1T (initial density 2.25 g per cubic centimeter) can be effectively studied in the liquid state. Without a new experiment the problem of the liquid carbon density cannot be solved, as the calculations in the field of graphite melting extremely complex (there is no reliable model of graphite melting), and the reliable equation of state for graphite (including melting) is missing in the literature, in spite of the fact that there are many different published modeling data.

There are various options of methods for physical properties investigation of materials using the heating current pulse. The main difference between these techniques—it is the duration of the pulse. Techniques are the most demanded with millisecond pulse and with microsecond pulse heating. We have chosen a technique using a microsecond pulse. This technique has several advantages over methods with millisecond heating. This is primarily due to the lack of energy losses (heat losses) by the specimen during heating. For example, in the study of Togaya [11], the specimen was heated by a current pulse duration of ~ 1.5 ms. When calculating the energy input into the specimen it needs a correction for heat losses. This correction makes tens of percent. Bundy [25] in their studies also used a heating current pulse with the duration of a few milliseconds. In this case the heat loss of the specimens was the same as in the works by Togaya, tens percent. By calculation way it is established that at microsecond heating the loss of heat practically are absent (fraction of one percent).

Another disadvantage of a millisecond heating is the loss of the shape of a specimen under the transition of the specimen into the liquid state (due to the action on the liquid specimen gravity and surface tension forces). This action splits the specimen into droplets before all the energy will be introduced (for slow heating). The heating the specimen at the microsecond time interval simply has no time to lose shape, which has been confirmed by an experiment [26].

Moreover, today there are many high-speed devices (digital oscilloscopes, current monitors, photo-detectors), capable of recording parameters with high accuracy of the heating process of sub-microsecond duration. Therefore at high temperatures —it is favorable to apply microseconds pulse heating technique for investigation of physical properties for materials, especially in liquid state.

6.2.3 *Resistivity of the Carbon in a Broad Range of Liquid State (with the Expansion Included)*

6.2.3.1 The Electrical Resistivity of Carbon in Solid and Liquid States

The ability to measure high temperature properties, such as enthalpy, density, volume resistivity favorably distinguishes graphite electrical heating current from a laser surface-heating. Experiments fulfilled by Korobenko and Savvatimskiy [13, 15, 27, 28] (under pulse heating by electrical current) included the use of thick-walled capillary tubes (glass, quartz, sapphire). Heating graphite specimens inside the isolated tube allows one to fix the moment of filling the inner tube volume by expanding graphite, i.e. to measure the density of graphite at a specific energy input. Fast heating technique (1–5 μs) by pulse electrical heating is very effective in the study of graphite properties in the liquid state. In the discussed experiments a pyrolytic graphite of low initial density (1.9 g/cm^3) and quasi-single-crystal graphite UPV-1T of high density (2.2 g/cm^3) were used.

The results of the first experiments confirmed that the graphite specimens of low initial density show no any peculiarities in electrical resistivity under graphite melting (from 10.5 to 20.5 kJ/g) for both low and high pressures involved. Furthermore, there is a direct dependence of the resistivity of the liquid carbon (above 20.5 kJ/g) on the pressure: the higher the pressure, the lower the resistivity of the liquid phase. Specimens were made of various types of low density graphite (1.5–1.9 g/cm^3), usually have a source of heterogeneity in the structure (experimental fact), which may cause non-uniform heat dissipation throughout the specimen volume. Nevertheless, the first series of experiments with low-density graphite specimens led to the following conclusions. The results for the liquid phase of carbon in the melting curve at a specific energy of E = 20.5 kJ/g: the density γ = 1 g/cm^3 and under low pressure, the electrical resistivity ρ (including expansion) equals $\sim$2200 μΩ cm;

at a density of γ = 1.12 g/cm^3 resistivity ρ = 1500 μΩ cm;
at a density of γ = 1.36 g/cm^3 resistivity ρ = 1100 μΩ cm;
at a density of γ = 1.81 g/cm^3 resistivity ρ = 734 μΩ cm.

In the latter case, it was obtained a pressure maximum ($\sim$50 kbar).

Table 6.4 gives data for graphite of low initial density (γ = 1.9 g/cm^3), which presents: the electrical resistivity ρ^0 (related to the initial size of the specimen) and resistivity ρ (including expansion) for different values of the specific energy input E. Density γ was calculated taking into account the compression of graphite to a density γ = 2.2 g/cm^3 (at 4000 K) and subsequent expansion (see Fig. 6.12).

We note that for the same grade of graphite, its expansion gives the result of a monotonic increase in resistivity ρ. The growth of resistivity ρ from № 4 to № 6 (Table 6.4) under the same density, is due to the simultaneous increase in temperature and pressure under conditions of isochoric heating.

The following Table 6.5 shows the results of those experiments in which the resistivity was obtained for the liquid carbon at E = 20.5 kJ/g. The results in

Table 6.4 The electrical resistivity ρ and density γ for graphite with low initial density (γ_0 = 1.9 g/cm^3) at the different input energy E

№	ρ^0 μΩ cm	$\rho = \rho^0$ V/V_0μΩ cm	γ g/cm^3	V/V_0 Volume expansion	E kJ/g	Pressure P rise from E_1 to E_2 kJ/g
1	750	**890**	**1.85**	1.19	7.9	–
2	800	**1100**	**1.57**	1.4	20.5	From 15 to 20.5
3	880	**1500**	**1.29**	1.7	20.5	–
4	900	**1650**	**1.2**	1.84	14	–
5	1200	**2200**	**1.2**	1.84	20.5	From 14 to 20.5
6	2170	**4000**	**1.2**	1.84	38	From 14 to 38

Table 6.5 The electrical resistivityρ and density γ for liquid carbon in the melting curve at the input energy E = 20.5 kJ/g

№	ρ^0μΩ cm	$\rho = \rho^0(V/V_0)$ μΩ cm	γ g/cm^3	γ_0 g/cm^3	V/V_0
1	1200	**2200**	**1.2**	1.9	1.84
2	880	**1500**	**1.29**	1.9	1.7
3	800	**1100**	**1.57**	1.9	1.4
4	590	**730**	**1.8**	2.25	≤1.2

Table 6.5 are settled (approximately) with increasing of external pressure. The pressure has a maximum value (∼50 kbar) in the position number 4.

The results of microsecond heating of graphite with initial density γ_O = 1.83 g/cm^3 at a gas pressure of 4 kbar are published in [3]. It was obtained a constant electrical resistivity of liquid carbon ∼1000 μΩ cm, up to a temperature of 6000 K. This value is consistent with the resistivity results presented at the third line of Table 6.5.

The Table 6.5 gives the next result: the density of liquid carbon at the melting line rises with the pressure increases, while decreasing the resistivity ρ (from 2200 to 730 μΩ cm). The experiment indicates a high compressibility of graphite at low pressures. The density of liquid carbon increases with pressure rising like it is the compressed gas (it was noted by us in [14]) and, accordingly, the electrical resistance decreases.

The experiment indicates the high compressibility of graphite at low pressures (up to 1 kbar). It seems that the sublimation of graphite, which has begun in the solid phase from the surface at T ∼ 3000 K, replaced by sublimation of carbon in the entire volume for the liquid phase (at T higher 4800), and only pressure keeps the liquid carbon from further expansion. Upon completion of the melting point (for small external pressure) there is a loss of the carbon-carbon bonds and carbon "sublimates" throughout the volume. "Sublimation" in this context does not mean that the individual atoms evaporate (just as for metals). On the contrary, if we create conditions for further expansion of liquid carbon along the melting curve, the different structures can be formed: from individual atoms and their complexes to the

extended fragments. Apparently the structure of these formations will depend on ambient pressure and on the conditions of the further cooling of a carbon.

The estimation of graphite expansion during melting gives ~70 % at low external pressure (up to ~1 kbar), ~20 % at high pressure (~50 kbar). Another fact has to do with it: graphite resistivity for the specimen heated in a water (Fig. 4.14, curve 1) or free expansion in a capillary (curve 3) with a small external pressure begins to increase rapidly at E ~ 16–17 kJ/g, i.e. before the completion of melting (20.5 kJ/g). We can assume that the accelerated growth of the resistivity ρ, during melting (for low pressures), is associated with an intensive expansion of graphite at a temperature T ~ Tm (4800 K).

For low pressures there is a direct dependence of the resistivity of the liquid carbon (above 20.5 kJ/g) on the pressure: the higher the pressure, the lower the resistivity of the liquid phase. The results for the liquid carbon in the melting curve at a specific energy E = 20.5 kJ/g: the density $\gamma = 1$ g/cm^3 and under low pressure, the electrical resistivity (including expansion) equals ~2200 μΩ cm.

At a density of $\gamma = 1.12$ g/cm^3 $\rho \sim 1500$ μΩ cm;
at a density of $\gamma = 1.36$ g/cm^3 $\rho \sim 1100$ μΩ cm;
at a density of $\gamma = 1.8$ g/cm^3 $\rho \sim 730$ μΩ cm.

In the latter case, the pressure has a maximum (~50 kbar). There is a good agreement between our results and data of Togaya [11] for the reduced electrical resistivity ρ^0 (referred to initial dimensions) in the melting line for pyrolytic graphite with high initial density of 2.2 g/cm^3.

For a low external pressures (about 1 kb) the liquid carbon density in the melting curve is very small (~1.2 g/cm^3), in contrast to theoretical calculations (1.6 g/cm^3) in previous years [20]. Electrical resistivity in the melting curve is about 2000 μΩ cm for the mentioned pressure.

Mentioned conclusions about the role of external pressure on the expansion of carbon may have important technological applications. Influencing by the external pressure on the liquid carbon one can obtain an intermediate product of different density, under using, further, the density, which will give the most efficient further transformation of carbon. Despite the high temperature of the liquid carbon (T ~ 4800 K), used pressure transformation can vary widely, starting from atmospheric pressure. Therefore, the efficient conversion of liquid carbon (representing a mixture of graphite fragments of different configuration), it is quite possible in pulsed processes.

Close value of resistivity was obtained by Shaner (USA) with microsecond pulse heating of graphite (about 1000 μΩ cm). As it was shown [6] for pure graphite was obtained about 700 μΩ cm, using analog oscilloscopes, and later (study of Korobenko Savvatimskiy) 600–640 μΩ cm with a digital oscilloscope used for the case of high pulse pressure in sapphire capillaries. The latter result coincides with measurements by Togaya (630 μΩ cm) [11]. If previously Togaya argued that liquid carbon—it is rather a non-conductor, a such lowest recorded value of the electrical resistance, that they declared in 2010, allowed M. Togaya (in his last study) assert that liquid carbon—is a "*weakly conductive metal.*"

6.2.4 Resistivity of Dense Isotropic Graphite MF-307 Higher Melting Point (with the Expansion Included)

6.2.4.1 Introduction

This chapter describes experiments with pulse heated graphite (in microseconds time scale) and the recording the electrical resistivity of liquid carbon. Specimen's density (2 g/cm^3) for isotropic graphite grade MF-307 (Nippon Techno-Corporation Ltd., Japan). The carbon content is more than 99 %, ash content of 0.1 %. The thermal conductivity is equal to 116 W/m K, the initial resistivity 1250 μΩ cm. Section of the specimens 0.3 × 0.3 mm and a length of 10–15 mm were heated in water or in a thick-sapphire (outer diameter 10 mm, inner ~0.5 mm) capillary tubes. It is confirmed that the heating in water at atmospheric pressure does not allow to obtain and investigate of liquid carbon properties. In the best case achieved the start of the liquid state. The heating inside the sapphire tubes gives rise a pulse pressure (up to several tens kbar) after the stop expanding graphite by the wall of the tubes. This growing pressure (within microseconds) allows you to explore the liquid state of carbon in a limited volume. Isochoric heating led to the possibility of measuring the electrical resistivity of liquid carbon at high specific energies (up to ~32 kJ/g) and high pressures, such measurements are extremely costly in stationary studies.

Isotropic graphite of high density 2 g/cm^3 can be used as a durable structural material in the space and nuclear industries at high temperatures. The principal advantage of this graphite—high temperature resistance with satisfactory strength. Moreover, an important factor in its practical application is the possibility of machining.

However, its high temperature properties at temperatures of 3000 K and above have been insufficiently studied, which hinders its application in widespread industrial use.

This chapter demonstrates the possibility of experimental investigation of the graphite properties (brand MF-37 graphite, manufactured by Nippon Techno-Corporation Ltd., Japan) to the maximum possible working temperatures up to the melting of graphite at 4800 K, and further heating in the liquid state. The method of investigation—a pulsed electrical heating during several microseconds. After melting liquid carbon retains the original shape of the specimen within a few microseconds, which allows you to explore its properties, recording parameters of the heating process by fast oscilloscope and fast pyrometer recording. Due to the short duration of the heating process (~5 μs) all kinds of heat losses (due to heat conduction in contact with the electrodes and the external environment; due to radiation from the surface over the entire spectral range; due to the sublimation from the surface of the specimen)—are insignificant and amounts to fractions of a one percent of the input Joule energy E. The procedure for calculating the properties of graphite (electrical resistivity, density, enthalpy) at high temperatures for pulsed heating process appears to be quite simple. For example, the input energy E is

provided by a pulse of electric current: $E = \int UIdt$, where U—voltage, I—current, t—the time of heating. Input energy can be considered in this case as enthalpy, because, despite the short time of the experiment, the specimen is realized the work of expansion in the radial direction (the small specimen size) is almost unchanged at ambient nearly constant pressure. It is enough to measure voltage, current and heating time to get Joule heat. The use of modern digital technology allows performing such measurements with a high accuracy; all the recorded signals are strictly correlated to time.

Specimens in the form of the planes ($\sim$0.15–0.5 mm thick) were prepared by cutting the diamond blade (thickness of the disk 0.1 mm) from the bulk graphite. Then, the same planes are cut by diamond blade to obtain specimens of rectangular cross section and a length of 10–20 mm. Error voltage and current measurements was $\sim$1 % (digital oscilloscope Tektronix 3034B), but considering the dividers used in the experiment can reach $\sim$1.5 %. The basic error was given by measurement of geometrical dimensions of the specimens (by IZA-2 meter and caliper) to give a final estimate of the error of measurement for resistance of 4 and 5 % for input energy E.

6.2.4.2 Experiments with MF-307 Graphite Under Pulsed Heating in a Water

Under pulse heating of the graphite specimen in the open air at a pressure of 1 bar, it will be shunted by the surface discharge at the beginning of heating (due to ionization under carbon sublimation from the surface)—the input a significant amount of energy into the graphite will not succeed. Moreover, since the graphite the triple point corresponds to pressure of 100–110 bar, graphite melting at a lower pressure is failed. Therefore, a graphite specimen must be placed in an insulating medium—water, oil, or tight enough to place in an insulating tube (glass, quartz, or sapphire). As an example, the heating of an isotropic graphite specimen is shown in Fig. 6.15 in water. Pre-boiled water was used to degas the medium, as in the case of ordinary water the small bubbles are appeared on the specimen surface, causing the formation of a longitudinal shunt electrical discharge during pulse heating. The short of the heating process is achieved by applying a high voltage to the capacitor bank. If you heat the graphite specimen in the open air at a pressure of 1 bar, it will appear shunting discharge on the surface and the input a significant amount of energy into the graphite will not succeed.

But even more serious reasons for heating graphite at elevated pressure are exist. Since, according to the results of most experimental studies, the triple point of graphite corresponds to the pressure of 100–110 bar, to melt graphite at a lower pressure impossible. Therefore, a graphite specimen must be placed in a restricted volume—insulating tube (glass, quartz, sapphire), creating increased pressure during the pulse heating (thermal compression due to thermal expansion of the graphite).

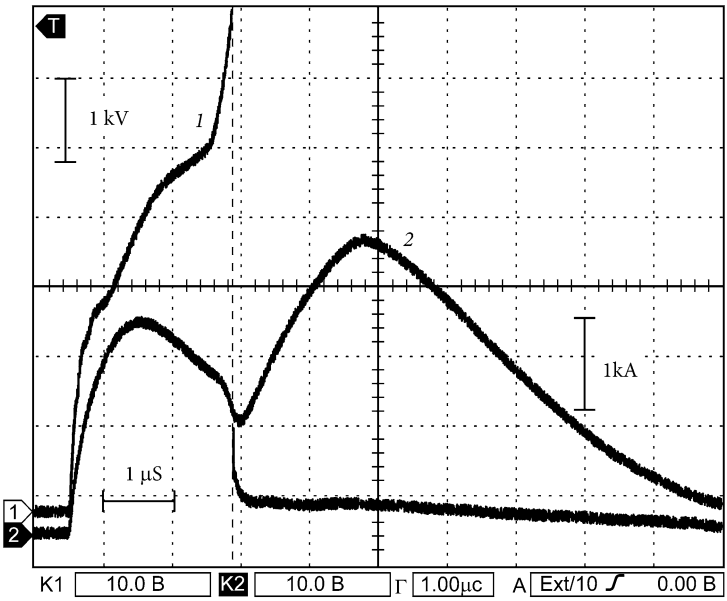

Fig. 6.15 Oscilloscope traces under heating of graphite specimen MF-307 in a water. Section of the specimen 0.63 × 0.14 mm, length 16 mm. *Curve 1* voltage U along the specimen; *curve 2* current I

Strictly speaking, for the pulse heating graphite specimen in a restricted volume or simply in a water it will appeared pinch-pressure (due to the magnetic field of the current). In our experiments, pinch-pressure reached 45 bar for the current 5 kA. It will be seen later (Fig. 6.27) that this pressure has a maximum value in the center of the cylindrical specimen and on the surface it equals zero, so it does not interfere the surface graphite layers to sublimate. Evidently, the total pressure of water around the specimen in these experiments does not exceed 100–110 bar, i.e. it is not achieved the triple point of carbon.

As an example, Fig. 6.15 shows the case of an isotropic graphite specimen heating (made of MF-307) in water at an initial voltage of the capacitor bank—8 kV. Pre-boiled water was used.

After ~2 μs after the start of heating, the specimen voltage begins to rise sharply due to increased resistance of the specimen, resulting (in the presence of high voltage on the specimen) to the occurrence of a shunt discharge along the surface of the specimen. After a current decrease (curve 2), it again begins increase in the discharge. After a sharp increase of the voltage U (curve 1), which we associate with the bulk sublimation in volume, there is a bypass discharge. The voltage—falls to near zero, and further heating does not occur, all the remaining energy is emitted in the discharge, bypassing a specimen.

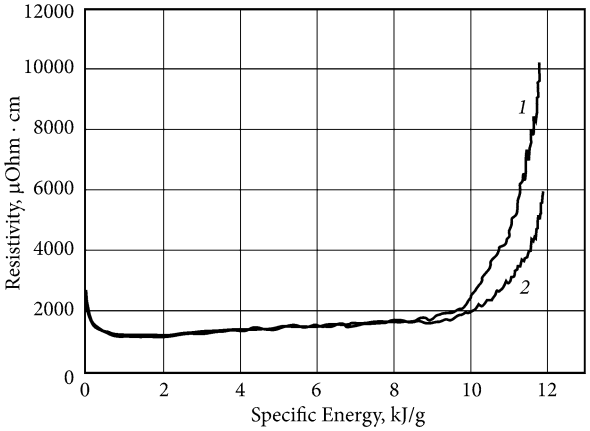

Fig. 6.16 The dependence of the resistivity of graphite MF-307 (referred to the initial dimensions) against specific energy under heating in a water. *1* Specimen Section 0.148 × 0.587 mm, length—19.9 mm; *2* Specimen Section 0.19 × 0.735 mm and a length of 17.5 mm. The two curves coincide in the most parts of input energy values

Figure 6.16 presents the results for the dependence of the resistivity against injected energy obtained for two graphite specimens in the same conditions under heating in a water (charging voltage 8 kV).

In our opinion the reason for the observed loss of conductivity (at the input energy of about 10 kJ/g) is the volume expansion. The experimental fact that when a pressure increase this loss of conductivity disappears (as it will be shown below in the experiments with sapphire tubes), supports the hypothesis that the loss of conductivity is most likely due to the volumetric expansion (the concept "volume sublimation" was introduced by Savvatimskiy in [14]), which occurs under a small external pressure and at a high input energy, near to melting region. To melt graphite with low initial density (less than 2 g/cm^3) at low pressure, is not possible. Therefore, further experiments were carried out by heating the isotropic graphite specimens of the initial density 2 g/cm^3, when they are placed in the sapphire capillary tubes. Sapphire tubes—capable of withstanding high thermo-compression pressure (due to thermal expansion of the graphite).

6.2.4.3 Experiments with MF-307 Graphite Under Pulse Heating in Sapphire Capillary Tubes

Several experiments were performed with sapphire tubes with different inner diameter under the initial voltage on the capacitor bank—12 kV. Figure 6.17 presents one of the most successful pulse heating of graphite in the sapphire capillary tube with inner diameter of 0.48 mm; the length of the graphite specimen

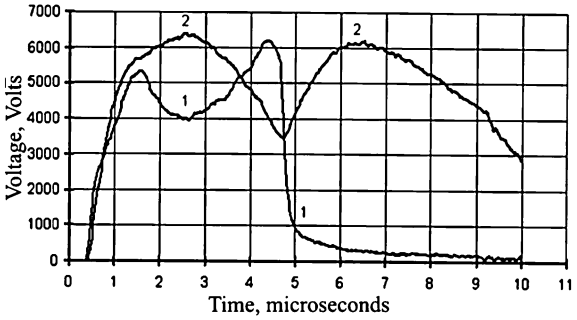

Fig. 6.17 The oscilloscope traces of heating the specimen of graphite (Section 0.307 × 0.347 mm, length 9 mm); sapphire capillary tube (internal diameter 0.48 mm, outer—10.2 mm). *Curve 1* voltage along the specimen, *curve 2* a current (in arbitrary units)

equal to the length of the tube (9 mm). The specimen was entered into the tube tightly, since the angles of the square specimen' section touches the inner cylindrical surface of the tube. Ends of the specimen and the sapphire tube impacting on both sides by the steel screw clamp (insulated from the electrodes) through the pads of aluminum foil (to ensure contact with the graphite electrodes). Note that such "blind " fixation of the ends in the sapphire tube could lead to a further increase in pressure due to the expansion of the air heated inside the tube and the appearance inside the tube a sublimate (as a vapor) from the graphite surface.

In the case of a capillary tube due to the thermo-compression (at the moment it stops expanding graphite in the tube wall) it is greatly increases the pressure in the graphite. The further input of energy occurs in the conditions of isochoric heating at a reasonable assumption that in a short time (about 6 μs) the internal diameter of the tube is not changed. The ratio of the internal volume of the sapphire capillary V to the initial volume V_0 of graphite was $V/V_0 \sim 1.7$.

As we have seen (Fig. 6.17) the time of heating in the sapphire tube is limited by 4.5 μs; it is defined by dynamic strength of the sapphire at a given heating rate, depending on the current density. Obviously, accelerating the heating process (by increasing the density of the heating current), you can achieve higher pressures while maintaining the strength of the tube. This requires the use of even higher voltages. Increasing the voltage increases the probability of shunting the surface discharges along the specimen in the free volume of air in the tube.

Figure 6.18 shows processing of waveforms shown in Fig. 6.17.

The upper arrow (bottom curve) marks the start of the drag reduction before the isochoric heating (one of the reasons is the compression of solid graphite to a higher density, this effect has been confirmed by us in 1986 [6] after reading the pulse experiment [19] executed in 1974). Furthermore, from this point can be established through pressurizing and heating of the air admission carbon sublimate into a closed volume. Right upper arrow (curve 2) indicates the time of destruction of the sapphire tube under pulsed heating of graphite in the sapphire capillary.

The lower left arrow (curve 1) marks the beginning of melting (10.5 kJ/g), and the lower right arrow—the end of melting (20.5 kJ/g). These values have been obtained in previous works under pulsed heating graphite [15, 28].

Thermal expansion of the graphite is about 30 % prior to the start of melting, and the expansion during the melting time is estimated as 70 % [13, 14]. Isochoric heating is realized near the end of the melting (right arrow in the curve 1). Calculated density of the liquid carbon for this experiment under isochoric heating (curve 2) is 1.18 g/cm^3, the calculated resistivity (including expansion) of liquid carbon at the melting point (E = 20.5 kJ/g): ρ^0 = 600 μΩ cm (excluding expansion) and $\rho^0 \times V/V_0 \sim 900$ μΩ cm (including expansion). V—internal volume of the tube, V_0—initial volume of graphite ($V/V_0 \sim 1.7$).

Under input the energy E = 10.5 kJ/g (start of melting) the expandable graphite still does not fill the free volume of the tube. Under the input energy E = 20.5 kJ/g (end melting) the tube is filled with melted graphite and liquid carbon resistivity ρ^0 (related to its original size) is about 600 μΩ cm and the resistivity ρ (taking into account the filling volume of the tube), ~900 μΩ cm). In the liquid state the electrical resistivity of liquid carbon increases from ~900 μΩ cm up to 2000 μΩ cm at the input energy E ~ 32 kJ/g. The picture presented in Fig. 6.18 is repeated virtually unchanged for all six specimens tested under the same experimental conditions.

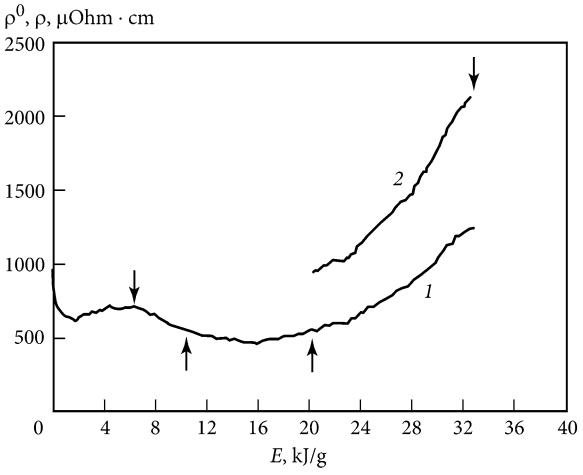

Fig. 6.18 Electrical resistivity ρ^0, referred to its initial size, (*lower curve 1*) and taking into account the expansion ρ (*upper curve 2*, only for the liquid state), depending on the specific energy input E (kJ/g). Pulse heating in sapphire capillary tube. The *upper arrow* in the curve 1—the onset of the failure of the sapphire tube

6.2.4.4 Discussion

During the contact of the liquid with the inner wall of the carbon tube a thin layer of sapphire may be melted. The penetration depth of the heat wave in the sapphire estimated by the expression:

$$\delta = (a\,\Delta t)^{1/2} \tag{6.1}$$

where: a—thermal diffusivity of a sapphire before melting ($a = \lambda / Cp\ \gamma$; λ—thermal conductivity, Cp—specific heat; γ—density). The thermal conductivity of sapphire is ($\lambda = 6 \times 10^{-2}$ J/cm s C at T = 1600 °C [29]); the heat capacity of a sapphire (Cp = 1.43 J/g K for T = 2300 K [30]); duration of the experiment $\Delta t = 6 \times 10^{-6}$ s. The density of solid sapphire before melting $\gamma = 3.764$ g/cm^3 [31]. Calculations show that the layer thickness of the sapphire ~3 μ can be melted during the time of heating 6 μs. This will lead to a change in the inner diameter by a small amount (about 3 μ), i.e. diameter will be ~(500 ± 3 μ) that can be ignored when calculating the resistivity.

The resistivity of the liquid sapphire at the melting point (~4×10^5 μΩ cm) was obtained in the experiment [32] (the resistivity of a solid phase at the melting point is 10^3 times more). Decrease in the resistance of a thin layer of the sapphire (up to ~4×10^5 μΩ cm) will not have a noticeable effect on the resistance of a liquid carbon (~800–2000 μΩ cm). Thus, under rapid heating of carbon in the sapphire tubes actually was measured the resistivity of the liquid carbon.

6.2.5 *Critical Sensitivity of Graphite Melting to the Magnitude of the Pressure (Experiments in the Sapphire Capillary Tubes)*

Since the pulse heating of graphite in water cannot provide liquid carbon research above its melting point, further experiments were performed by heating specimens of graphite, placed in sapphire capillary tubes capable of withstanding of high pressure thermo-compression.

Figure 6.19 presents the pulsed heating of graphite in the sapphire capillary tube with inner diameter of about 0.7 mm, which housed a graphite specimen size of 0.367 × 0.315 mm. In the case of capillary tube the expansion of the graphite limited by emphasis in the wall of the tube (at the same time because thermo-compression increases the pressure). Further, the energy input takes place in conditions of nearly isochoric heating, assuming that in a short time (about 4 μs), the internal diameter of the tube is not changed.

The initial voltage of the capacitor bank—9.2 kV.

1—voltage along the specimen, arrow shows the start of the discharge appearance; 2—current recorded by current monitor. Full-time in the figure (the horizontal axis)—10 μs.

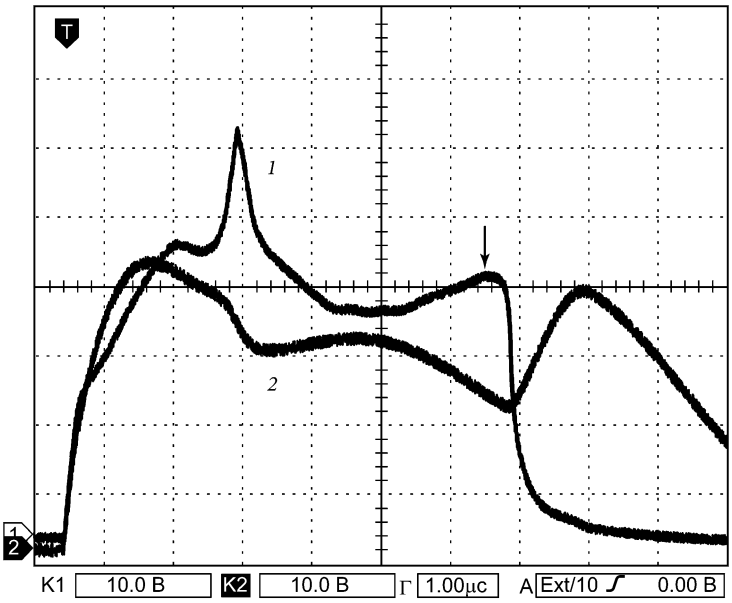

Fig. 6.19 Oscilloscope traces at heating graphite specimen MF-307 with the cross-section 0.367 × 0.315 mm, length 11.75 mm. Sapphire capillary tube was not accurately measured and accounted for ≈0.7 mm, thus, $V/V_0 \sim 3$ (V—internal volume of the tube, V_0—initial volume of graphite)

The moment it stops graphite in the wall of the capillary tube, in our opinion, comes at a time of transition from a sharp decline in voltage to much smoother. Figure 6.20 shows the dependence of the electrical resistivity ρ (μΩ cm) from the specific energy input E (kJ/g) for this specimen.

Under the experiment, when the energy input consists of 10–10.5 kJ/g, the resistance begins to increase sharply (we assume due to thermal expansion of carbon at low external pressure, i.e., it stops at the wall of the tube yet). However, further increasing the pressure in the sapphire tube restricts this expansion (increase in resistance is replaced by a fall). Graphite at high pressure melts and the completion of melting occurs at E = 20.5 kJ/g. Further heating occurs in the quazy-isochoric conditions under continuous increase in temperature and pressure. Achievable pressure can be roughly estimated as several kbar (up to 10 kbar). When the input specific energy reaches of about 27 kJ/g, the sapphire tube is destroyed with explosion effect—the voltage along the specimen is dropped, and the current increases during the development of the discharge in the products of the destruction of the tube and carbon (Fig. 6.20).

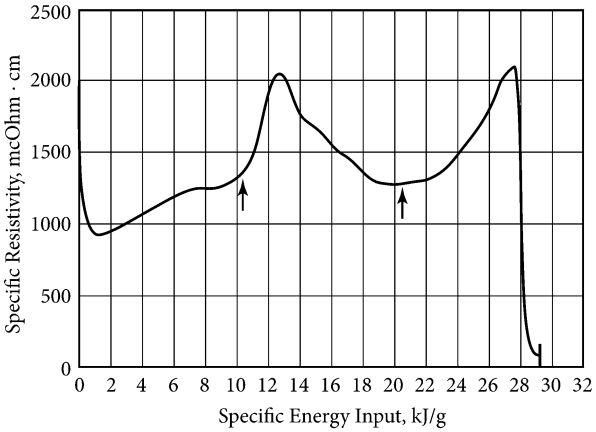

Fig. 6.20 The dependence of the electrical resistivity ρ^0 (related to the original dimensions) of the specific energy input E (kJ/g) under pulsed heating graphite MF-307 in the sapphire capillary tube (processing of the Fig. 6.19). The *left arrow* marks the beginning of a possible melting point (rather the beginning of a bulk sublimation at low pressure), and the *right arrow* shows the end of melting at 20.5 kJ/g, the last value was obtained in previous works under pulse heating [41, 42]. Calculated density of liquid carbon under quasi-isochoric heating (above 20.5 kJ/g) is $\gamma \approx 0.66$ g/cm^3, resistivity (including expansion) $\rho = 1250\ \mu\Omega$ cm $\times$ $V/V_0 = 1250 \times 3 = 3800\ \mu\Omega$ cm. (V—internal volume of the tube, V_0—initial volume of graphite; $V/V_0 \approx 3$)

The same type of experiment is shown in the following Fig. 6.21. Figure 6.22 shows the dependence of ρ^0 against E, calculated for the Fig. 6.21.

6.2.5.1 Heating Graphite in a Control Restricted Volume

To complete the picture of our study we represent experiment of different character under heating graphite in sapphire tube (Fig. 6.23). The ends of the tube were plugged by metallic pads and compressed by steel vise (through insulating plates). In this case, there is not a sharp peak on the waveform of voltage before melting, which we associate with the possible bulk sublimation (sharp expansion) at low pressure. It is possible that the nature of the seal ends of the capillary (we could compress sapphire tube ends with different strengths)—depends the level of maintaining the pressure during the experiment. Unfortunately, the press force of the compression from experiment to experiment—was not controlled.

As we have seen (Fig. 6.23), the heating time is limited by sapphire tube in 6th microseconds defined dynamic strength of sapphire at a given speed of heating, depending on the current density. Obviously, the accelerating of the heating process (by increasing the density of the heating current), you can achieve higher pressure while maintaining the strength of the tube. This requires even higher voltage (for a given pulse installation). Increasing the voltage increases the probability of bypass

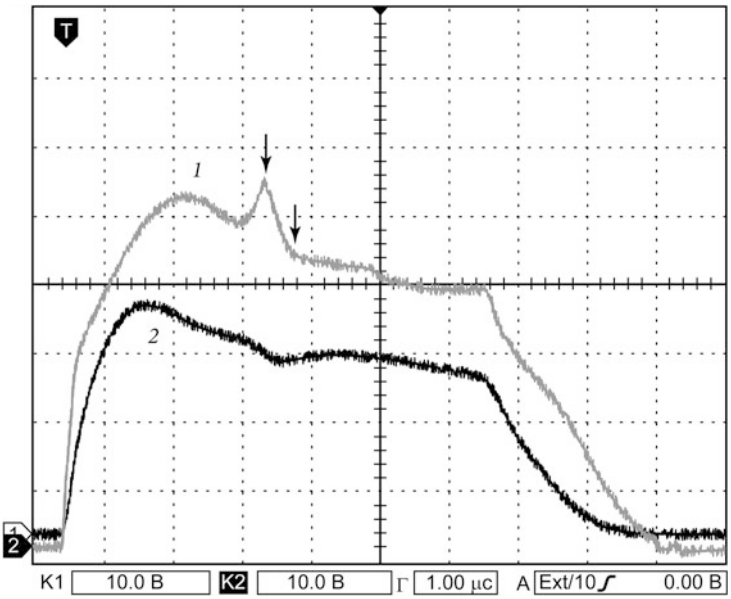

Fig. 6.21 Oscillogram of heating graphite specimen MF-307 cross-section 0.348 × 0.315 mm, length 16.45 mm sapphire capillary tube, an inner diameter of about 0.48 mm. The initial voltage on the capacitor bank—9 kV. *1* voltage across the specimen, (*left-hand arrow* shows supposed pressure higher triple point value, *right-hand arrow* shows supposed filling the volume by expanding graphite); *2* current recorded by monitor. Full-time heating in the figure (the horizontal axis)—10 μs. In this experiment, V—the internal volume of the tube, V_0—initial volume of graphite: $V/V_0 = 1.65$

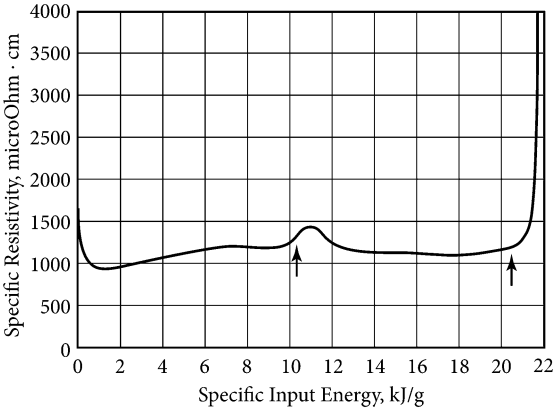

Fig. 6.22 The dependence of the electrical resistivity ρ^0 (related to the initial dimensions) against specific energy input E (kJ/g) under pulse heating graphite MF-307 in the sapphire capillary tube (processing of Fig. 6.21). The *left-hand arrow* marks the beginning of a possible melting (10.5 kJ/g), and the *right-hand arrow* the end (20.5 kJ/g). Near the *right-hand arrow* an abrupt of the heating current takes place (see Fig. 6.21), so a sharp increase in resistance after the input energy E = 20.5 kJ/g should not be taken into account. Calculated density of liquid carbon for quasi-isochoric heating (at 20.5 kJ/g) is $\gamma = 1.21$ g/cm^3; the resistivity (including expansion) $\rho = 1200\ \mu\Omega$ cm × $V/V_0 = 1200 \times 1.65 = 1980\ \mu\Omega$ cm. (V—internal volume of the tube, V_0—initial volume of graphite ($V/V_0 = 1.65$)

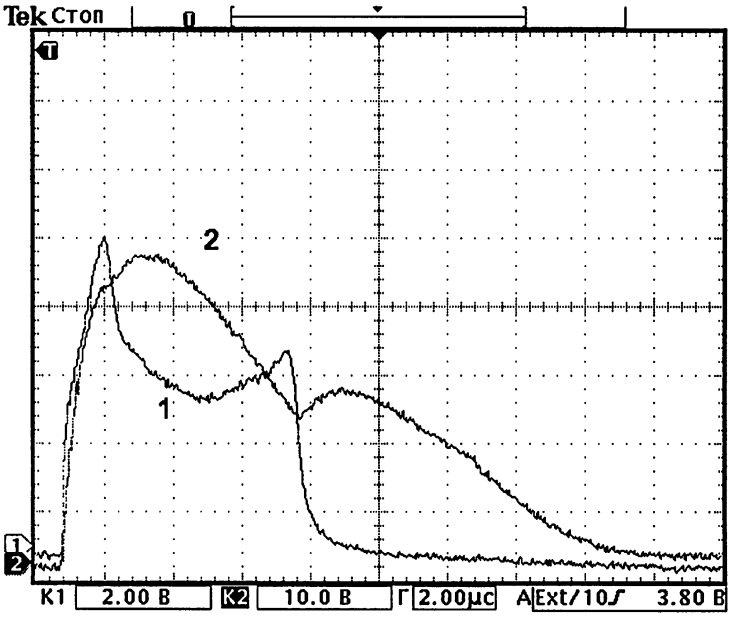

Fig. 6.23 Oscillogram traces for heating graphite specimen MF-307 with cross-section 0.45 × 0.46 mm, length 12.4 mm, in the sapphire capillary tube (inner diameter 0.78 mm, outer—10.2 mm). The ends of the tube were tightly closed and locked with a steel vise (through an insulating gasket). *1* voltage along the specimen; *2* the current detected by a current monitor. The entire heating process in the figure—20 μs. The initial voltage of the capacitor bank —14 kV. (V—internal volume of the tube, V_0—initial volume of graphite, $V/V_0 = 2.3$)

discharges along the surface of the specimen (at the beginning of heating) in the free volume of the tube placed in air. Therefore, the heating of the graphite specimen with the highest possible cross-section ($S \sim 0.5 \times 0.5$ mm) is the limit of our possibilities pulsed setup. At the same time, technically to produce the quality specimens of this size (and smaller) is a realistic procedure.

Figure 6.24 shows the processing of the waveforms shown in Fig. 6.23.

For waveforms, the nature of which is shown in Fig. 6.23 and calculated data in Figs. 6.24 and 9.15 at $V/V_0 > 2$, (under the larger gap it is not guaranteed that the bypass discharge along the specimen is not formed inside the tube).

Figure 6.25 shows another similar experiment (there were six of the experiments with the control volume heating).

Note that after the melting under isochoric heating conditions, the resistivity of liquid carbon—increases (Fig. 6.20) with input energy rising (i.e. with increasing temperature). At a pressure of less than 25 kbar in Togaya study [9, 11] it was failed to fix the melting point through the resistivity (Fig. 6.6). One can see that for 14 kbar (1.4 Gpa) in the Fig. 6.6 the resistivity of liquid carbon has a growing character (wherever occurred end of the melting).

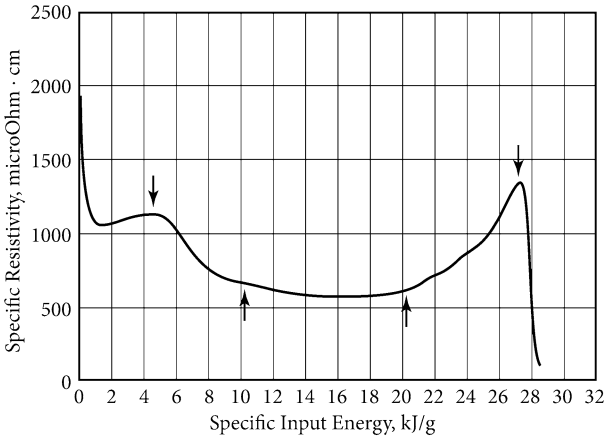

Fig. 6.24 The dependence of the electrical resistivity ρ^0 (related to the initial dimensions) against specific energy input E (kJ/g) under pulse heating of the graphite specimen MF-307 in the sapphire capillary tube (processing of the Fig. 6.23). Charging of the capacitor battery—14 kV. The *lower left-hand arrow* marks the beginning of melting (10.5 kJ/g), and the *lower right-hand arrow*—the end of melting (20.5 kJ/g). These values have been obtained in previous works under pulse heating [41, 42]. The *upper left-hand arrow* marks the beginning of the transition region from the thermal expansion from the free volume to heat in a restricted volume (very roughly at 6−10.5 kJ/g, i.e., near or before the onset of melting). *Right-hand upper arrow* indicates the time of destruction of the sapphire tube. Calculated density of liquid carbon for this experiment at isochoric heating is ~0.9 g/cm^3, the calculated electrical resistivity of liquid carbon (including expansion) at the melting point $\rho = 600\ \mu\Omega\ \text{cm} \times V/V_0 = 600 \times 2.3 = 1380\ \mu\Omega\ \text{cm}$. (V—the internal volume of the tube, V_0—the initial volume of graphite, $V/V_0 \approx 2.3$)

Most likely, the pulse pressure in our experiments does not reach 14 kbar, i.e. the minimum fixed pressures recorded in [11, 12]. Under the isochoric heating conditions it is shown in Fig. 6.24, the density of liquid carbon was 0.9 g/cm^3 (and for Fig. 6.26—1 g/cm^3). Electrical resistivity (including expansion) of the liquid phase at the melting point ~1380 μΩ cm; resistivity, excluding expansion, referred to its original size—600 μΩ cm (which also indicated in Fig. 6.24 at the end of melting). It must be recalled that the electrical resistivity of liquid carbon depends on the pressure. The higher pressure, the lower the electrical resistance. For example, at a pressure of ~50 kbar the specific (i.e., including expansion) electrical resistivity of liquid carbon at the melting point ~700–800 μΩ cm [13], and for low pressures (but more than 110 bar) ~2200 μΩ cm [14]. The obtained value ~1380 μΩ cm (see Fig. 6.24) shows a slight pressure (rough estimate gives several kbar, in any case, up to 10 kbar). Therefore, the behavior of the electrical resistivity of liquid carbon in our experiments, for this level of pressure, consistent with experimental data of Togaya [11, 12].

Most experimenters until recently used stationary methods of the study the properties of materials. However, these methods do not allow to achieve very high levels of temperature and pressure. For example, for carbon up to now, there is no complete phase diagram and have not been fully investigated liquid state for

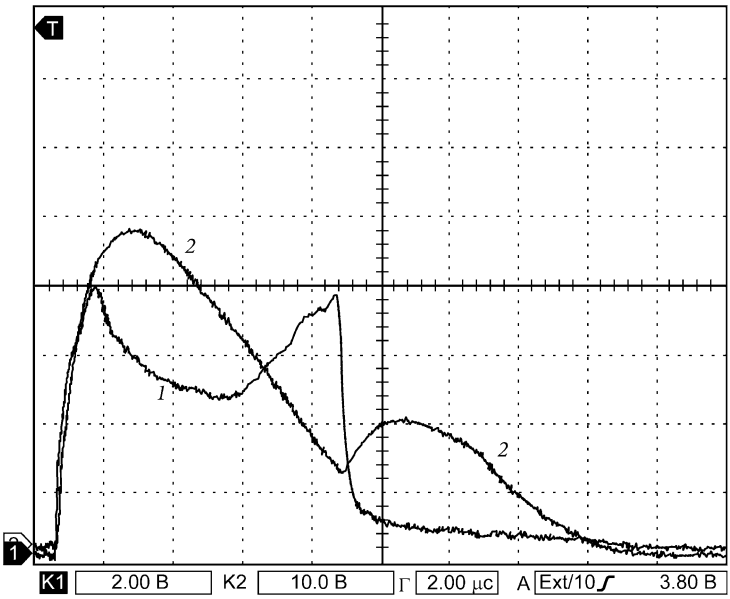

Fig. 6.25 Oscillogram traces of heating graphite specimen MF-307 (initial density of 2.0 g/cm^3), cross-section 0.625 × 0.415 mm, length 10.3 mm in a sapphire capillary tube (inner diameter 0.81 mm, outer—10.2 mm; $V/V_0 = 2$). *1* voltage along the specimen; *2* the current detected by a current monitor. The entire screen in the figure—20 μs. The initial voltage of the capacitor bank—14 kV. Graphite density under the filling the entire cross-section of the sapphire tube is 1 g/cm^3

carbon; the conflicting data of stationary measurements exist for the melting point of carbon. Discussed in this monograph experiments based on the use of pulse current heating methods enable us to solve the problem of achieving high temperatures and study the properties of carbon at high temperatures.

Prospects for further studies of liquid carbon we associate with increasing heating rate, with a corresponding decrease in the pulse time of the experiment (up to 1 μs and shorter). This will increase the relative time of the liquid state for carbon (before the destruction of the capillary tube). Thus, we can more confidently determine the properties of liquid carbon in a wide range of the liquid state.

6.2.5.2 A Short Conclusion on Experiments with Graphite Grade MF-307

1. In recent years, the most reliable experimental results were obtained for the triple point of carbon: ~100–110 bar pressure, the temperature of 4800 K. The melting of different graphite initial structures studied in detail in [33], concluded a non-metallic nature of liquid carbon after melting in the pressure range of 110–2500 bar. Possible expansion of carbon during melting is estimated as 45 % in [33] and 70 % in [14].

2. These experiments in water showed that the loss of conductivity for isotropic graphite at low ambient pressure (less than 100 bar) prevents to obtain a liquid state of carbon. In most cases, pulsed heating in the water leads to premature (near the proposed onset of melting at E ~ 10.5 kJ/g) growth of the electrical resistivity that is the characteristics of sublimation for the bulk graphite [14]. In particular, it prevents the correct measurements of melting temperature for graphite heated in a steady-state conditions or at a slow (seconds) pulse heating.
3. The application of sapphire capillary tubes, significantly increase the pressure and increase the energy input. Furthermore, quasi-isochoric heating is allowed to measure the specific resistivity (including expansion) of the liquid phases; as at the melting point ~900 μΩ cm (excluding extension it gives 600 μΩ cm), and in a wide range of the liquid state.
4. It is observed an increase of the electrical resistivity (including expansion) for liquid carbon up to 2000 μΩ cm above the melting point for relatively low pressure levels (presumably 10–20 kbar) at the input energy up to 32 kJ/g. The same behavior of the electrical resistivity of liquid carbon can be found in [12] for stationary pressure of about 14–25 kbar, as well as in pulsed heating process [13, 14]. This book demonstrates the ability to achieve and study of liquid carbon under pulse heating under standard laboratory conditions that do not require the maintenance of a stationary high- pressure equipment. High pulse pressure in graphite can be measured by the spectral method demonstrated in [34, 35] for a flat loading, just as it demonstrated during the study of super-critical states of metals. For more details, this technique is described in [23].

6.2.6 *Pulse "Pinch" Pressure at Fast Electrical Heating [36]*

6.2.6.1 Isotropic (Disordered) and Dense Graphite MF-307

Isotropic graphite MF-307 (Nippon Techno-Corporation, Japan) was used with initial density of 2 g/cm^3, initial resistivity 1250 μΩ cm. The specimens were placed in a container with previously boiled water. This ensures the absence of shunting discharge along the specimen at the start of heating. The pressure in the graphite due to the electric current pulse (the pinch effect) can be calculated by the equation:

$$\overline{P} = \frac{I^2}{2\pi R^2 C^2},$$

where $\overline{P}$—the average pressure, dyne/cm^2; I– current, CGS units. R—radius in cm; C = 3 × 10^{10} cm/s. Calculation of "pinch" pressure was produced in the CGS

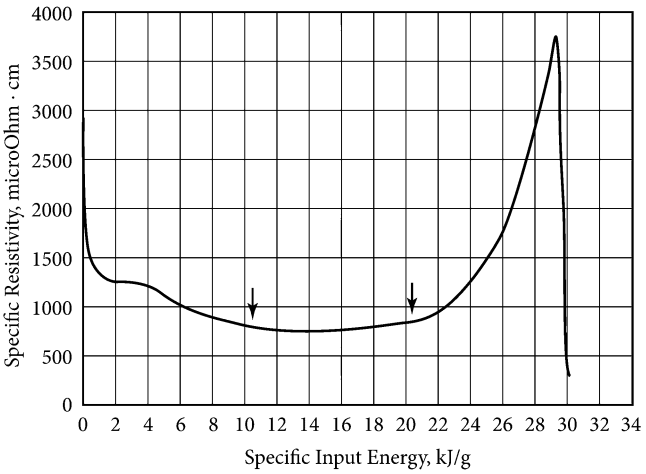

Fig. 6.26 The dependence of the electrical resistivity ρ^0 (related to the original dimensions) against specific energy input E (kJ/g) under pulsed heating of the graphite specimen MF-307 in the sapphire capillary tube (processing of the Fig. 6.25). Area of the supposed melting region (10.5—20.5 kJ/g)—marked by two arrows. Charging voltage of the capacito battery—14 kV. ($V/V_0 = 2$). Graphite density under the filling the entire cross-section of the sapphire tube is 1 g/cm^3

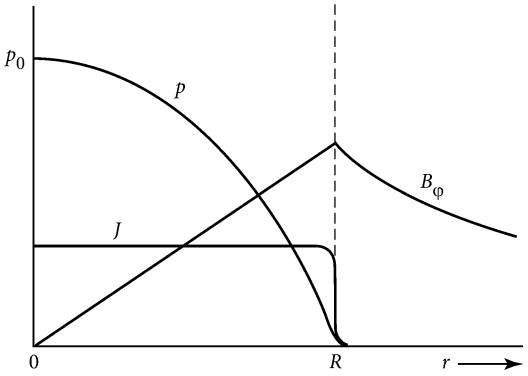

Fig. 6.27 Is taken from [23]. The current density (J), the pressure (p) and magnetic field induction ($B\varphi$) depending on the radius (R) of the conductor. *Dashed line* the outer surface of the conductor. p_σ—pressure value in the center of the conductor of cylindrical shape

system. In this unit system 1 atmosphere = 10^6 dyne/cm^2. Figure 6.27 shows the dependence of the pinch pressure of the specimen against radius [23].

Under the maximum current, for example, I = 5 kA (15×10^{12} units CGS),—the average (over the cross-section), the pressure P = 44 bar, the maximum—in the center of the specimen P = 88 bar, which is lower than the pressure at the triple point of carbon (107–110 bar). For the Figs. 6.26, 6.27 and 6.28 current consists of ~3 kA, so the pinch pressure was even less. It is noted that the pinch pressure on the surface of

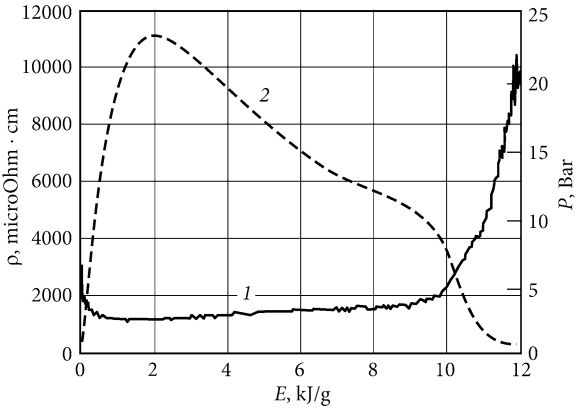

Fig. 6.28 The electric resistivity of graphite MF-307 (*curve 1*) against input energy E. The average (over the cross-section) pinch pressure P for the specimen of graphite (*curve 2*) depending on the input energy E

the conductor is always equal to zero (for an arbitrarily large value of current). As a result, nothing prevents the substance to evaporate from the surface at any pulse current value; respectively, at any values for the pinch pressure.

Summing up the consideration of characteristics of the pinch pressure, let us give an important conclusion: you can melt the bulk of the carbon contained in the specimen by pinch pressure. But pyrometer that record the temperature of the carbon surface will never show you the temperature plateau at the melting area, since the surface of carbon will not melt and will only be sublimated.

The dependence of the resistivity ρ and pinch pressure P (due to the current flowing) against input energy E for isotropic graphite MF-307 are shown (Fig. 6.28). It can be seen that the electrical resistivity begins rising sharply at the energy input ∼10 kJ/g. Under the energy input ∼12 kJ/g the resistivity reaches 10000 μΩ cm; later the specimen is destroyed.

Estimation of the pressure in this experiment gives a value of less than 100 bar. Taking into account that 10.5 kJ/g is the energy of the onset of melting [13, 15] and that the pressure at the triple point of graphite is not less than 107 bar [37–39], we can conclude that the effect of higher resistivity may be caused by the expansion in the volume of sublimation graphite (at a pressure lower than the pressure at the triple point).

6.2.6.2 Anisotropic Graphite (with Ordered Structure) UPV-1TMO

The experiments were performed with anisotropic graphite, brand UPV-1TMO (like HOPG, highly oriented graphite). The initial density of 2.25 g/cm^3 and the initial electrical resistance ρ = 50−100 μΩ cm (after annealing at 3000 °C). Specimens of graphite also dipped in a bath of previously boiled water to avoid shunting discharge. Dependencies of the resistivity and the pinch pressure from the energy input are shown below. The electrical resistivity of anisotropic graphite along the planes of deposition is much lower, than for the isotropic graphite. Due to

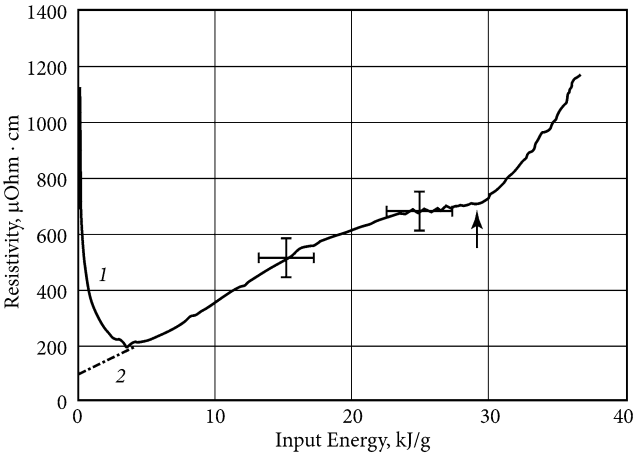

Fig. 6.29 The electrical resistivity ρ^0 (referred to initial dimensions) of anisotropic graphite (UPV-1TMO) depending on the input energy. The diminishing of the resistivity at the start of heating (1) connects with the inductance. The initial resistivity of graphite was ~100 μΩ cm (it was measured before the experiment and show by the start of the *dashed line* 2). *Arrow* marks the moment of decreasing the pinch pressure below 100 bar

this fact, at the same voltages on the capacitor bank, the heating current is much higher in the case of the experiment with the anisotropic graphite. Current was reached 10 kA or more. For such a current the average value of the pinch pressure higher than the triple point pressure of the graphite (107–110 bar). The specimen (as a whole) in Fig. 6.29 begins to melt at the energy input 10.5 kJ/g, melting ends at the energy input ~20.5 kJ/g [13]. The arrow indicates the time when the average pinch pressure becomes lower than 107–110 bar (the pressure at the triple point of graphite).

Increased electrical resistivity in the figure (at the beginning of the heating) is mainly associated with the spike voltage due to the inductance of the circuit (L) near the point of contact with the specimen and the steep increase in the current I at the beginning of heating ($\Delta U = L \times dI/dt$). Extrapolation (2) of the resistivity line (from 15 kJ/g to the start point) gives the starting resistivity of 100 μΩ cm. A sharp resistivity rise starts at ~30 kJ/g, that is, after the melting of the specimen as a whole. The following Fig. 6.30 shows the close relationship of pressure and electrical resistivity of carbon.

At the input energy equals 30 kJ/g, pressure is diminishing to 100 bar (!). So after 30 kJ/g, when the pressure falls, it begins a sharp increase in resistivity (volume sublimation at a pressure less than the pressure at the triple point).

You should pay attention to the fact that the input energy of 30 kJ/g, when the pressure drops to 100 bar (Fig. 6.30), the electrical resistivity begins to grow rapidly due to the volume sublimation at a pressure lower than the triple point (less than 100 bar). Nevertheless, in this experiment a graphite specimen was melted as a whole (except for the surface layer, where the pinch pressure is practically zero).

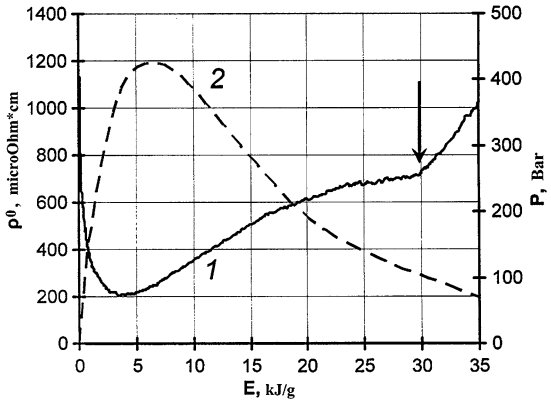

Fig. 6.30 Electrical resistivity ρ^0 (referred to initial dimensions) for graphite UPV-1TMO (*left-hand axis*) as a function of input energy E (*curve 1*). The average (over the cross-section) of pinch pressure P (*right-hand axis*) in a specimen of graphite UPV- 1TMO depending on the input energy E (*dotted curve 2*)

Melting of the main bulk specimen is confirmed by the value of the electrical resistivity at the beginning of the liquid state in Fig. 6.30 near the input energy 21 kJ/g ($\sim$620 μΩ cm), that is near to the result of Motohiro Togaya investigation.

6.2.6.3 The Results of Comparative Experiments of Anisotropic and Isotropic Graphite

1. Experiments with isotropic graphite showed that graphite MF-307 with high initial electrical resistance (1250 μΩ cm) can be melted only at elevated pressure (as well as any other graphite). In our experiments: the average pressure of the pinch for the isotropic graphite—less than the pressure at the triple point of graphite—because of the high initial electrical resistance of the graphite grade MF-307. Therefore, isotropic graphite cannot melt in water. Theoretically, one can melt and in a water, if to provide a passage of a larger current. However, for the large current, the voltage must increase considerably, which may lead to appearing the shunt discharge along the specimen.
2. Experiments with the anisotropic graphite UPV-1T with low initial resistivity showed that this graphite can be melted (as a whole), even when heated in water, as the magnitude of the heating current (in this case higher) provides a high pressure, above 110 bar. In our experiments: the average pressure of the pinch in the anisotropic graphite exceeds the pressure of the triple point of graphite due to low initial electrical resistance, i.e. due to higher current, and consequently, the increasing pinch-pressure. Despite the possibility of melting the graphite as a whole, the upper layer of the specimen (in which the pinch pressure is always zero) will not melt. It has been verified experimentally by us in these experiments:

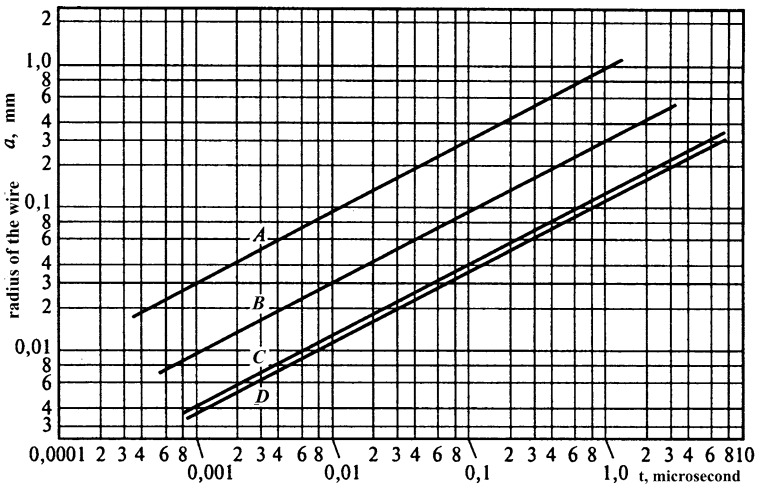

Fig. 6.31 (It is taken from [23]). The dependence of the radius "*a*" of the wire against the heating time *T* in microseconds [23, 40]. *T* time required for the current density in the center of the wire is reached the value of 99 % of the surface density: *A* Nichrome, resistivity ρ = 100 μΩ cm; *B* Platinum, ρ = 9.8 μΩ cm; Copper, ρ = 1.72 μΩ cm; *D* Silver, ρ = 1.47 μΩ cm

the light emission from the surface does not give a temperature plateau corresponding to the melting point (10.5–20.5 kJ/g), whereas at a high pressure at the surface—this plateau is recorded. To record melting area of graphite by optical methods for surface luminescence is necessary to create pressure on the surface. For example, to place a specimen between two insulating plates: under heating graphite, the latter creates excess pressure due to inertia of the outer plates (thermo-compression).

In conclusion, we present one of the most important figure [40] (previously published in [23]). Under electrical heating a field penetration depth (or current) depends on the current frequency and the resistivity of the test conductor. For simplicity of estimates gives Fig. 6.31 with a current penetration depth (for different heating time) obtained for various metal conductivity [23, 40].

According to the Fig. 6.31, in the case of heating for example for 1 microsecond, a specimen of pyrolytic graphite (of high density, quazy-mono-crystal) having an initial resistivity of about 100 μΩ cm (equaled to the resistance of Nichrome), the radius of the wire may be 1 mm (diameter 2 mm). In that case the time of 1 μs is sufficient that the current density in the center of the wire has reached 99 % of the surface density. For the case of copper with a resistivity of about 2 μΩ cm for all other things being equal, the diameter of the wire must be no more than 0.3 mm. This provides uniformity of heating throughout the volume of specimen (within 99 %). Figure 6.31 is important to evaluate the ability of a homogeneous heating; it includes as the heating rate and the value of electric resistance of the material tested. It is recommended that the experimenters to use this figure to evaluate the

possibilities of uniform heating of the conductor by single current pulse. This is especially important for very fast heating (nanoseconds) when the skin effect becomes crucial to assess heterogeneity of heating.

References

1. M. Togaya, Pressure dependences of the melting temperature of graphite and the electrical resistivity of liquid carbon. Phys. Rev. Lett. **79**(13), 2474–2477 (1997)
2. M. Togaya, Electrical resistivity of liquid carbon at high pressure, science and technology of high pressure, in *Proceedings of AIRAPT-17*, ed. by M.H. Manghnani, W.J. Nellis, M.F. Nicol (Universities Press, Hyderabad, India, 2000), pp. 871–874
3. J.W. Shaner, Bull. Am. Phys. Soc. **32**, 608 (1987)
4. J. Heremans, C.H. Olk, J.L. Eesley et al., Observation of metallic conductivity in liquid carbon. Phys. Rev. Lett. **66**(2), 452 (1988)
5. M. Togaya, S. Sugiyama, E. Mizuhara, Melting line of graphite. AIP Conf. Proc. **309**(1), 255–258 (1994)
6. S.V. Lebedev, A.I. Savvatimskiy, The electrical resistivity of graphite in a wide range of condensed state. High Temp. **24**(5), 671–678 (1986)
7. A.I. Savvatimskiy, V.E. Fortov, R. Cheret, Thermophysical properties of liquid metals and graphite, and diamond production under fast heating. High Temp.- High Press. **30**, 1–18 (1998)
8. D.H. Reitze, X. Wang, H. Ahn, M.C. Downer, Femtosecond laser melting of graphite. Phys. Rev. **40**, 11986–11989 (1989)
9. D.H. Reitze, H. Ahn, M.C. Downer, Phys. Rev. **45**, 2677 (1992)
10. N. Bloembergen, First light on liquid carbon. Nature **356**, 110 (1992)
11. M. Togaya, Electrical property changes of liquid carbon under high pressures. J. Phys. Conf. Ser. **215**, 012–081 (2010)
12. M. Togaya, in *Behaviors of liquid carbon at high pressure*. ed. by V.V. Brazhkin et al., New Kinds of Phase Transitions: Transformations in Disordered Substance (Kluwer Academic Publishers, Printed in the Netherlands, 2002), pp. 255–266
13. A.I. Savvatimskiy, Measurements of the melting point of graphite and the properties of liquid carbon (a review for 1963–2003). Carbon **43**, 1115–1142 (2005)
14. A.I. Savvatimskiy, Liquid carbon density and resistivity. J. Phys.: Condens. Matter **20**, 114112 (2008)
15. V.N. Korobenko, A.I. Savvatimskiy, Electrical resistivity of liquid carbon. High Temp. **36**(5), 700–707 (1998)
16. M.A. Sheindlin, V.N. Senchenko, Experimental study of the thermodynamic properties of graphite near the melting point. Sov. Phys. Dokl. **33**, 142–145 (1988)
17. V.N. Korobenko, A.I. Savvatimski, R. Cheret, Graphite melting and properties of liquid carbon. Int. J. Thermophys. **20**(4), 1247–1256 (1999)
18. F.P. Bundy, R.H. Wentorf, Direct transformation of hexagonal Boron Nitride to denser forms. J. Chem. Phys. **38**, 1733815 (1963)
19. G.R. Gathers, J.W. Shaner, D.A. Young, High temperature carbon equation of state, UCRL-51644. Livermor, 1–13 (1974)
20. H.R. Leider, O.H. Krikorian, D.A. Young, Thermodynamic properties of carbon up to the critical point. Carbon **11**, 555–563 (1973)
21. G.I. Kerley, L. Chhabildas, *Multicomponent-multiphase equation of state for carbon, sandia report: SAND2001-2619* (Sandia National Laboratories, USA, 2001), pp. 1–50
22. M.S. Downer, H. Ahn, D.H. Reitze, X.Y. Wang, Dielectric function and electrical resistivity of liquid carbon determined by femtosecond spectroscopy. Int. J. Thermophys. **14**(3), 361–370 (1993)

23. A.I. Savvatimskiy, V.N. Korobenko, High-temperature properties of metals for nuclear industry (zirconium, hafnium and iron during melting and in the liquid state), MEI Publishing House, 216 p., ISBN 978-5-383-00800-3 (2012) (in Russian)
24. V.N. Senchenko, Enthalpy and heat capacity of graphite in the region of melting point. Ph. thesis, Institute for High Temperatures, Moscow (1987) (in Russian)
25. F.P. Bundy, Melting of graphite at very high pressure. J. Chem. Phys. **38**, 618–630 (1963)
26. S.V. Lebedev, Phenomena in tungsten wires prior to their explosion by a high current, JEPT **27**(5), 605–614 (1954)
27. V.N. Korobenko, A.I. Savvatimskiy, in *Blackbody design for high temperature* (*1800 to 5500 K*) *of metals and carbon in liquid states under fast heating, temperature: its measurement and control in science and industry*, ed. by D.C. Ripple. AIP Conference Proceedings, vol. 7, part 2, pp. 783–788 (2003)
28. A.I. Savvatimskiy, Melting point of graphite and liquid carbon. Phys. Usp. **46**, 1295–1303 (2003)
29. Refractory materials in mechanical engineering, (reference-book), ed. by A.T. Tumanov, K.I. Portnoi (Mashinostroenie, Moscow) (1967) (in Russian)
30. L.V. Gurvich, I.V. Weitz, D.F. Medvedev et al., Termodinamicheskte properties of individual substances. Nauka **3**(2), 1–395 (1981) (in Russian)
31. S.V. Stankus, P.V. Tyagelsky, Thermal properties of Al_2O_3 in the melting region. Int. J. Thermophys. **15**(2), 309 (1994)
32. E.E. Shpil'rain, D.N. Kagan, L.S. Barhatov, L.I. Zhmakin, The electric conductivity of alumina near the melting point. High Temp.- High Press. **8**, 177–181 (1976)
33. M. Musella, C. Ronchi, M. Brykin, M. Sheindlin, The molten state of graphite: an experimental study. J. Appl. Phys. **84**(5), 2530–2537 (1998)
34. A.I. Savvatimskiy, Physical properties of conductors at high temperatures, in the book "Results and Prospects (50 years JIHT)" (Publisher "Chance" (JIHT RAS), in Russian, 2010), pp. 89–114
35. V.N. Korobenko, A.D. Rakhel, Electrical resistivity and equation of state measurements on hot expanded aluminum in the metal–nonmetal transition range. Phys. Rev. B **75**, 064208 (2007)
36. A.I. Savvatimskiy, A.M. Kondratyev, S.V. Onufriev, Experiments on the melting of graphite under pulse electrical heating. Izvestia Vuzov. Chem. Chem. Technol. **56**(7), 53–56 (2013)
37. D.M. Haaland, Graphite-liquid-vapor triple point pressure and the density of liquid carbon. Carbon **14**(6), 357–361 (1976)
38. D.M. Haaland, Determination of the solid-liquid-vapor triple point pressure of carbon. Report SAND **76–0074**, pp. 1–48 (1976)
39. A.Y. Basharin, M.V. Brykin, M. Marin, I.S. Pakhomov, S.F. Sitnikov, Ways to improve the measurement accuracy in the experimental determination of the melting temperature of graphite. High Temp. **42**(1), 60–67 (2004)
40. R. Manninger, in *Radial distribution of current and its impact on the exploding wire, in the book* "*Exploding Wires*"*, translated from English*, ed. by Rukhadze (Foreign Literature Publishing House, Moscow, 1963) pp. 142–154 (in Russian)
41. V.N. Korobenko, PhD dissertation for the degree of candidate of physical and mathematical sciences, experimental study of the properties of liquid metals and carbon at high temperatures, (Institute for High Temperatures RAS, Moscow, 2001) (in Russian)
42. A.V. Baitin, A.A. Lebedev, S.V. Romanenko, V.N. Senchenko, M.A. Sheindlin, The melting point and optical properties of solid and liquid carbon at pressures up to 2 kbar. High Temp.-High Press. **21**, 157–170 (1990)
43. V.E. Fortov, V.N. Korobenko, A.I. Savvatimskiy, Liquid metals and liquid carbon: some similar properties at high temperatures. Eur. Phys. J. B (EPJ WEB of the Conferences) **15**, 02001 (2011)

Chapter 7
Experimental Setup in Fast Heating of Carbon

Abstract Two installations are shown: with a small current pulse (upper limit 15 kA) for training students and the largest one with a high current pulse (upper limit 400 kA). The features of these two systems discussed in all the details that are the most important to the experimenters. It was given a choice of a blackbody design and fast pyrometer for recording melting and liquid state of carbon under fast heating in JIHT. A detailed description of the arrangements in pulse electrical heating is shown. Pulse heating results on measuring carbon temperature (up to 12,000 K) are shown.

7.1 Pulse Experimental Arrangements in Laboratory of Electro-exploding Processes (JIHT)

7.1.1 Introduction

As was shown in monograph [1]: the time of transferring energy from the electrons to the lattice under the pulse volume heating of the metals by electric current consist of picoseconds. For the case of graphite heating by current pulse or by laser pulse approximately the same picture takes place (laser pulse transmits photon energy to the outer electrons that carry the energy further, to lattice). For example, the calculation [2] shows how fast the establishment of equality of electron does and ion temperatures in the absorption of the laser pulse by graphite surface (Fig. 7.1).

It was observed electron-ion relaxation within 1 ps (τ_L), while the thermal diffusion τ_D is considered infinite. Inset shows the estimated pair potential for liquid phase of low density at high temperature. Estimated cell contains 240 atoms.

The influence of heating rate on the measured conductor properties under pulse heating was studied in detail [1]. In the [1, p. 33] there is a diagram to evaluate a uniform heating over a specified time of the experiment, it includes accounting, as the heating rate, and the magnitude of the electrical resistance of the material under investigation. There are also schemes and description of the pulse installations for

A. Savvatimskiy, *Carbon at High Temperatures*, Springer Series in Materials Science 134, DOI 10.1007/978-3-319-21350-7_7

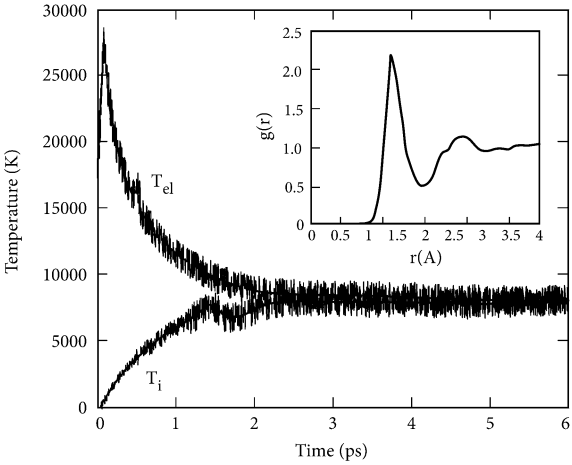

Fig. 7.1 [2]. Ion and electron temperature (calculated values) in the absorption of laser pulse energy 3.5 eV/atom. T_{el} electron temperature; T_i ion temperature

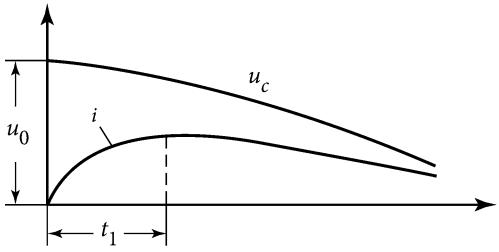

Fig. 7.2 The shape of the current pulse (i) and voltage (U_C) at the discharge aperiodic depending on time t. U_0—initial battery voltage; t_1—time to reach the maximum current; $t_1 = 2L/(R_{SPECIMEN} + R_{BALLAST})$

investigation of the thermophysical properties for metals. To set out earlier in [1] it should be added that the most advantageous mode of pulse heating (for optimal use of energy in the first half-cycle battery discharge) is a discharge of a capacitor bank at the border aperiodicity. Critical is called loop resistance expressed by the formula:

$r = 2\sqrt{L}/C$, (L—circuit inductance; C—battery capacity). If the total resistance of the circuit ($R_{SPECIMEN}$ + $R_{BALLAST}$) is less than the critical value r, there is a periodic discharge takes place. Under equality is observed boundary aperiodicity, there is unipolar pulse takes place (Fig. 7.2).

If the total resistance of the circuit ($R_{SPECIMEN}$ + R_{BALL}) more than critical, there is a deep aperiodicity until almost it has nearly a constant current (with a weak diminishing)—it is usually a slow heating process. Figure 7.2 shows the case of aperiodicity boundary which is realized usually in the presence of ballast resistances

in the circuit. Then the total resistance of the circuit will be the sum of the resistances $R_{SPECIMEN}$ and $R_{BALLAST}$ ($R_{SPECIMEN} + R_{BALL}$). Usually pulsed facilities intended for thermal measurements, the ballast resistor R_{BALL} (the main part of the total resistance) is about 0.5–1 Ω.

At lower resistances it may obtained a periodic change of the current ($r < 2\sqrt{L/C}$), which is disadvantageous in many ways. We only mention three main reasons. First, the calculation of input energy for AC signal it is required to enter into the calculation of effective current value. Secondly, when calculating the energy input and the electrical resistivity (in the program of Exel or Origin) it requires fixing only positive values of the functions (negative values are not allowed). Thirdly, the modern pulse capacitors accumulate although a high energy density in a small volume (i.e. have low weight), but do not maintain a significant negative potential (no more than 10 % from the maximum positive pulse value).

7.1.2 *Pulse Experimental Setup for Training Students and Postgraduates*

Schematic electrical diagram of the pulse installation is shown in Fig. 7.3. According to Fig. 7.3 one can use the ignition (T_1) of the pulse current and shunt this pulse by using the second thyratron (T_2).

Block diagram of operation of the installation shown in Fig. 7.4.

The pulse generator G5-63 operates in the mode of paired pulses. In this mode when you manually start the generator it has 2 electrical pulse: 1—sync-pulse and 2—the main pulse. Time shift (delay) between the sync-pulse and the main pulse is determined depending on the required length of the working pulse (i.e. a pulse current applied to the specimen). The sync-pulse is used for triggering the thyratron

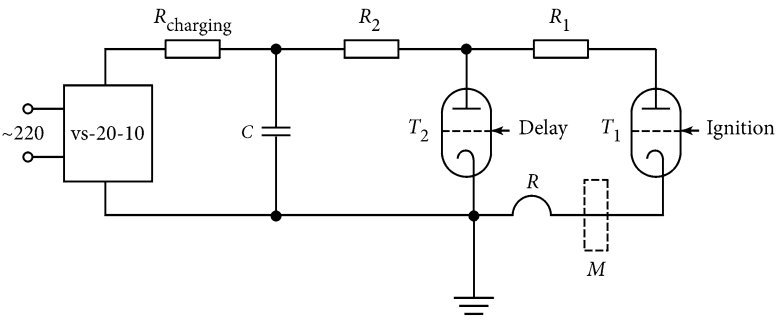

Fig. 7.3 Schematic diagram of pulse installation with the shunting pulse. Recharging—charging resistor type TVO-60 (~200 kΩ); R—test specimen; R_1—resistor of the main circuit (~0.8–1 Ω); R_2—resistor of the cutting circuit (~0.3 Ω); C—capacitor bank (6–12 μF); M—Monitor of the current (A-110 or 5046, Pearson Electronics); *T*1, *T*2 hydrogen thyratron TGI1-1000/25 (25 kV, 1000 A for continuous operation); VS- 20-10—the rectifier unit (20 kV, 10 mA)

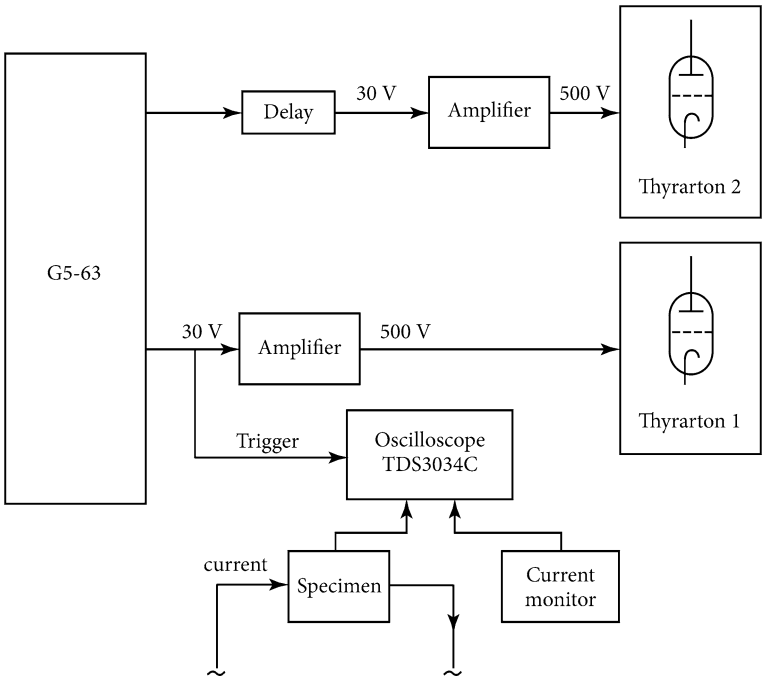

Fig. 7.4 Block operation diagram of the installation

No. 1 and oscilloscope operating in the run mode from an external source. When this happens, the start thyratron No 1 takes place and we have a unit pulse of current from the capacitor bank. Simultaneously, the sync-pulse starts the oscilloscope and recorded waveforms of current and voltage along the specimen.

The main pulse, which follows with a delay after sync-pulse, is used to run the thyratron No. 2. Then the start of thyratron No. 2 takes place. The heated specimen is shunted (abrupt of the current), as the current begins to flow through the thyratron of the circuit No. 2 (Fig. 7.3). Thus, the thyratron No. 1 includes current and the thyratron No 2 interrupts it, resulting in the current pulse of desired duration whose length is equal to the time shift (delay) between the sync pulse and the main pulse.

We use the installations (for the current pulse on the order of 1–10 kA) which includes hydrogen thyratrons TGI1-1000/25 (continuous current 1000 A under 25 kV). Two-three capacitors IKM-50/3 (3 microfarad capacity each under 50 kV maximum) are connected in parallel and the whole capacitor bank gives 6–9 μF capacitance. They are charged by the rectifier unit VS-20-10 (20 kV, 10 mA). Between VS-20-10 and capacitors it was placed resistor (200 kΩ) for limiting the charging current. The start current occurs through the disc low-inductance ballast resistances R1 and R2 (Fig. 7.3), resulting in a current pulse. R1 and R2 represent a two serially connected resistor disk HVR APC with the value from 0.3 up to 1 Ω.

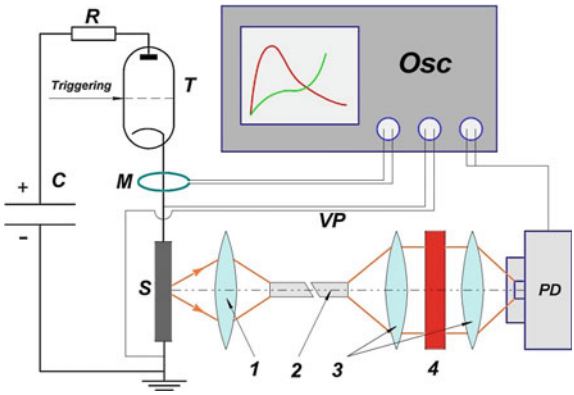

Fig. 7.5 Schematic diagram of the experimental installation. Main electrical circuit and optical scheme of the pyrometer are shown. C—capacitor bank; R—current-limiting resistor; *T* hydrogen thyratron; M—current monitor; VP—voltage probe; S—specimen; PD—photodetector; *1* pyrometer objective; *2* light guide; *3* lenses; *4* interference filter (856 nm)

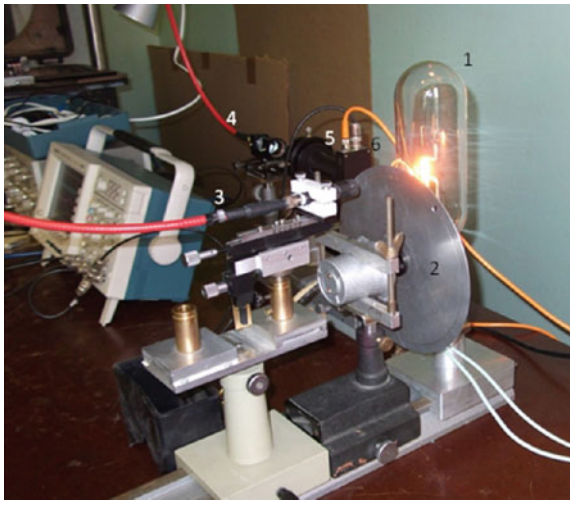

Fig. 7.6 Calibration of the pyrometer by constant glow of a tungsten lamp through a rotating disc (3000 rpm). In the disk (on one diameter) it was drilled 2 holes. When the disk rotates, the light signal of the glow lamp is converted into an AC signal at the input to the pyrometer

In the most experiments it is enough to use only one discharger; in that case one can use the scheme shown in the Fig. 7.5. Besides, this figure shows the optical scheme to measure temperature during short pulse heating.

Pyrometer was calibrated through tungsten lamp (Fig. 7.6).

1 Pyrometric tungsten lamp.
2 Rotating disk (chopper) with two holes along the diameter.
3 Light guide.
4 Fiber (to pyrometer).

5 Interference filter for wavelength 853 nm.
6 Pyrometer(photodetector PDA-10A, firm Thorlabs)

Hydrogen thyratrons (T) are the incandescent model TGI1-1000/25. Filament voltage is required for 6.3 V. The cathode heat of the thyratron number 2 (T2) is constantly connected to the ground circuit. For filament cathode thyratron number 1 (T1) is placed in the transformer oil due to the fact that in case of excessively high voltage cathode filament circuit may be at high voltages. In fact, the heating of the thyratron cathode 1 (T1) can operate at high voltage. The inclusion of the thyratrons in the operating mode is not less than 5 min, it is associated with the work of hot cathode.

The output signal of the generator G5-63 (output 20–80 V) requires an increase voltage up to 500 V as thyratrons start needs signal with a voltage of 500 V. In this connection, voltage amplifiers are used, a scheme of one of them is shown in Fig. 7.7. Surely it may be a simpler scheme for the up to date electronic devices (the common feature is using two transformers in the circuit).

To measure the charging voltage the static high voltage voltmeter C-196 was used. This voltmeter is convenient because it shows the true voltage without current consumption.

To work without significant interference (for the all the pulsed installations) it needs to earth the electrical scheme only at one point. This allows you to get rid of multiple ground loops that can lead to disturbance of the recorded pulse signals. So this installation is grounded at a single point of attachment of the test specimen.

As a current sensor we used monitor of Pearson Current Monitor 5046 (production of Pearson Corporation, USA, Fig. 7.8), which gives inaccuracy 1 % under measurement of pulse current up to 25 kA.

The advantage of using this type of monitor is that they can be placed in the high voltage circuit, because the current measurement takes place in a contactless manner. Proximity method involves measuring the current flowing in the monitor

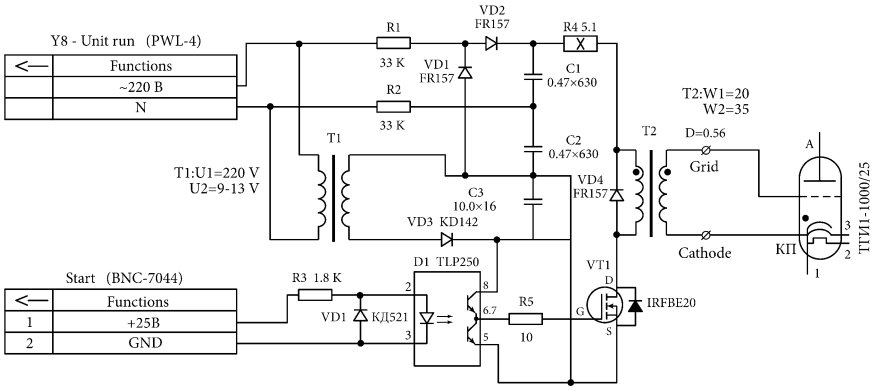

Fig. 7.7 Scheme of the amplifying voltage unit (from 20 up to 500 V) by Maxim Kruchinin (start unit for ignition of thyratron TGI1-1000/25)

Fig. 7.8 Sensor (monitor) of the current (Pearson Current Monitor model 5046). Outer diameter 48 mm, inner diameter 13 mm, thickness 23 mm

circuit, due to the electromagnetic field. Monitor 5046 is designed to operate at 20 MHz, the current rise time is 20 ns (the upper limit 25 kA). This allows using it at the heating times of the order of a few microseconds.

To verify the installation it were conducted the experiments with materials whose properties are already known. In particular, it was investigated Nickel, molybdenum and tungsten in the region of their melting. The results of these trial experiments were correlated with the data available in the literature, and had no differences with them. After that, experiments were started by pulse heating of graphite in different media–air, water and sapphire capillary tubes.

Parts of the installation (Fig. 7.9) include:

- Rectifier unit for charging the capacitor VS-20-10 (maximum output voltage of 20 kV, a current of 10 mA)—1 piece;
- Capacitor IKM 50/3 (switching low-inductance capacitor, 50 kV, 3 μF, production by Serpukhov condenser plant)—2–4 pieces (together they form the capacitor battery);
- The thyratron TGI-1000/25 (gas-filled pulse thyratron with a filling of hydrogen, 1000 A and 25 kV)—2pcs;
- Start device for thyratron switching (output voltage 500 V)—2 pcs;
- Low-inductance disk ballast resistor HVR APC (0.1 Ω, 20 kV)—2 pcs;
- Low-inductance disk ballast resistor HVR APC (0.43 Ω, 20 kV)—2 pcs;
- Carbon resistor TWO-60 ($\sim$200 kΩ)—1;
- Pearson Current Monitor 110A production Pearson Corporation (USA) (maximal measured current 10 kA with an error of 0.43 % (certified), designed to operate at 20 MHz)—1; or monitor 5046 (for 25 kA)—1

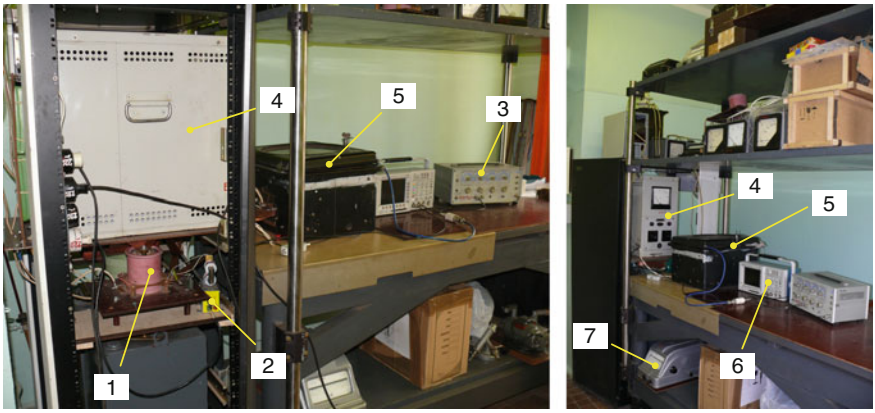

Fig. 7.9 Photo of pulse installation. Numbers denote: *1* thyratron TGI-1000/25; *2* unit run for thyratron (voltage amplifier); *3* pulse generator G5-63; *4* rectifier setting VS-20-10; *5* working camera; *6* oscilloscope Tektronix TDS3034B; *7* kilovoltmeter-(C-196)

- High voltage voltmeter C-196 (measured voltage up to 30 kV with an error of a reference voltage of 1.5 %)—1 piece;
- The pulse generator G5-63 (duration of about 0.1–1000 μs, amplitude of 0.1–60 V; modes: single pulse sequence, paired pulses, the time difference between the pulse pair 3–2000 μs)—1 piece;
- Digital oscilloscope Tektronix TDS3034B, 4-channel (300 MHz, digital, the sampling frequency of 2.5 GHz, the length of a record 10,000 points/channel, synchronization usual and video, 5 arithmetic functions automatic measurement 21 parameter, color DPO)—1 piece;
- Transformers (separation for power installation—1 unit, filament transformer for the glow thyratrons 2 items);
- Working (explosive) camera.

As the test material it was used isotropic graphite (grade MF-307), with 2 g/cm^3 density produced by the Japanese company Nippon Carbon-Corporation. The carbon content—99 %; ash—0.1 %. The thermal conductivity is 116 W/m•K. Initial resistivity 1250 μΩ cm according to the passport data; it was confirmed in the experiment.

The part of graphite block 2 × 2 × 2 cm was cut into flat plates with a thickness of about 0.3 mm with the help of diamond disc (rotation speed of 300 rpm). Upon rotation the disk was moistened with water for cooling and removal of the carbon particles. Next, a set of plates in a stack of graphite was cut in the transverse direction. As a result, we obtained specimens of rectangular cross-section ~0.3 × 0.25 mm, a length of about 10–15 mm.

In the case of heating in water the specimens were fixed in the tool holder—electrodes using the "soldering" by tin solder. Under the "soldering" we mean a

tight binding end of the specimen holder in the electrode during the solidification of tin solder.

Since graphite is melted only at a pressure greater than 100 bar, and we are interested in liquid carbon at much higher temperatures than the melting temperature (4800 K) it was necessary to create a high pressure in the graphite specimens to within a short time to investigate the liquid carbon at higher temperatures. This was accomplished by restricting the thermal expansion of solid graphite, which will cause pressure thermo-compression. For this purpose, the specimens were placed in isolation capillary tube which was made of sapphire (Al_2O_3) or silica (SiO_2). As a result, when the expansion of the graphite stops it was appeared high pressure.

Under rapid heating the pressure can reach tens of thousands of bar as dynamic yield strength of the tube is much higher than during steady load. Besides the compression pressure in the specimen, a pressure due to electromagnetic forces was appeared (due to the magnitude of the own pulse current)—pinch effect. Value of the "pinch" pressure depends on the square of the electrical current and the specimen cross-section (for the details see Sect. 6.2.6). In this paper, "pinch" pressure was calculated, and for the current 5 kA and it equals $\sim$50 bar. Under microsecond experiments in the water it arises minor inertial pressure also (it was not considered). Estimation of the compression pressure in the capillaries was made on the basis of the behavior of the resistivity and a comparison with results of other studies, where this pressure was recorded. Subsequently, the pressure can be measured by the shift of the ruby luminescence (but this requires a special expensive equipment), or using other pressure sensors.

Input energy under pulse electrical heating was calculated from the known [1] formula:

$$E(t) = \int_0^t \frac{I(t)U(t)}{m} dt,$$

where m—mass of the specimen.

Calculation of the skin effect [1] shows that the graphite specimen of 0.4 mm in diameter, heated by a current pulse with a 10 μs duration, the energy input at the surface of only 1–1.5 % higher than the release of energy in the center of the specimen.

Figure 7.10 presents the attachment methods for graphite specimen (placed inside the sapphire capillary tubes) in the removable brass holders.

The apparatus was used to 15–20 kV of operating voltage, with current reaching 5–10 kA. These limiting parameters allow to heat specimen in the form of the rods with an effective diameter of not more than $\sim$0.4 mm in the range of heating time is not more than 7–10 μs. During this time, the input energy reaches 15–30 kJ/g that is enough to melt and further heating the liquid phase. The main problem was how to introduce this Joule energy E (E = U × I × t, where U—voltage; I—current; t—time) at high pressure, because to achieve the triple point of carbon it is required pressure of at least 100–110 bar.

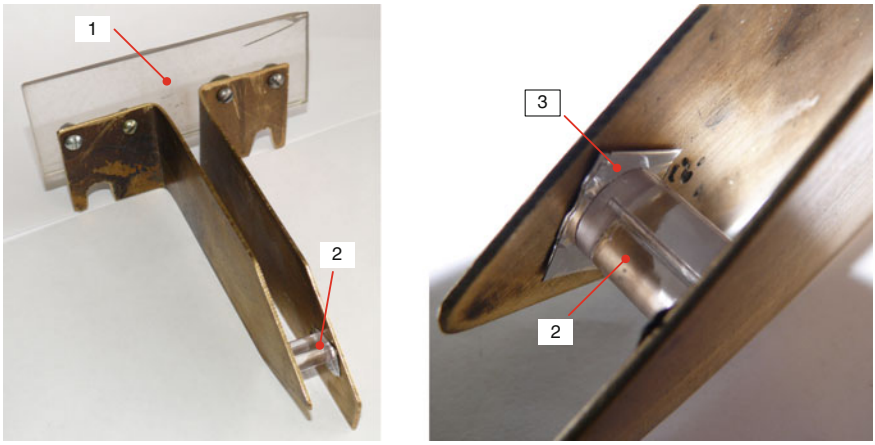

Fig. 7.10 Holder-electrode, supply current to the graphite specimen which placed inside a sapphire capillary tube. *1* Insulating plate; *2* sapphire tube with the specimen of graphite inside; *3* thin pads are made of soft aluminum (or copper)

Prepared holder-electrode with the specimen is installed in the explosive camera and tightened by metal vice, which is isolated from the potential electrode. The voltage along the specimen is applied to the cables of the oscilloscope.

7.1.3 *Powerful Pulse Installation for Fast Heating of Graphite Plates*

To allow heating of thin graphite plate at high pulse pressure this thin plate was placed between two thick plates of sapphire. In the experiments it was measured the time dependence of the current through the specimen $I(t)$ and the voltage drop on it $U(t)$. The Rogowski coil and voltage divider were used for recording signals from 4-channel digital oscilloscope TDS-S (time resolution ~ 1 ns). The active voltage drop in the sample was calculated by the formula:

$$U_R = U - L_f dI/dt$$

where L_f is the inductance of the foil. Active resistance and the heat absorbed in the specimen (per unit mass) were obtained from the equations:

$$R = \frac{U_R}{I} \quad q = \frac{1}{m}\int_0^t I(t')U_R(t')dt'$$

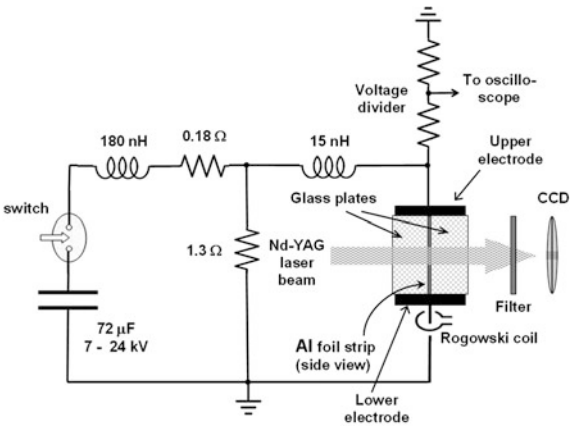

Fig. 7.11 Diagram of the electric circuit for pulsed heating of the specimen, the recording of current and voltage, as well as obtaining the high-speed pictures of the specimen

(where m is the mass of the specimen). Conductivity was determined from the relation:

$$\sigma = l/(SR),$$

where $S = hd(t)$—cross-section sample. The thickness of the foil as a function of time $d(t)$ was calculated using the hydrodynamic model, assuming that l and h—are constant (Fig. 7.11).

Show the picture (Fig. 7.12) of a powerful installation, built by V.N. Korobenko and used for rapid input of energy into the graphite specimen with a diameter of about 1 mm. It was obtained the maximum value of input energy into the graphite with the help of this installation.

Vacuum discharger allocates in a metal shell (#4 at the top of the picture) initiates two more powerful spark gap RVU-2, #5). Maximum possible pulse current 500 kA in the microseconds time scale.

Capacitor Bank contains 6 capacitors IKM25-12, (25 kV, 12 μF for each capacitor).

1. Charging transformer.
2. Chamber (diameter 30 cm) with exploding specimen placed inside.
3. Metal room for operator and equipment.
4. 1st vacuum discharger in metallic shield (which ignites the two power discharges RVU-2).
5. Two power discharges RVU-2.
6. Two heavy white Teflon block press tape resistance with low inductance for forming a short current pulse.

Fig. 7.12 Powerful pulse installation by V.N. Korobenko

7. Cable line; the flat bus-bar goes into the cable line #7 (24 cables, each 1 m long). Plane way of current, which changes to cableway (from right side to the left).
8. Condenser battery: 6 condensers IKM25-12, (25 kV, 12 μF each).

The main pulse installation was built by V.N. Korobenko and used to study metals and graphite. We (both with Korobenko) published a book (Fig. 7.13) devoted to experimental investigation of refractory metals at high temperatures (MEI Publishing House, 2012, 216 pages, ISBN 978-5-383-00800-3, in Russian). Later (2014 year) a second monograph has appeared (Fig. 7.14), devoted to carbon melting.

The installation is structurally designed as a flat bus bars (starting from the capacitors to the ballast resistance), passing in the 12 cables leads supplying current to the specimen, that was located coaxially, in the center of the explosion chamber.

Figure 7.15 shows a section of the explosion chamber, which was used during rapid heating of graphite electric pulses (time of heating 1–3 μs). This ensured the input of high specific energy into the graphite (sometimes higher the sublimation energy for carbon).

It was used a capacitor bank in a low-inductance performance, with stored energy of 20 kJ. The test specimens consisted of metal foil (thickness ~20–50 μ for metals and ~200–300 μ for graphite), a component of which was mounted as a blackbody design for temperature measurement. It was not necessary to take into account the heat losses and chemical reactions due to the short duration of the

Fig. 7.13 The first monograph by Savvatimskiy and Korobenko "High-temperature properties of metals for nuclear industry (zirconium, hafnium and iron during melting and in the liquid state)". The book was published with the support of the RFBR (project 12-08-07016) in 2012 year

experiment (1–3 μs). Due to such a short heating time of the electric discharge along the surface of the metal in an air atmosphere usually is not appeared (up to 6000 K) even under a tungsten study. With the specimens of graphite it was different. Previously, we tried to heat the graphite specimens within tens of microseconds in an air pressure of 1 atmosphere, trying to melt it. We did not succeed, since the bypass discharge was flushed along the graphite at the specific energy input nearly 8–9 kJ/g, i.e. before melting.

Fig. 7.14 The second monograph "Graphite melting and liquid carbon properties", Moscow, Fizmatkniga, 257 pages, ISBN 978-589155-240-1. The book was published with the support of the Russian Foundation for Basic Research, project 14-08-07009 in 2014 year

Bypass discharge appeared around the specimen, interrupting the heating of the graphite specimen. Therefore, further we use a solid insulating jacket around the specimen prior to heating it, that contributed to the measurement of the specific properties of liquid carbon.

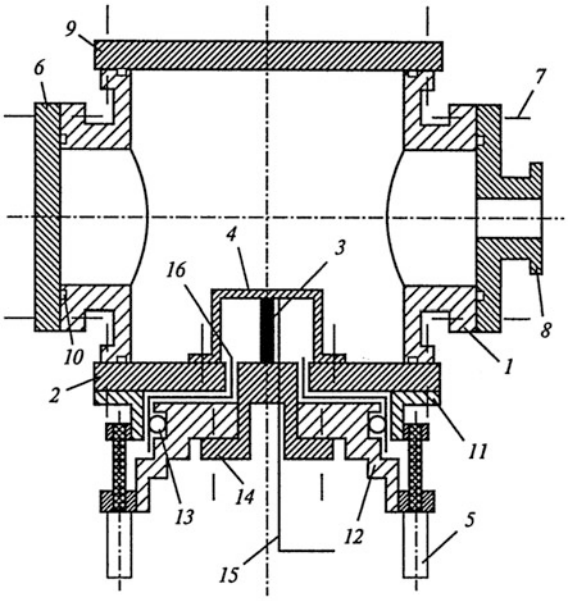

Fig. 7.15 [1]. The cut of explosion chamber (of about 20 liters in volume). In the lower part there is a Rogowski coil for measuring pulse current. *1* steel case; *2* a base; *3* graphite specimen; *4* copper bracket or coaxial cylinder; *5* coaxial cables, located on a circle; *6* viewing windows; *7* axes of bolt; *8* flange to supply gas (nitrogen); *9* steel cover; *10* rubber ring; *11* collector (aluminum); *12* collector "earth"; *13* Rogowski coil; *14* steel insert with a specimen from above; *15* insulated wire (for output and measure the voltage across the specimen; *16* insulation (polyethylene layers with a total thickness of 1 mm)

7.1.4 Specimens

A diamond tools were used to obtain thin (0.2 mm) graphite strips. The block of quasi-monocrystal graphite UPV-1T were cut to the narrow (width 1, 40 mm long) bars, that was then split into thin (0.2 mm) strips. Finally, the specimens had a size of 1 × 0.2 × 40 mm.

Specimen size and weight were determined with the use of optical methods and balance VLR-200 (measurement error is 0.15 mg). The copper layers were deposited to the ends of the graphite specimens by electrolytic method. The electrodes were soldered to the copper layers. Two such strips folded one by one, with a small (0.1 mm) gap from one side of this sandwich. A flat tip of an optic cable was inserted in this gap. A flat tip of an optic cable has 20–50 optical fibers (diameter of 50 μ each) that was arranged in one row. Then, the whole unit was fixed laterally by quartz plates, and the spacing between the plates was filled with epoxy glue. Thus the light transmitting medium is an epoxy glue and glass fiber. Under a short-time heating (1–5 μs) the heat losses are negligible, so the calculation of input energy absorbed by a unit mass of graphite was

$$E(t) = \int_0^t [I^2(t) \cdot R(t)/m]dt$$

where m—mass of the specimen; I—current; R (t)—the electrical resistance, which is calculated by the formula $R(t) = [U(t) - L(dI/dt)]/I(t)$, where U—voltage along the specimen; L—inductance of the specimen.

Diagnostic equipment includes a digital 4—channel oscilloscope Tektronix TDS-754C for recording voltage and current signal, as well as high-speed pyrometer response.

Under the heating of the anisotropic pyrolytic graphite (that was grown in a cylinder form) the expanding in radial direction (plane "C") becomes impossible because the cylindrical surface (plane "a") restricts expansion—specimen may breaks before melting. We used a special method for the manufacture of cylindrical graphite specimens having the opportunity to expand in two axes (graphite grade UPV-1T). We applied serial pushing the specimens of square cross section UPV-1T through the diamond filers of all decreasing (step by step) diameter. Specimens were obtained with a diameter 0.87 mm. They were placed into a thick (outer diameter 11 mm) sapphire tubes which had an internal diameter slightly larger than the diameter of the specimens. Heating of such specimens in the tubes gave the results on the specific electrical resistivity of liquid carbon, assuming that the tube has not changed the inner diameter of sapphire tube during short heating of graphite. Recording the radiation from the graphite plane "c" through the wall of the sapphire tube, it was managed in the same experiments to fix the inclined temperature plateau of graphite at melting point [3].

Our experiments in a limited volume showed that the electrical resistivity of liquid carbon equals 730 μΩ cm at a density 1.8 g/cm^3 (specific volume of 0.55 cm^3/g) for pressures of a few tens of kbar and temperatures of 5000–7000 K (see lower Fig. 7.25). In our opinion (based on the results of the experiments) the electrical resistivity of liquid carbon at high pressure has a metallic character. Numerically, it corresponds to the resistivity of extended (by four times) liquid refractory metals (W, Ta, Mo) [4].

7.2 Choice of a Blackbody Design and Fast Pyrometer for Recording Melting and Liquid State of Carbon

7.2.1 Select a Blackbody Design

In 1895, Otto Lummer proposed method of obtaining the blackbody radiation with blacken cavity with a small hole. This radiation is the desired equilibrium thermal radiation. In addition to the interest in fundamental physical laws, the motivation for creating artificial black body was the need for the standard absolute intensity of

the radiation. In 1897/98 year Lummer with Ernst Pringsheim completed the practical implementation of the black body: it was a spherical or cylindrical metal cavity (used iron and copper), which on the inner side was coated with soot or uranium oxide. To stabilize the temperature of the cavity it was placed in various liquids (liquid air, boiling water, hot nitrate and so on). In 1897 the Lummer and Pringsheim checked the Stefan—Boltzmann law, and confirmed the Wien displacement law. Later the other scientists improved blackbody design.

Mendenhall is the author of a wedge blackbody model, which it was first proposed, designed and published in 1911 year [5] (Fig. 7.16). For the calculation Mendenhall used the angle shown in Fig. 7.17.

It should be noted that wedge blackbody model must have the polished planes, it gives more reflections. The angle α at the top of a blackbody model in Mendenhall calculations was 10°. Mendenhall [5] draws attention to the prominent role of the thermal conductivity for the material at temperature measurement for the specimen

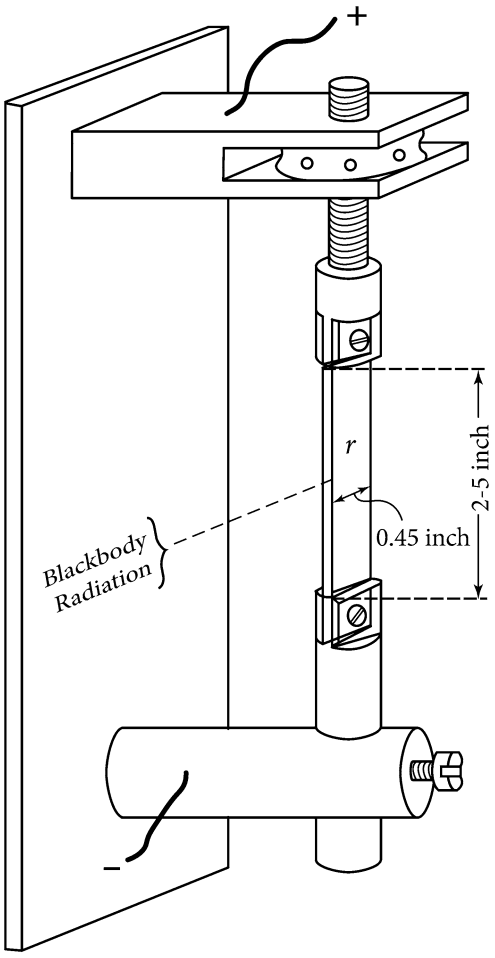

Fig. 7.16 The assembling of a blackbody model in the experiments by Mendenhall [5]

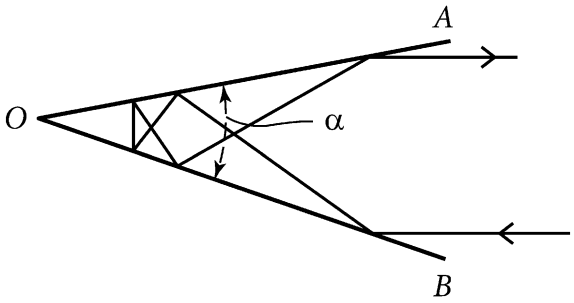

Fig. 7.17 The form of a blackbody model in the experiments by Mendenhall [5]

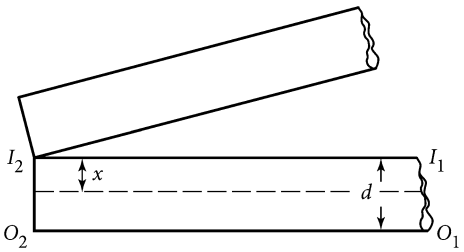

Fig. 7.18 [5] A scheme of wedge blackbody model for subsequent calculation

of finite size. This is essential under the stationary temperature measurements when there are significant redistribution of heat flows.

In the Fig. 7.18 [5] it is presented a scheme of wedge blackbody model.

Calculation in the Mendenhall study has the following outcome:

$$t_0 - t_d = {}^1\!/_2\,(d/k \times W/bl),$$

where, t_0—temperature at the center of the side plate; t_d—temperature at the edge of the side plate; d—plate thickness; k—thermal conductivity of the material under the measured temperature; W—a heat in calories per unit length and for unit cross section; b—the width of the plate; l—length of the plate.

For the case of the heating plate (at W = 8.6; d = 0.0035 cm; b = 0.6; l = 2.8 cm) Mendenhall obtain $t_0 - t_d = 0.05$ °C, which is negligible. If the plate thickness is three times more the difference is 0.75 °C, under measuring a temperature above 1000 °C and it is a small quantity also. However, according to Mendenhall, for materials with significantly lower thermal conductivity, such as carbon, especially with thicker plates, this difference can be substantial. Therefore Mendenhall offers to evaluate the thermal conductivity at high temperatures for three experiments with different thickness of the plates, and after that to extrapolate thermal conductivity graphically to zero thickness.

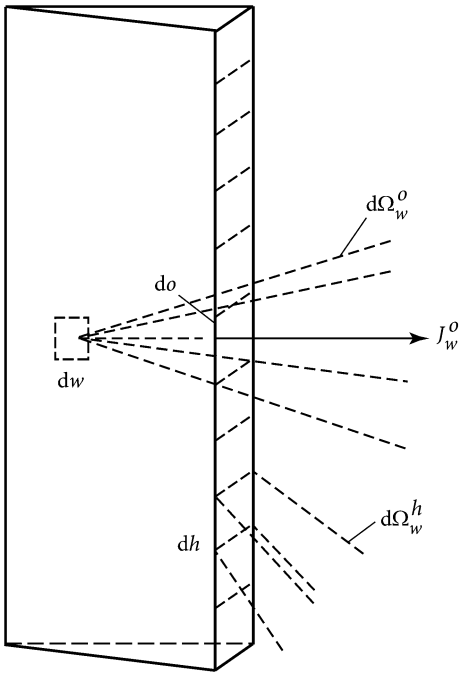

Fig. 7.19 The central part of the V—wedge blackbody design. dw—the element observed through the slit; $d\Omega_w^0$ and $d\Omega_w^h$—are the solid angles subtended by the surface elements of the slit d_0 and d_h when viewed from d_w

Next Mendenhall gives the example of processing of the experimental results for the blackbody model made of platinum. And obtain 1700 °C whereas the temperature measured with a polished surface gives 1500 °C (plate thickness 0.032 mm). Note in particular, that Mendenhall calls the surface temperature as a temperature of a blackbody (blackbody temperature), and the temperature of the blackbody model calls a true temperature. This is somewhat different from the modern interpretation in the literature devoted to optical pyrometry.

In conclusion of its work, Mendenhall notes that for wedge models of a blackbody with rounding at the top corner, there is a black strip is visible due only normal reflection in this area. Mendenhall suggested investigating this effect further. This problem was investigated by De Vos in 1954 [6].

In 1954 it was published a paper by De Vos [6], which shows the specific model of a black body (wedged, cylindrical, spherical) with the formulas for calculating the performance of the models. For example, Fig. 7.19 shows the wedge shaped model, which was used in determining the emissivity of the metals. De Vos spoke negatively about the properties of this model, which cannot give an exact calculation result of the temperature. Emphasize the word "calculation" as in practical optics this model is widely used. The main "claim" by De Vos to this model—is the presence of a dark band at the top corner of the model, in the case when this angle is a smooth rounded curve.

De Vos commented the properties of wedge model:

"*The radiant intensity of the different elements of the inner surface observable through the slit varies much .... The surface elements near the edges will have a lower intensity particularly when the partial reflectivities... have relatively high values... These elements must be eliminated by diaphragming. This diaphragming however is seriously encumbered by the dark stroke in the centre of the slit caused by the high values of the partial reflectivity of the elements in the neighborhood of the fold, especially if the reflection is basically a mirror (This diaphragming however seriously encumbered by the dark stroke in the centre of the slit caused by the high values of the partial reflectivity of the elements in the neighborhood of the fold especially when the reflection is specular for the greater part*" [6].

Recall that a dark band appears in the case when the vertex angle is not sharp. Further, De Vos makes a final conclusion:

"*Since the radiant intensity so strongly depends on the position of the elements and the nature of the reflection the V-wedge blackbody is not appropriate to accurate measurements. An accurate calculation which moreover would require a great number of terms is not worthwhile*".

After such a "heavy blow" (which, by the way, the practice by the optical pyrometry was ignored) De Vos goes to the recommendations.

As the most suitable model of a blackbody De Vos considering tubular model with a small hole on the side surface (Fig. 7.20). Such a model of a black body

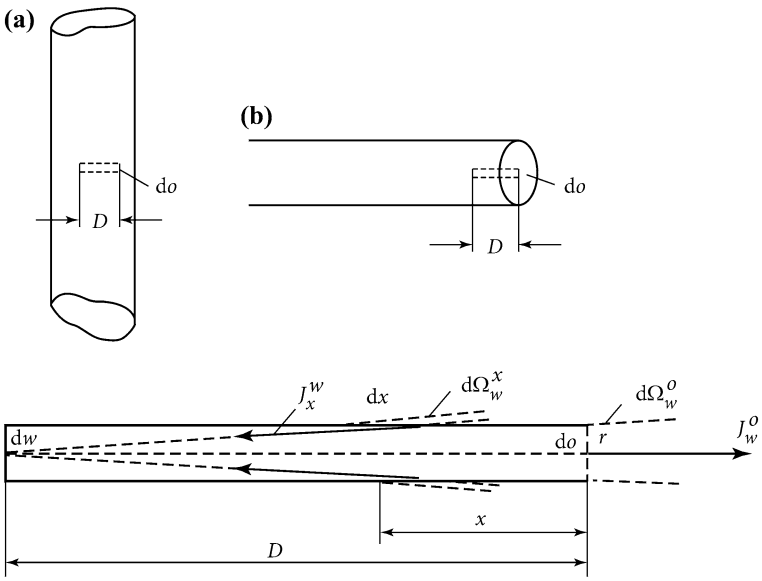

Fig. 7.20 Cylindrical blackbody model, closed at one end. D—the "depth" of the cylindrical hole; d_w—the surface element observed; d_x—the elementary annulus of the cylinder whose contribution to I_w^0 is calculated. **a** and **b** show two different constructions of the cylindrical blackbody

successfully used in stationary studies by many authors, including Ared Cezairliyan [7–9], with millisecond pulse heating of metal and graphite cylinders.

In the conclusion De Vos says:

> "*From the preceding calculations it can be concluded that with the aid of all blackbodies considered, except the V-wedge, it is possible to attain a good approximation to pure blackbody radiation. It appears from literature that as a rule the blackbodies used in practice meet the requirements as far as concerns the dimensions of the holes in comparison with other dimensions. Often insufficient attention has been paid, however, to the prevention of temperature gradients along the walls. Many errors in experiments with blackbodies should be ascribed to lack of uniformity in the temperature*" [6].

Despite the criticisms by De Vos to the address of wedge-model, it was actively used in the measurement of the radiative properties of solids [10].

Wedge design blackbody model was used for the study of metals by V.N. Korobenko (Fig. 7.21), who improved this model by the two strips used with acute angle between the strips while De Vos offered one bending metal strip (with not so acute angle).

The blackbody model was developed by V.N. Korobenko, especially for use in the investigation of the temperature dependence of the thermal properties of liquid zirconium and liquid hafnium [11], and then for liquid carbon [12].

The tip of the solid-state light guide is located on the side, in the vicinity of the gap between the foil strips. In order to extend the "lifetime" of the model, both strips were bent outwards. In this case, given the employed heating rate, the model

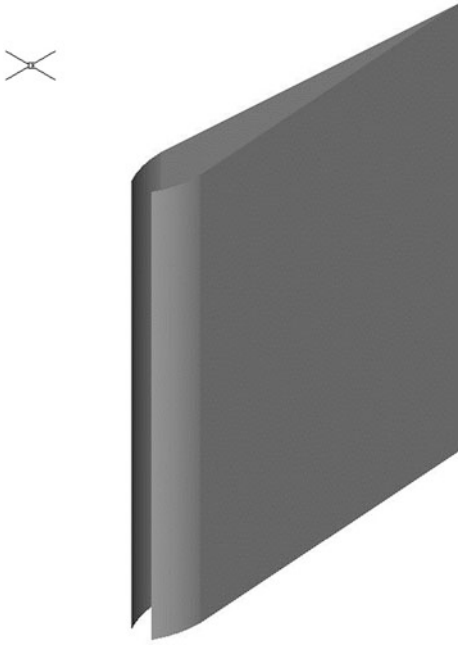

Fig. 7.21 Wedge-shaped blackbody design made of two polished foils (a middle section of the specimen made of two strips of metal foil). *Foils* width—1.5 mm, thick—0.055 mm. The current is going through the foils from the *top down* or from the *bottom* to *top*

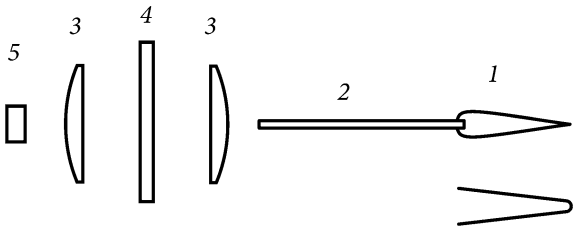

Fig. 7.22 Registration scheme for radiation measurement of twin-belt blackbody model. *1* two-tape blackbody model (cross-section), both ribbons are curved outward. Downstairs—the model investigated in [5, 6]. It is the same that was used in the study of graphite. *2* The general fiber (*2*) consists of 10–50 individual fibers, with a diameter of 50 μ each. On the *right side* of general fiber (*2*) the small fibers are distributed in a single layer along the lateral gap of a blackbody model. On the *left side* of (*2*) the small fibers look as a circle in cross section. *3* Lenses. *4* Interference filter. *5* PIN-photodiode

retained its working capacity up to 5000 K. The melting temperature of zirconium and hafnium was calibrated against the radiation of blackbodies made of these metals in the region of their melting. In so doing, the temperature at the beginning of the temperature plateau of melting was equated to the known melting temperature for Hf (2504 K) [13].

7.2.2 Fast Pyrometer Made by V.N. Korobenko (JIHT)

The investigated specimen of wedge-shaped blackbody model consisted of two superimposed foil strips about 2 mm wide. On one side of the sample, these strips were separated by a small gap of ~100 μm into which a flat (about 80 μm thick) tip of a light guide was introduced. The other end of the light guide was directed, via interference light filter, to a pin-photodiode of a pyrometer (Fig. 7.22). In this manner, the radiation from the space of the blackbody model was recorded; this made possible the measurement of the true temperature of solid and liquid refractory metal in the process of its heating in the air during 1.5 μs.

The expansion of liquid Hf with measuring temperature up to 5750 K (that is higher boiling point) was published in [13] (2007 year) by Korobenko and Savvatimskiy.

Evaluation of the emissivity of this blackbody model gives 0.99, provided that the reflection likes a mirror. Before the experiment the metal foils were polished in oil. The tips of the glass fiber cores have a maximum angle of propagation of light within 30° around the central axis. Thus, the pyrometer recorded light radiation within this solid angle, for a black body radiation, and for a flat surface. For further temperature calculations it was used Planck equation. As a result, there was obtained the dependence of the specific energy input (enthalpy) against temperature for tungsten, and the specific heat capacity against temperature for metals (Zr, W):

for zirconium, up to 4100 K [14, 15], for tungsten up to 5,600 K [12, 16]. A good agreement took place with the measured equilibrium properties of the metals; further the authors have transferred the experience of creating wedge blackbody model to the graphite investigation.

The main components of the pyrometer were: silicon PIN- photodiode, an interference filter with half bandwidth of 16 nm at a wavelength of 855 nm, two lenses, trans-impedance amplifier and a glass fiber (Fig. 7.22). A settling time of the pyrometer with an accuracy of 1 % was 12 ns. The same pyrometer signal fed into two channels of a digital oscilloscope with different sensitivity. Sensitivity of one of the channels is set so that you can record a temperature plateau at the melting of metals or graphite with high resolution. Give an example for zirconium (melting point 2128 K) as a representative of metals. Signal for that channel was limited to a temperature T $\sim$ 2300 K. The second channel (with low sensitivity) recorded spectral brightness temperatures up to 4000 K or more. Joining the both signals allowed to get one smooth curve with a high dynamic range. We tested the linearity of the photodiode (up to 1800 mV) depending on the value of the spectral radiation density.

The next step was calibrated photodiode by temperature. Starting temperature plateau at a specimen from a metal melting (melting point of which is known) was used as a calibration point for registration of temperatures above the melting point. If the specimen was a blackbody model, the true temperature was calculated (according to Planck's law). Melting point of the metals was used as reference points for subsequent heating of a graphite specimen in the same conditions.

Linearity of the pyrometer (output voltage to 1.8 V) was verification under recording a spectral density of LED AL-124A, having a linear dependence of the radiation power from the current flowing through the emitting diode.

The efficiency of a blackbody model of this design has been previously tested in obtaining of the thermal properties (heat capacity, enthalpy, electrical resistivity) of liquid zirconium from the melting point to 4100 K and a comparison with the equilibrium data [11, 15].

The dependence of the output signal of the pyrometer from the current through the infrared emissivity of the diode AL124A shown in Fig. 7.23. Emitting diode AL124A has a linear dependence of the output power from the flowing current.

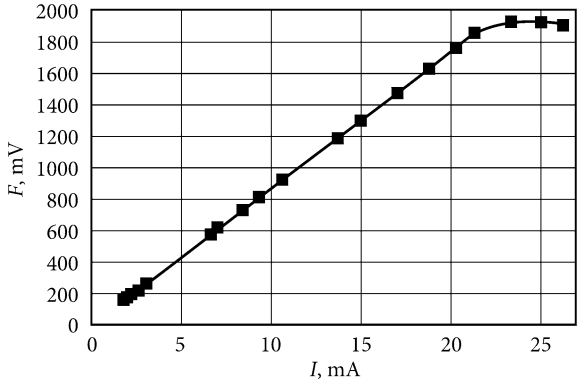

Fig. 7.23 The dependence of the output signal of the pyrometer from the current through the infrared emissivity of the diode AL124A

As a result of this validation of the linearity emitting diode it was found that the deviation of its ampere-watt dependence based on the linear no more than 0.5 % in the range of input currents 2–50 mA. The time setting signal of the pyrometer with an accuracy of 1 % is not exceeded for at least 12 ns.

The temperature was calculated from measurements of the output voltage of the pyrometer, is proportional to the spectral brightness of the thermal radiation from the surface of the foil or of the cavity according to the Planck law:

$$T = \frac{c_2}{\lambda \ln(1 + \frac{U(t)}{U_m}(e^{hc/\lambda kT_m} - 1))}$$

where c_2 = hc/k—is the second radiation constant, λ—the central wavelength bandwidth of the interference filter, U(t)—output of the pyrometer, U_m—output voltage pyrometer on the plateau of melting, Tm = 2128 K the melting point of zirconium.

7.3 Melting and Liquid State Recorded at Fast Pulse Heating

7.3.1 Melting of Anisotropic Graphite Placed Between Two Sapphire Plates

In these experiments, a low-inductance capacitor bank was used, with stored energy of 20 kJ. The specimens represented graphite plates (thickness is 300 μ). Around the specimen, before the heating it was created solid insulating shell which reduce sublimation of graphite and leads to high pressure increased for 1–5 μs, which give a chance, in the future, to measure specific thermophysical properties for liquid carbon [12, 16].

Diagnostics of the experimental setup was changed into digital recording. The results of fast (2 μs) pulse of electric current heating were obtained for the annealed at 3000 C graphite UPV-1T and presented in [3, 12, 16, 17]. A number of problems on the melting graphite was resolved in these experiments: the specimens in the form of flat strips were placed in a solid insulating medium (Canadian balsam) between two glass plates (Fig. 7.24). This limited sublimation of graphite at high temperatures (3000–10,000 K), and also prevents a bypass discharge along the graphite surface.

Calculation of input specific energy E absorbed by a unit mass of graphite (Joule heat) was made by the measured current and voltage with the inductance included by the 4-channel digital oscilloscope Tektronix 754C used.

Calibration of the pyrometer signal was made under specific energy E = 9.1 kJ/g —corresponding to the graphite temperature 4500 K, according to [18]. It was

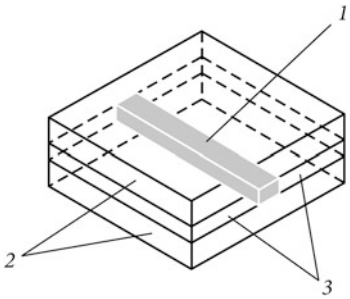

Fig. 7.24 [17] A specimen of highly oriented graphite UPV-1T (in a *rectangular* form) is enclosed in a hard cell made of glass. *1* Specimen of graphite; *2* glass plates; *3* Canadian balsam (analog of epoxy glue). The copper layers were electrolytic deposited to the ends of the graphite specimen which was connected by solder to electrodes

assumed that above 4500 K the emissivity of graphite is constant and does not depend on temperature.

The two vertical lines mark the melting region, measured by surface radiation (in the Fig. 7.25). The start of melting takes place at ~5,500 K (under elevated but not measured pressure), the end—at ~6000 K (even at higher pressure). Electrical resistivity ρ—refers to the initial size of the specimen.

1 Cusp at this point shows the start of melting if we consider melting by volume properties (voltage and resistivity);
2 Cusp at this point shows the finish of melting which is determined by the volume properties (voltage and resistivity).

Melting region measured by volume properties for the six specimens (11 ± 1 kJ/g—the start of melting and 20 ± 1 kJ/g—the finish of melting).

We say at once that the melting region measured by radiation plateau (two vertical lines) is shifted in the E axis to the right-hand side. The reason – is in the absorbed a part of input energy by a glass plate during a short time of heating. Thus the both parts of the melting region (the start and the finish of melting) are shifted to higher input energy approximately one and the same value (~10 % as an average for six studied specimens).

There is a mismatch moments of start and finish under melting for radiation and voltage (resistance) curves in Fig. 7.25. Later we realized that despite the rapid heating process, there is an outflow of heat from the heated graphite in close contact with the glass. During the heating (a few microseconds), nearly ~ 7–10 % of the input energy is absorbed in the glass plate. Therefore, the curve of temperature measurement should be shifted to the left (Fig. 7.25) along the energy axis by 10 %, and it will give a full match for the onset of melting temperature and voltage curve U (point 1). The finish of melting temperature will be close to the position of the maximum of the curve U (point 2) in Fig. 7.25.

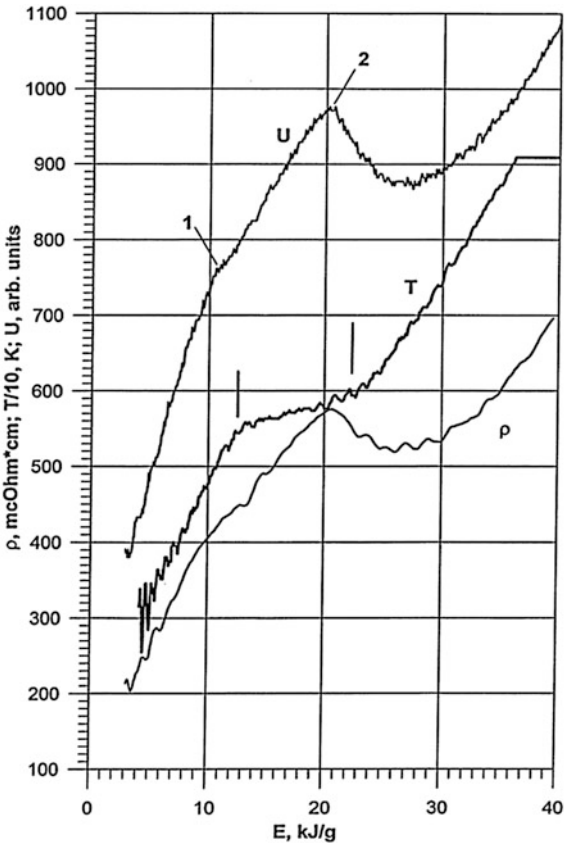

Fig. 7.25 [3] The result as it is. The dependencies of the specimen voltage (U), the temperature (T), the resistivity (ρ) against the energy input (E) for the pulsed electrical heating of a graphite strip

A total of 6 specimens were studied, below it is shown one of them (Fig. 7.26).

Rapid heating of the flat graphite specimens in a solid medium creates a high pressure in the graphite. The modeling this process of heating by A.D. Rakhel in [12, 16] allowed us to estimate the level of pressure at the beginning of melting (5–10 kbar) for our experiments (Fig. 7.27); 5 kbar for the surface layer and 10 kbar in the center of the specimen.

We obtained in the Fig. 7.26 [3, 17] that the graphite specimen begins to melt near 5000 K. Thus, we have measured 5000 K at 5 kbar pressure (surface layer), which means (taking into account dP/dT = 54 bar/K [19–21]) that the temperature at the start point of graphite melting is 4900 K at low (0.1–1 kbar) pressure. V.N. Korobenko obtained a similar result by measuring the melting temperature of graphite blackbody design under pulsed heating (4800 ± 200 K).

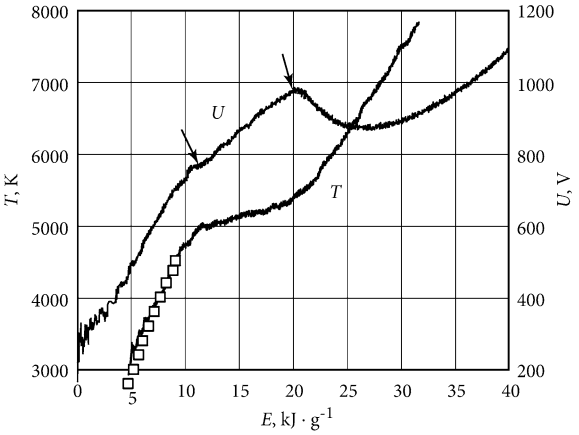

Fig. 7.26 [12, 16] Improved (shifted) result relative to Fig. 7.25. The melting region of highly oriented pyrolytic graphite (temperature was recording at "a" plane of deposition). Full heating time—1.5 μs. Graphite strip (1 mm × 10 mm, thickness 0.3 mm) was placed between two thick glass plates. The start and the finish of melting are indicated by arrows on the voltage curve U. The experimental data [18] is shown by the hollow squares

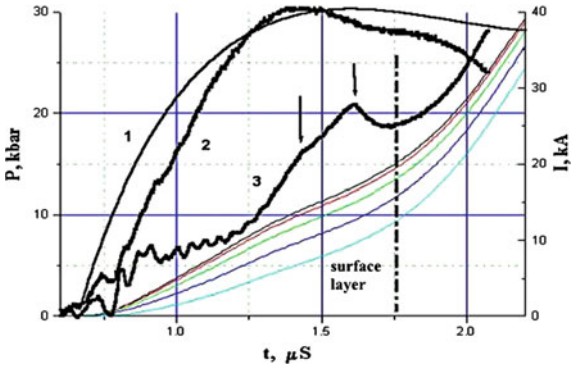

Fig. 7.27 [12, 16] The pressure in the specimen of a flat graphite HOPG (simulation results were obtained by A.D. Rakhel for the heating of graphite specimen) *1* Current (modeling). *2* Current (experiment). *3* The voltage for the specimen U (experiment), melting region is marked by arrows

Temperature calibration was performed in the linear range of the pyrometer signal by a standard reference data in the dependence of the input energy E of graphite against temperature (E = 9.14 kJ/g corresponds to 4500 K) [18].

Five curves in the lower part of the figure—the calculation of the pressure for the 5 layers of the specimen (the top—layer in the center; the lower—layer in the surface). The vertical dotted line—limit of reliable calculations of pressure; to the right of the dotted line the calculation model is not working (error more than 20 %).

7.3.2 *Melting of Anisotropic Graphite Placed Inside the Sapphire Capillary Tube*

In the further experiments, we used highly oriented pyrolytic graphite UPV-1T (quasi-monocrystal) in a rectangular form, it gives the opportunity for the specimen to expand independently along two axes. Electric current is passed along the basal plane of a high conductivity "a", i.e. along the specimen. We used the annealed specimens resulted in the continuous growth of electrical resistance, providing more uniform heating.

It was fabricated the cylindrical (anisotropic!) specimens of UPV-1T graphite grade (using diamond tools), which were placed in a thick sapphire tubes (Fig. 7.28). Temperature was recorded from a cylindrical surface "c" through the wall of the tube and the glass plate which was fixed on the top of the tube by optical glue.

The benefits of recording temperature on this plane "C" are essential: the contact cooling of the surface layer of graphite with the sapphire is negligible. As inserted into the specimen energy efficiently feeds the cooled surface (due to the high thermal conductivity along the layers of graphite). That is why the start of melting point (Fig. 7.29) equals 10.5 kJ/g, whereas for the temperature measurement on another plane "a" requires a correction for the amount of heat of cooling (about 7–10 % of the input energy, Fig. 7.25).

The ratio of the internal volume of the sapphire tube (V) to the volume of the specimen of graphite (V_0) was $V/V_0 = 1.24$. Therefore, prior to the onset of graphite melting a specimen expanded freely (according to the literature data a solid graphite expansion before melting consists ≈ 20 %). The increased temperature (inclined) plateau corresponds to the melting of graphite in the increasing pressure, which was reached ~50 kbar (Fig. 7.29).

Pyrometer records temperature through the sapphire wall from a plane "c" of graphite specimen. Onset of melting is at fixed input energy E = 10.5 kJ/g and it is

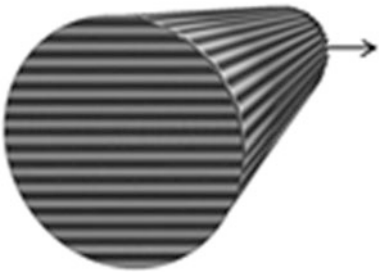

Fig. 7.28 Anisotropic specimens of UPV-1T graphite grade (scheme). Temperature measurement was recorded from the side of plane "C" (*arrow*)

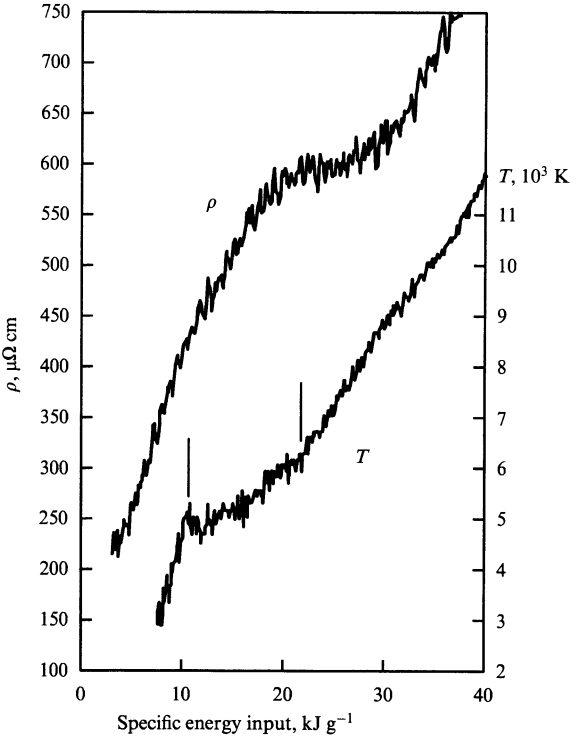

Fig. 7.29 [3] Melting point of graphite UPV1-T in the form of a rod, in a thick-walled sapphire capillary tube. Pressure is low (about 5 kbar) at the beginning of the melting. The inclined plateau is indicated by vertical bars under the melting of graphite at high pulse pressure (estimate yields 54 kbar at the completion of melting) in a thick-walled sapphire capillary tube. Y-axis—the electrical resistivity ρ (*upper curve*), referred to initial dimensions of the specimen

coordinated with the energy input at the beginning of fusion (Figs. 7.25 and 7.26). The melting onset temperature for low pressures (of the order of hundreds of atmospheres) should be somewhat lower than 5000 K (estimated by 200 K lower), since the pressure at the start of melting in Fig. 7.29 is slightly elevated.

Since liquid carbon was heated in quazy-isochoric conditions the isochoric heat capacity of liquid carbon could be estimated (Cv ~ 3 J/g K) [3]. The input energy at the beginning of fusion (10.5 kJ/g, according to our measurements) is close to the results of experiments by other authors under the microsecond heating experiments: 10.4, 9.5 and 10.45 kJ/g for millisecond electric heating . It is also close to the calculated data of stationary studies (10.7 kJ/g) [23].

We used a high current pulse at the above mentioned two series of the experiment (Fig. 7.30).

Vertical arrows mark the beginning and the end of melting that match the specific energy E = 10.5 and 20.5 kJ/g, respectively. 1 μs after the current switching, the specimen begins to melt; from that moment the average pressure in the specimen due to pinch-effect equals 4.5 kbar, which is stored in the broad area of the liquid phase of carbon (before time 2 μs). Figure 7.30 shows that the heating current (68 kA) during melting (the time between the vertical arrows) and further to

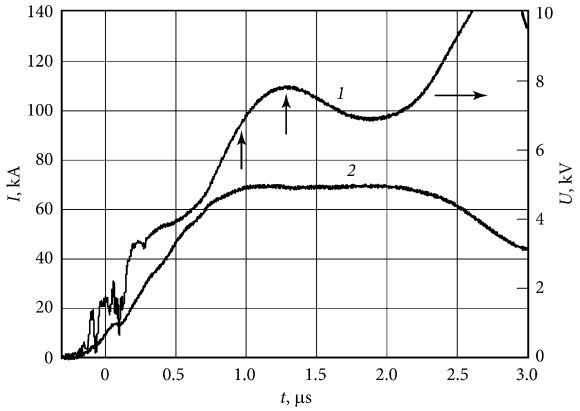

Fig. 7.30 The voltage U (*curve 1*) and the current I (*curve 2*) against time, for the case $V/V_0 = 1.25$

the liquid phase of carbon, is a constant. Calculation of the pinch effect for this current value, including diameter of graphite specimen 0.8 mm, giving an average pressure in the specimen $P \sim 4.5$ kbar (maximum at the center of the specimen 9 kbar and $P = 0$ at the surface). This pressure in the specimen, first, provides melting of the main part of the graphite specimen ($P \geq 110$ bar) and, secondly, it must be added to the pressure arising due to the restricted volume (thermo-compression).

The transition of the liquid carbon's electrical resistivity from semi-metal to metal-like characteristics was obtained at a high input energy (35–45 MJ/kg). It was obtained that the liquid carbon of higher density has higher electrical resistivity under the same input energy. Pressure was not measured in the experiments but a comparison was shown with the data of M. Togaya (Japan), which were fulfilled with the measured static data up to 94 kbar. For example, Fig. 7.31 shows the change of electrical resistivity for liquid carbon versus input energy in isochoric pulse heating for different liquid density.

The electrical resistivity of liquid carbon at the melting point decreases with the increase of density, as seen in the figure (arrows show 790, 690, and 640 μΩ cm for curves 1, 2, and 3, respectively). One may consider $d\rho/dP < 0$ for liquid carbon just at the melting point, which coincides with the data published in [24] for pressure $P < 50$ kbar, also at the melting point under slow pulse heating.

For the lower density (1.1 and 1.76 g/cm^3), the electrical resistivity decreases just after the melting. It looks like a nonmetallic behavior. The increasing of the resistivity ρ, at higher energy input, more than 35–45 MJ/kg gives $d\rho/dE > 0$. The second item should be mentioned that the higher liquid carbon density has the higher resistivity. For example, at $E = 45$ kJ/g for the curve 1 ($\gamma = 1.1$ g/cm^3), the resistivity ρ is the lowest, while for curve 3 ($\gamma = 1.88$ g/cm^3), the resistivity has the highest value.

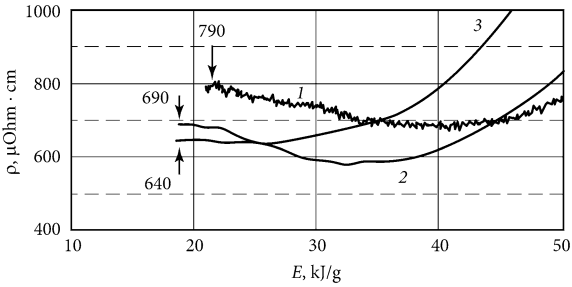

Fig. 7.31 Specific resistivity ρ (with the expansion included) of the carbon versus input energy E. Only the data for liquid state is shown in the figure. The initial part of heating from room temperature to melting temperature (4800 K) is excluded in the figure. Thermal expansion (filling the inside volume of the sapphire) is included, starting with the finish of the melting (arrows). A quasi-isochoric heating is shown at the right-hand side from the arrows. *Curve 1* $V/V_0 = 2.0$; density $\gamma = 1.1$ g/cm^3 (graphite specimen with the diameter ∅ 0.79 mm in the sapphire tube of outer diameter 1.15 mm/8 mm (inner diameter). The length l = 14.4 mm. *Curve 2* $V/V_0 = 1.25$; density $\gamma = 1.76$ g/cm^3. (∅ 0.79 mm in the tube 0.885 mm/10 mm (l = 15.18 mm). *Curve 3* $V/V_0 = 1.17$; density $\gamma = 1.88$ g/cm^3. (∅ 0.79 mm in the tube 0.85 mm/10 mm (l = 18.4 mm)

7.3.3 *Estimation of Sapphire Melting and the Possible Destruction of a Sapphire Tubes*

The main question arises: would it be isochoric heating, when a high temperature liquid carbon contacts with the solid sapphire? There is a possible melting of the inner layer of sapphire tube during short time of heating. The depth of thermal wave penetration δ to sapphire may be estimated through

$$\delta = (a\Delta t)^{1/2},$$

where: a—thermal diffusivity for sapphire before melting ($a = \lambda/C_p \cdot \gamma$; λ—heat conductivity, C_p—heat capacity γ—density). For the heat conductivity we may use experimental and reference data. For the time interval $\Delta t = 3 \cdot 10^{-6}$ s calculations give $\delta \sim 2$ μ for liquid thin sapphire layer that may be melted. This value (2 μ) is too low to change the inner diameter ($\sim$1000 μ) of the tube. There are no arguments to take this small inner tube volume expansion or contraction (sapphire expands during melting) into consideration in the fast heating. So, our fast experiments are really isochoric heating of the liquid carbon of nearly constant density.

The diminishing of the resistivity for sapphire thin layer (up to $\sim 4 \cdot 10^5$ μΩ cm for liquid sapphire) has no marked influence on the resistivity of liquid carbon ($\sim$600–1000 μΩ cm in the figure). Thus, we have really measured the liquid carbon resistivity in the experiment at the high input energy level.

The only problem is not solved. The rise of the resistivity at the latest studies of heating may be connected not with the liquid carbon properties but also with the destruction of the sapphire tube. Especially due to the fact that the destruction of the

Fig. 7.32 The result of the destruction of sapphire capillary tube with outer diameter of 10 mm (length 18 mm) after heating graphite MF-307 in the form of a rod placed inside the tube

sapphire tube takes place on a separate sectional pieces. It gives an impression that the tube collapses on a separate part symmetric to the axis of the tube (2 or three, or four parts), as if in the radial direction, there are areas of lower strength (Fig. 7.32).

Remind that the assumption of constant cavity volume of capillary in our experiment in question—is not obvious, and was not supported by the possible control experiments. It is not excluded that a monotonous increase in the electrical resistance (up to 3000 μΩ cm at the very high energy input) is associated with the destruction of sapphire capillaries of this kind: the tube is broken down into 2–3 segments (along the specimen, Fig. 7.32) that was watched sometimes after the experiment. The reason in such kind of destruction connects with the quite hard technology of capillaries growing from liquid sapphire (the weak areas are always remaining in grown tube); the boundaries of these areas are less strong relatively perfect sapphire crystal. These segments have been broken and expanded during heating as we supposed. These expanded segments, may increase the volume occupied by carbon itself; as a result monotonically rise of the resistivity may be connected with the appearing gap between segments. Such a control experiment remains to be done.

The increase in resistance at higher energy input (higher 40 kJ/g) may be connected with the possible destruction of the sapphire tube into the separate segments accompanied by monotonic increase in resistivity (see the "result" of the experiment in Fig. 7.32).

7.3.3.1 Discussion

According to Motohiro Togaya data [24] the peak maximum of resistivity means the completion of melting. We used the peak in electrical resistivity as evidence of

melting at the end of input energy E ~ 19–21 kJ/g (Figs. 6.14 and 7.25) as a sign of the end of melting, particularly, according to [24]. Togaya [24, 25] used this method by observing the texture of the specimens after current interruption (just as Francis Bundy used earlier [26, 27]).

Conclusions about the role of external pressure may have important technological applications. Influence of the external pressure on the liquid carbon it can be obtained the intermediate product of different density. And further, one can use the carbon density, which gives the most efficient carbon transformation. Despite of the high temperature for liquid carbon (T ≥ 4800 K), the used pressure transformation may vary within wide limits, starting from the atmospheric one. Therefore, efficient conversion of liquid carbon (representing a mixture of graphite fragments of various configurations) is quite possible in pulsed processes.

At the completion of graphite fusion (20.5 kJ/g) the density of liquid carbon is ~1.2 g/cm^3, that is close to the experimental result of the American scientists (~1 g/cm^3) obtained for low initial density of graphite (Fig. 6.12). Thus, the density of liquid carbon in the melting curve (at low pressures) is quite small, in contrast to theoretical calculations (1.6 g/cm^3 in previous years). The resistivity (referred to initial dimension) of the carbon in the liquid phase at high pressure (~50 kbar) is about 700 μΩ cm that substantially coincides with the experimental data by Motohiro Togaya (Japan) corresponding to the same pressure. The manifestation of nonmetallic properties for liquid carbon near the melting point, observed by us in the last series of experiments, also coincides with the experimental data of Motohiro Togaya.

Heating by pulse current has a major advantage in volumetric heat release that allows you to measure the specific material properties (density, electrical resistivity, input energy). Experiments have shown that the pulse heating allows to increase the power density of the heat dissipation (with respect to the stationary experiments) and provide a graphite melting in a short time experiment (a few microseconds and even shorter). An important conclusion of our first pulsed experiments with graphite became the confidence to use pulse electric heating for the study of graphite (first used by Lebedev S.V. for investigation of metals). The heat losses are negligible at this rate of heating ($5 \cdot 10^9$ K/s) identified in the study of metals, led to the use of short-time heating of the graphite, ~1–3 μs in our further experiments. The originality of our experiments consists of:

- First, rapid heating (which prevents the molten liquid specimen to lose its shape during heating);
- And secondly, to use thick-walled insulating tubes (or thick-walled plates), creating a short time experiment under isochoric heating conditions at high pulse pressure, arises due to the thermo-compression process. Pulse experiment in a single act of electrical heating allows watching of both solid and liquid states, comparing the properties of different phases and recording possible phase transitions.

Assuming a weak expansion of the sapphire tube during a short time of the experiment, you can get isochoric heating at a nearly constant density of liquid

carbon. Isochoric heating conditions consistent with a constant density of carbon for three experiments: 1.1, 1.76 and 1.88 g/cm^3 (Fig. 7.31).

The estimation showed that during the experiment (3 μs) a thin layer inside the tube (~2 μ) of the sapphire could be melted—it was impossible to apply the fast pyrometer for temperature measurement. (It is known that sapphire near the melting point ceases to transmit radiation). Temperature above the melting point is estimated by the formula $\Delta E = C_V$ (T—Tmelting), where ΔE—input specific energy, C_V = 3 J/g K- specific heat at constant volume for liquid carbon (earlier it was calculated by the authors in the experiment [3, 12]); Tmelting = 4800 K (measured earlier [3, 16]). A comparison with the experiment [25, 28, 29] was under consideration, which used a constant pressure (from 14 to 94 kbar) by electric pulse of milliseconds heating. A good agreement has been obtained in two different experiments: liquid carbon exhibits semiconducting properties immediately after melting at pressures up to 50 kbar, and at higher pressure (more than 50 kbar), its electrical resistance is growing, shows a metallic character.

The heating of liquid carbon occurs in conditions of limited volume (isochoric process) and the falling character of the referred resistance ρ^0 characterizes the behavior of electrical resistivity ρ ($\rho = \rho^0 \times V/V_0$, where V/V_0 = 2.0 and 1.25 for curves 1 and 2 in the Fig. 7.31 accordingly). After reaching the minimum of the resistivity it begins a monotonic increase of the resistivity. The observed changes (if it should be confirmed by the new experiment) can be attributed to a nonmetal-metal transition occurring in the liquid carbon under high pressure and at high energy input (but prior to reaching the sublimation energy of carbon under normal conditions). Thus, Fig. 7.31 demonstrates a new physical effect, characterizing of liquid carbon above the melting point, which has not been observed earlier. Recall that this conclusion would be fair if it is proved the constancy of the volume of liquid carbon in a sapphire tube.

As it turned out, the behavior of liquid carbon at high pressure resembles the behavior of liquid lithium. Neaton and Ashcroft [30] predicted growth of the resistivity of lithium at high pressure. This prediction was confirmed in an experiment that is discussed in [31, 32]. Theorists have consistently studied the behavior of liquid metals associated with increased density (see, for example, [33]).

7.4 Input Energy Versus Temperature for Liquid Carbon State (up to 12,000 K)

First, note the main requirements that apply to a specimen of graphite under heating by pulse of electric current. Graphite specimens that are heated to and above the melting point,—should have a high initial density (more than 2 g/cm^3). The best example is the specimen made of highly oriented pyrolytic graphite (HOPG) with initial density 2.26 g/cm^3. Electric current is applied, usually along the plane of high conductivity. Specimens made of various types of low density graphite

(1.5–1.85 g/cm^3) usually have initial inhomogeneity in the structure. For example, it was shown in [34] that graphite grade POCO (initial density 1.83 g/cm^3) have significant differences of electrical resistance at the small distances for the same specimen. This leads to non-uniform heat dissipation in the different points of a specimen under electrical heating. The faster heating for such specimens, the greater the temperature inhomogeneity is accumulated at the certain points. As the thermal conductivity (low, usually to such graphite specimen) cannot be able to level temperature by volume.

Graphite specimen may have a circular or square cross section. The worst case is when a specimen of pyrolytic graphite (even of high density) was grown in a form of a cylinder. For these specimens the plane "a"—is a cylindrical surface and a plane "c"—the plane in the radial direction. It is well known that the main expansion occurs in solid graphite along the "c" plane. The specimen is trying to expand generally along a radius, but a cylindrical surface which extends less far, resists radial expansion. As a result, a specimen with high initial density, but grown in the form of a cylinder, is destroyed before the fusion.

In 1986, we [35] obtained important experimental results on uniform heating graphite specimens by pulse of electric current. Summary results for pulsed electric heating of metals and graphite specimens were published in [36]. Since graphite specimen must be able to expand freely in both directions (along the plane "a" and along the plane "c"), we used a highly oriented HOPG specimen in a square form. Specimens were annealed in vacuum at 3000 °C to obtain a low initial resistivity ($\sim$50 μΩ cm). Only in this case, the subsequent resistance of the annealed specimens does not fall at the beginning of the electrical heating; there is only the continuous growth of the resistivity with increasing temperature.

Fast pulse heating by electric current of highly oriented pyrolytic graphite (in the form of flat strips) was studied in [3, 12, 16, 17].

To record radiation for measuring true carbon temperature it was constructed blackbody design. The block of quasi-single-crystal graphite was cut by diamond tools to narrow ribbons (width 1 mm), 40 mm long, and then cleaved into thin (0.2 mm) strips. Finally, the specimens had a size of (1 ± 0.2 mm) with the length 40 mm. A composite specimen was consisted of two graphite plates (thickness 0.3 mm, width of 1 mm, length 10 mm), superimposed on one another.

On the one hand (along composite specimen) plates were closed tightly, and the other had a gap of 100 μ. In this gap (on the side of a composite sample) it was introduced a flat glass fiber leading to fast pyrometer. Composite specimen (blackbody design) with a light guide was filled with epoxy resin to limit sublimation during heating and prevent electrical shunting discharge.

Fiber tip was a few tens of cores (50-μ diameter each) adjacent to form a planar system. Fast pyrometer provides recording spectral density at a wavelength of λ = 855 nm. The current, voltage and spectral density were recorded by 4 channel digital oscilloscope Tektronix 754C, (bandwidth 500 MHz). Duration in melting temperature plateau was 200 ns.

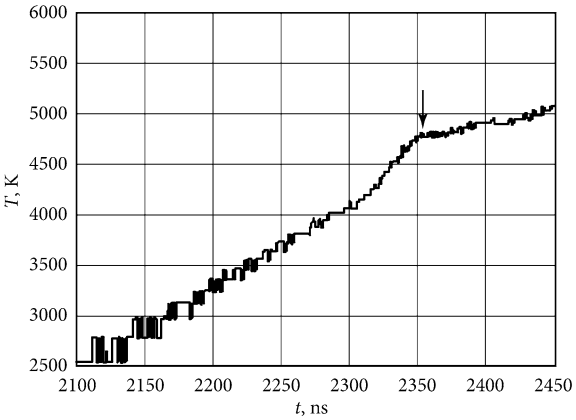

Fig. 7.33 Melting point of graphite in the form of a blackbody model (experiment by Korobenko V.N.). The *arrow* indicates the start of graphite melting; pyrometer calibrated on a melting plateau for tungsten (3690 K). Time to the onset of melting equals 2.35 μs

Calibration of the temperature measurement was performed by heating the graphite tungsten pattern in the form of a blackbody of the same design, the temperature plateau under tungsten melting attributed to equilibrium melting temperature (3690 K).

Linearity of the pyrometer (output voltage to 1.8 V) was checked under recording the spectral density LED AL-124A, having a linear dependence of the radiation power from the current flowing through the emitting diode.

The efficiency of a blackbody model of this design has been previously tested in the obtaining of thermal properties (heat capacity, enthalpy, electrical resistivity) of liquid zirconium from the melting point to 4100 K and a comparison with the equilibrium data (the start of the melting for the blackbody graphite design is shown in Fig. 7.33).

Specific heat Cp of solid graphite before melting is 3.2 J/g K according to our experiment, which is close to published equilibrium data. The data of our measurements of the specific heat of liquid carbon are shown in Fig. 7.34, as the derivative dE/dT. Specific heat Cp = 4.2 J/g K for the temperature range from 6000 K to 12,000 K (blackbody model is not used to obtain the results shown in Fig. 7.34). Therefore, the temperature in the range of 6000–12,000 K were measured under the assumption that the emissivity ε from 4500–12,000 K does not change.

We have prepared [3, 12, 17] HOPG graphite specimens of cylindrical shape with a diamond tool. Initial specimens of HOPG were a square cross-section rods (1 × 1 mm), a length of 30 mm. They were pushed through a series of diamond-ring dies with decreasing size diameter (from 2 to 0.9 mm). Thus, the cylindrical specimen was obtained of highly oriented (!) HOPG graphite with the diameter 0.9 mm and studied in [3, 12, 17]. These specimens were placed in a cylindrical thick-walled (12 mm outer diameter) sapphire tube which had an inner diameter

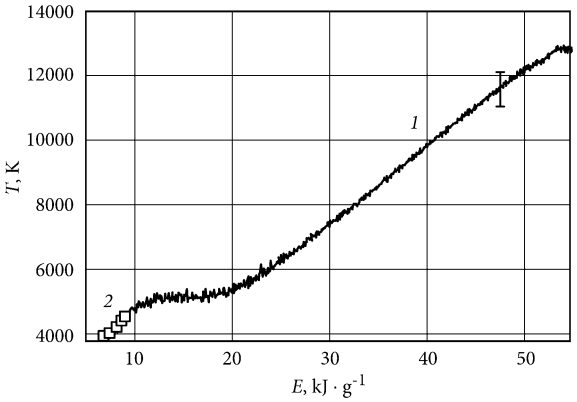

Fig. 7.34 The temperature of the liquid and solid carbon versus specific energy input. *1* Measurements by V.N. Korobenko (error of temperature measurements (±500 K) is shown above 10,000 K. Specific heat of liquid carbon (may be obtain as dE/dT in the figure) equals 4.2 J/g K (from 6000 to 12,000 K). *2* Hollow squares—experimental measurements of pulse heating [18] (tens of microseconds) of graphite in the solid state

slightly larger than the diameter of the specimens. Heating of such specimens inside of the thick-walled sapphire tubes yielded results in specific resistivity of liquid carbon—730 μΩ cm (referred to initial dimensions), assuming that a sapphire tube does not changed bore dimensions under heating.

Maximum systematic error for measuring the specific power includes the systematic error of measurement of electric current (2 %), systematic error of measuring voltage (3 %), the error of mass measurement (0.4 %). The total systematic measurement error of input power equals about 5 %. Maximum systematic error for the measurement of the specific input energy E (±6 %) throughout the range of input energy to the liquid state. Temperature measurement error near the melting point ±200 K, and about ±500 K at temperatures 10^4–1.2×10^4 (Fig. 7.34).

The new wedge blackbody (twin-belt) model is very useful for studying the properties of liquid metals and carbon [12, 16].

Especially it will be useful for specimens made from hardened steel and graphite, which cannot be deformed for the manufacture of a blackbody cavity in the form of a tube of small diameter. Wedge blackbody model may also be useful for research and development of high- melting point for metal-carbon compounds. For example, the maximum melting temperature for carbide HfC is 4220 K, for carbide TaC—4270 K. There is a possibility of obtaining in the pulse experiment calibration temperature scale for measuring the temperature radiation of a blackbody wedge specimens made of different metals (Zr, Hf, Mo, Ta, Re) and carbides. Tungsten is not useful for high temperature calibration due to the strong dependence of the melting temperature of carbon impurities (1.5 % carbon additive gives a reduction of the melting temperature of 1500 K). Since the metal carbides in the solid state have an increasing electrical resistance with increasing temperatures [37], it gives a homogeneous heating of these materials with pulsed electrical heating.

The problem under consideration is to create thin foils of metal carbides to obtain the wedge-shaped blackbody design. It gives you the chance to test the true melting temperature of graphite and determine the melting point of different carbide eutectics [38].

The wedge blackbody model (under the rapid electrical heating) is a simple and convenient tool for achieving and measuring the true temperature at its high value. We performed preliminary experiments with the wedge model blackbody made of two strips of graphite (grade like HOPG). As the calibration point it was used tungsten melting temperature for the blackbody model made of high purity tungsten. In both cases, the cavity of the specimens before heating was filled with the epoxy glue using one and the same fiber construction. Pyrometer recorded temperature plateau at the melting point of tungsten blackbody model for the known melting point (3690 K), which was used to calibrate the pyrometer signal upon subsequent heating graphite blackbody model. As it turned out, the melting temperature of graphite in these conditions is 4800 ± 200 K.

At the International Symposium in the USA (2009 year) we presented the reports on the study of carbon [39]. Due to the lack of financial capabilities, we refused to travel to a conference, but Daniela Gaal (Secretary of the organizing Committee) paid for us to stay at the conference.

Daniela GAAL—head of the Laboratory of Anter Corporation (later), nowdays, —TA Instruments, and organizer of the International Symposium on thermal expansion and thermal conductivity conference, 2009, Pittsburgh (USA). She is the publisher of the proceedings of this Symposium: “Thermal conductivity 30 and thermal expansion 18” (Proceedings of the Thirtieth International Thermal Conductivity Conference and Proceedings of the Eighteenth International Expansion Symposium), DEStech Publications, Inc., 2010, 985 pages.

References

1. A.I. Savvatimskiy, V.N. Korobenko, High-temperature properties of metals for nuclear industry (zirconium, hafnium and iron during melting and in the liquid state), MEI Publishing House (2012), 216 pp. ISBN 978-5-383-00800-3. in Russian
2. A. Cavalleri, K. Sokolowski-Tinten, D. Von der Linde et al., Generation of the low density liquid phase of carbon by non-thermal melting of fullerite. Europhys. Lett. **57**(2), 281–287 (2002)
3. V.N. Korobenko, A.I. Savvatimski, R. Cheret, Graphite melting and properties of liquid carbon. Int. J. Thermophys. **20**(4), 1247–1256 (1999)
4. A.I. Savvatimskiy, V.E. Fortov, R. Cheret, Thermophysical properties of liquid metals and graphite, and diamond production under fast heating. High Temp.-High Press **30**, 1–18 (1998)
5. C.E. Mendenhall, On the emissive power of wedge-shaped cavities and their use in temperature measurements (an international review of spectroscopy and astronomical physics). Astrophys. J. **33**(2), 91–97 (1911)
6. J.C. De Vos, Evaluation of the quality of a blackbody, Physica XX, pp. 669–689 (1954)

7. A. Cezairliyan, A.P. Miiller, Heat capacity and electrical resistivity of POCO AXM-5Q1 graphite in the range 1500–3000 K by a pulse-heating technique. Int. J. Thermophys. **6**(3), 285–300 (1985)
8. A. Cezairliyan, P. Miiller, Measurement of the radiance temperature (at 655 nm) of melting graphite near its triple point by a pulse-heating technique. Int. J. of Thermophys. **11**(4), 643–651 (1990)
9. A. Cezairliyan, F. Righini, Rev. Int. Hautes Temp. et Refract. **12**, 124 (1975)
10. L.N. Latyev, V.A. Petrov, V.Y. Chekhovskoi, E.N. Shestakov, Radiative properties of solid materials, in *Handbook*, ed. Sheindlin A.E., Moscow: Energiya, (1974), 471 pp. in Russian
11. V.N. Korobenko, A.I. Savvatimskiy, Liquid zirconium properties up to 4100 K (density, enthalpy, heat capacity, emissivity, and resistivity). Russ. J. Phys. Chem. **77**(10), 1564–1569 (2003). (in Russian)
12. Korobenko V.N., and Savvatimskiy A.I., Blackbody design for high temperature (1800–5500 K) of metals and carbon in liquid states under fast heating, TEMPERATURE: its measurement and control in science and industry, in *AIP Conference Proceedings*, ed. Dean C. Ripple, vol. 7, Part 2, pp. 783–788 (2003)
13. V.N. Korobenko, A.I. Savvatimskiy, The density of liquid hafnium from the melting point to the boiling point. High Temp. **45**(2), 159–163 (2007)
14. V.N. Korobenko, M.B. Agranat, S.I. Ashitkov, A.I. Savvatimskiy, zirconium and iron densities in a wide range of liquid states. Intern. J. Thermophys **23**(1), 307–318 (2002)
15. V.N. Korobenko, A.I. Savvatimskiy, Measurement of the zirconium temperature from the melting temperature to 4100 K using blackbody models in a liquid state. High Temp. **39**(3), 485–490 (2001)
16. V.N. Korobenko, Ph.D. dissertation for the degree of candidate of physical and mathematical sciences, Experimental study of the properties of liquid metals and carbon at high temperatures, (Moscow: Institute for High Temperatures RAS, 2001). in Russian
17. V.N. Korobenko, A.I. Savvatimskiy, Electrical resistivity of liquid carbon. High Temp. **36**(5), 700–707 (1998)
18. V.N. Senchenko, M.A. Sheindlin, Experimental study of the thermodynamic properties of graphite near the melting point. Sov. Phys. Dokl. **33**, 142–145 (1988)
19. N.S. Fateeva, L.F. Vereshchagin, V.S. Kolotygin, Optical method for measuring the melting temperature of graphite up to 3 kbar. Doklady USSR **152**(1), 88 (1963). in Russian
20. L.F. Vereshchagin, N.S. Fateeva, Melting curves of graphite, tungsten and platinum up to 60 kbar. JETP **28**(4), 597–600 (1969)
21. N.S. Fateeva, L.F. Vereshchagin, On the graphite melting curve to 90 kbar. JETP Lett. **13**(3), 110–111 (1971)
22. M.A. Sheindlin, V.N. Senchenko, Experimental study of thermodynamic properties of graphite in the vicinity of the melting point. Doklady **298**(6), 1383–1386 (1988). in Russian
23. L.M. Buchnev, A.I. Smyslov, I.A. Dmitriev, A.F. Kuteinikov, V.I. Kostikov, Experimental study of the enthalpy of kuazi-moncrystal graphite and glassy carbon in the temperature range 300–3800 K. High Temp. **25**(6), 816–821 (1987)
24. M. Togaya, Behaviors of liquid carbon at high pressure, in *New Kinds of Phase Transitions: Transformations in Disordered Substances*, ed. by V.V. Brazhkin (Kluwer Academic Publishers, Printed in the Netherlands, 2002), pp. 255–266
25. M. Togaya, Electrical resistivity of liquid carbon at high pressure, Science and Technology of High Pressure, in *Proceedings of AIRAPT-17*, eds. by M.H. Manghnani, W.J. Nellis, M.F. Nicol, (Universities Press, Hyderabad, India, 2000), pp. 871– 874
26. F.P. Bundy, Melting of graphite at very high pressure. J. Chem. Phys **38**, 618–630 (1963)
27. F.P. Bundy, Direct conversion of graphite to diamond in static pressure apparatus. J. Chem. Phys. **38**(3), 631–643 (1963)
28. M. Togaya, Pressure dependences of the melting temperature of graphite and the electrical resistivity of liquid carbon. Phys. Rev. Lett. **79**(13), 2474–2477 (1997)
29. M. Togaya, S. Sugiyama, E. Mizuhara, Melting line of graphite, in *AIP Conference Proceedings*, no. 309, pt. 1, pp. 255–258 (1994)

30. J.B. Neaton, N.W. Ashcroft, Pairing in dense lithium. Nature (Letters to Nature) **400**, 141 (1999)
31. V.E. Fortov, V.N. Korobenko, A.I. Savvatimskiy, Liquid metals and liquid carbon: some similar properties at high temperatures. Eur. Phys. J. B (EPJ WEB of the Conferences), **15**, 02001 (2011)
32. E.G. Maksimov, M.V. Magnitskaya, V.E. Fortov, Not a simple behavior of the simple metals at high pressure. Phys. Uspekhi **48**(8), 761–780 (2005)
33. G.S. Atwal, I.G. Khalil, N.W. Ashcroft, Dynamical local-field factors and effective interactions in the two-dimensional electron liquid. Phys. Rev. B **67**, 115107 (2003)
34. V.V. Mirkovich, Electrical resistance anisotropy of a POCO AXM-5Q1 graphite. Int. J. Thermophys. **8**(6), 795–801 (1987)
35. S.V. Lebedev, A.I. Savvatimskiy, The electrical resistivity of graphite in a wide range of condensed state. High Temp. **24**(5), 892–899 (1986)
36. S.V. Lebedev, A.I. Savvatimskiy, Investigation of metals and graphite under conditions of rapid electric heating, in *Thermal Physics Reviews*, eds. by A.E. Sheindlin, V.E. Fortov. Section B, vol. 5 part 3, (Yverdon, Switzerland: Harwood Academic Publishers GmbH, 1993), p. 1–79
37. R.B. Kotelnikov, S.N. Bashlykov, Z.G. Galiakbarov, A.I. Kashtanov, Especially refractory elements and compounds, (reference-book), Metallurgy, Moscow, (1969). 372 pp. in Russian
38. G. Machin, G. Beynon, F. Edler, S. Fourrez, J. Hartmann, D. Lowe, R. Morice, M. Sadli, M. Villamanan, HIMERT: A pan-European project for the development of metal-carbon eutectics as temperature standards, A report presented at 8th Temperature Symposium, Chicago, 21–24 Oct 2002
39. V. Korobenko, A. Savvatimskiy, Electrical resistivity of expanded liquid carbon at high temperatures and high pressures, in *Proceedings of the International Conference Thermal conductivity 30 and Thermal expansion 18*, DEStech Publication, Inc., 2010, 787–793

Chapter 8
The Evolution of Experimental Carbon Phase Diagram

Abstract Several diagram of Bundy are considered up to 1994 year, starting with combined diagram for C, Si and Ge (1964 year). The contribution to phase diagram by Motohiro Togaya for bulk carbon and modified diagram for nanocarbon of other investigators are also shown. A significant part of this chapter deals with the computational work on the melting of graphite and phase diagram of carbon, including high pressure level. Modeling of carbon phase diagram and the agreement with the experiments are discussed, including the new publications of 2014–2015 years.

8.1 Phase Diagram by Vereshchagin (1963 Year)

The survey [1] already contains the results obtained by a team headed by L.F. Vereshchagin.

Therefore we briefly mention the most significant achievements of this team as the detailed data were published in [1]. In the paper Fateeva, Vereshchagin, Kolotygin 1963 [2] it was investigated the dependence of the melting graphite temperature on the pressure in the gaseous medium. The authors [2] have measured the melting temperature by automatic fixing temperature at the time of melting at pressures up to 3000 bar. For the first time the authors [2] used a color pyrometer, and used quartz optical fiber to remove the effects of scattering due to convective flows in the gas environment.

It has been established that at pressures above 500 bar an application of standard optical pyrometer is impossible. Application of optical fiber gives possibility to measure temperature up to 3000 bar. The specimen is a rod with the length of 10 mm (1.5 mm in diameter) with a neck 0.8 mm in the middle. The measurements [2] showed that the graphite melting temperature increases with increasing pressure up to 3000 bar: from 4650 to 4750 K. The novelty of this research was to use optical fiber in combination with high-speed color pyrometer. The author of the review [1] notes that the melting moment recorded in the most previous experiments corresponds to the destruction of the rod during the formation in the center a small diameter of the molten zone. Thus, the maximum temperature is always measured by

A. Savvatimskiy, *Carbon at High Temperatures*, Springer Series in Materials Science 134, DOI 10.1007/978-3-319-21350-7_8

the surface of a solid specimen until failure, but not the temperature of the liquid surface. In the experiments [2], the error due to this effect is the smallest one.

In the studies under the direction of L.F. Vereshchagin it was shown that more than 50 % of the radiation scattered in the gas due to convective flows. This corresponds understated temperature exceeding 500 K at T = 4000 K using the brightness pyrometer.

In the paper of Vereshchagin and Fateeva in 1968 year [3] it was published the results of studies of the graphite melting curve from 3 to 60 kbar pressure using NaCl as the pressure medium. The melting temperature of graphite in [3] is very different from the data of the same authors previously obtained. For example, it was obtained Tm = 4037 K at P = 100 bar (previously 4650 K). Later such a strong contrast the authors [3] explained by the calibration error due to incorrect definition of attenuation filters in [3]. Note that all the previous experiments (by different authors) give melting temperature around the 4000 K during last years.

(The author of this monograph suppose that it may be the main reason to refute a novel data of 1963 year [2]. *It seems reasonable to explain the difference existing by strong absorption in a salt layer, tightly surrounding the graphite specimen in* [3]*).*

In 1971, Fateeva and Vereshchagin expanded the range of pressures up to 90 kbar (Fig. 8.1).

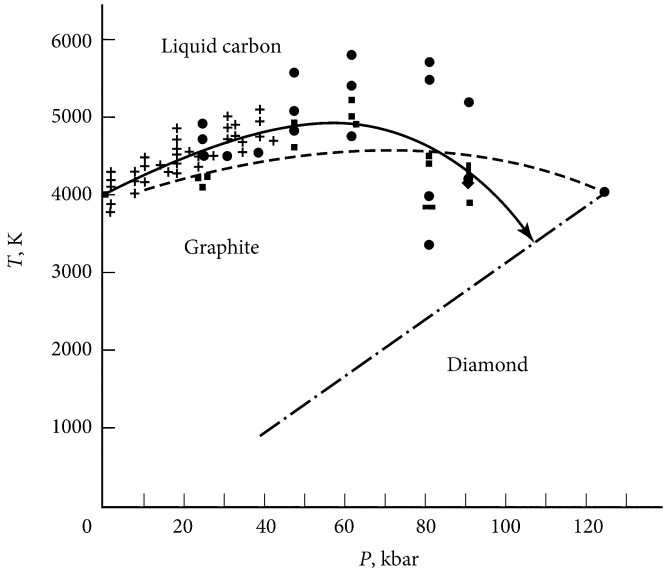

Fig. 8.1 Results for pressure 90 kbar. *Solid line* Averaged results [3]: 1—measurement on I_2/I_3; 2—on I_1/I_2; 3—on I_2/I_3. I_1, I_2, I_3 correspond to measurements at wavelengths of 0.420 μ, 0.622, 0.825. *Dotted line* Data of Bundy [4]. *Dash-dotted line* Equilibrium curve diamond–graphite (*direct crosses* The temperature is measured on the relative intensities of the spectral ranges (I_2/I_3 at the installation up to 40 kbar. *Inclined crosses* On I_1/I_2 at the installations up to 60 and up to 100 kbar). Inclined crosses in a circle—were measured on I_2/I_3)

The temperature was determined from the intensity ratio of two spectral lines. Each temperature measurement was performed independently by two pairs of intensity ratios of the three wavelengths of spectral regions (No 1 for the wavelength 420 nm, No 2 for 622 nm, No 3 for 825 nm).

A method of calibration temperature measurement is not mentioned in this paper. Apparently the calibration was based on calculation method. In determining the surface temperature for solid specimen the melting temperature may be severely underestimated (because of the sublimation from the surface).

As noted in the survey [1], one of the principal drawbacks of the work by Vereshchagin, like other previous ones, is to measure the temperature of the solid graphite surface before destruction, but not melted graphite. Temperature of the triple point in was not more than 4050 K at a pressure of 100 bar. A detailed discussion of the work can be found in [1].

Note the considerable scatter of the experimental points, especially in the pressure range of 60–90 kbar. It should have a sufficient independence of judgment, to draw a curve through these points (Fig. 8.1) and call it "measurements" (Since the measurements are represented by points and the curve is an interpretation of the authors). The authors of this study indicate that the probable error in measuring temperature does not exceed ±8 %, and in the measurement of pressure ±4 %. No methodological details of temperature measurement in this paper are omitted. It is unknown to consider the possibility of graphite sublimation and its influence on the temperature measurement—there is no any word in the publication.

8.2 Phase Diagram for Carbon Obtained by Francis Bundy

Graphite is a lot of different types arranged in a variety of structural forms.

However Bundy assumes that any solid form must be melted in the same liquid ([4], p. 623). Bundy analyze the known heat capacity data for graphite at high temperatures C_P, and comes to the conclusion to make a linear extrapolation of the heat capacity (known at T = 3200 K) up to 5000 K. Under these assumptions Bundy constructed carbon phase diagram (see Chap. 4, Fig. 4.6) which has a maximum melting point of 4600 K for a pressure of 60–70 kbar (accordingly about 4200 K at pressures of about 100 bar).

The first attempts by Francis Bundy to create the phase diagram for carbon, was presented in 1963 (Figs. 4.6 and 8.2).

It is known that silicon and germanium (the elements of carbon subgroup)—acquire properties of metal at high pressures and become a good conductor for electrical current. They all have the diamond crystal lattice. In response to this, and also used the built phase diagram of carbon, Bundy gives a supposition: at ultrahigh pressures from 600 to 700 kbar diamond is compressed into a dense metallic state of carbon (in the diagram in Fig. 8.2—upper circle with a dotted line). In this state, the density of carbon is 15–20 % greater than the density of diamond and, thereby,

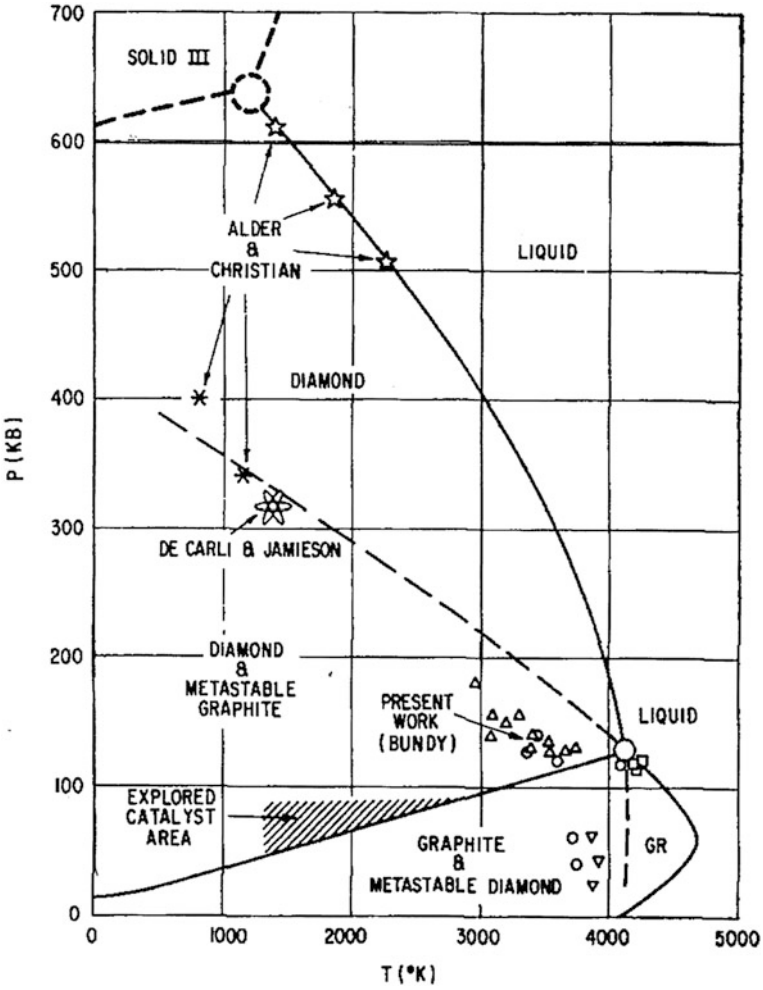

Fig. 8.2 The phase diagram of carbon: Solid state (*solid III*); data of Alder and Kristjan [5]; Data De Carli and Jamieson [6]; The data of Bundy are shown in [7]

it acquires the properties of the metal. Bundy noted that the density of the "solid state III" is greater than the density of the liquid, and hence the melting point will rise with the pressure rising as shown in Fig. 8.2. Note the interesting moment: the experimental threshold of reaction graphite-diamond and graphite melting line continuation. The latter may be regarded as a line of metastable graphite melting. In experiments on shock compression, in which the application time of pressure is extremely short, Bundy suggests that graphite should quickly melt to turn into a diamond. Concluding the discussion of Fig. 8.2, Bundy says, "*From the foregoing it follows that graphite is the only phase of carbon, which can exist in the region between the metastable melting line of diamond and graphite melting line*."

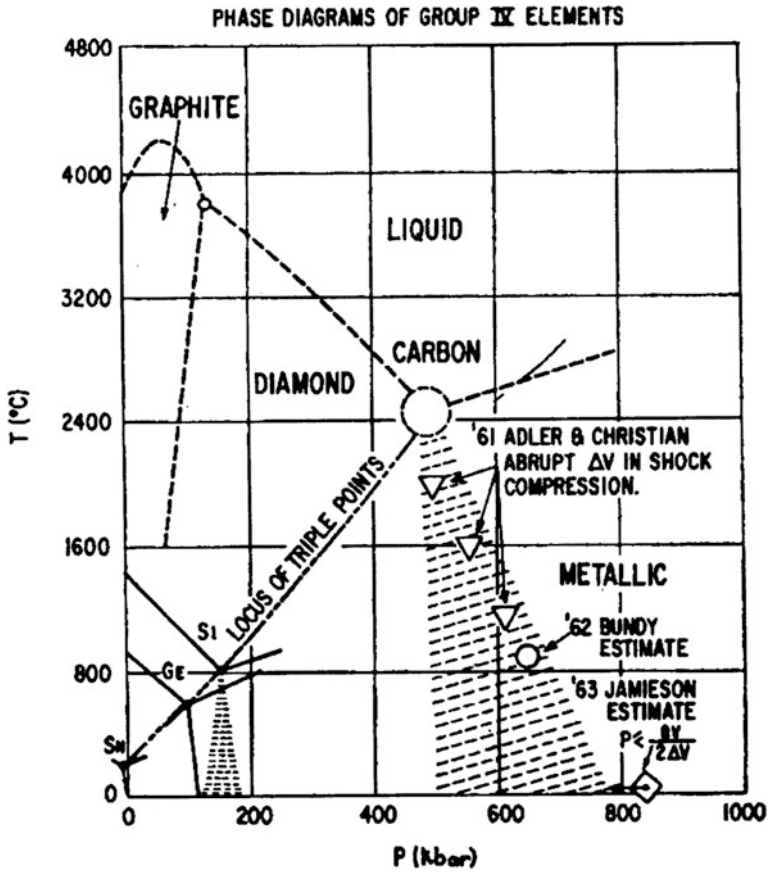

Fig. 8.3 P, T phase diagram of Bundy [8] for Sn, Ge and Si with the assumption about the carbon phase diagram [8]

The following, in 1964, after a study of the phase diagrams of silicon and germanium (neighbors of carbon in periodic table), Bundy publishes combined phase diagram of silicon, germanium and carbon corresponding experimental studies [8] (Fig. 8.3). Temperature in triple points for germanium and silicon were measured by thermocouples.

This phase diagram is mainly dedicated to the triple point diamond at high pressure and relatively low temperatures. Direct (dash-dotted) line drawn through the triple points Sn, Ge and Si, as suggested by Bundy, leads to the triple point of carbon diamond-metal-liquid with parameters 500 kbar and a temperature of 2400 ° C. It should be noted that in all given phase diagram Bundy indicates the melting point of carbon (at low pressures) as 4000 K, which corresponds to the results published in those years. In subsequent years, due to the improvement of methods of temperature measurements of carbon, melting point in his subsequent

publications was indicated much higher. Bundy closely followed the changes of carbon melting temperature in the literature and make changes in the phase diagram of carbon. This is clearly evident in the subsequent publication Bundy [9] in 1989, in the phase diagram (Fig. 8.4) contains the melting temperature of 4200 K at low pressures. This phase diagram is the most famous and the most perfect in its practical application.

Abstract of [9]: Carbon atoms form very strong bonds to each other yielding solid crystalline materials like graphite and diamond. Because of the high bonding

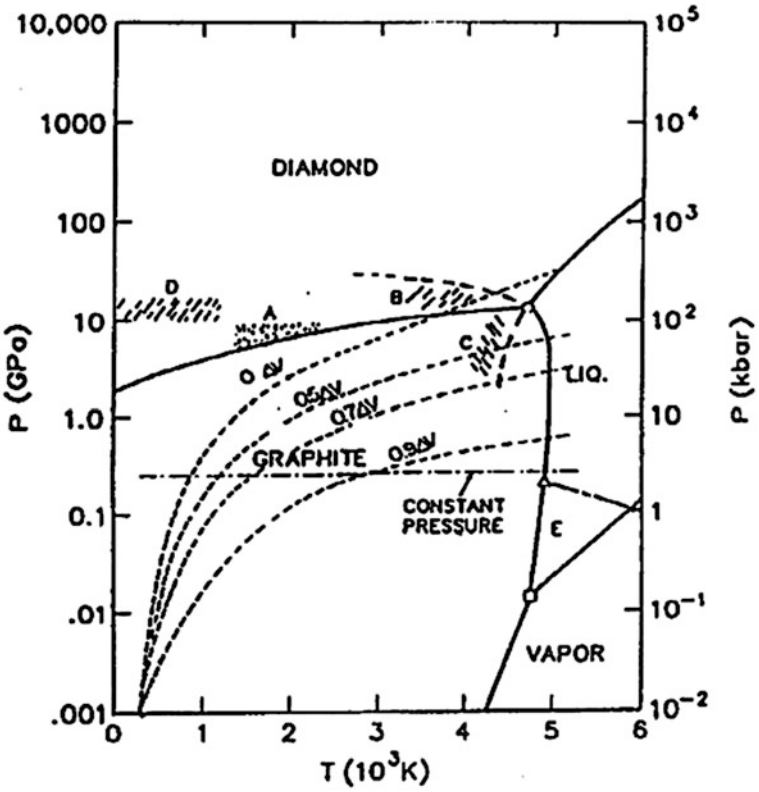

Fig. 8.4 [9] The phase diagram of carbon according to Francis Bundy (1989). In this P, T carbon phase diagram the way of fast heating is indicated. The P, T path of graphite specimen undergoes a different expansion with input energy is shown by *dashed lines*. "0 ΔV" means heating at a constant volume. If the temperature increases with the energy input so that 0.5 to possible thermal expansion is realized, such P, T trajectory is indicated as "0.5 ΔV". *A* The area of the catalytic synthesis of diamond from graphite; *B* a region of rapid spontaneous transition of graphite into diamond; *C* a region of rapid spontaneous transition of diamond to graphite; *D* martensitic transition region of hexagonal graphite to hexagonal diamond. The *direct curve* at constant pressure—experiment [10] at 2.5 kbar. This *straight line* falls on the melting line of graphite, just between the metallic and non-metallic liquid carbon (just above the *E* region). Area *E* The proposed nonmetallic state

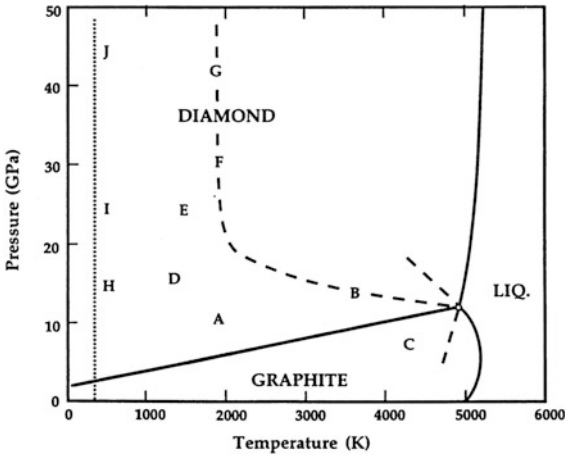

Fig. 8.5 [16] P, T phase (and phase transitions) diagram of carbon as it is understood by Bundy, on the basis of experimental studies until 1994 year. The *solid lines* represent the equilibrium phase boundaries. *A* The commercial synthesis of diamond from graphite using catalysis; *B* P/T threshold is very fast (less than 1 ms) transition (solid-solid) of graphite into diamond; *C* P/T threshold is very fast transition of diamond to graphite; *D* Monocrystalline hexagonal graphite turns into hexagonal recovered diamond; *E* the upper limit of shock cycle compression/hardening, which converts graphite particles in the hexagonal type of cubic diamond; *F* the upper limit of shock cycle compression/hardening, which converts the hexagonal graphite particles into the cubic diamond; *B*, *F*, *G* the threshold of fast P/T cycles which is the transformation of either graphite or hexagonal diamond into the cubic diamond; *H*, *I*, *J* the way in which the hexagonal single crystal graphite, compressed in the *C* direction at room temperature, loses some of the characteristics of graphite and acquires properties diamond-like polytype, but returns to graphite if the pressure is removed

energies, the vaporization and melting temperatures are very high. Different kinds of atom-to-atom bonding make many solid forms possible, ranging from pure graphite to pure diamond, as well as many types of molecules in liquid or gaseous carbon. Rigorous conditions of high temperature, high pressure, or both, are required to change a given elemental phase of carbon to another.

Phase diagram of carbon published by Bundy in 1989 (Fig. 8.4)—the most known and expressive. In this diagram, the experimental results taken into account the carbon made in the picosecond time range of heating. Note that Bundy himself used in 1963 [4] a pulse heating within 5 ms of time interval.

According to calculations by Bundy [9] the time passage of a shock wave through the thickness of the zone of energy input—a lot longer than the nanosecond laser and femtosecond laser pulse. In this case, heating should occur at an almost constant volume, as this zone is no time for expansion. Using data of Gustafson 1986 [11] according to the molar volume of graphite depending on pressure and temperature, Bundy identified "thermal pressure" generated in the specimen allowed for various permitted (by acceleration time) thermal volumetric expansion, ΔV.

For example, in Fig. 8.4 it can be seen that the thermal expansion on heating from 300 to 4500 K can be suppressed by compression at 240 kb, which is required for the case $\Delta V = 0$, i.e. in the case of heating at a constant volume. Thus, it is possible to construct a T-P dependencies corresponding $\Delta V = 0$; $\Delta V = 0.5$, etc.

If the growth of the temperature is such that 0.9 can be realized by possible thermal expansion, then the path P-T will be as follows according to the curve 0.9 ΔV. Microsecond experiments by Shaner [10] are shown in the diagram at a pressure of 2.5 kbar and intersect the melting curve of graphite near the proposed boundary between metallic and non-metallic liquid carbon (Fig. 8.4, [9]).

The path of rapid heating of graphite by uniform electrical heating in our experiments may be specified in the phase diagram of carbon. The trajectory of microsecond heating of graphite ($V/V0 \sim 1.2$) [12–14] (melting at a pressure $\sim$10–15 kbar) is close to the shown in Fig. 8.4 as "0.7 ΔV".

In 1990 it was published a clarifying result of the measurement of the melting temperature of carbon (5080 K) at low pressures (but above 110 bar) made by Baitin et al. [15] at the millisecond heating by pulse of electrical current. This new result is immediately was reflected in the phase diagram by Bundy, published in 1996 [16] (Fig. 8.5). The transition temperature of the graphite-liquid was shown as 5000 K at relatively low pressures.

In the study of 1996 year [16] (Bundy with colleagues), the authors in the Abstract claim: "*The liquid (carbon) is metallic and there appears to be no evidence for a transformation between electrically conducting and non-conducting forms, melted droplets of carbon less than 0.2 μm in diameter quench to a giant fullerene structure, even in the stability field of diamond; graphite transforms to a transparent phase on compression at room temperature, this phase reverts to graphite on decompression at this temperature from pressures as high as 1 Mbar.*"

And further in the text: "*Graphite melting temperature* $\sim$*5000 K.*" and on, p. 143: "*At high temperatures below melting there is some evidence for transformations from graphite to other solid phases, which are proposed to be carbine (linear molecules) or chaoite-like, but this remains controversial and unresolved*". We will remind that carbine–solid condensation form of linear molecules of carbon.

The authors [16] in p. 144: "*The temperature assigned to the triple point has been moved up from about 4000 K in the 1940s to about 5000 K in recent years. We show 5000 K as being the most probable value for the temperature at the triple point.*" (Bundy gives a reference to the study by Baitin with the colleagues [15]). And further: "*The study of Togaya et al.* [17] *utilized the most sophisticated apparatus and instrumentation, so it may be considered the most reliable. In this work, the temperatures were based on his measured values of enthalpy to melting, which were then converted to temperatures by applying the data of Sheindlin and Senchenko* [18] *on enthalpy versus temperature at conditions near the melting point.*" And further: "*…the enthalpy increase of graphite from room temperature to melting, lies in the range of 92–115 kJ/mol. The value 115 kJ/mol is probably the*

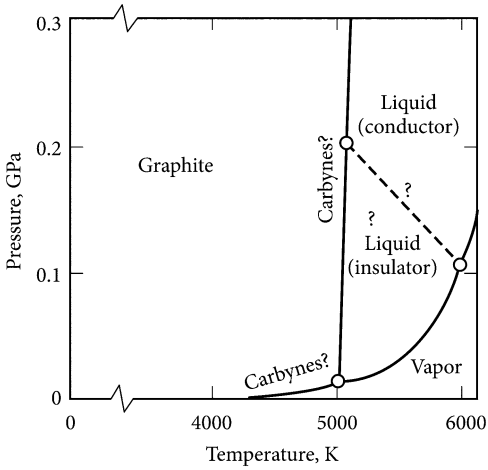

Fig. 8.6 P-T phase diagram for the low-pressure region [16]

most reliable". Mention that 115 kJ/mol means 9.6 kJ/g, and our pulse experiments gave subsequently 10 kJ/g [12, 13, 19, 20].

Authors of work [16] make comments to the Fig. 8.6:

The questions raised at the name "carbynes" specify that existence of carbines in a solid phase in this area of the phase diagram is disputable (see the text below). The questions standing in the field of a liquid phase, specify that the latest carefully executed experimental results don't support earlier published interpretation of experiment about existence of not conducting liquid phase of carbon (see the text below) [16].

And that's what gives the actual text in the publication [16].

"Evidence has been reported that the low pressure liquid is electrically non-conducting whereas the higher pressure liquid is conducting. Indeed, a phase boundary between the two kinds of liquids has been suggested, as illustrated in the Fig. 8.6. The liquid/vapor line should end at a critical point which has been estimated to be roughly in the vicinity 2 kbar/6800 K. At high temperatures below melting there is some evidence for transformations from graphite to other solid phases, which are proposed to be carbyne (linear molecules) or chaoite-like, but this remains controversial and unresolved" (p. 143 in [16]).

Discussing the topic of liquid carbon properties and graphite melting line position, the authors [16] note that there is a difference of hundreds degrees for the temperature of graphite/liquid/vapor triple point. With increasing quality pyrometric equipment and techniques the results were improved. Temperature of the triple point shifted from 4000 K (fortieth years) to about 5000 K at the moment. The authors [16] note that the last value is the most likely for the triple point of carbon. The same temperature (5000 K) is a basic value for a triple point graphite/diamond/liquid (Fig. 8.5).

8.3 Phase Diagram for Carbon, Obtained by Motohiro Togaya

Carbon phase diagram published by Motohiro Togaya (with colleagues) in their work in 1994 [21] (Fig. 8.7).

Melting temperature in Fig. 8.7 was calculated in the measurements of input energy using specific heat value near the melting point, that was given in the study of Sheindlin and Senchenko in 1988 [18]. According to [18] the influence of carbon sublimation on the temperature measurement was excluded using an inert gas at a pressure of 1 kbar. The melting temperature is increased in [21] from ~4600 K (triple point graphite-gas-liquid at a pressure of 100 bar) to 4800 K at a maximum pressure of 55 kbar and then reduced to 4600 K under a pressure of 100 kbar (Fig. 8.7). Togaya argues that the estimation error for melting temperature measurement is less than 1.7 %. Triple point temperature T = 4600 K is in good agreement with the experimental data of Cezairliyan and Miiller in 1990 [22] (4530 ± 150 K), but differs from the data of Baitin with employees of the same year [15] (5080 ± 70 K). The gentle slope of the melting line of graphite near the triple point of graphite-diamond-liquid assumes a positive slope of the melting line of diamond, which is consistent with theoretical predictions.

It should be added that in the experiment by Togaya [21] it was used a spectroscopic graphite with initial density of 1.6 g/cm^3, and in the study of Sheindlin and Senchenko [18] it was another brand of graphite (UPV1-T) with the density 2.25 g/cm^3. Evaluation of the phase diagram of Togaya based on measurements of enthalpy (error 2.3 %) with the summation of heat losses during the millisecond experiment (heat losses were calculated by a series of experiments using the extrapolation). Besides, a pressure was not more than 1 kbar in [18] whereas in the study of Togaya [21] a pressure was considerably higher—tens kbar. Moreover, Togaya noted in earlier studies that the energy need for the melting of graphite with increasing pressure—is reduced. According to his results (Table 3.2) with increase

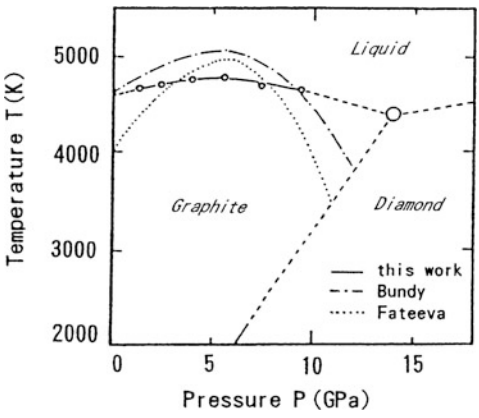

Fig. 8.7 Melting line of graphite and the P-T phase diagram of carbon published by Togaya [21]. The walls of the compressible cell were made of MgO/pyrophyllite

in pressure from 25 to 94 kbar the needed input energy required for graphite melting is reduced by 30 %. How this affects the related properties, specific heat and temperature—is unclear. This uncertainty leads to increased uncertainty of phase diagram construction, and the last uncertainty is difficult to estimate. In light of the mentioned uncertainties there is no reason to abandon Bundy's phase diagrams (Figs. 8.3 and 8.4).

In particular, according to Fig. 8.4 for Togaya experiments [17, 23] at 94 kbar pressure are (presumably) to the curve ~0.3 ΔV (the point of intersection of the dotted curve with the melting curve in Fig. 8.4), and in the melting line according to phase diagram of Bundy it should be fixed temperature T ~ 4900 K whereas the calculation in the studies of Togaya [17, 23] gives the temperature of 4630 K.

In one of our experiments (Figs. 7.25 and 7.27, [13]), the graphite specimen was expanded freely on ~20 % of its original volume ($V/V_0 = 1.2$), and then melting occurs in a quasi-isochoric conditions, with a significant increase in pressure. So the path of microsecond heating in our experiments [13] is near the specified curve in Fig. 8.4 as "0.7 ΔV". The melting temperature under these conditions is according to [8] of about 5000 K. The same temperature value is also recorded in our experiment in Figs. 7.25 and 7.27, at the beginning of melting.

8.4 The Dependence of Tmelting Against Pressure

According to Bundy (Fig. 8.4), the derivative dP/dT = 80 bar/K for a range of pressures from 200 bar to ~20 kbar. The results of Fateeva and Vereshchagin give dP/dT = 54 bar/K in the range from 200 bar to 40 kbar (Fig. 8.1).

Note, in particular, that the question about the the equilibrium condition of diamond with different carbon materials described by L.F. Vereshchagin with colleagues in [24].

Many authors have assumed that graphite phase equilibrium curve solid–liquid has a positive derivative (dP/dT > 0) with increasing temperature at pressures up to 56 kbar (Fig. 8.8, [17]) or at pressures up to ~80 kbar [9] (Fig. 8.4). Thus the melting point of graphite with increasing pressure will be slightly larger. According to Togaya data (Fig. 8.8, [17]) a positive derivative dP/dT is constant (299 bar/K) in the range of 0–56 kbar. Above 56 kbar the derivative dP/dT is negative and also a constant: dP/dT = −258 bar/K (Fig. 8.8, [17]).

Thus, at the pressures above ~56 kbar [17] (or above ~80 kbar according Bundy [9], Fig. 8.4) graphite will be compressed under melting and the melting temperature will decrease. Pay attention to the assessment of errors in the experimental study of M.Togaya. At the level of 4500 K the error of the measurement for the enthalpy H is 2.3 %, and for the temperature 1.7 % [21]. But since the author [21] calibrate their measurements through the dependency of H (T), taken from [18], then you need to add errors from [19]: in addition, 2.5 % for the enthalpy H (the sum for H should be 4.8 %) and additional 2 % for the temperature T.

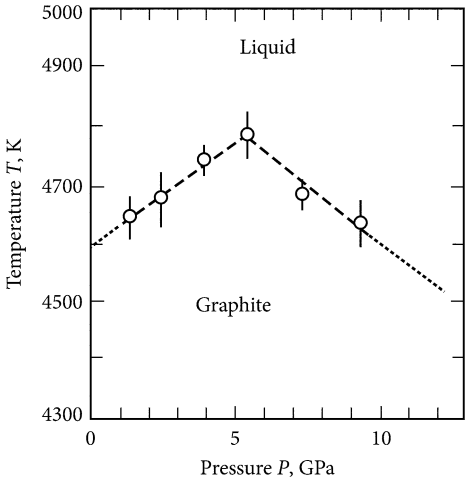

Fig. 8.8 [17] The *dotted line* shows a possible line of graphite melting—it is a smoothed curve for several experimental points. At the pressures below 56 kbar it was observed a derivative 33.4 K/GPa (299 bar/K) and at the pressures higher 56 kbar—38.7 K/GPa (258 bar/K)

The graphite melting temperature has low depending on the pressure according Togaya [17]: T = 4651 K at 14 kbar and T = 4786 K (maximum melting point) at 56 kb (Fig. 8.8, [17]).

Previously, in [25], 1973 year, it was calculated the data for carbon: carbon density dependence against temperature for the solid phase, liquid phase, and vapor. The density of the liquid phase at the triple point is taken to be $\gamma_{TP} = 1.611$ g/cm^3 (it was obtained **by averaging the data** in the literature of previous years up to 1973—the increase in graphite expansion by 15–30 % during melting). The pressure at the triple point is 103 bar; the temperature is 4765 K; the density of vapor is 0.01445 g/cm^3. The estimation of the critical point gives $T_C = 6810$ K, Pc = 2.2 kbar; $\gamma_C = 0.64$ g/cm^3. The significant difference of [25] from our measurements is the difference between the density of the liquid phase: 1.611 g/cm^3 for the triple point [25] and $\gamma = 1.2$ g/cm^3 in our measurements.

In the paper of 1991 year [26] it was published, as the authors write, the generalized phase diagram of carbon (slightly differs from other published. In this paper, the authors still believe that melting temperature for graphite equals 4000 K at low pressures. The authors of [26] indicate that "*at sufficiently high pressure layered structures are converted to tetrahedral as a result of direct phase transitions, and in the low-temperature region is formed Lonsdale while in the high-temperature region is formed diamond … often both versions are formed together*."

The interesting features of the behavior of graphite at high pressure and normal temperatures were watched in experimental study [27]. It was found that the specimens of graphite completely opaque in the initial state, under pressure begin transmitting light in the visible wavelength range. With the increasing pressure they turn to dark brown in color, then gradually become lighter and become transparent and uncolored. This effect is noticeable, since pressure is 35 GPa. The transparency of such specimens reaches 15 % at P = 55 GPa. Under reducing the pressure graphite specimens remain transparent until to 5 GPa, and then dramatically darken. These data, along with the measurement of

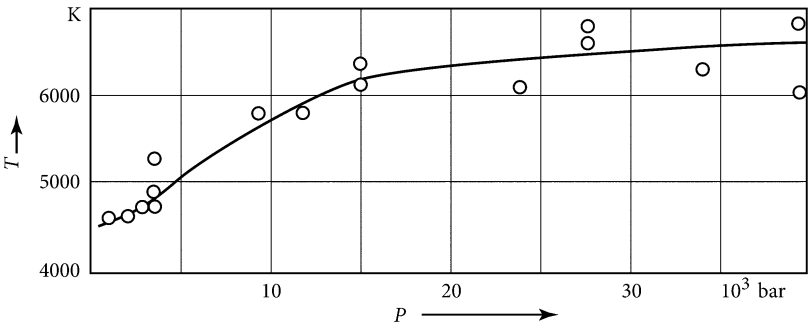

Fig. 8.9 [30] The dependence of the melting temperature of graphite against pressure (up to 40 kbar) according to data of L.F. Vereschagin

the reflection coefficient in the pressure range 15–35 GPa, allowed the authors of [27] to suggest that "*at pressures above 20 GPa graphite goes into a new state semiconductor carbon. A similar conclusion was made by Bundy* [28]*, in which there was an increase in the electrical resistance of the graphite at pressures of 15–20 GPa. The authors of* [28] *attribute this effect to the formation of the hexagonal phase of diamond. However, our measurements do not confirm this assumption because the Raman spectra of graphite at high pressures does not contain a "diamond" lines* [28, C. 672]". Moreover, in [27] it was reported that there are signs of amorphization of the original structure, leading to the formation of a new hybrid state of carbon which was mentioned by Leipunsky [29]. It is possible that the compression of a particular class of covalent substances (carbon and quartz SiO_2) at sufficiently low temperatures occurs at substantially nonequilibrium path—note the authors of [27].

The true dependence of the melting temperature of graphite against pressure is still not established. According to experimental data of Fateeva and Vereshchagin [30] even under the pressure is increased to 30 kbar the melting temperature increases from 4500 to 6500 K (Fig. 8.9).

The points for the curve (up to the 30 kbar) were obtained from the smoothed curve of the dependence of T(P) for the graphite as measured in the gaseous medium.

According to the estimated data of M. Togaya [31, 32], the melting temperature is increasing only by 200 K under the pressure rise up to 56 kbar. Our direct experiment [13] under quazy-isochoric heating (Fig. 7.29) shows that the melting temperature of graphite at melting point grows by $\sim$1000 K when pressure is increased to $\sim$50 kbar. It is hoped that future experimental efforts in the study of rapid heating of graphite will aim to measure the pulse pressure by the shift of the ruby luminescence, i.e. the use of already developed in stationary conditions (diamond anvils) method. Such measurements are already performed in a flat loading for metal foils with rapid (microseconds) electrical heating [33, 34].

The carbon phase diagram shows the data Togaya, Bundy, and Fateeva et al. The lowest melting temperature T $\sim$ 4000 K (triple point according to [3]) in the study of the latter authors increases with pressure up to a maximum temperature T $\sim$ 4800 K at the pressure P = 60 kbar. In contrast to this result, in the same

laboratory of L.F. Vereshchagin, it was indicated the melting point of 6500 K for the pressure ~30 kbar (Fig. 8.9, [30]). The question of the true melting point of graphite, depending on the pressure—is not clarified until now due to problems with the measurement of the melting temperature of graphite.

8.5 Phase Diagram for Small Particles of Carbon

The authors of several published works on the carbon phase diagram consider changing it for the very small carbon particles that are at high pressures and temperatures. For example, in [35] of A.L. Vereshchagin, the three-dimensional phase diagram of carbon is considered, built in coordinates pressure–temperature–dispersion on the basis of published data on the properties of detonation diamonds. As usual, the consideration of carbon phase diagram for small particles leads to a decrease in melting temperatures with decreasing their size.

The study [36] presents the P-T phase diagram, taking into account the small size of the particles (Fig. 8.10). The feature of this latest work is the latest result of published experimental studies of melting carbon, including and received by our measurements.

In more detail the phase boundary of the G-L shown in the following figure by the same authors (Fig. 8.11).

In [42], 1993, it was published another calculated phase diagram of carbon. This work is mainly devoted to the phase stratification in liquid carbon. As the triple point for carbon the authors [42] gives: T = 4550 K, P = 110 bar, liquid density γ = 1.11 g/cm^3. Derivative dP/dT at low pressures is ~70 bar/K. Calculated phase separation in the liquid leads to: a diamond-like (non-conductive) fluid and graphite (conductive) fluid. The straight line

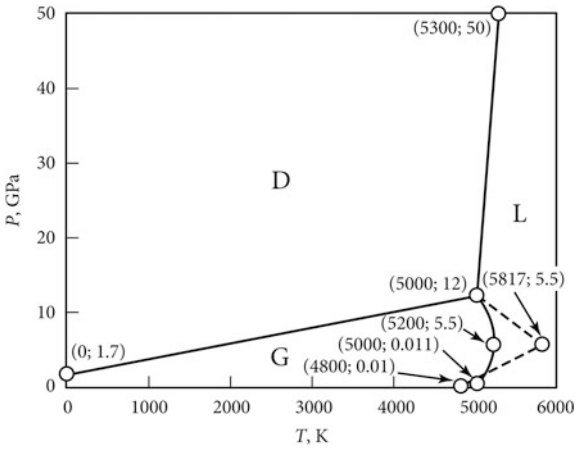

Fig. 8.10 [36] P-T phase diagram for the bulk carbon as it was predicted Bundy with the colleagues in 1996 [37] (*solid line*), where the phase boundary G-L is adjusted (*dotted line*) according to the results of recent experimental studies of Korobenko and Savvatimskiy, 4800 K [14, 38–40], as well as the work of Basharin with the colleagues, 4800 K [41]. *Circles* indicate the characteristic points on the phase diagram. In parentheses are the appropriate temperatures and pressures (in GPa)

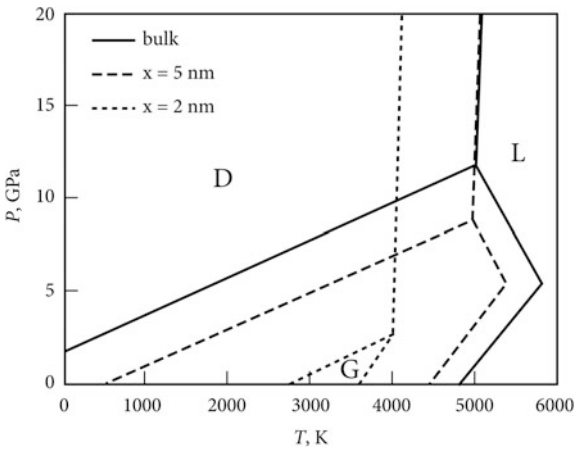

Fig. 8.11 [36] P-T phase diagram for the bulk carbon and nano-crystalline carbon. *Lines*: *solid, dashed* and *dotted* are for the bulk carbon; having a particle size of 5 nm; having a particle size of 2 nm, respectively

has the derivative dP/dT ~40 bar/K and ends at the critical point of liquid-liquid separation at the parameters: T = 5520 K, P = 70.5 kbar with the density $\gamma = 2.32$ g/cm^3. At one time, Bundy doubted about the real existence of such a bundle [16].

It should be mentioned again the review Bundy et al. in 1996 [16] which focuses on the relevance of the phase diagram of carbon and recent experimental results for the carbon at high temperatures. In particular, for the melting temperature of graphite it was adopted the value of 5000 K (with a reference to M. Sheindlin and V. Senchenko [18]) for low pressures, instead of the previous ~4000 K (Fig. 8.5).

In Fig. 8.12 (skeletal form of which is taken from [43]) shows the phase diagram of carbon near the triple point and the melting region. The results of our experiment at a high temperature (Fig. 7.27, [13]), at pressures up to about 60 kbar, are presented in Fig. 8.13 (at the axis pressure P-specific volume V). To calculate the pressure (at the melting temperature of 4800 K) it was used the derivative dP/dT (equals 54 bar/K) given in the study of L.F. Vereschagin with coworkers [2, 3, 44].

Graphite with initial density $\gamma = 2.2$ g/cm^3 reaches melting point at density of about 1.8 g/cm^3(0.56 cm^3/g) at a pressure of approximately 54 kbar. Figure 8.13 allows us to represent the behavior of graphite heated to high temperatures at high pressures. Note that the curves "m" and "n" (the lines for the start and the end of melting, respectively) under they extend upwards, must intersect at the melting point, where the density of the solid phase equals the density of the liquid phase.

According to Bundy (Fig. 8.5, [9, 45]) this point corresponds to the pressure ~80 kbar (in the region of the phase diagram where the derivative dP/dT becomes negative). According to Togaya this transition can occur at ~50 kbar [23]. Thus, under the high pressure and temperature parameters the curves "m" and "n" are swapped, so that at the beginning of melting the density of the liquid phase becomes higher than the density of the solid phase.

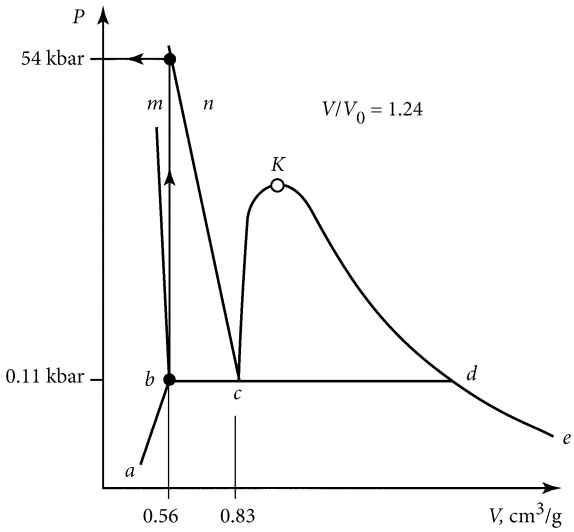

Fig. 8.12 Phase diagram of carbon in the axis: the pressure P and specific volume V (0.56 cm^3/g with a density 1.8 and 0.83 cm^3/g with a density of 1.2 g/cm^3). *Bold lines* (*a*, *b*) The line of start sublimation. (*d*, *e*) The line of complete sublimation. (*b–d*) The line for triple point; *m* the start of melting; *n* the completion of melting. *K* critical point. *Thin line* (marked by the *arrows*) shows the course of the experiment [13] (Fig. 7.29)

8.6 Modeling of Carbon Phase Diagram

8.6.1 Data of Ghiringhelli and Meijer

In 2010 year a book was published (by Springer) as a collection of different articles devoted to modeling of carbon properties [46].

Chapter 1 (authors Luca Ghiringhelli and Evert Meijer) of the book titled "Liquid Carbon: Freezing Line and Structure Near Freezing". The authors of the Chap. 1 publish the approach to the selection of the potential for calculation "1.3 Modeling Carbon":

"*A viable alternative is to model the inter-atomic interactions by a functional description, whose parameters are (partly) fitted to a selected database. Such a functional description (also referred to as empirical, semi-empirical or classical potentials) serves several purposes, ranging from the modeling of minimum energy structures for surface reconstructions, grain boundaries or related defects, to the description of the liquid structure and thermodynamic stability.*

According to Brenner potential (reference [47] for this paragraph,—see in [46]), *an analytic potential needs to be:*

- ***Flexible*** *The function should be flexible enough to accommodate the inclusion of a relatively wide range of structures in a fitting database.*

- ***Accurate*** *The potential function must be able to accurately reproduce quantities such energies, bond lengths, elastic constant, and related properties entering a fitting database.*
- ***Transferable*** *The functional form of the potential should be able to reproduce related properties that are not included in the fitting database. In practice the potential should be able to give a good description of the energy landscape for any possible realistic configuration characterized by the set of atomic positions* $\{\mathbf{r}_i\}$.
- ***Computationally Efficient*** *The function should be of such a form that it is tractable for a desired calculation, given the available computing resources. Focusing on carbon, there is a noble lineage of increasingly successful parameterizations of the empirical potentials, from the Tersoff potential, via the Brenner potentials* [44] *and their modifications* [2, 3, 47] *up to Los-Fasolino LCBOP . The crucial characteristic of these potentials is that they account for the "bond order": the potentials formalize and parameterize the idea that for covalently bonded systems an increasing number of bonds per atom modifies (typically decreases) the bond energy per bond"* (These references [2, 3, 44] see in the [46] only).

One of the motive for the calculation of multiple phases in liquid carbon comes from the following fact: "*Sulfur has at least three liquid phases: two insulating phases and a metallic phase*" (Reference 18, also see in [46]).

In spite of the well theory approach to the calculation procedure the results near the melting point in this paper (Ghiringhelli and Meijer) differ from the experimental data at the phase transition area (first triple point parameters). Pay attention to the choice of the authors of the experimental data for phase transitions (Fig. 8.13) in particular the melting of graphite. It is known that almost all phase transitions are difficult to calculate, so the attraction of reliable experimental data is necessary. In the part of the Chap. 1 ("1.2 Carbon Phase Diagram: Some Important Characteristics") the authors (Ghiringhelli and Meijer) stated:

"*The experimental estimates for the melting temperatures show a large spread. It appears that the estimated melting temperature depends significantly on the heating rate of the sample [47, 55], yielding values from 3,700 to 5,000 K below 0.01 GPa. In a recent comprehensive review of graphite melting [40] the melting temperature is proposed to be in the range of 4,600–5,000 K.*" [46, p. 2] (These references [40, 46–48] are according to this monograph).

In spite of the fact that the survey [40] gives in 2005 year the most reliable data (4600–5000 K) the authors (Ghiringhelli and Meijer) published the unreliable data with low melting temperature [47, 48] for the graphite melting line: melting temperature (at the pressure value $\sim$0.2 kbar) is lower than 4000 K, see Fig. 8.13. We must remind that it was shown in [40] that the data [47] obtained at atmospheric pressure under slow heating are unreliable data. Besides there is no any depending on the heating rate for the most reliable experimental data for graphite melting temperature, starting from 1963 year. After [40] these points are established in this monograph in detail also (see Sect. 3.5 in this monograph).The result of the calculation of Ghiringhelli and Meijer is shown in Fig. 8.13.

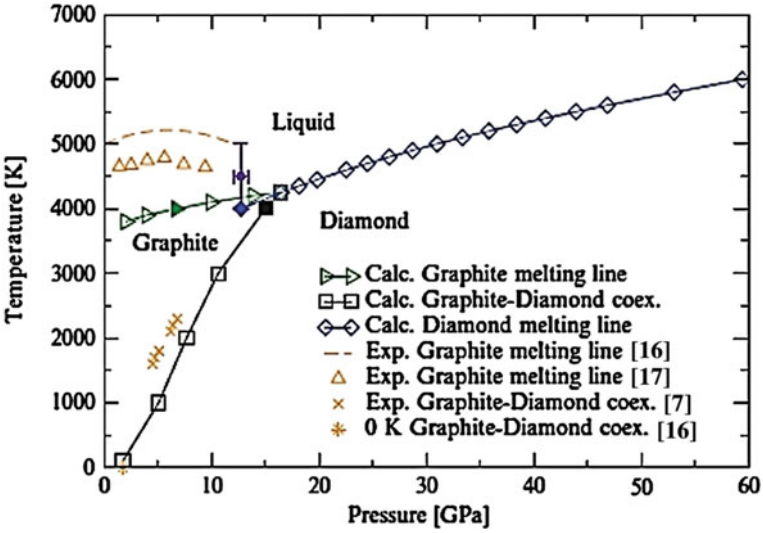

Fig. 8.13 [46] Phase diagram of carbon up to 60 GPa. The *solid right triangle*, *square*, and *diamond* are the three coexistence points found by equating the chemical potentials at 4,000 K (see text). The *open right triangles*, *squares*, and *diamonds* are the calculated coexistence points, propagated via Gibbs–Duhem integration. The *solid circle* with *error bars* indicates the experimental estimate for the liquid/graphite/diamond triple point [16, 42, 49]. The *dashed line* is the experimental graphite *melting line* from [16]. The *up triangles* are graphite melting state points from [17]. The *crosses* represent experimental graphite/diamond coexistence from [7]. The *asterisk* represent the theoretical graphite/diamond coexistence at zero kelvin, as reported in [16] (*The links shown in the figure and in figure legends—according to Reference of this monograph*)

Pay attention to the sentence in figure captions: "*The solid circle with error bars indicates the experimental estimate for the liquid/graphite/diamond triple point* [17, 42, 49]". The reference [16] is really an experimental estimation, but [42, 49]—are just the calculations. The reader clearly sees the graphite melting line (green in color) in the Fig. 8.14 goes to the temperature lower 4000 K at low pressures. This result is based on unreliable data of the authors [47, 48] (mentioned in [46]) who stated that graphite triple point (graphite/liquid/vapor) has a pressure near 1 bar and temperature near or lower 4000 K. The authors of [46] continue: "*It appears that the estimated melting temperature depends significantly on the heating rate of the sample* [47, 48], *yielding values from 3,700 to 5,000 K below 0.01 GPa. In a recent comprehensive review of graphite melting* [40] *the melting temperature is proposed to be in the range of 4,600–5,000 K.*". The authors [46] new our justified criticism [40] to the data [47, 48] (see Chap. 3 in this book) but choose the result of [47, 48]. May be they believed that melting temperature really depends on velocity of heating. In the Sect. 3.5 we have shown that this depending is absent. Moreover, fast heating gives possibility to avoid sublimation (with appearing a soot that gives an underestimated temperature) and fulfill temperature measurements correctly. (*The references are shown according to this monograph*).

In fairness it should be said that the publication of [42] contains an excellent review, including experimental works also (without giving the most reliable results). Conclusion of [42] is as follows. Despite the analysis of a considerable number of experiments of different duration for different pressures (before 1993 year), the authors [42] failed to set the behavior of the electrical resistance of the liquid phase of carbon during melting (whether accompanied the melting of the increase of the electrical resistance or fall). Next, the authors [42] of 1993, continues: "*Ferraz and March [50] do interpret Bundy"s experiments as an indication of a liquid-liquid transition*" [42, p. 3592]. However, Bundy [16, p. 145] said: "*There appears to be no firm evidence from the most recent experiments that supports the existence of an electrically insulating form of liquid carbon.*" It is obvious that this conclusion applies to the state of liquid carbon near the first triple point of graphite-vapor-liquid. As Bundy in the same work (and in the same page) concludes: "*There is some experimental evidence that liquid carbon at pressures above the graphite/diamond/liquid triple point does contain graphite-like and diamond-like linkages*" [16]. Thus, according to Bundy, we can talk about the stratification of liquid carbon only above second triple point graphite/diamond/liquid, higher 15 GPa according to Fig. 8.13 (*Above mentioned links are shown according to this monograph*).

We may show comparison result of calculation [46] and Bundy phase diagram [16] in a rough composition (Fig. 8.14).

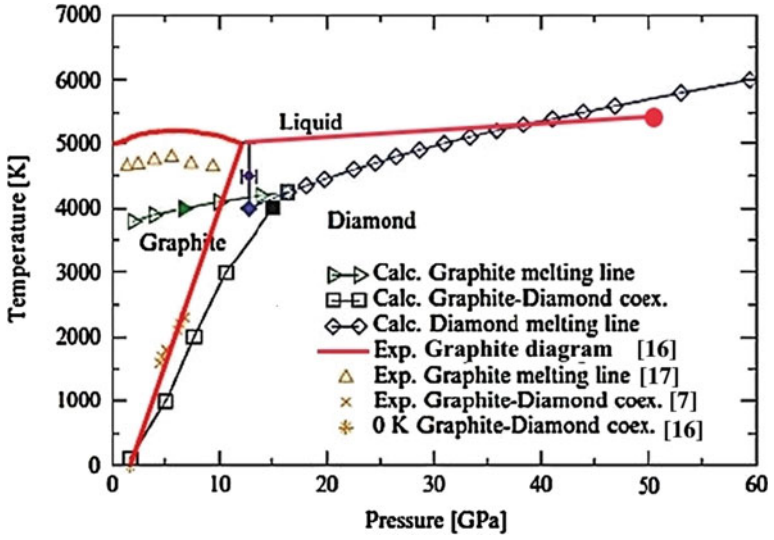

Fig. 8.14 P-T phase diagram (experimental and calculated approach). [16] in *red color*—Bundy, the *solid red dot* is the limit value published in [16, 17]—Togaya's data. One can see that the computations are slightly inaccurate in the graphite/diamond separation; they are much more inaccurate in the prediction of the melting line at low pressures (too low). Usually authors of the calculations do not know which of the experiments more reliable, and these lead to additional questions. One of the main purpose of this monograph—to give readers formed the own opinion on the reliability of the data based on the results of the analysis of experimental data published in this book

The authors of calculation in [46] (2010) refer to the estimated work of other authors [42] (1993) just as if there were summed up the results of carbon melting line studies. Note that the authors of estimations [44] (published in1993 year) did not know the works of Togaya, while Bundy et al. [16] (of 1996 year) knew the clue experimental data of Togaya published in 1994 year (liquid carbon resistivity diminishing with imparted energy before 50 kbar pressure, and rise higher 50 kbar pressure). That's why we prefer the opinion of Bundy and Togaya (who are the experimenters) in assessing the behavior of liquid carbon before diamond triple point.

As to the carbon at the highest pressures (higher graphite/diamond/liquid triple point) the reader should see the original publications devoted to this area. The authors (Ghiringhelli and Meijer in Colombo) investigated by calculation (specifying the data of the shock wave experiment) the behavior of carbon phase diagram up to 400 GPa.

For clarity, we note that usually the phase diagram of carbon gives the dependence of carbon on temperature and pressure only. The experiment allows us to give the phase diagram of a deeper meaning in the measurement of the electrical resistance. Next take action the calculation studies, arguing about the presence or absence of conductivity at various parameters (including the separation of carbon to conductive and non-conductive phase). But the experiment goes even deeper, measuring other properties (enthalpy, heat capacity, optical properties).

8.6.2 Data of Glosli and Ree

Data of Glosli and Ree. In 1999 year Glosli and Francis Ree [49] took into account the data of Togaya and calculated phase transition in carbon above ~ 2 GPa pressure. A first order phase transition was found in liquid carbon using atomistic simulation methods and Brenner's bond order potential. The phase line was terminated by a critical point at 8801 K (*pay attention: the accuracy in calculation is 1 K!, this demonstrates the endless faith of the estimator in their results*) and 10.56 GPa and by a triple point on the graphite melting line at 5133 K and 1.88 GPa. The phase change was associated with density and structural changes. The low-density liquid was predominantly *sp* bonded with little sp^3 character. The high-density liquid was mostly sp^3 bonded with little *sp* character. This was the first non-empirical evidence of a liquid-liquid transition between thermodynamically stable fluids.

8.6.3 Data of Umantsev, and Akkerman

Data of Umantsev, and Akkerman. Next theoretical study [51] was published in the Journal Carbon (2010 year).

The authors [51] constructed a continuum theory of carbon phases based on the Landau theory of phase transitions. The authors note that the theory ties up many seemingly unrelated data on the carbon system. Transformations between graphite, diamond, and liquid-carbon are described by the Landau–Gibbs free-energy which depends on two order parameters: crystallization and structural. The barrier-height and gradient-energy coefficients were calculated from the nucleation data obtained in the studies of diamond/graphite and diamond/liquid-carbon systems. The boundary of the absolute stability of the graphitic phase was interpreted as the spinodal point of the free-energy, which allowed authors to calculate the pressure dependence of the barrier-height coefficient. The continuum model yielded a value of 1.66 J/m^2 for the graphite/liquid-carbon interface energy, which continues the trend of the elements of Group IV. The authors [51] also analyzed stability of nanostructured amorphous carbon and interpreted it as the transition state of the free-energy function. This conjecture helped the authors to explain results of the experiments on the focused ion-beam irradiation of CVD-diamond nano-films. The authors stated that present theory may be used for the large-scale modeling of graphite and diamond crystallization; it can also be extended to include other structural modifications of carbon or an entirely different element such as silicon.

The authors [51] has received a phase diagram in the upper pressure limit equals 100 GPa, **According to [51] the authors give almost the same data (and figure) for carbon triple point at low pressures as published in the previous work of Ghiringhelli and Meijer** (Fig. 8.13): at low pressure the temperature at the triple point (graphite-liquid-vapor) is lower than 4000 K and temperature at the "diamond" triple point (graphite-liquid-diamond) is not high than 4300 K. In addition the co-existence line between these two triple points is growing with the increase of pressure (see above mentioned Figs. 8.13 and 8.14). This is fundamentally different from the experimental data of Bundy, Tagaya and Vereshchagin, in which there is the maximum of this curve in the region of 5 GPa (see Chap. 3 in this book).

8.6.4 Data of Colonna, Fasolino, and Meijer

In the Journal Carbon it was published the result of calculation [52] for carbon equation of state at low temperature (up to 4000 K) but up to high pressure (20 GPa). Apparently the calculation for high pressure is much easier than at the phase transitions.

The thermoelastic behavior of graphite [59] was experimentally accessible in a limited range of pressures and temperatures. It was performed Monte Carlo simulations based on the accurate long range carbon bond-order potential (LCBOPII) in order to study graphite in a wider range of thermodynamic conditions. It was presented the volume-pressure equation of state and related thermoelastic properties up to 4000 K and 20 GPa.

We mentioned this study of the solid graphite to show the privilege of the calculators to pressure but not temperature. Obviously, many hoped that the calculation is cheaper and gives the desired properties without great financial cost of conducting the experiment. It should be mentioned that all physics was born from the experiments. Experiment must give the clue points for the calculations, and it's impossible to ignore.

8.6.5 Data of Shabalin

A new book [53] by Igor I. Shabalin was published (Springer) in 2014 year titled: "Ultra-High Temperature Materials I: Carbon (Graphene/Graphite), and Refractory metals". The number of pages 800, but Chap. 2, named "Carbon (Graphene/Graphite)" consist 188 pages, and only 70 pages are devoted to thermal, electromagnetic, optical, physico-mechanical, and nuclear properties of carbon.

There are a lot of references and numerical data in the book, but the choosing the most reliable results is absent in the book (as far as we can judge from the fragmentary data available online). For the temperature at the triple point of carbon is given: 3800, 4000, 4200, 4500, 4760 K (with the references included), but the reader does not know which values to believe.

Carbon melting temperature is shown in Table 1.3 (p. 4) as 3700–4100 °C. In the Table 2.4 (p. 34) the author of [53] mentioned "*true melting temperature and triple point of graphite … 4000–5000 K*". I think that it is a very useful publication on the all aspects of high temperature materials (and chemical properties), but it contains unsufficient reliable data on carbon itself at the first carbon triple point (graphite/liquid/vapor).

The reluctance of the authors of reference books to identify the most reliable data, leads to the arbitrary behavior of the estimator when selecting the source of the experimental data to build the calculation model. In the case of a large scatter of the experimental data for the estimator is much easier to justify their results, as these results will be in agreement with the scatter of the experimental data. In this respect, the objective of this monograph was to identify the most reliable information from numerous experimental studies of the properties of carbon in the vicinity of the first triple point and in the liquid state.

8.6.6 Data of Orekhov and Stegailov

Just in 2014 and 2015 year it was appeared calculation study [54] and then [55] on the possible explanation of the scatter of the experimental data with very different values of melting temperature (3800–5000 K). The main advantage of work is keeping the velocity of the melting front at different heating rates. Note that front velocity was also calculated.

The conclusion of [54] publication gives the following.

"*The main aim of this work was to study the kinetics of melting of graphite and clarify the behavior of the phase diagram of carbon on the basis of the obtained data. It was made of two-phase MD simulation of melting of graphite. The calculated dependence of the front velocity of the melt from overheating degree. The front velocity is about 1 m/s, which is about two orders of magnitude less than the velocity of the melting front in metals. While on the dependence of the speed of the front melting temperature detected two areas: clearly manifested in the MD calculations of high-temperature linear section of the site and slow motion front at low temperatures. By extrapolation of the linear section it was determined melting point in the range of 2–14 GPa. The obtained melting curve has a maximum at pressures 6–8 GPa.*

It is noted that the ideal graphite structure can withstand large temperature rises (up to 400–500 K) for times greater than 10 ns, especially at relatively low pressures P < 2–3 GPa, when the concentration of interlayer defects is negligible. The formation of interlayer defects is an important mechanism of melting of graphite, which, apparently, may explain the decrease in melting temperature with increasing pressure and thus there is a maximum on the melting curve.

It is noteworthy that the phenomena described here within a single model, specifying the nature of the interatomic interactions using the AIREBO potential, with good accuracy fall within the range of experimental melting temperatures (3800–5000 K). In this wide temperature range there are different mechanisms of melting, which probably reduces the task of explaining the differences of experimental data on the melting temperature of graphite to the problem of determining the mechanisms for fixing melting in different experiments."

Note that the authors [54] consider the result of their approach "*with good accuracy fall within the range of experimental melting temperatures (3800–5000 K)*", so we may supposed that the uncertainty of the approach is not better than the scatter in experimental values.

Even more interesting is the article [55] of the same authors published in 2015 year.

To study the kinetics of heterogeneous process of melting, the front velocity calculations are carried out using the twophase simulation method.

Conclusions of the [55].

"*Using the molecular-dynamics method we have shown that melting in graphite proceeds much slower than in other solids. We have calculated the rates of heterogeneous and homogeneous melting mechanisms as well as the thermodynamic melting temperature of graphite and the* ***single graphene layer*** *decay temperature for the AIREBO interatomic potential. These results combined in a simple mesoscopic model that takes into account a typical microstructure of graphite specimens, have allowed us to describe a large set of experimental results on the detected graphite melting temperatures at different heating rates. These results suggest that at the heating rates higher that* $\sim 10^6$ *K/s graphite specimens in most cases become superheated, the solid–liquid transition temperature becomes higher than the equilibrium melting temperature and is influenced mainly by the specimen microstructure and the energy deposition process.*

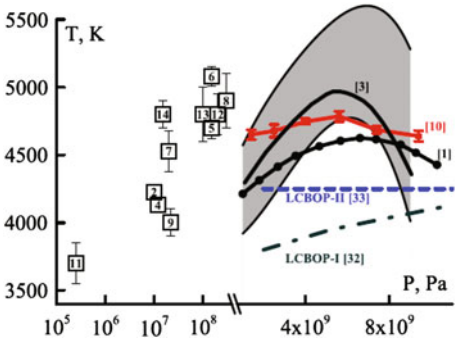

Fig. 8.15 [55] The experimental results on the graphite melting temperature in two pressure ranges from different experiments [1, 4 (see this references only in [55]) (*the numbers* match the corresponding citations in the reference list). The data from are shown as the average line as well as the *upper and lower envelope curves* that show the scatter of the individual measurement results. The results of atomistic calculations for LCBOP-I [2] and LCBOP-II models [3] are shown as well (see all the references [2, 3] only in [55])

The slow melting kinetics of graphite together with the pressure and temperature effects on porosity of commonly used graphite specimens can explain the observed maximum on the experimentally detected melting temperature dependence on pressure as a kinetic effect without the hypothesis about a liquid–liquid phase transition in liquid carbon."

Consider Figs. 8.15 and 8.16 as they are shown in [55].

The clarification of the authors [55] to the Fig. 8.15:

"*Atomistic simulation methods became mature enough to handle the graphite melting problem as soon as the sophisticated interatomic potentials for carbon had been created (AIREBO and LCBOP). However despite considerable effort no confirmation of the LLPT in liquid carbon was found [44]. The pressure dependencies of the graphite melting temperature calculated for the LCBOP type models using thermodynamic integration [2, 3] are located in the region 3800–4250 K and display no evidence of the maximum (see Fig. 8.15). Therefore the nature of the observed maximum of the melting curve remains unexplained.*" (References [2, 3, 44] of this paragraph see only in [55], but not in this monograph).

For a clearer understanding give the references numbered as they were shown in [55] for the Figs. 8.15 and 8.16 and for the legends to this figures.

[1] Bundy FP. Melting of graphite at very high pressure. J Chem Phys 1963;38 (3):618–30.
[3] Fateeva NS, Vereshchagin LF. Concerning the melting point of graphite up to 90 kbar. JETP Lett 1971;13:110.
[10] Togaya M. Pressure dependences of the melting temperature of graphite and the electrical resistivity of liquid carbon. Phys Rev Lett 1997;79(13):2474–7.
[31] Stuart SJ, Tutein AB, Harrison JA. A reactive potential for hydrocarbons with intermolecular interactions. J Chem Phys 2000;112(14):6472.

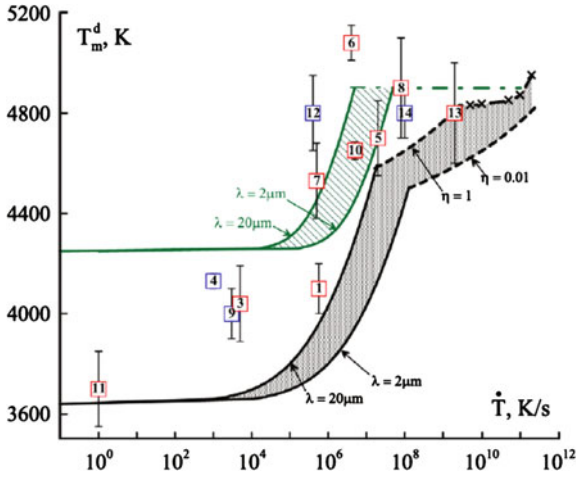

Fig. 8.16 [55] The dependence of the graphite melting temperature detected in experiment on the heating rate. The *symbols* meaning is as on Fig. 8.16 (here *red* shows electrical and *blue* shows laser heating experiments). The *solid lines* show the region of T_m^d (Ṫ) determined by (*5*) for the average grain size λ = 2–20 μm. The *dashed lines* show the region determined by (*6*) for the critical liquid phase fraction η = 0.01–1. The *black curves* are our results for AIREBO and the *green curves* are our estimates for LCBOP-II (without data for homogeneous nucleation). The *dash-dotted lines* show the graphene melting determined in this work (the crosses) and in *(References are shown in the legend according to* [55]*)*

[32] Los JH, Fasolino A. Intrinsic long-range bond-order potential for carbon: performance in Monte Carlo simulations of graphitization. Phys Rev B 2003;68 (2):1–14.
[33] Wu CJ, Glosli JN, Galli G, Ree FH. Liquid–liquid phase transition in elemental carbon: a first-principles investigation. Phys Rev Lett 2002;89:135701.
[34] Kum O, Ree FH, Stuart SJ, Wu CJ. Molecular dynamics investigation on liquid–liquid phase change in carbon with empirical bond-order potentials. J Chem Phys 2003;119(12):6053–6
[35] Ghiringhelli LM, Valeriani C, Los JH, Meijer EJ, Fasolino A, Frenkel D. State-of-the-art models for the phase diagram of carbon and diamond nucleation. Mol Phys 2008;106(16–18):2011–38.
[36] Ghiringhelli LM, Los JH, Meijer EJ, Fasolino A, Frenkel D. Modeling the phase diagram of carbon. Phys Rev Lett 2005;94(14):145701
[37] Colonna F, Los JH, Fasolino A, Meijer EJ. Properties of graphite at melting from multilayer thermodynamic integration. Phys Rev B 2009;80(13):1–8.

It is very useful that the authors [55] compare the capabilities of different potentials. Particularly it opens up some weak points of such calculations. The readers should see themselves this notable work. Figure 8.16 gives probably all the experimental results considered by the authors [55].

As the authors [55] note in the Abstract:

"*The unusually slow melting kinetics results in the existence of the superheated graphite at the* ***microsecond timescale*** *and thus biases the measurements of its equilibrium melting temperature*". In response to this show almost stationary study [56, 57] (10-s laser heating) which received the melting temperature of graphite equals 5000 K, or [58] (20–30 ms heating) with the melting temperature 4800 ± 150 K, see Sect. 3.5, Table *3.3* in this book. So the true reasons are hidden in the analysis of reliable experimental data. (*References in this paragraph are shown according to this monograph*).

8.6.7 The Resume for All Considered Papers of the Sect. 8.6

(1) Almost all the authors of calculation studies do not distinguish between reliable data of experimental studies from the false. They accept everything "as it is". Almost none of the calculaters realise that there were two different stages during experimental carbon melting investigation. The first, when the carbon sublimation preventing correct measurement of the melting temperature was not considered, and the second, when have learned to avoid the influence of sublimation on temperature measurements (particularly by fast heating). Some even try to make calculations so that they could explain all of the difference of the experimental data, as the advantage of their calculations. But this does not solve the problem, so does not allow establishing the truth. Unfortunately, at the present time calculations and experiments are going in parallel paths, not trying to converge. The study [55] is may be the first attempt to bring closer the positions of estimation and the experiment.

(2) Since in the calculations is not allocated the reliable result among all the experiments, it seems that there is a dependence of the melting temperature on the speed of heat. We may understand the position of the authors [55] who try to explain this supposed effect by the slow melting kinetics of graphite. As the authors [55] say: "*the scatter of the measured Tm values can be explained by the ease of graphite superheating due to its unusually slow melting kinetics*". (Remind that we have shown in the Sect. 3.5 (Table 3.3) that the reliable experiments did not show the dependence on the heating rate on the carbon melting temperature).

In the case of rapid heating of a defect-free crystal there paired defects of Frenkel have appeared (just before the beginning of melting). Under melting of rapidly heated substances the low speed of diffusion of the defects from the specimen surface or from grains does not have time to saturate the metal by the equilibrium defects. Fast experiments prove (for metals [59], carbides [60] and carbon [61]) that before the melting of a crystal, there appeared the Frenkel point defects ensured melting and the effect gives increasing in heat capacity just before melting.

References

1. M.A. Sheindlin, The phase diagram of carbon at high temperatures. High Temp. **19**(3), 467–488 (1981)
2. L.F. Vereshchagin, N.S. Fateeva, Melting curves of graphite, tungsten and platinum up to 60 kbar. JETP **28**(4), 597–819 (1969)
3. N.S. Fateeva, L.F. Vereshchagin, On the graphite melting curve to 90 kbar. JETP Lett. **13**, 110–111 (1971).
4. F.P. Bundy, Melting of graphite at very high pressure. J. Chem. Phys **38**, 618–630 (1963)
5. B.J. Alder, R.H. Christian, Phys. Rev. Letters **7**, 367 (1961)
6. P.S. DeCarli, J.C. Jamieson, Science **133**, 1821 (1961)
7. F.P. Bundy, Direct conversion of graphite to diamond in static pressure apparatus. J. Chem. Phys. **38**(3), 631–643 (1963)
8. F.P. Bundy, Phase diagrams of silicon and germanium up to 200 kbar, 1000 C. J. Chem. Phys. **41**(12), 3809–3813 (1964)
9. F.P. Bundy, Pressure-temperature phase diagram of elemental carbon. Phys. A **156**(1), 169–178 (1989)
10. J.W. Shaner, Equation of state and electrical conductivity of carbon, pulse heated up to 6000 K. Bull. Am. Phys. Soc. **32**(607), 133 (1987)
11. P. Gustafson, An evaluation of the thermodynamic properties and the P, T phase diagram of carbon. Carbon **24**(2), 169–176 (1986)
12. V.N. Korobenko, A.I. Savvatimskiy, Electrical resistivity of liquid carbon. High Temp. **36**(5), 700–707 (1998)
13. V.N. Korobenko, A.I. Savvatimski, R. Cheret, Graphite melting and properties of liquid carbon. Int. J. Thermophys. **20**(4), 1247–1256 (1999)
14. V.N. Korobenko, PhD dissertation for the degree of candidate of physical and mathematical sciences, Experimental study of the properties of liquid metals and carbon at high temperatures, (Moscow : Institute for High Temperatures RAS, 2001) (in Russian)
15. A.V. Baitin, A.A. Lebedev, S.V. Romanenko, V.N. Senchenko, M.A. Sheindlin, The melting point and optical properties of solid and liquid carbon at pressures up to 2 kbar. High Temp.-High Press **21**, 157–170 (1990)
16. F.P. Bundy, W.A. Basset, M.S. Weathers, R.J. Hemley, H.K. Mao, A.F. Goncharov, Review article The pressure-temperature phase and transformation diagram for carbon; updated through. Carbon **34**(2), 141–153 (1996)
17. M. Togaya, Pressure dependences of the melting temperature of graphite and the electrical resistivity of liquid carbon. Phys. Rev. Lett. **79**(13), 2474–2477 (1997)
18. M.A. Sheindlin, V.N. Senchenko, Experimental study of thermodynamic properties of graphite in the vicinity of the melting point. Doklady **298**(6), 1383–1386 (1988). (in Russian)
19. A.I. Savvatimskiy, V.E. Fortov, R. Cheret, Thermophysical properties of liquid metals and graphite, and diamond production under fast heating. High Temp.-High Press **30**, 1–18 (1998)
20. S.V. Lebedev, A.I. Savvatimskiy, The electrical resistivity of graphite in a wide range of condensed state. High Temp. **24**(5), 671–678 (1986)
21. M. Togaya, S. Sugiyama, E. Mizuhara, Melting line of graphite. AIP Conf. Proc. **309**, 255–258 (1994)
22. A. Cezairliyan, P. Miiller, Measurement of the radiance temperature (at 655 nm) of melting graphite near its triple point by a pulse-heating technique. Int. J. Thermophys. **11**(4), 643–651 (1990)
23. M. Togaya, Behaviors of liquid carbon at high pressure, in *New Kinds of Phase Transitions: Transformations in Disordered Substances*, ed. by V.V. Brazhkin, et al. (Kluwer Academic Publishers, Printed in the Netherlands, 2002), pp. 255–266
24. L.F. Vereshchagin, E.N. Yakovlev, L.M. Buchnev, B.K. Dymov, The question about the conditions of equilibrium of diamond with different carbon materials. High Temperatures **15**(2), 316–321 (1977). in Russian

25. H.R. Leider, O.H. Krikorian, D.A. Young, Thermodynamic properties of carbon up to the critical point. Carbon **11**, 555–563 (1973)
26. V.I. Kostikov, N.N. Shipkov, Y.A. Kalashnikov, et al., Graphitization and diamond formation, M. Metallurgy (1991)
27. A.F. Goncharov, I.N. Makarenko, S.M. Stishov, Graphite at pressures up to 55 GPa: optical properties and combination scattering of light, amorphous carbon? JEPT **96**(2), 380 (1989)
28. F.P. Bundy, Science **137**, 1057 (1962)
29. O.I. Leipunsky, About artificial diamonds. Chem. Uspekhi **8**(10), 1519 (1939)
30. L.F. Vereshchagin, Solid state at a high pressure. Nauka 1981, 286 p. (in Russian)
31. M. Togaya, Electrical property changes of liquid carbon under high pressures. J. Phys.: Conf. Ser. 215 012 081 (2010)
32. M. Togaya, Electrical resistivity of liquid carbon at high pressure, Science and Technology of High Pressure. In Proceedings of AIRAPT-17, ed by M.H. Manghnani, W.J. Nellis, M.F. Nicol (Universities Press, Hyderabad, India, 2000), pp. 871–874
33. V.N. Korobenko, A.D. Rakhel, A.I. Savvatimskiy, V.E. Fortov, Measurement of the electrical resistivity of hot aluminum passing from the liquid to gaseous state at supercritical pressure. Physical Review B **71**, 014208 (2005)
34. V.N. Korobenko, A.D. Rakhel, Observation of a first-order metal-to-nonmetal phase transition in fluid iron. Physical Review B **85**, 014208 (2012)
35. A.L. Vereshchagin, Phase diagram of ultrafine carbon. Combust. Explosion Shock Waves **38**(3), 358–359 (2002). in Russian
36. C.C. Yang, S. Li, Size-dependent temperature–pressure phase diagram of carbon. J. Phys. Chem. **112**, 1423–1426 (2008)
37. F.P. Bundy, R.H. Wentorf, Direct transformastion of hexagonal boron nitride to denser forms. J. Chem. Phys. **38**, 1733815 (6 pages) (1963)
38. V.N. Korobenko, A.I. Savvatimskiy, Blackbody design for high temperature (1800 to 5500 K) of metals and carbon in liquid states under fast heating, Temperature: its measurement and control in science and industry. AIP Conf. Proc. Ed. Dean C. Ripple, 7, Part 2, pp. 783–788 (2003)
39. A.I. Savvatimskiy, Melting point of graphite and liquid carbon. Phys. Usp. **46**, 1295–1303 (2003)
40. A.I. Savvatimskiy, Measurements of the melting point of graphite and the properties of liquid carbon (a review for 1963–2003). Carbon **43**, 1115–1142 (2005)
41. Basharin A. Yu, M.V. Brykin, M. Marin, I.S. Pakhomov, S.F. Sitnikov, Ways to improve the measurement accuracy in the experimental determination of the melting temperature of graphite. High Temp. **42**(1), 60–67 (2004)
42. M. Van Thiel, F.H. Ree, High-pressure liquid-liquid phase change in carbon. Phys. Rev. B (condensed matter) **48**(6), 3591 (1993)
43. V.A. Kirillin, V.V. Sychev, A.E. Sheindlin, *Technical Thermodynamics* (Energoatomizdat, Moscow, 1983). in Russian
44. N.S. Fateeva, L.F. Vereshchagin, V.S. Kolotygin, Optical method for measuring the melting temperature of graphite up to 3 kbar. Doklady USSR **152**(1), 88 (1963). in Russian
45. F.P. Bundy, The P, T phase and reaction diagram for elemental carbon. J. Geophys. Res. **85** (B12), 6930–6936 (1980)
46. L. Colombo, A. Fasolino (eds.), *Computer-Based Modeling of Novel Carbon Systems and Their Properties*, Carbon Materials: Chemistry and Physics 3, Springer Science + Business Media B.V. (2010)
47. E.I. Asinovsky, A.V. Kirillin, A.V. Kostanovskii, On the carbon phase diagram in the vicinity of the triple point of the solid-liquid-vapor. High Temp. **35**, 716 (1997). in Russian
48. E.I. Asinovsky, A.V. Kirillin, A.V. Kostanovskii, V.E. Fortov, On the parameters of carbon melting. High Temperatures **36**(5), 716–721 (1998)
49. J.N. Glosli, F.H. Ree, Phys. Rev. Lett. **82**, 4659 (1999)
50. A. Ferraz, N.H. March, Phys. Chem. Liq. **8**, 289 (1979)
51. A. Umantsev, Z. Akkerman, Continuum theory of carbon phases. Carbon **48**(1), 8–24 (2010)

52. F. Colonna, A. Fasolino, E.J. Meijer, High-pressure high-temperature equation of state of graphite from Monte Carlo simulations. Carbon **49**(2), 364–368 (2011)
53. Igor I. Shabalin "Ultra-High Temperature Materials I: Carbon (Graphene/Graphite), and Refractory metals" (Springer, 2014)
54. N.D. Orekhov, V.V. Stegailov, Molecular dynamics simulation of graphite melting. High Temp. **52**(2), 198–204 (2014)
55. N.D. Orekhov, V.V. Stegailov, Graphite melting: atomistic kinetics bridges theory and experiment. Carbon **8**(7), 358–364 (2015)
56. A.V. Kirillin, S.P. Malyshenko, M.A. Sheindlin, V.N. Evseev, Study of phase transformations of condensed phase—carbon gas in the vicinity of the triple point of graphite-liquid-vapor under pressure up to 400 bar. Doklady **257**(6), 1356–1359 (1981). in Russian
57. A.V. Kirillin, M.D. Kovalenko, S.V. Romanenko, L.M. Heifetz, M.A. Sheindlin, Apparatus and methods for examining the properties of refractory substances at high temperatures and pressures by stationary laser heating. High Temp. **24**(2), 286–290 (1986)
58. M. Musella, C. Ronchi, M. Brykin, M. Sheindlin, The molten state of graphite: an experimental study. J. Appl. Phys. **84**(5), 2530–2537 (1998)
59. A.I. Savvatimskiy, V.N. Korobenko, High-temperature properties of metals for nuclear industry (zirconium, hafnium and iron during melting and in the liquid state). MEI Publishing House, 216 p., (2012). ISBN 978-5-383-00800-3 (in Russian)
60. Arseniy Kondratyev, Sergey Muboyajan, Sergey Onufriev, Alexander Savvatimskiy, The application of the fast pulse heating method for investigation of carbon-rich side of Zr–C phase diagram under high temperatures. J. Alloy. Compd. **631**, 52–59 (2015)
61. A.M. Kondratyev, S.V. Onufriev, A.I. Savvatimskiy Melting of HAPG graphite Joint Institute for High Temperatures, Moscow, Russia, (unpublished), see the Chapter 10

Chapter 9
Pulse Heating Application to Study High-Pressure Carbon State

Abstract The advantages of fast carbon heating to measure properties at high temperatures and some practical applications of carbon heating are considered. It was commented a complicated study of converting diamond—to liquid carbon under high pulse pressure with temperature recording (nanosecond experiment by Jon Eggert et al., USA). The more high pressure (terapascal value) is obtained in 2015 year with laser energy up to 0.76 MJ in a 20-ns time to convert diamond to the highest pressure (experiment by R.F. Smith et al. USA).

9.1 The Advantages of Fast Carbon Heating to Measure Properties at High Temperatures and Some Practical Applications

The advantages of fast electrical heating are as follows.

Because the pulse laser heating is widely used in the experiments, we note the overall benefits of heating by electrical current to the laser heating of the surface. Pulsed electric heating enables uniform heating of the specimen volume, in particular in the form of a blackbody model [1–3]. One can measure the specific thermal properties (as an example, for metals) depending on the actual temperature of up to 8000 K (in the air), and by using a sapphire plates and thick-walled sapphire capillaries—up to tens of thousands of degrees. For example, a rapid heating of graphite in a thick-walled capillary sapphire allowed to reach the temperature of liquid carbon from 4800 K (melting point) to 20,000 K (estimation) [4, 5]. Another significant advantage is the ability to use a higher rate of heating with volume heat dissipation (it does not take time for heating of the entire specimen as in the case of surface laser heating). It is possible to achieve a higher energy density embedded in carbon, i.e. to reach the higher temperatures. It is possible to determine the equilibrium thermal properties of matter, despite the very high heating rate. Overview of the study of metals and graphite under pulsed heating is published as a separate chapter in the book [6] (2010 year).

A. Savvatimskiy, *Carbon at High Temperatures*, Springer Series in Materials Science 134, DOI 10.1007/978-3-319-21350-7_9

What happens to the graphite if it is limited in its ability to expand under pulsed heating? If we limiting the expanding graphite by a non-conducting wall (in the short-time heating process), as the loss of conduction does not occur. It was obtained a large number of experiments with different graphite grades: to limit expansion leads to increased pressure and, as a consequence, the new substance properties have appeared which typical for high pressure. Moreover, there is a drop in electrical resistance of liquid carbon near the melting point, and higher the melting point the increase in resistance is observed. Under pulse experiments the quartz and sapphire capillary tubes, were used, which kept high pulse pressure (up to tens of kbar). The use of such tubes has allowed investigating the properties of the liquid carbon at high pressure. It is a chance to measure the expansion of the liquid carbon during limit stop housing in the wall during the expansion of the substance. During the stop of the expanding graphite into the wall of the tube, the derivative of resistivity against input energy is reflected in the oscilloscope traces.

To measure pressure in the pulsed heating process the most useful is a plane system: a thin layer of material sandwiched between two thick sapphire plates. When the metal or graphite is heated between sapphire plates its inertia prevents the expansion of the substance—there is high (up to 100 kbar) pulse pressure appears for a short time (fraction of a microsecond). This time is enough to measure the properties of the liquid carbon and its compounds, as well as the pressure itself. The questions of measuring pulse pressure partially presented in the monograph of Savvatimskiy and Korobenko [7] in 2012 year.

As an example, we note below the works, which addressed different aspects of investigations of the properties of graphite but are of practical interest.

(1) Summary of [8] (Journal Carbon, 1985).
It is known that carbon is vaporized by mixture of molecules such as C1, C2, C3, and so on. More poly-nuclear particles have a more significant influence on the thermodynamic properties at high temperatures and high pressure. While little is known about the composition higher than C5, usually accepted estimates of the dominance of C3 in various conditions. To overcome the lack of experimental data for the liquid carbon in the [8] it is calculated thermodynamic properties of a liquid carbon in a wide range from the triple point temperature to the critical point of the liquid using the model structures have been successfully applied to many other liquids.

(2) Part of the abstract from [9] (Journal Applied Surface Science, 2003).
It was found that the surface of the emitting layer of carbon becomes liquid-like during the explosive electron emission (EEE), forming a very thin tabs with a radius of curvature $r < 10$ nm. These tabs are uniformly distributed over the surface of the carbon emitting surface with the surface density of 10^8 per 1 cm^2. It is assumed that these tabs provide high stability and reproducibility of EEE emitting carbon surface (discussion on the possible causes of EEE published in [7] of 2012 year).

The phenomenon of "electropolishing" of carbon surface was found when recording ions from the plasma of an explosive emission. The experiment demonstrates that the recording of the ion current (actually under the recording of the electron emission current, *note the author of the monograph*) it appears discontinuous micro-sources of emitting surface, and the emitting surface becomes more smooth (polished).

As we see, it is continued an active research of carbon with important practical applications. Therefore, investigation of carbon (including thermophysical aspect) will certainly be explored further. The future of the pulse heating of carbon will develop in more short processes of heating, at least in the nanosecond time scale (under creation of dense and thin deposits on the insulating substrate). Transition to a minimum specimen size (including the thin sputtered layers of micron and submicron size), along with the transition to fast heating time, would input very high specific energy to carbon compounds. This will give a chance to examine non-equilibrium processes and extreme states of matter at high temperatures and pressures.

Recently, there has been a new area of research by pulse method—heating not only carbon but also more complex compounds such as carbides [10–12] and nitrides [13]. Besides, due to the possibilities of magnetron sputtering is possible to sputter layers onto substrates of nanometric layers of different metals, semiconductors, and their compounds—this makes it possible to investigate high-speed diffusion, followed by unexpected thermal effects. Recall that the uniformity of the heating by pulse of electric current is only possible for those conductors which have electrical resistance growing with increasing energy input (or with the increase in temperature). It occurs for carbides (excluding SiC) and nitrides [13]. High temperature refractory properties of these compounds (as well as graphite) are important in practice, as the refractory carbides and nitrides are included in the tract of gas turbine and in the coating of nozzles of aircraft, missile defense systems, protective tiles spacecraft, matrix of nuclear fuels.

The results of studies of carbon presented in this monograph may find practical application in industries (aerospace, nuclear engineering and aviation), under using graphite and their compounds with metals for work at high temperature conditions.

9.2 From Diamond—to Liquid Carbon with Temperature Recording (Experiment by Eggert et al. USA [14])

Give a description of the experiment according to the publication of Nature "Diamond molted under Pressure" [15] and according to Russian information portal [16].

In their experiments, American scientists used a small natural diamond with a mass of about one-tenth of a carat. The melting of the material held in the shock wave created by using nanosecond laser pulse; liquid diamond was obtained at a pressure of 40 million times above normal atmospheric pressure.

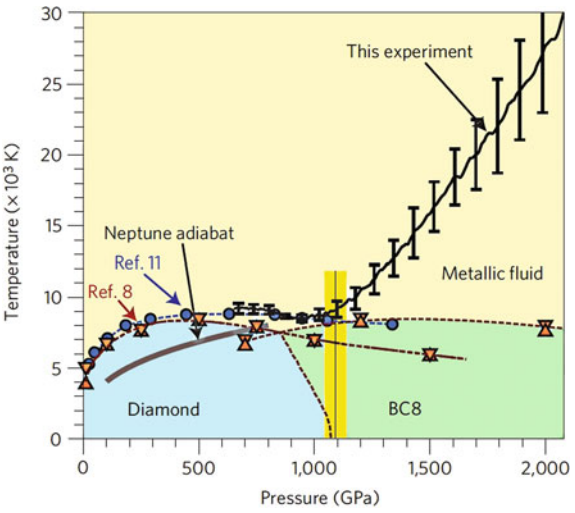

Fig. 9.1 [14] Temperature versus pressure data compared with simulations

During a gradual pressure reduction to 11 million atmospheres and temperatures up to 50,000 K on the surface of the liquid it were appeared solid formations. Physics did not expect that the pieces of solid diamond, do not sink, but remain afloat, like pieces of ice. With further decreasing pressure, the temperature remained constant, and on the surface accumulated more solid pieces of diamond, forming the "icebergs".

It is the first temperature measurements for shock-compressed diamond at conditions of (6–40 Mbar) and 8000–100,000 K. These data reveal the melting curve for carbon up to 1.1 TPa and a complex fluid state between 1.2 and 2.5 TPa. Similar conditions exist inside the gas giants Uranus and Neptune, of which 10 % are composed of carbon. Authors [14] observe a plateau in T between 600 and 1100 GPa (Fig. 9.1), which they interpret as the transition of diamond from liquid to solid (corresponding to a two-phase region). Thus, the diamond melts at about 9,000 K and at mentioned pressure.

The black line denotes new experimental shock temperature data [14]. The blue circles and blue dashed line represent the melt curve from density functional theory calculations, that include diamond and liquid phases. The brown triangles that bracket the phase transitions and the brown dashed lines represent similar calculations, that include the diamond, BC8 and fluid phases. The graphite phase is omitted for clarity. The uncertainties represent the weighted standard deviation of all measurements.

Using Hugoniot temperature measurements, the authors can extract the specific heat. Just before melting, the sample is at a temperature much higher than the Debye temperature of diamond (2200 K), so the specific heat should be close to the Dulong-Petit limit of $3Nk_B$ (k_B is Boltzmann's constant). In the fluid, the specific heat shows a broad peak with $C_V \sim 4$–$6\ k_B$ between 10,000 and 30,000 K, implying an excess energy sink. At higher temperature, C_V eventually approaches $3Nk_B$ at about 70,000 K after first dropping below the Dulong-Petit limit (Fig. 9.2).

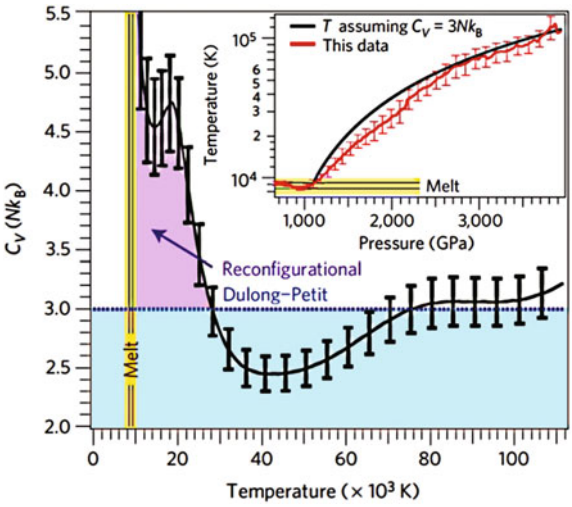

Fig. 9.2 [14] Specific heat of diamond in liquid state versus temperature showing the Dulong–Petit limit, $C_V = 3Nk_B$, which should hold for the solid below the melting temperature, and the peak attributed to atomic reconfiguration above the melting temperature

The uncertainties represent the standard deviation of results of a variety of assumptions.

The inset compares temperature versus pressure from our measurements (red line) with the values calculated assuming a constant specific heat (black line). The temperatures for a hypothetical fluid obeying the Dulong–Petit limit are well above our uncertainties for pressures of 1:2–2:4 TPa.

The authors [14] consider it unlikely that this peak in C_V is due to a change in ionization, because the reflectivity remains constant at about 30 % over this entire P–T range. High values of specific heat are similarly observed just above the melt temperature of quartz, fused silica, many alkali halides, silicon and germanium, and have been interpreted in terms of dissociation of a short-range ordered fluid. The high specific heat of Si and Ge is correlated with an anomalous liquid structure factor, and there is an explicit relationship between the structure factor and specific heat for a liquid described by pairwise interactions. Thus, the observed peak in C_V is probably due to a reconfiguration of atomic packing, from a partially bonded complex fluid to an atomic fluid above 60,000 K.

In a Sect. 7.3.2 we measured C_V for liquid carbon in the temperature range ~6000–9000 K and obtained the data (3 J/g K) that is closed to result of [14].

The data [14] indicate that diamond melts to a denser, metallic fluid—with the melting curve showing a negative Clapeyron slope—between 0.60 and 1.05 TPa, in good agreement with predictions of first-principles calculations. Temperature data at still higher pressures suggest diamond melts to a complex fluid state, which dissociates at shock pressures between 1.1 and 2.5 TPa (11–25 Mbar) as the temperatures increase above 50,000 K.

9.3 From Diamond—to Liquid Carbon at the Highest Pressure (Experiment by R.F. Smith et al. [17] 2014, USA)

"Give a description of this experiment and its interpretation as described in publication [17].

The recent discovery of more than a thousand planets outside our Solar System, together with the significant push to achieve inertially confined fusion in the laboratory [18] (references [18–20] of this paragraph see in [17])*, has prompted a renewed interest in how dense matter behaves at millions to billions of atmospheres of pressure. The theoretical description of such electron-degenerate matter has matured since the early quantum statistical model of Thomas and Fermi, and now suggests that new complexities can emerge at pressures where core electrons (not only valence electrons) influence the structure and bonding of matter* [19]*. Recent developments in shock-free dynamic (ramp) compression now allow laboratory access to this dense matter regime. Here we describe ramp-compression measurements for diamond, achieving 3.7-fold compression at a peak pressure of 5 terapascals (equivalent to 50 million atmospheres). These equation-of-state data can now be compared to first-principles density functional calculations* [20] *and theories long used to describe matter present in the interiors of giant planets, in stars, and in inertial-confinement fusion experiments. Our data also provide new constraints on mass–radius relationships for carbon-rich planets".* (References referred to [17]).

9.4 Methods Summary

Experiments used 176 laser beams from the National Ignition Facility (NIF) (in Livermore, California, USA) focused onto the inner walls of a gold hohlraum (a gold cylinder that converts the laser light to X-rays) with a combined laser energy up to 0.76 MJ in a, 20-ns temporally ramped pulse. This generates a spatially uniform near-blackbody distribution of thermal X-rays in the hohlraum with a characteristic radiation temperature Tr, which increases with time to a peak of Tr < 235 eV.

The subsequent X-ray ablation of the diamond, over a 3-mm diameter, produces a uniform ramp-compression wave, which outruns the thermal wave produced by ablation. As the pressure wave reaches the back surface of the diamond the free surface velocity of each step is recorded with animaging velocity interferometer. Samples consist of a 50-mm-thick diamond plate used as an ablator, a 10-μm Au layer preheat shield, and a diamond sample having four steps.

The diamond was synthesized by chemical vapour deposition to yield a layered microstructure with an average grain size of 200 nm and a density of 3.2491 g cm^{-3} (±0.01 %).

The final sample had alternating 0.35-μm layers of 20-nm grains and ~350-nm grains. X-ray diffraction showed a < 110 > texture in the growth direction. The thickness of the composite sample is determined to ±1 μm, and the differences in step thickness are determined by optical interferometry to ±0.1 μm. The Au layer was incorporated into the target design to serve as a radiation preheat shield for the step diamond sample. Detailed radiation transport simulations estimate a temperature rise of 33 K due to X-ray preheating.

Although temperature was not measured in these experiments, it is useful to comment on such estimates from theoretical calculations. The temperature calculated from DFT along the diamond principal isentrope is quite low even at the most extreme compressions studied here (~600–700 K at multi-terapascal pressures). For this reason, the principal isentrope and the room-temperature isotherm are predicted to be nearly coincident in stress–density space. It is certainly possible that ramp compression path have higher temperatures than these isentrope predictions and this may be responsible for the higher stress versus density. However, because temperature, material strength, and phase transformation kinetics can each cause a stiffer response with respect to the isentrope, current estimates for the ramp compression temperature into the terapascal regime are quite speculative.

References

1. V.N. Korobenko, A.I. Savvatimskiy, in *Blackbody Design for High Temperature (1800 to 5500 K) of Metals and Carbon in Liquid States under Fast Heating*, Temperature: its measurement and control in science and industry, ed. by Dean C. Ripple, 2003, vol.7, Part 2, pp. 783–788
2. A.I. Savvatimskiy, Melting point of graphite and liquid carbon / Phys. Usp. **173**, 12, 1371–1379 (2003) in Russian
3. A.I. Savvatimskiy, Liquid carbon density and resistivity. J. Phys.: Condens. Matter **20** (114112), 6 (2008)
4. A.I. Savvatimskiy, Experimental electrical resistivity of liquid carbon in the temperature range from 4800 to 20,000 K. Carbon **47**, 2322–2328 (2009)
5. V. Korobenko, A. Savvatimskiy, Electrical resistivity of expanded liquid carbon at high temperatures and high pressures, in *Proceedings of the International Conference Thermal conductivity 30 and Thermal expansion 18*, DEStech Publication, Inc., pp. 787–793 (2010)
6. A.I. Savvatimskiy, Physical properties of conductors at high temperatures, in *Results and Prospects (50 years JIHT)*, 2010, pp. 89–114, Publisher Chance (JIHT RAS) (in Russian)
7. A.I. Savvatimskiy, V.N. Korobenko, in *High-temperature properties of metals for nuclear industry (zirconium, hafnium and iron during melting and in the liquid state)*, MEI Publishing House , 2012, p. 216, ISBN 978-5-383-00800-3 (in Russian)
8. Man Chai Chang, Mu Ryoo Ryong, Shik Jhon, Thermodynamic properties of liquid carbon. Carbon **23**(5), 481–485 (1985)
9. G.N. Fursey, M.A. Polyakov, L.A. Shirochin, A.N. Saveliev, Liquid carbon surface during explosive emission. Appl. Surf. Sci. **215**(1–4), 286–290 (2003)
10. A.M. Knyazkov, S.D. Kurbakov, A.I. Savvatimskiy, M.A. Sheindlin, V.I. Yanchuk, Melting of carbides by electrical pulse heating. High Temp.-High Pressures **40**, 349–358 (2011)

11. S.V. Onufriev, A.I. Savvatimskiy, Yanchuk V.I., Measurement of thermophysical properties of zirconium and tantalum carbides at high temperatures (up to and above the melting point), Measurement Techniques, 2011, № 8, pp. 49–52 (in Russian)
12. Arseniy Kondratyev, Sergey Muboyajan, Sergey Onufriev, Alexander Savvatimskiy, The application of the fast pulse heating method for investigation of carbon-rich side of Zr–C phase diagram under high temperatures. J. Alloy. Compd. **631**, 52–59 (2015)
13. S.V. Onufriev, A.M. Kondratyev, A.I. Savvatimskiy, G.E. Val'iano, S.A. Muboyajan, High-temperature properties investigation of ZrN by pulse current heating. High Temp. **53**(3), 3 (2015)
14. Eggert J.H., Hicks D.G, Celliers1 P.M, Bradley D.K, McWilliams R.S, Jeanloz R, Miller J.E, Boehly T.R, and Collins G.W, (2010). Melting temperature of diamond at ultrahigh pressure, Nature Physics 6, 9–10
15. Nature Physics, January 2010, V.6, P.9
16. http://temperatures.ru/articles/
17. R.F. Smith, J.H. Eggert, R. Jeanloz, T.S. Duffy, D.G. Braun, J.R. Patterson, R.E. Rudd, J. Biener, A.E. Lazicki, A.V. Hamza, J. Wang, T. Braun, L.X. Benedict, P.M. Celliers, G.W. Collins, Ramp compression of diamond to five terapascals. Nature (Letter) **511**, 330–333 (2014)
18. M.J. Edwards, et al. Progress towards ignition on the National Ignition Facility. Phys. Plasmas **20**, 070501 (2013)
19. J.B. Neaton, N.W. Ashcroft, Pairing in dense lithium. Nature **400**, 141–144 (1999)
20. M. Martinez-Canales, C.J. Pickard, R.J. Needs, Theormodynamically stable phase of carbon at multiterapascal pressures. Phys. Rev. Lett. **108**, 045704 (2012)

Chapter 10
Graphene Investigation

Abstract The calculation of Graphene melting is shown that gives melting temperature of one carbon layer equals 4900 K. It was shown the broad experimental and estimated methods to investigate Graphene: theory and the experiments of Alexander Balandin (USA). It was mentioned the first experiments of measuring melting temperature of the HAPG graphite under fast electrical heating in 2015 year.

10.1 Calculation of Graphene Melting

In the calculation study [1] of 2011 year, on the base of the selected interatomic potential for carbon it was obtained that the molten carbon is not a simple liquid and forms the carbon chains. The temperature of melting of graphene (one atom layer of the solid graphite) according to the authors [1] is 4900 K. It should be noted that references in the literature of this article contains our previous study [2], which shows the experimental melting temperature for graphite 4800–4900 K.

Abstract [1]: The high temperature behavior of graphene is studied by atomistic simulations based on an accurate interatomic potential for carbon. We find that clustering of Stone–Wales defects and formation of octagons are the first steps in the process of melting which proceeds via the formation of carbon chains. The molten state forms a three-dimensional network of entangled chains rather than a simple liquid. The melting temperature estimated from the two-dimensional Lindemann criterion and from extrapolation of our simulation for different heating rates is about 4900 K.

Atomistic simulations in [1] give a scenario of the melting of graphene as the decomposition of the 2D crystal in a 3D network of 1D chains. The molten phase is similar to the one found for fullerenes [3]. Similar structures can be seen in simulations of nanotubes [4, 5]. We find that, for graphene, a crucial role is played by SW defects. It is the clustering of SW defects that triggers the formation of octagons which are the precursors for the spontaneous melting around T_m = 4900 K in our

A. Savvatimskiy, *Carbon at High Temperatures*, Springer Series in Materials Science 134, DOI 10.1007/978-3-319-21350-7_10

simulations. This temperature is higher than the value of 4000 K found for fullerenes [3] and close to the 4800 K found for nanotubes [4], but not as high as the value of 5800 K estimated for graphene by extrapolation to infinite-radius nanotubes in [5].

Zakharchenko et al. [1] study the melting of graphene by Monte Carlo simulations in the *NVT* and *NPT* ensembles (constant number of particles *N*, constant volume *V* or constant pressure *P* and constant temperature *T*) with periodic boundary conditions in the plane for samples of $N = 1008$, 4032 and 16,128 atoms. The interatomic interactions are calculated with the LCBOPII potential [6] that the authors of [1] have shown to describe well the elastic and thermal properties of graphene [7] as well as the liquid phase [6].

When melting is completed the carbon chains form an entangled 3D network with a substantial amount of threefold-coordinated atoms, linking the chains. Therefore, this low density structure reminds us rather of a polymer gel than a simple liquid. In fact, the radial distribution function shown a very sharp peak at distances smaller than the interatomic distance in graphene, due to the formation of shorter double bonds in the chains. In typical simple liquids, instead, the first peak shifts to larger values of interatomic distances when going from a crystal to a liquid [8]. This high temperature phase has also been found for molten fullerenes [3].

The Lindemann criterion [8, 9] $\sqrt{\langle u^2 \rangle_m}/d \approx 0.2$ (where $(u^2)_m$ is the mean-square atomic displacement at the melting temperature and d is the interatomic distance at $T = 0$) is commonly used to estimate the melting temperature in 3D systems. Since in 2D the mean-square displacement (u^2) is divergent at finite temperatures, we need to consider differences in atomic displacements [10, 11]. Adapting the melting criterion used in [10] to the honeycomb lattice of graphene Zakharchenko et al. [1] define the average quantity

$$\gamma_n = \frac{1}{a^2} \left\langle \left| \mathbf{r}_i - \frac{1}{n} \sum_j \mathbf{r}_j \right|^2 \right\rangle, \tag{10.1}$$

where $a = 1/\sqrt{\pi \rho 0}$, ρ_0 is the 2D particle density at $T = 0$ K, $\mathbf{r}_i$ is the position of the ith atom and the sum over j runs over the n atoms closest to atom i. In Fig. 10.1 Zakharchenko et al. [1] show γ_n for $n = 3$, 9 and 12, namely including one, two and three coordination spheres (see the inset in Fig. 10.1). Since the difference between second- and third-neighbour distances is relatively small, the distinction between second and third neighbours becomes fuzzy at very high temperatures. Therefore the authors [1] think that γ_{12} is more meaningful than γ_9. Interestingly, as shown in Fig. 10.1, melting occurs when $\gamma_{12} = 0.1$, as found for the strictly 2D triangular lattice in [10]. Instead, γ_3 remains much smaller due to the rigidity of the covalent nearest-neighbour bonds.

The closest system to graphene is graphite. The melting temperature of graphite has been extensively studied experimentally at pressures around 10 Gpa and the results present a large spread between 4000 and 5000 K [2]. With LCBOPII, free energy calculations give $T_m = 4250$ K, almost independent of pressure between 1 and 20 Gpa [12]. At zero pressure, however, graphite sublimates before melting at 3000 K [2]. Monte Carlo simulations with LCBOPII at zero pressure show that, at 3000 K,

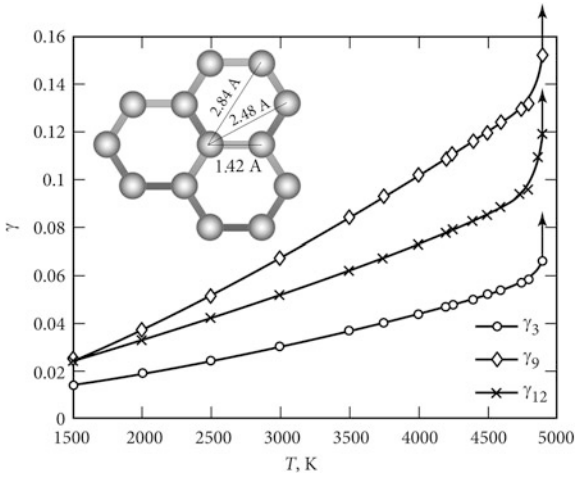

Fig. 10.1 [1] Temperature dependence of γ^3, γ^9 and γ^{12} calculated including the closest three, nine and 12 neighbours (see *inset*). The last points indicated by *arrows* correspond to the onset of the liquid phase for which these quantities diverge for infinite systems

graphite sublimates through detachment of the graphene layers [12]. The melting of graphene in vacuum that [1] have studied here can be thought of as the last step in the thermal decomposition of graphite, the 2D graphene layers melting into a 3D liquid network of 1D chains. Interestingly, formation of carbon chains has been observed in the melt zone of graphite under laser irradiation [13]. Although the temperature $T = 4900$ K of spontaneous melting represents an upper limit for T_m, our simulations suggest that T_m of graphene at zero pressure is higher than that of graphite.

10.2 Thermal Properties of Graphene: Experiments and Theory of Alexander Balandin and Co-authors

Graphene has already gained a unique reputation among novel synthetic materials. Dedicated efforts and enormous resources are being invested in creating viable commercial products. The high electrical and thermal conductivities in graphene are well known, and most of the applications of this material are pivoted to these properties. In addition to electronic and thermal management applications there are several other vital areas where graphene can be used successfully.

The unique thermal properties of graphene have been discovered by Alexander Balandin and co-workers at the University of California—Riverside. It has been established that graphene has extremely high intrinsic thermal conductivity, which can exceed that of carbon nanotubes (CNTs) [14–18]. Few-layer graphene retains excellent thermal properties [14, 15, 19]. Graphite, which is the 3D bulk limit for the few-layer graphen with the number of layers $n \rightarrow \infty$, is still an outstanding heat conductor with the intrinsic $K \approx 2000$ W/m K at RT. For comparison, $K \approx 430$ W/m K for silver. Balandin and his group members have also offered the first detailed theory of heat conduction in graphene.

The first experimental studies of thermal conductivity of graphene were carried out using an original non-contact optothermal technique based on Raman spectroscopy. Taking into account the temperature shift of Raman G-peak, the temperature profiles for large-area suspended graphene flakes were determined. The thermal conductivity values were extracted from numerical simulations, taking into account temperature profiles and actual size and shape of the flakes. It was established that graphene demonstrates very high thermal conductivity in the range from 2000 W/m K to 5000 W/m K for the high quality large flakes [14–18]. The measurements were performed with large-area suspended graphene layers exfoliated from bulk graphite.

Below we discuss the results of Prof. Alexander Balandin in more details, most closely to the text, often quoting his work. Several years ago we declared [20] that to obtain and investigate carbon in liquid state you should give the most high density graphite without any pores and possible point defects inside. The better carbon with such initial properties at that time was anisotropic graphite (brand HOPG). As one can see through this book we investigated liquid carbon under fast heating just HOPG grade (Russian production UPV-1T). To know the whole (bulk-carbon), you need to explore private, which is graphene. There is a mutual interest in the study of graphene and bulk carbon of these two research groups (investigating graphene and bulk-carbon).

Balandin et al. published in 2010 year a very useful study on graphene thermal conduction [21].

Abstract [21]: "*We review the results of our experimental and theoretical investigation of heat conduction in suspended graphene layers. Through direct measurements using a noncontact optical technique, we established that the thermal conductivity of the suspended graphene flakes is extremely high, and exceeds that of diamond and carbon nanotubes. By invoking Klemens' theoretical model, we explained the physical mechanisms behind such unusual thermal conduction in two-dimensional graphene layers. Our detailed theory, which includes the phonon-mode dependent Gruneisen parameter and takes into account phonon scattering on graphene edges and point defects, gives results in excellent agreement with the measurements. Superior thermal properties of graphene are beneficial for all proposed graphene device applications*".

And further:

"*In order to measure the thermal conductivity of suspended graphene layers, we developed our own noncontact optical approach. We took advantage of the fact that graphene has distinctive signatures in Raman spectra with clear G peak and 2D band. Moreover, we also found that the G peak of graphene's Raman spectra exhibits strong temperature dependence. The latter means that the shift in the position of G peak in response to the laser heating can be used for measuring the local temperature rise. The correlation between the temperature rise and amount of power dissipated in graphene, for the sample with given geometry and proper heat sinks, can give the value of the thermal conductivity K* (*see the schematic of the experiment in Fig.* 10.2)".

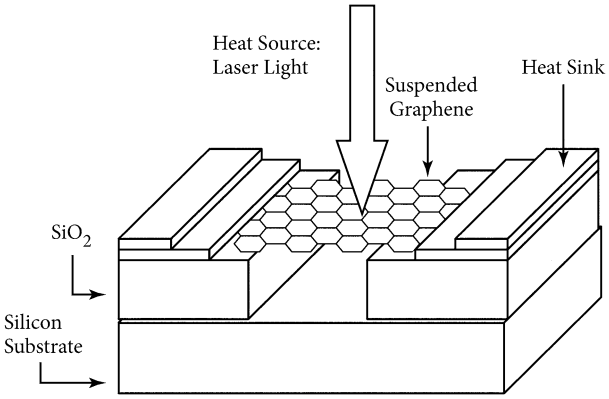

Fig. 10.2 [21] Schematic of the experiments for direct measurements of the thermal conductivity of the suspended graphene layers attached to heat sinks

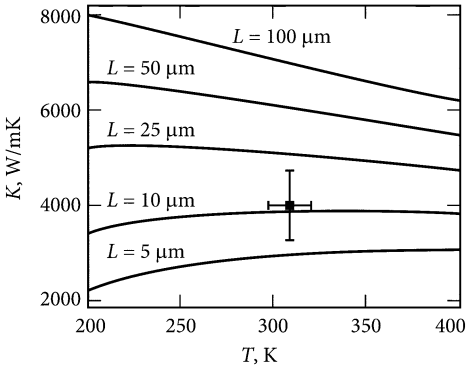

Fig. 10.3 [21] Theoretical thermal conductivity of graphene as a function of temperature. An experimental data point after Balandin et al. is also shown for comparison

Baladin et al. give a theory of heat conduction in Graphene and show the result of their experiment (Fig. 10.3). Using the equations summarized in the Chap. 4 (in [21]) Balandin et al. calculated the Umklapp-limited intrinsic thermal conductivity of graphene as a function of temperature. The results are shown in Fig. 10.3 for several lateral sizes of graphene flakes. An experimental data point after Balandin et al. is also shown for comparison. There is a good agreement between the model predictions and the available experimental data.

Balandin et al. reported the evolution of the thermal conductivity in few-layer graphene with addition of atomic layers. The intrinsic thermal conductivity of few layer graphene approaches the bulk graphite limit as the number of atomic planes increases.

In 2011 year [14] Balandin published a clue study devoted to thermal properties of graphene.

Abstract [14] gives next information. The room-temperature thermal conductivity of carbon materials span an extraordinary large range–of over five orders of

magnitude—from the lowest in amorphous carbons to the highest in graphene and carbon nanotubes. The review [14] gives thermal and thermoelectric properties of carbon materials focusing on recent results for graphene, carbon nanotubes and nanostructured carbon materials with different degrees of disorder. A special attention was given to the unusual size dependence of heat conduction in two-dimensional crystals and, specifically, in graphene. It was also described prospects of applications of graphene and carbon materials for thermal management of electronics.

Balandin gives a very useful figure on the thermal conductivity of different graphite grades including diamond (Fig. 10.4).

In the several chapters in [14] Balandin gives detailed overview on the thermal properties of bulk carbon allotropes, disordered and nanostructured carbon materials, carbon nanotubes, and graphene. Balandin mentioned [14] that different studies with suspended graphene found K in the range from $\sim$1500 to $\sim$5000 W/m K. The author gives the experimental thermal conductivity of graphene as a function of temperature for different studies.

Balandin [14] gives the chapter "Theoretical and Experimental Uncertainties": Thermal properties of low-dimensional carbon materials and experimental thermal conductivity of graphene as a function of temperature up to 700 K.

Next, Balandin [14] gives further chapters: Thermal Transport at Graphene-Substrate Interfaces; Graphene and Carbon Based Composites; Thermoelectric

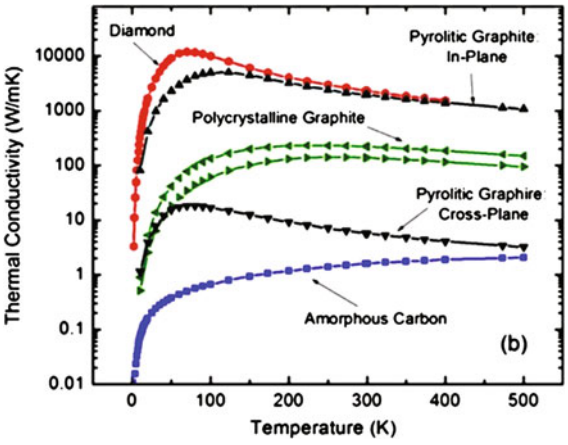

Fig. 10.4 [14]: Thermal conductivity K of bulk carbon allotropes as a function of T. The plots are based on commonly accepted *recommended* values from [24]. The curve "Diamond" is for the electrically insulating diamond of type II-*a*; Polycrystalline Graphite" is for AGOT graphite—a high-purity pitch-bonded graphite; and "Pyrolytic Graphite" is for high-quality graphite analog to HOPG. *Note* An *order of magnitude* difference in K of pyrolytic graphite and polycrystalline graphite with disoriented grains. The K value for pyrolytic graphite constitutes the bulk graphite limit of $\sim$2000 W/m K at RT. At low T, K is proportional to T^{γ}, where γ varies in a wide range depending on graphite's quality and crystallites size [24–39] (*References in the legend are indicated according to* [14])

Effects in Graphene; Appendix A: Methods for Measuring Thermal Conductivity of Graphene; Appendix B: Unique Features of Heat Conduction in 2D Crystals.

In the conclusion the author [14] mentioned; an important issue is the effect of the defects, grain size and orientation on $K(T)$ of graphene. Recently, two similar studies [22, 23] suggested that $K(T) \sim T^{1.4}$ or $\sim T^{1.5}$ dependences prove that ZA modes are dominant in graphene heat transport. However, it is well known that $K(T)$ dependence is strongly influenced by the material quality [24] (Fig. 10.5). The K values below bulk graphite and $K(T)$ dependence in [22, 23] likely indicate polycrystalline graphene with small and misoriented grains or a high concentration of defects due to processing as suggested in [25]. The isotope effects in graphene have been considered only computationally [26, 27] and await experimental investigation (*References* [22–27] *of this paragraph are indicated according to* [14] and one can see [22–27] in [14]). The author [28] shows the dependence of thermal conductivity of ultrathin films as a function of the thickness (H) in Fig. 10.5.

Alexander Balandin in 2011 year published a review article: "Thermal properties of graphene and nanostructured carbon materials" [28].

Starting with the Fig. 10.5 (shown above) the author consider other problems in the next chapters: "Basics of heat conduction" and "Bulk carbon allotropes". In the last chapter the author [28] noted: "*Revisiting the thermal properties of bulk carbon allotropes—graphite, diamond and amorphous carbon—provides proper reference for the discussion of graphene and nanostructured carbons. It also helps to distinguish new physics emerging in low-dimensional structures from mundane material-quality issues. It is hard to find another material where K has been studied as rigorously as it has in graphite. One of the reasons for this was the needs of the*

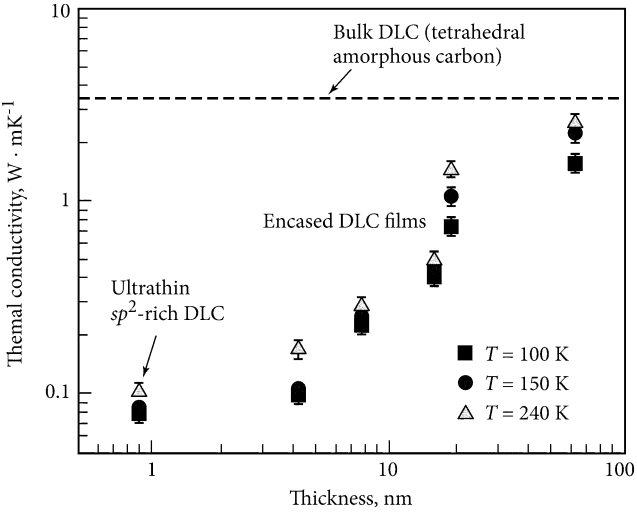

Fig. 10.5 [28]. Thermal conductivity of encased ultrathin DLC films as a function of H (the thickness of the specimen), indicating a similar trend to the encased FLG. Fig. 10.5 *is indicated according to* [28]

nuclear industry. Ironically, the data for graphite are sometimes difficult to find because the studies were conducted in the last century and often published in reports of limited circulation. Correspondingly, there is confusion among modern-day researchers about what is the K value for basal planes of high-quality graphite. Figure 10.5 (see above) shows K values for two types of high-purity graphite (sp^2 bonding), diamond (sp^3) and amorphous carbon (disordered mixture of sp^2 and sp^3). These plots are based on the recommended values reported in [29] (see reference [29] of this paragraph in [28]), *which were obtained by compilation and analysis of hundreds of research papers with conventionally accepted experimental data.*

Pyrolytic graphite, which is similar to highly oriented pyrolytic graphite (HOPG), has an in-plane K of ∼2000 W/m K *at room temperature. Its cross-plane K is more than two orders of magnitude smaller. Another type of chemically pure pitch-bonded graphite, produced by different technique, has an order-of-magnitude-smaller in-plane K of* ∼200 W/m K. *The K anisotropy is much less pronounced. This difference is explained by the fact that HOPG is made from large crystallites, which are well aligned with each other, so that the overall behavior is similar to that of a single crystal*".

To show the wide interests of the Balandin and his colleagues we give a brief description of their work [29].

Abstract of the authors [29]: "*We report on the development of a new technique for the growth of graphene and graphite nanocrystals from a metal–carbon melt. The process involves dissolving carbon inside molten nickel or copper at a specified temperature and then allowing the dissolved carbon to nucleate and grow on top of the melt at a lower temperature. The morphology of graphite forming inside nickel is shown to depend on the melt composition and cooling rate. The results indicate that the graphene layers contain a wrinkled structure due to thermal expansion coefficient mismatch between the grown layers and substrate. The graphene layers, however, preserve their continuity over these wrinkles. Although the formation of wrinkles was found not to depend on the type of metal substrate, the substrate had strong effect on the quality of grown layers. The films on copper contained quite a few defects including cracks and entrapped vacancies, whereas the films grown on nickel were pristine and defects free*".

The melt growth technique basically rely on dissolving carbon atoms inside a molten metal at a certain temperature, and then allowing the dissolved carbon to grow as graphite films on top of the melt at lower temperatures. In this process, as described previously [30], nickel and copper were melted in contact with a carbon source at a given temperature to saturate with carbon at a concentration that was determined from the binary phase diagram of metal–carbon. Upon cooling, as the solubility of carbon in the molten metal decreased, the excess carbon formed on top of the melt as well as other sites within the melt. The floating graphite layer could be either skimmed or allowed to freeze on the metal. The Cu–C system was selected because of the limited solubility of carbon in molten copper and no carbide formation has also been reported for this binary. The Ni–C system, on the other hand, consists of a simple eutectic reaction at 1356.5 C with limited terminal solubility of

carbon in nickel. The samples were prepared by arc melting process, melting in resistance furnace, induction melting, and electromagnetic levitation.

In this research, a new technique for growing graphite nano-crystals was utilized. The technique involved dissolving carbon in a molten metal at a specified temperature and then allowing the dissolved carbon to nucleate and grow on defects. Mentioned above reference [30] is very interesting and demonstrates the ability to establish a bridge between studies of graphene to the study of bulk graphite.

It was demonstrated a new method for the large-area graphene growth, which can lead to a scalable low-cost high-throughput production technology. The method is based on growing single layer or few-layer graphene films from a molten phase. The process involves dissolving carbon inside a molten metal at a specified temperature and then allowing the dissolved carbon to nucleate and grow on top of the melt at a lower temperature. The examined metals for the metal-carbon melt included copper and nickel. For the latter, the high-quality single layer graphene was grown successfully. The resulting graphene layers were subjected to detailed microscopic and Raman spectroscopic characterization. The deconvolution of the Raman 2D band was used to accurately determine the number of atomic planes in the resulting graphene layers and access their quality. The results indicate that this technology can provide bulk graphite films, few-layer graphene as well as high-quality single layer graphene on metals. Balandin et al. approach can also be used for producing graphene-metal thermal interface materials for thermal management applications.

For phonon transport in graphene Nika and Balandin gives a special publication [15].

Abstract [15]: "*Properties of phonons—quanta of the crystal lattice vibrations—in graphene have recently attracted significant attention from the physics and engineering communities. Acoustic phonons are the main heat carriers in graphene near room temperature, while optical phonons are used for counting the number of atomic planes in Raman experiments with few-layer graphene. It was shown both theoretically and experimentally that transport properties of phonons, i.e. energy dispersion and scattering rates, are substantially different in a quasi-two-dimensional system such as graphene compared to the basal planes in graphite or three-dimensional bulk crystals. The unique nature of two-dimensional phonon transport translates into unusual heat conduction in graphene and related materials. In this review, we outline different theoretical approaches developed for phonon transport in graphene, discuss contributions of the in-plane and cross-plane phonon modes, and provide comparison with available experimental thermal conductivity data. Particular attention is given to analysis of recent results for the phonon thermal conductivity of single-layer graphene and few-layer graphene, and the effects of the strain, defects, and isotopes on phonon transport in these systems*".

The very important result is shown in Fig. 10.6.

The publication [31] of Balandin et al. is devoted to thermal properties of graphene and graphene nanoribbons. In 2014 year Balandin with co-workers published fashionable and important result of the study of practical application: Graphene Thermal Properties: Applications in Thermal Management and Energy Storage [31].

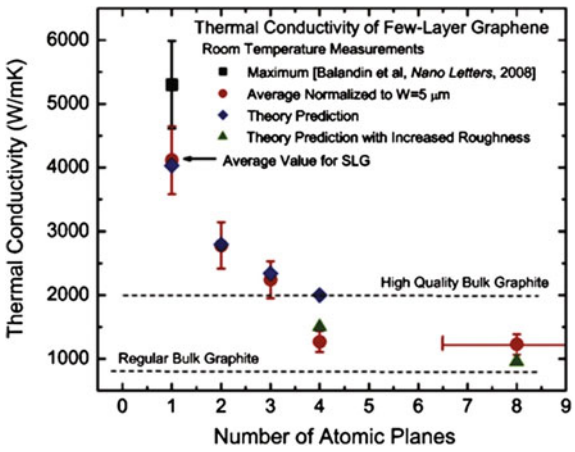

Fig. 10.6 [15]. Measured thermal conductivity as a function of the number of atomic planes in suspended FLG. The *dashed straight lines* indicate the range of bulk graphite thermal conductivities. The *blue diamonds* were obtained from the first-principles theory of thermal conduction in FLG based on the actual phonon dispersion and accounting for all allowed three-phonon umklapp scattering channels. The *green triangles* are Callaway–Klemens model calculations, which include extrinsic effects characteristic of thicker films. Reproduced with permission from [40]. Copyright 2010 Nature Publishing Group (*References in the legend are indicated according to* [15])

Abstract [31]: "*We review the thermal properties of graphene, few-layer graphene and graphene nanoribbons, and discuss practical applications of graphene in thermal management and energy storage. The first part of the review describes the state-of-the-art in the graphene thermal field focusing on recently reported experimental and theoretical data for heat conduction in graphene and graphene nanoribbons. The effects of the sample size, shape, quality, strain distribution, isotope composition, and point-defect concentration are included in the summary. The second part of the review outlines thermal properties of graphene-enhanced phase change materials used in energy storage. It is shown that the use of liquid-phase-exfoliated graphene as filler material in phase change materials is promising for thermal management of high-power-density battery parks. The reported experimental and modeling results indicate that graphene has the potential to outperform metal nanoparticles, carbon nanotubes, and other carbon allotropes as filler in thermal management materials.*"

There are several chapters are discussed in [31].

1. Introduction and Terminology
2. Motivations for Graphene Applications in Thermal Management
3. Intrinsic Thermal Conductivity of Graphene
4. Theory of the Thermal Conductivity of Graphene and GNR
5. Graphene Applications in Thermal Phase-Change Materials
6. Thermal Conductivity of Graphene-Enhanced Phase Change Materials

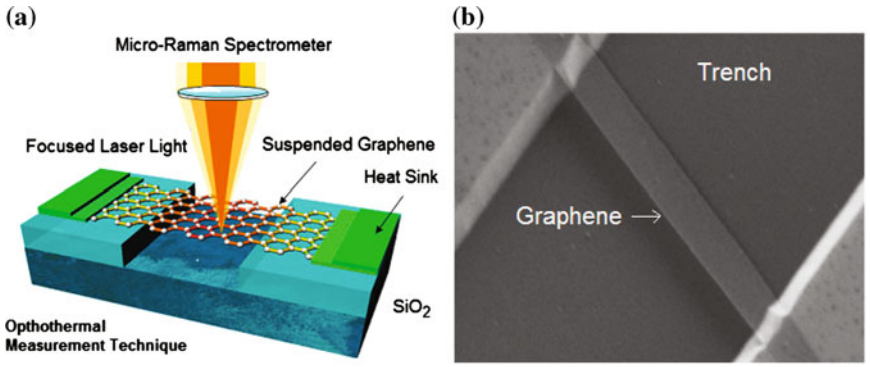

Fig. 10.7 [31] **a** Schematic of the suspended graphene structure used for measurements of the thermal conductivity of graphene. Graphene was heated with the laser light focused in the middle of the suspended part. The temperature rise was determined from the shift of the G peak position in graphene Raman spectrum. **b** Scanning electron image of the bilayer graphene ribbon suspended across the 3-μm trench in Si/SiO2 wafer for optothermal measurements. The image is reproduced with permission from [41] (see reference [41] in [31]). Copyright 2010 Nature Publishing Group (*The figure, text and* [41] *are indicated according to* [31])

7. Application of Graphene-Enhanced PCMs in Battery Packs
8. Modeling-Based Optimization of Thermal Management with Graphene-Enhanced PCMs

Give only one figure from Chap. 3 in [31] on the scheme of experimental investigation (Fig. 10.7).

As we see Professor Balandin with colleagues develops research in the broad area of experimental and calculation research.

10.3 Measuring of Melting Temperature of the HAPG Graphite Under Fast Electrical Heating in 2015 Year

HAPG—it is highly annealing anisotropic pyrolytic graphite.

German researchers [32] give such an Introduction: "*Nowadays HAPG is significantly important since this material becomes popular among the community of high-energy density physics at both laser facilities and x-ray free electron lasers A mosaic crystal is generally considered as numerous small perfect crystallite domains of micrometer and sub-micron size which are oriented, almost but not exactly, parallel to one another. The term Highly Annealed Pyrolytic Graphite (HAPG) is present in the literature since the 1960s for bulk specimen* [33]*, and was re-introduced by* Legall et al. [34] *in 2006 for a new kind of pyrolytic graphite developed by Optigraph GmbH (Berlin, Germany). HAPG is optimized for spectroscopy because it can be adhered as a single layer of desired thickness,*

pertaining its low mosaic spread" (References in this paragraph refer to this monograph).

In fairness it should be noted that Russian scientists (Grigorieva and Antonov) one of the first drew attention to the special properties of graphite HAPG and created a company to produce this grade of graphite. In just the above-mentioned article [32] provides links to the publication of Russian scientists [35, 36] dated back to 2000, 2003 years. I myself have met with Grigorieva and Antonov (in NIIGRAPHITE Institute, Moscow) in those years and they demonstrated me a thin highly annealed graphite foils which later were called HAPG.

The specimens (which we have obtained from Grigorieva and Antonov laboratory) have a density 2.25 g/cm^3 and thickness 20 and 30 microns. It looks like HOPG, but as a result of annealing the specimen in this experiment has the mosaicity to be ~0.08 on a 1 × 1 mm^2 scale. And the one more advantage: they have no any impurities and also almost all defects (extended and point), which leads to loosely coupled layers. It makes them look like a layered specimen with weak bonding between layers.

We report the first result of fast heating HAPG graphite. The first result of fast heating is shown in Fig. 10.8.

Specimen has 20 micron thick (width 5 mm, 15 mm long). Current pulse heating 16 kA; melting point was reached in the time interval ∼2 μs. The specimen was sandwiched between two thick quartz plates.

Pay attention to the fact that the heat capacity (as dE/dT) in the Fig. 10.8 equals constant in a broad range of temperature (from 2000 to ∼4500 K). It is the result of the small number of defects in the initial specimen HAPG. The derivative dE/dT (that is heat capacity) has increased only before the beginning of the melting providing the appearance of paired Frenkel's point defects (interstitial atom and vacancy) [37].

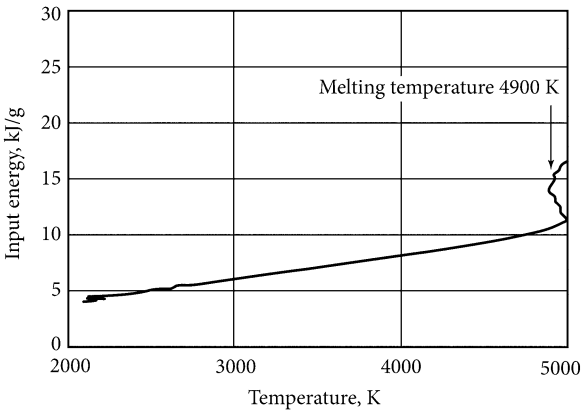

Fig. 10.8 [42] (Unpublished). Experimental dependence of input energy E against temperature T for HAPG graphite. Temperature was measured by optical pyrometer calibrated on the tungsten ribbon lamp. Emissivity ε = 0.6 was used to convert radiance to the true temperature

The small roughness of the original surface of the graphite specimen leads to a higher emissivity before melting. After reaching the melting temperature roughness disappears, providing a smooth surface with a smaller value of emissivity. Therefore, the temperature signal after the start of melting is somewhat reduced in line with lower emissivity. That's why melting temperature is shown by arrow in the Fig. 10.8 (4900 K) but not at 5000 K. One may camparison the diminishing of the temperature signal after starting of melting with the Fig. 4.20 (Chap. 4), where the carbon grade UPV-1TMO (like HOPG) was under investigation (under slow pulse electrical heating) [38].

For the liquid phase it was previously taken emissivity equals 0.6 (and 0.71 for solid state at 4000 K) [38].

In the experimental work [38] (milliseconds pulse heating) it was received the maximum melting temperature (5080 K) of graphite among all considered pulsed experiments (see Sect. 3.4 in this book). Pay attention to the fact that in our experiment with HAPG (Fig. 10.8) and in [38] for anisotropic graphite it was obtained a linear dependence of input energy against temperature. It is concluded that the heat capacity is constant. We suppose that the high quality of the specimens (with small number of defects) were used in both experiments, that's why (as we supposed) the both results have a linear dependence of input energy against temperature (up to ~ 4500 K).

References

1. K.V. Zakharchenko, A. Fasolino, J.H. Los, M.I. Katsnelson, Melting of graphene: from two to one dimension. J. Phys.: Condens. Matter **23**(202202), 4 (2011)
2. A.I. Savvatimskiy, Measurements of the melting point of graphite and the properties of liquid carbon (a review for 1963–2003). Carbon **43**, 1115–1142 (2005)
3. S.G. Kim, D. Tomanek, Phys. Rev. Lett. **72**, 2418 (1994)
4. K. Zhang, G.M. Stocks, J. Zhong, Nanotechnology **18**, 285703 (2007)
5. Y. Kowaki, A. Harada, F. Shimojo, K. Hoshino, J. Phys.: Condens. Matter **19**, 436224 (2007)
6. J.H. Los, L.M. Ghiringhelli, E.J. Meijer, A. Fasolino, Phys. Rev. B **72**, 214102 (2005)
7. K.V. Zakharchenko, M.I. Katsnelson, A. Fasolino, Phys. Rev. Lett. **102**, 046808 (2009)
8. N.H. March, M.P. Tosi, *Introduction to Liquid State Physics* (World Scientific, Singapore, 2002)
9. J.M. Ziman, *Principles of the Theory of Solids* (Cambridge University Press, Cambridge, 1972)
10. V.M. Bedanov, G.V. Gadyak, YuE Lozovik, Phys. Lett. A **109**, 289 (1985)
11. X.H. Zheng, J.G. Earnshaw, Europhys. Lett. **41**, 635 (1998)
12. F. Colonna, J.H. Los, A. Fasolino, E.J. Meijer, Phys. Rev. B **80**, 134103 (2009)
13. A. Hu, M. Rybachuk, Q.B. Lu, W.W. Duley, Appl. Phys. Lett. **91**, 131906 (2007)
14. A.A. Balandin, Thermal properties of graphene and nanostructured carbon materials. Nat. Mater. **10**, 569–581 (2011)
15. D.L. Nika, A.A. Balandin, Two-dimensional phonon transport in graphene. J. Phys.: Condens. Matter **24**, 233203 (2012)

16. A.A. Balandin, D.L. Nika, Phonons in low-dimensions: Engineering phonons in nanostructures and grapheme. Mater. Today **15**, 266–275 (2012)
17. A.A. Balandin, S. Ghosh, W. Bao, I. Calizo, D. Teweldebrhan, F. Miao, C.N. Lau, Superior thermal conductivity of single layer grapheme. Nano Lett. **8**, 902–907 (2008)
18. S. Ghosh, I. Calizo, D. Teweldebrhan, E.P. Pokatilov, D.L. Nika, A.A. Balandin, W. Bao, F. Miao, C.N. Lau, Extremely high thermal conductivity in graphene: Prospects for thermal management application in nanoelectronic circuits. Appl. Phys. Lett. **92**, 151911 (2008)
19. S. Ghosh, W. Bao, D.L. Nika, S. Subrina, E.P. Pokatilov, C.N. Lau, A.A. Balandin, Dimensional crossover of thermal transport in few-layer graphene. Nat. Mater. **9**, 555–558 (2010)
20. A.I. Savvatimskiy, V.E. Fortov, Cheret R. (1998) Thermophysical properties of liquid metals and graphite, and diamond production under fast heating, High Temp.-High Press, 30, pp. 1–18
21. A.A. Balandin, S. Ghosh, D.L. Nikaande, P. Pokatilov, Thermal conduction in suspended graphene layers. Fullerenes, Nanotubes, Carbon Nanostruct. **18**, 474–486 (2010)
22. B.J. Alder, R.H. Christian, Phys. Rev. Lett. **7**, 367 (1961)
23. P.S. DeCarli, J.C. Jamieson, Science **133**, 1821 (1961)
24. Yu.M. Korolev, New forms of crystalline carbon, Doklady T. **394**(1), 36–39 (2004) (in Russian)
25. F.P. Bundy, Pressure-temperature phase diagram of elemental carbon. Phys. A **156**(1), 169 (1989)
26. G.R. Gathers, J.W. Shaner, D.A. Young, High temperature carbon equation of state, UCRL-51644, Livermor, pp. 1–13 (1974)
27. A.F. Goncharov, I.N. Makarenko, S.M. Stishov, Graphite at pressures up to 55 GPa: optical properties and combination scattering of light, amorphous carbon?, JEPT, **96**(2), 670–673 (1989) (in Russian)
28. Alexander Balandin, Nat. Mater. **10**, 569–581 (2011)
29. S. Amini, H. Kalaantari, J. Garay, A.A. Balandin, R. Abbaschian, Growth of graphene and graphite nanocrystals from a molten phase. J. Mater. Sci. **46**, 6255–6263 (2011)
30. S. Amini, J. Garay, G. Liu, A.A. Balandin, R. Abbaschian, Growth of large-area graphene films from metal-carbon melts. J. Appl. Phys. **108**, 094321 (2010)
31. J.D. Renteria, D.L. Nika, A.A. Balandin, Graphene Thermal Properties: applications in thermal management and energy storage. Appl. Sci. **4**, 525–547 (2014)
32. U. Zastrau, A. Woldegeorgis, E. Förster, R. Loetzsch, H. Marschner, I. Uschmann, Characterization of strongly-bent HAPG crystals for von-Hámos x-ray spectrographs, Preprint typeset in JINST style—HYPER VERSION. J. Instrum. **8** (2013)
33. C.A. Klein, W.D. Straub, R.J. Diefendorf, Evidence of single-crystal characteristics in highly annealed pyrolytic graphite. Phys. Rev. **125**, 468–470 (1962)
34. H. Legall, H. Stiel, et al., A new generation of x-ray optics based on pyrolytic graphite. In *Proceedings of FEL, BESSY Berlin Germany*, pp. 798 (2006)
35. A.P. Shevelko, A. Antonov, et al., Focusing crystal von hamos spectrometer for x-ray spectroscopy and x-ray fluorescence applications. In *International Symposium on Optical Science and Technology*, International Society for Optics and Photonics, pp. 148–154 (2000)
36. I.G. Grigorieva, A.A. Antonov, HOPG as powerful x-ray optics. X-Ray Spectrom. **32**(1), 64–68 (2003)
37. Ya.I. Frenkel, *Kinetic Theory of Liquids* (Clarendon Press, Oxford, 1946)
38. A.V. Baitin, A.A. Lebedev, S.V. Romanenko, V.N. Senchenko, M.A. Sheindlin, The melting point and optical properties of solid and liquid carbon at pressures up to 2 kbar. High Temp.-High Press. **21**, 157–170 (1990)
39. D.M. Haaland, Graphite-liquid-vapor triple point pressure and the density of liquid carbon. Carbon **14**(6), 357–361 (1976)

40. V.N. Senchenko, M.A. Sheindlin, Experimental investigation of caloric properties for tungsten and graphite in the vicinity of their melting point. High Temp. **25**(3), 492–496 (1987) (in Russian)
41. M.J. Kuchner, S. Seager, Astrophys. J. Lett. **0504214**, 2 (2005)
42. A.M. Kondratyev, S.V. Onufriev, A.I. Savvatimskiy, Melting of HAPG graphite. Joint Institute for High Temperatures, Moscow, Russia, (unpublished), see the Chapter 10

Chapter 11
Conclusion

As we can see, carbon is diverse and multifaceted, even the pure form of carbon gives a lot of forms (diamond, graphite, graphene, nanotubes, fullerene), and the various compounds of carbon cover the whole industries—from medical (heart valves) to rocket technology. Experiments prove that the melting point of carbon is the highest of all substances on Earth (4800–4900 K). In addition, melting can take place only at pressures above 110 bars. These high parameters, along with good strength properties make carbon a universal working material in mechanical engineering. Even the seemingly negative property of carbon to begin actively sublimate at pressures below 110 bar and temperatures above 3000 K has practical application. At the entrance of missiles in the Earth's atmosphere a sublimation of carbon protects the surface from overheating, carrying away the excess energy.

Worldwide, the activities to study carbon are continued due to the importance of carbon for different industries. Therefore, carbon (including thermophysical aspects) will surely be explored further. In the future, studies on carbon may be developed in the field of even shorter heating times, for instance in the range of nanoseconds. Going to smaller size of specimens (including thin sputtered layers of micron and submicron size), along with nanosecond time heating will allow the injection of very high specific energy in carbon compounds. This will provide an opportunity to investigate non-equilibrium processes, as well as extreme states of matter at high temperatures and pressures, corresponding to astrophysical conditions.

In recent years, a new area of research in pulse heating methods—applied not only to carbon, but also to more complex compounds, like carbides [1].

In addition, by using magnetron sputtering there is an opportunity to create nanometer substrate layers of different metals or carbon-based compounds—this opens the opportunity to explore high-speed diffusion accompanied by thermal effects.

In recent years we have seen the development of scientific and engineering activities for the study of the properties of graphene (see Chap. 10 in this book). A similar study of complex carbon compounds (with the subtle effects of mixed electronic states)—may be yet to be implemented. The prospect of development of the properties for graphene will lead to the creation of a graphene crystal (bulk-carbon with properties of graphene) without any defects; it should be the ideal

A. Savvatimskiy, *Carbon at High Temperatures*, Springer Series in Materials Science 134, DOI 10.1007/978-3-319-21350-7_11

material for electronics. Homogeneous pulsed electric heating is only possible for those conductors which have increasing resistance with increasing input energy (or with increasing temperature). This is the case for carbides [1–3] (except SiC), and nitrides [4]. High temperature properties of these refractory compounds (as well as graphite) are important for practical applications, because refractory carbides and nitrides are included in the coating composition used in gas turbine tracts and nozzles of aircraft, protective plates of missile systems, matrix of nuclear fuels.

Besides the historical aspect of carbon studies at high temperatures during last 70 years, the results presented in this monograph can find practical application in different branches of industry (aerospace, nuclear engineering and aviation) which prepare different grades of graphite and of refractory carbides for use at the highest temperatures. We emphasize again that the study of the properties of carbon at temperatures 4000–10,000 K is possible only with rapid pulsed heating, a fact we have demonstrated in this monograph. Unfortunately, as shown by the last chapters of this book, calculation and experiment in the area of carbon properties are evolved often independently. The author believes that the development of experimental research and calculation methods have to go hand in hand with the constant comparison of the results. You cannot split up the physics on the two branches (calculated and experimental); physics (of processes and materials) should be one and indivisible which will ensure its successful development.

The author is extremely grateful to the reviewers of this book, Professor Gerard L. Vignoles (University of Bordeaux) and Dr. Alexander Balandin (University of California at Riverside), who carefully read the manuscript and gave useful advices. The author is also grateful to Dr. hab. Claus E. Ascheron (Springer) who took on the job of promoting this book for publication.

References

1. A. Kondratyev, S. Muboyajan, S. Onufriev, S. Savvatimskiy, The application of the fast pulse heating method for investigation of carbon-rich side of Zr–C phase diagram under high temperatures. J. Alloy. Compd. **631**, 52–59 (2015)
2. A.M. Knyazkov, S.D. Kurbakov, A.I. Savvatimskiy, M.A. Sheindlin, V.I. Yanchuk, Melting of carbides by electrical pulse heating. High Temp. -High Pressures **40**, 349–358 (2011)
3. S.V. Onufriev, A.I. Savvatimskiy, V.I. Yanchuk, Measurement of thermophysical properties of zirconium and tantalum carbides at high temperatures (up to and above the melting point). Measur. Tech. **54**(8), 926–930 (2011)
4. S.V. Onufriev, A.M. Kondratyev, A.I. Savvatimskiy, G.E. Val'iano, S.A. Muboyajan, High-temperature properties investigation of ZrN by pulse current heating. High Temp. **53**(3), 455–457 (2015)

Index

A. Savvatimskiy, *Carbon at High Temperatures*, Springer Series in Materials Science 134, DOI 10.1007/978-3-319-21350-7